

Identification of novel antagonists against skin relevant molecular targets in mediation of itch and inflammation



TECHNISCHE
UNIVERSITÄT
DARMSTADT

Vom Fachbereich Chemie
der Technischen Universität Darmstadt

zur Erlangung des akademischen Grades eines
Doctor rerum naturalium (Dr. rer. nat.)

Dissertation

von

Anita Jäger, M. Sc.
aus Darmstadt

Erstgutachter:
Zweitgutachter:

Prof. Dr. Harald Kolmar
Prof. Dr. Dipl.-Ing. Jörg von Hagen

Darmstadt 2023

Jäger, Anita: Identification of novel antagonists against skin relevant molecular targets in mediation of itch and inflammation

Darmstadt, Technische Universität Darmstadt,

Jahr der Veröffentlichung der Dissertation auf TUprints: 2024

Tag der mündlichen Prüfung: 20.02.2023

Veröffentlicht unter CC BY-SA 4.0 International

<https://creativecommons.org/licenses/>

Die vorliegende Arbeit wurde unter der Leitung von Herrn Prof. Dr. Harald Kolmar am Clemens-Schöpf-Institut für Organische Chemie und Biochemie der Technischen Universität Darmstadt sowie bei Merck KGaA in Darmstadt in der Abteilung Active Ingredient Innovation von Januar 2020 bis November 2022 angefertigt.

Publications derived from related projects

Termer, M., Jaeger, A., Carola, C., Salazar, A., Keck, C. M., Kolmar, H., & von Hagen, J. (2022). Methoxy-Monobenzoylmethane Protects Skin from UV-Induced Damages in a Randomized, Placebo Controlled, Double-Blinded Human In Vivo Study and Prevents Signs of Inflammation While Improving the Skin Barrier. *Dermatology and Therapy*, 12(2), 435-449.

Contribution to conferences

Talks:

Merck Science Academy 2022, virtual

Poster:

11th World Congress of Itch 2021, virtual (International Forum for the study of itch)

Cold Spring Harbor Laboratory 2020, virtual (Mechanisms of Aging)

Table of contents

Table of contents.....	v
1 Abstract.....	1
2 Zusammenfassung.....	2
3 Aim of the project.....	3
4 Introduction.....	4
4.1 Morphology of the skin.....	4
4.2 Inflammation and Itch in skin.....	7
4.3 Targets.....	12
4.4 Skin diseases with the involvement of 11 β HSD1 and NK1R.....	16
5 Materials & Methods.....	18
5.1 Materials.....	18
5.1.1 Reagents.....	18
5.2 Methods.....	18
5.2.1 Cell culture.....	18
5.2.2 Cell treatment.....	19
5.2.3 ATP Quantification.....	19
5.2.4 Interleukin 8 Quantification.....	19
5.2.5 Interleukin 6 Quantification.....	20
5.2.6 CCL2/MCP-1 Quantification.....	20
5.2.7 CCL20/MIP3 Quantification.....	20
5.2.8 Interleukin 1 β Quantification.....	20
5.2.9 Interleukin 18 Quantification.....	21
5.2.10 Caspase 1 Inflammasome Assay.....	21
5.2.11 Western Blot analysis.....	22
5.2.12 Sample preparation for 2D-LC-MS/MS analysis.....	22
5.2.13 2D-LC-MS/MS analysis.....	23
5.2.14 Gene set enrichment analysis.....	23
5.2.15 In-silico molecular docking.....	23
5.2.16 Fluorescence Imaging Plate Reader (FLIPR) Assay.....	24
5.2.17 Statistical analysis.....	24
6 Results.....	25
6.1 Results for 11 β HSD1.....	25
6.1.1 Molecular docking indicates target specific binding of three tested compounds... 25	
6.1.2 Proteome analysis of pro-inflammatory induced HaCat cells by 2D-LC-MS/MS labeling-assisted proteomics.....	26
6.1.3 Decreasing inflammatory response after treatment with FPCM, TPCA and DPAAM in HaCat cells.....	29
6.1.4 Differences in chemical analogue structure influence effectivity in modulating downstream targets.....	31
6.1.5 Decreased phosphorylated protein of ERK after treatment with NCEs.....	32
6.1.6 Proteome analysis of pro-inflammatory induced primary keratinocytes by 2D-LC-MS/MS labeling-assisted proteomics.....	33

6.1.7	Confirmation of three significant 11 β HSD1 inhibitors significantly affect downstream targets in primary keratinocytes.....	35
6.1.8	Proteome analysis of pro-inflammatory induced THP-1 cells by signal transfer from treated HaCat cells by 2D-LC-MS/MS labeling-assisted proteomics.....	37
6.1.9	Secretome of treated HaCat cells significantly reduced inflammatory response of THP-1 cells.....	39
6.1.10	Confirmation of involvement of caspase 1 in processing IL-1 β	40
6.1.11	Phosphorylation analysis of key inflammatory kinases after supernatant transfer of treated HaCat to THP-1 cells.....	42
6.2	Results for NK1R.....	44
6.2.1	Molecular docking supports hypothesis of target specific binding of two tested compounds.....	44
6.2.2	Ca ²⁺ influx after activation of NK1R in CHO-K1 and CHO-K1-NK1R cells.....	45
6.2.3	Proteome analysis of pro-inflammatory induced HaCat cells by 2D-LC-MS/MS labeling-assisted proteomics.....	46
6.2.4	Decreasing pro-inflammatory cytokine concentration after treatment with MAPA and OPMA in HaCat cells.....	47
6.2.5	Differences in chemical analogue structure influence effectivity in modulating downstream targets.....	49
6.2.6	Decreased phosphorylation protein after treatment with MAPA and OPMA.....	49
6.2.7	Proteome analysis of pro-inflammatory induced primary keratinocytes by 2D-LC-MS/MS labeling-assisted proteomics.....	51
6.2.8	Confirmation of two significant NK1R inhibitors on downstream targets.....	52
6.2.9	Proteome analysis of secretome of pro-inflammatory induced HaCat cells transferred to THP-1 cells y 2D-LC-MS/MS labeling-assisted proteomics.....	54
6.2.10	Secretome of treated HaCat cells significantly reduce inflammation response of THP-1 cells.....	56
6.2.11	Confirmation of involvement of caspase 1 in processing IL-1 β	57
6.2.12	Elucidation of phosphorylated protein after supernatant transfer of treated HaCat cells to THP-1 cells.....	58
7	Discussion.....	60
7.1.1	11 β HSD1 as molecular inflammatory target.....	60
7.1.2	NK1R as molecular itch target.....	65
8	Executive summary.....	74
9	Outlook.....	75
10	Appendix.....	76
10.1	Abbreviations.....	76
10.2	List of figures.....	79
10.3	References.....	82
10.4	Appendix.....	96
10.5	Danksagung.....	133
10.6	Curriculum Vitae.....	135
10.7	Affirmations.....	136

1 Abstract

Inflammation and itch are common symptoms of various skin diseases and have major influence on the quality of life of affected patients. In the treatment of individuals with sensitive and psoriatic skin, several inflammation and itch related molecular and cellular targets have been identified but many of these have yet to be characterized. In this study, we present two potential targets in skin that can be linked to the inflammation and itch cycle.

The enzyme 11 β HSD1 is responsible for converting inactive cortisone to active cortisol, which is used to transmit signals downstream. The activation of the receptor NK1R correlates with promoting inflammation and the perception of itch and pain in skin. In this study, both targets have been investigated based on their involvement in inflammation. The role of both identified targets were characterized based on the secretion of inflammatory cytokines- IL-6, IL-8, and CCL2, as well as phosphorylation and signaling pathways in keratinocyte like cells and primary keratinocytes.

Mimicking signal transfer in cell culture with secretome transmission from treated keratinocyte like cells to immune like cells showed significant reduction of tested compounds.

Treating skin cells with molecules able to inhibit inflammatory pathways result in the reduction of inflammatory signaling molecules secreted by skin cells. Therefore, these molecular targets and their associated pathways show therapeutic potential and can be mitigated via small molecules. This research can be used for further studies in inflammation and itch pathways and can help to treat the pathological symptoms.

2 Zusammenfassung

Entzündung und Juckreiz sind häufige Symptome bei verschiedenen Hautkrankheiten. Diese haben einen sehr großen Einfluss auf die Lebensqualität der erkrankten Patienten. Bei der Behandlung von Patienten mit empfindlicher und erkrankter Haut wurden mehrere mit Entzündung und Juckreiz zusammenhängende molekulare und zelluläre Zielstrukturen identifiziert, von denen viele jedoch noch charakterisiert werden müssen. In dieser Studie stellen wir zwei potenzielle Targets der Haut vor, die mit dem Entzündungs- und Juckreizzyklus in Verbindung gebracht werden können.

Das Enzym 11 β HSD1 ist für die Umwandlung von inaktivem Cortison in aktives Cortisol verantwortlich ist. Die Aktivierung des Rezeptors NK1R löst eine Reizweiterleitung von Entzündung und der Wahrnehmung von Juckreiz und Schmerzen in der Haut aus. In dieser Studie wurden beide Targets auf ihre Beteiligung an Entzündungen und Juckreiz hin untersucht. Die Rolle der beiden identifizierten Targets wurde anhand der Sekretion von Zytokinen - IL-6, IL-8 und CCL2 - als Entzündungsmarker sowie der Phosphorylierung von Signalwegen in keratinozytenähnlichen Zellen und primären Keratinozyten charakterisiert.

Ein Model der Signalübertragung in der Zellkultur mit Sekretübertragung von behandelten keratinozytenähnlichen Zellen auf immunähnliche Zellen, ergab eine signifikante Reduzierung von getesteten Entzündungsmarkern.

Es wurde festgestellt, dass die Behandlung von Hautzellen mit Molekülen, die in der Lage sind, Entzündungswege zu hemmen, zu einer Verringerung der von den Hautzellen ausgeschütteten Entzündungssignalmoleküle führt. Diese Zielstrukturen und die mit ihnen verbundenen Signalwege weisen also ein therapeutisches Potenzial auf und können durch kleine Moleküle gemildert werden. Diese Forschungsergebnisse können für weitere Studien im Bereich von Entzündung und Juckreiz genutzt werden und können zur weiteren Behandlung der pathologischen Symptome beitragen.

3 Aim of the project

Inflammation and itch are elicited by various cellular and molecular changes and restrict the normal function which promotes related pathologies. Uncontrolled increase of pro-inflammatory cytokine concentration lead to tissue damage compromised function. For skin diseases like atopic dermatitis, psoriasis, and epidermolysis bullosa is an appropriate medication still an unmet medical need for most patients. As a new approach NK1R and 11 β HSD1 have been investigated to be relevant molecular targets in the context of skin pathologies. Therefore, the identification of novel chemical entities for specific inhibition of NK1R and 11 β HSD1 to reduce signal transduction and further decreased cytokine secretion are of therapeutic interest.

Thus, the aims of this thesis are

- Identify novel chemical entities as potent mitigators of inflammation and itch, targeted towards NK1R and 11 β HSD1
- Identify the mode of action by analyzing the inflammation pathways downstream of NK1R and 11 β HSD1 that are inhibited by the identified NCEs
- Further characterize role of the NCEs in inflammation signaling pathways
- Evaluate the role of new chemical entities in primary keratinocytes to get closer to an in vivo model with biological variety
- Investigate signal transfer from keratinocytes like cells to immune like cells to analyze secreted immune response

4 Introduction

With a surface area of approximately 1,5-2m², skin is the biggest organ and one of the most important barriers for the human body (Richardson 2003). The primary function of the skin is to protect the organism against physical, chemical and biological influences. This could be pathogens like bacteria, viruses and fungi, UV exposure, temperature variations, dehydration and mechanical forces (Elias 2007). Also, the skin is responsible for regulating physiological processes, such as body temperature. Eventually, the skin contains mechano- and thermoreceptors for tactical and thermal sensitivity to the organism (Pedersen and Jemec 2006).

4.1 Morphology of the skin

The skin is structured in three main layers; the epidermis, the dermis and the subcutaneous tissue (Figure 1).

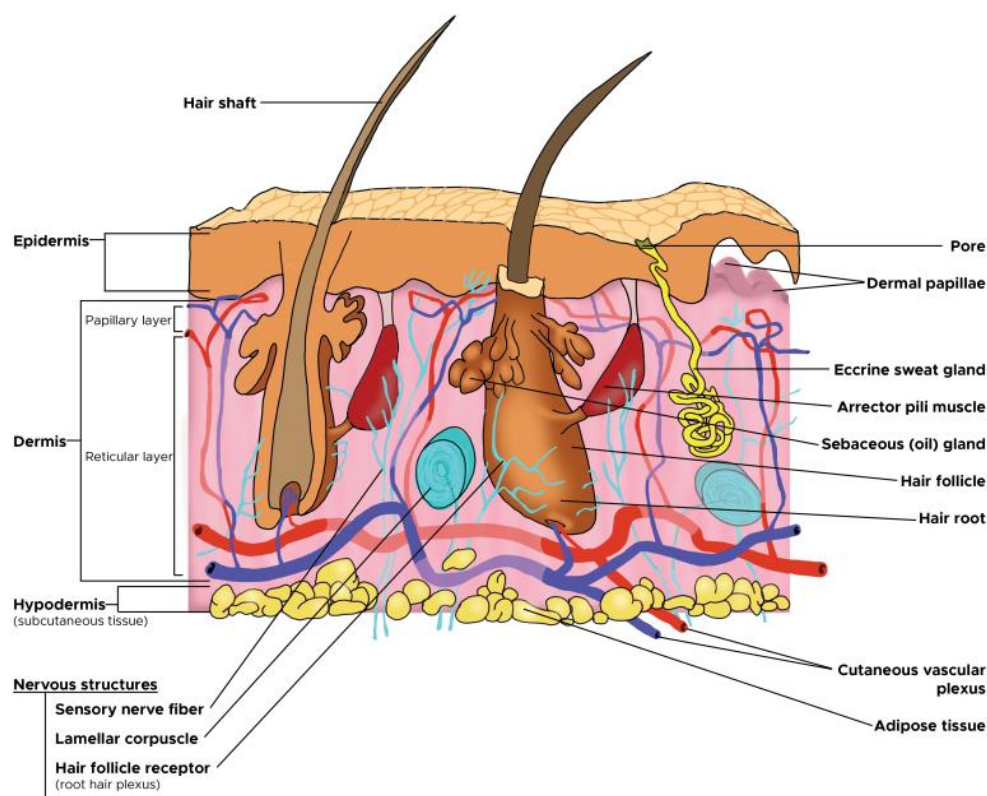


Figure 1: Morphology of the skin with epidermis, dermis and hypodermis (Yousef et al., 2017)

Epidermis

The Epidermis is the outermost layer of the skin and functions as a barrier from the environment and protects from potential pathogens and epidermal water loss (Boer et al., 2016).

The epidermis is up to 100µm thick and has a self-renewing character and consists deeper of four varying layers mainly dividing in a viable and non-viable epidermis layer (de-Souza et al., 2019). Keratinocytes are the most abundant cell type beside immune cells or melanocytes in the epidermis. So, keratinocytes differentiate and mature from the *stratum basale* as lowermost layer with proliferating cells to the *stratum spinosum* and *stratum granulosum* and therefore form the viable epidermis part. Furthermore, the keratinocytes differentiate to the *stratum lucidum* to the *stratum corneum* and build up the fully cornified non-viable and nucleus free epidermis as a strong compactable skin barrier. But the *stratum lucidum* is only build in hairless skin like foot or palms of the hand. Each stage of differentiation is characterized by expression of specific proteins like keratins and lipids. This process of cornification takes approximately 28 days. The differentiation is triggered in part through increasing Calcium (Ca^{2+}) concentration in the ascending layers of the epidermis (Colombo et al., 2017; Bikle et al., 2012).

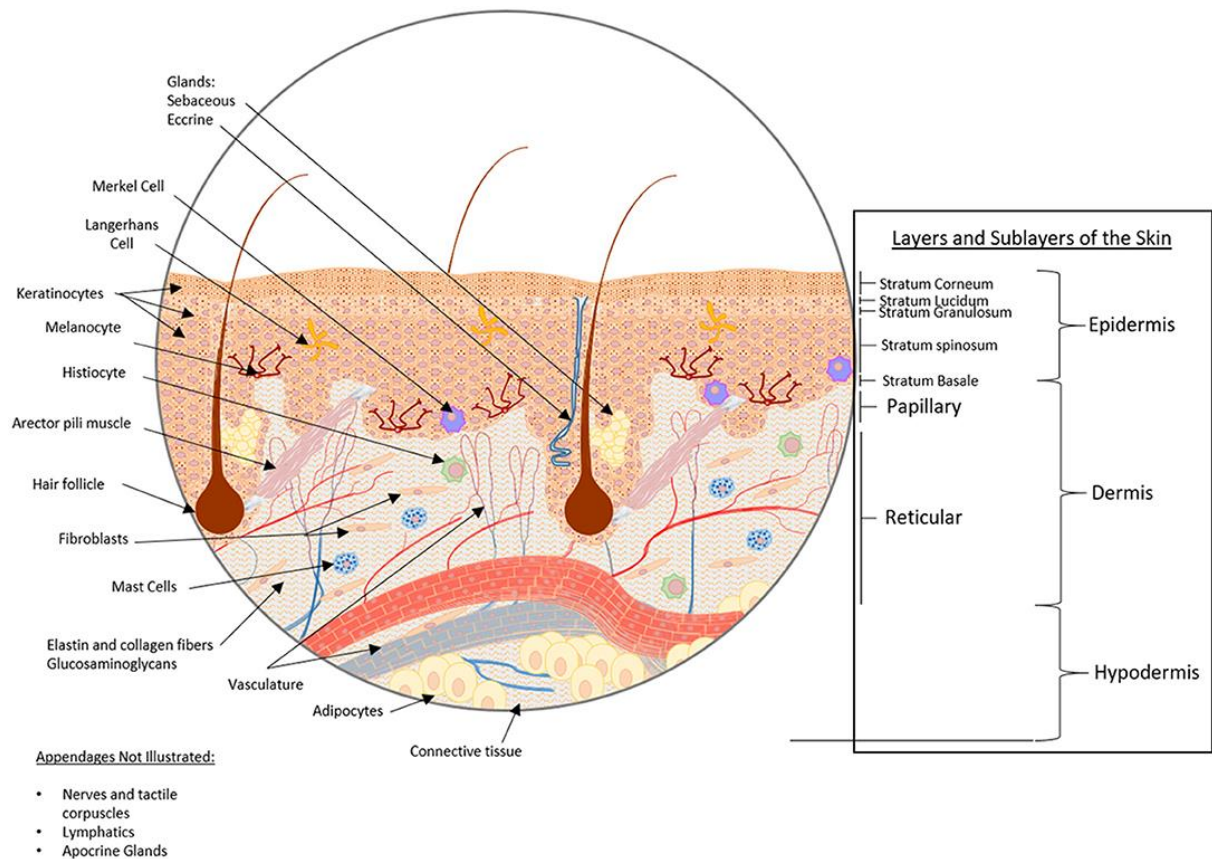


Figure 2: Morphology of the epidermis (Randall et al., 2018)

Primary human keratinocytes using for routine monitoring of inflammation and itch seems to be difficult. Firstly, primary human keratinocytes have a short live span in vitro and once differentiated they rapidly undergo senescence and apoptosis. Primary keratinocytes are very sensitive and require additional nutrients in growth media. So, a long-term investigation of proliferation and differentiation of human keratinocytes with constant data is difficult. Secondly, donor-to-donor variability through growth characteristics and in vitro responses, different plating density and a short lifetime in vitro complicates the interpretation of data. Also changes in proliferation and differentiation characteristics with increasing number of passages from different donors impede consistent interpretation (Ip and Wong 2012; Anderson et al., 2018). Therefore, the spontaneously immortalized human keratinocyte cell line HaCat from adult skin is an often-used model to minimize problems with primary cell culture (Wilson 2013). HaCat cells are nontumorigenic and are adapted to long-term growth without supplemented factors. Also, upon stimulation HaCat cells can differentiate and express specific markers of differentiation comparable with primary keratinocytes (Colombo et al., 2017).

Dermis

The dermis with 1-3mm thickness joins the epidermis and exhibits a lower cell density compared to the epidermis (de-Souza et al., 2019). The dermis contains primarily of extracellular matrix (ECM), consisting predominantly of different collagen and elastin fibers. Mainly 75% of the dermis consisting of collagen type I and III and build along with glycoproteins and proteoglycans the dermal network. Fibroblasts represent the main cell type and are responsible for the synthesis of the ECM material like the collagen and elastin fibers (Nguyen and Soulika 2019). Together building a connective tissue with functions like skin elasticity and resistance. Besides, the dermis provides blood vessels, hair follicles, sensory nerve endings, different type of glands and macrophages, mast cells and adipocytes. Macrophages be part of inflammatory cells and are therefore involved in the inflammatory response, wound healing and remodeling of the collagen fibers (Shin et al., 2019). THP1 cells which are of a monocyte lineage, are often-used as an analogous model to immune cells of the skin. Different studies revealed that THP1 cells suggest a useful examination to inflammation response (Schroecksnadel et al., 2011; Chanput et al., 2010). THP1 cells convince with less mature state compared to other immune like cells. THP1 cells are differentiated with phorbol-12-myristate-13-acetate (PMA) resulting in adherent non proliferating cells with properties of mature macrophages (Richter et al., 2016) which were used by default in our laboratory. Adipocytes in the dermis mainly contribute for energy storage and thermal protection but are also known for wound healing. Dendritic cells are involved in

immunological tasks like the regulation and initiation of inflammation, tissue remodeling and also wound healing (Driskell et al., 2014).

Subcutis

Also known as subcutis, the subcutaneous layer is the innermost layer and consists of adipocytes, fibroblasts, and macrophages. Primary function ascribed to this thickest skin layer is fat storage, providing energy and thermoregulation, hormone production, and attachment support for the upper layers (Rodrigues et al., 2019).

Furthermore, the skin layers are seamless connected through blood vessel and sensory nerves. Through communication between each cell layer different signaling of stimulation or inhibition takes place. Stimuli like environmental influences or dermal signals from blood vessels lead to different cell signaling pathways and further to different cell activities like inflammation and itching (Nguyen and Soulika 2019). This study investigates inhibited cytokines and signaling pathways related to inflammation and itch which were activated in keratinocytes mediated by drug treatment.

4.2 Inflammation and Itch in skin

Inflammation is a response by the immune system to stimuli like pathogens, irritants and toxic compounds (Chen et al., 2018). Itching is “the fact of having or producing an uncomfortable feeling on the skin that makes you want to rub it with your nails” (Han and Dong 2014). Inflammation and itch in skin tissue can be triggered by different intrinsic and extrinsic causes such as insect bites, allergies, and eczemas (Chung et al., 2020). An increased release of different pro-inflammatory cytokines is accompanied by itch and inflammation in skin cells (Erickson et al., 2021). Often used treatments are glucocorticoids but in long term treatment these often have side effects such as skin atrophy fragility and have unconvincing specificity which lead to increased research for alternative specific medications (Alan and Alan 2018).

Inflammation

Inflammation is a response from the immune system to extrinsic and intrinsic stimuli like pathogens, irradiation and damaged cells (Chen et al., 2018). Inflammation is a following defense mechanism to remove the stimuli and to initiate wound healing (Figure 3) (Ansar and Ghosh 2016). Uncontrolled acute inflammation can become chronic and may lead to a variation of inflammatory diseases. Symptoms that are associated with inflammation in tissue are swollen, pain, heated, and red tissue accompanied by a loss of tissue function which were identified by Celsus in 47 AD (Ansar and Ghosh 2016; Köckerling et al., 2013).

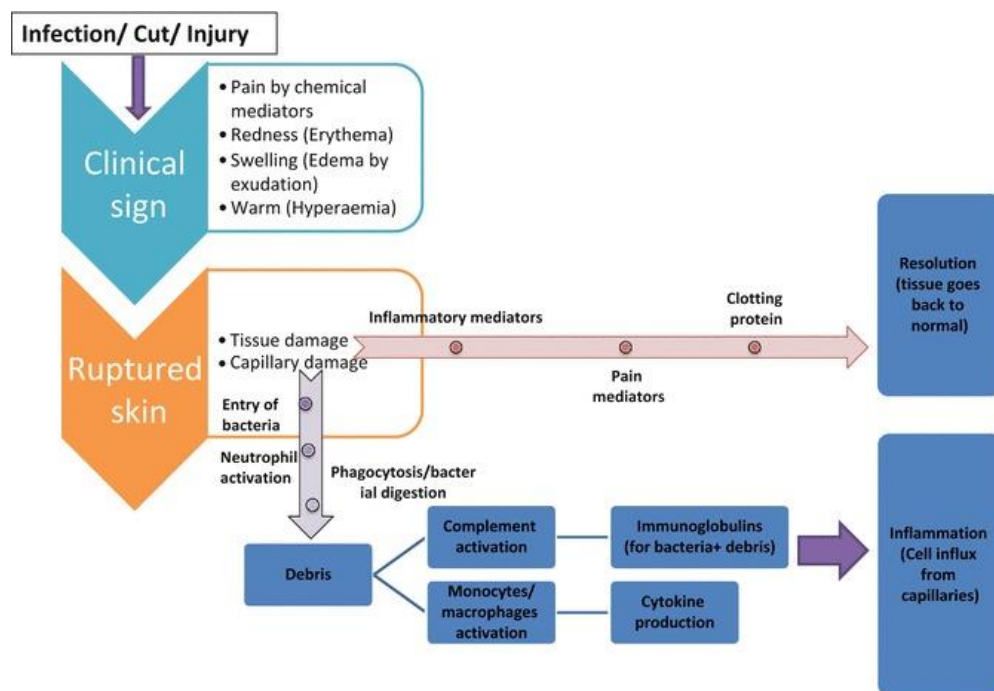


Figure 3: Symptoms and mediators in inflammation (Ansar and Ghosh 2016)

A common cause for inflammation is an allergic irritation reaction and penetration of pathogens like bacteria, virus or fungi triggered through a broken skin barrier in the epidermis (Pasparakis et al., 2014). These pathogenic microbial structures are known as pathogen-associated molecular patterns (PAMPs) activate germline-encoded pattern-recognition receptors (PRRs) in non-immune and immune cells. Damage-associated molecular patterns (DAMPs) can also be recognized and activated by PRRs and can initiate anti-inflammatory responses. PRRs include well studied Toll-like receptors (TLRs) which activate internal signaling pathways with triggering transcription factors (TF) such as activator protein-1 (AP-1) and nuclear factor kappa-B (NF κ B) (Chen et al., 2018).

Inflammatory signaling pathways are stimulated by inflammatory trigger and then activate the secretion of cytokines such as Interleukin-6 (IL-6), Interleukin-8 (IL-8), Interleukin-1 β (IL-1 β) or

CC-Chemokine-Ligand-2 (CCL2). Through receptor activation with secreted cytokines signaling pathways like mitogen-activated protein kinase (MAPK), Nuclear Factor κ B (NF κ B), Protein kinase B (Akt), and Janus kinase (JAK)-Signal Transducers and Activators of Transcription (STAT) are stimulated and activate immune response cascade (Chen et al., 2018; Ansar and Ghosh 2016; Pasparakis et al., 2014) (Figure 4).

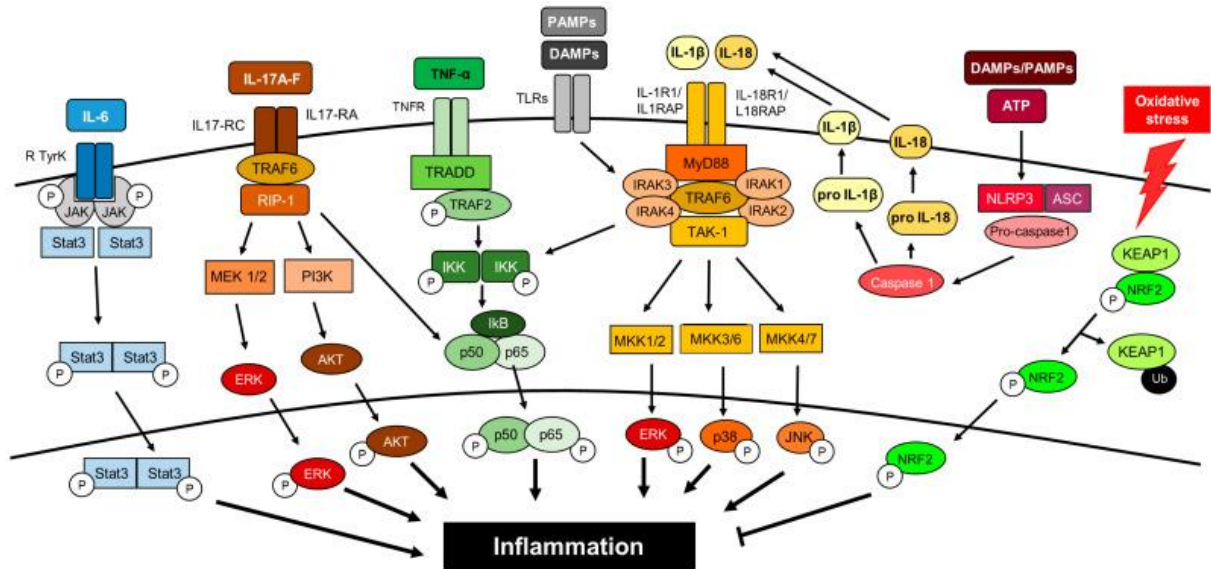


Figure 4: Schematic overview of pro-inflammatory signaling pathways (Rayego-Mateos et al., 2020)

NF κ B pathway plays a crucial role in pro-inflammatory cytokine production, cell recruitment, immune response and apoptotic processes. MAPK signaling pathway includes p38 MAP Kinase, extracellular signal-regulated kinase (ERK1/2) and Jun N-terminal Kinase (JNK) and activated by mitogens, cellular stress and inflammatory cytokines (Kim and Chio 2010) (Figure 4). Phosphorylation of MAPKs leads to activation of transcription factors and mediating inflammatory response (Sabio and David 2014; Rayego-Mateos et al., 2020). Activation of JAK/STAT signaling through growth factors or cytokines translate the stimulation in inflammatory response and secretion of more cytokines (Hu et al., 2021). Imbalance of signaling pathways NF κ B, JAK/STAT or MAPK activity is related to inflammation, metabolic diseases or cancer. Activation of transcription factors regulate expression of inflammatory genes and secretion of cytokines as immune response (Pearson et al., 2001; Raingeaud et al., 1996).

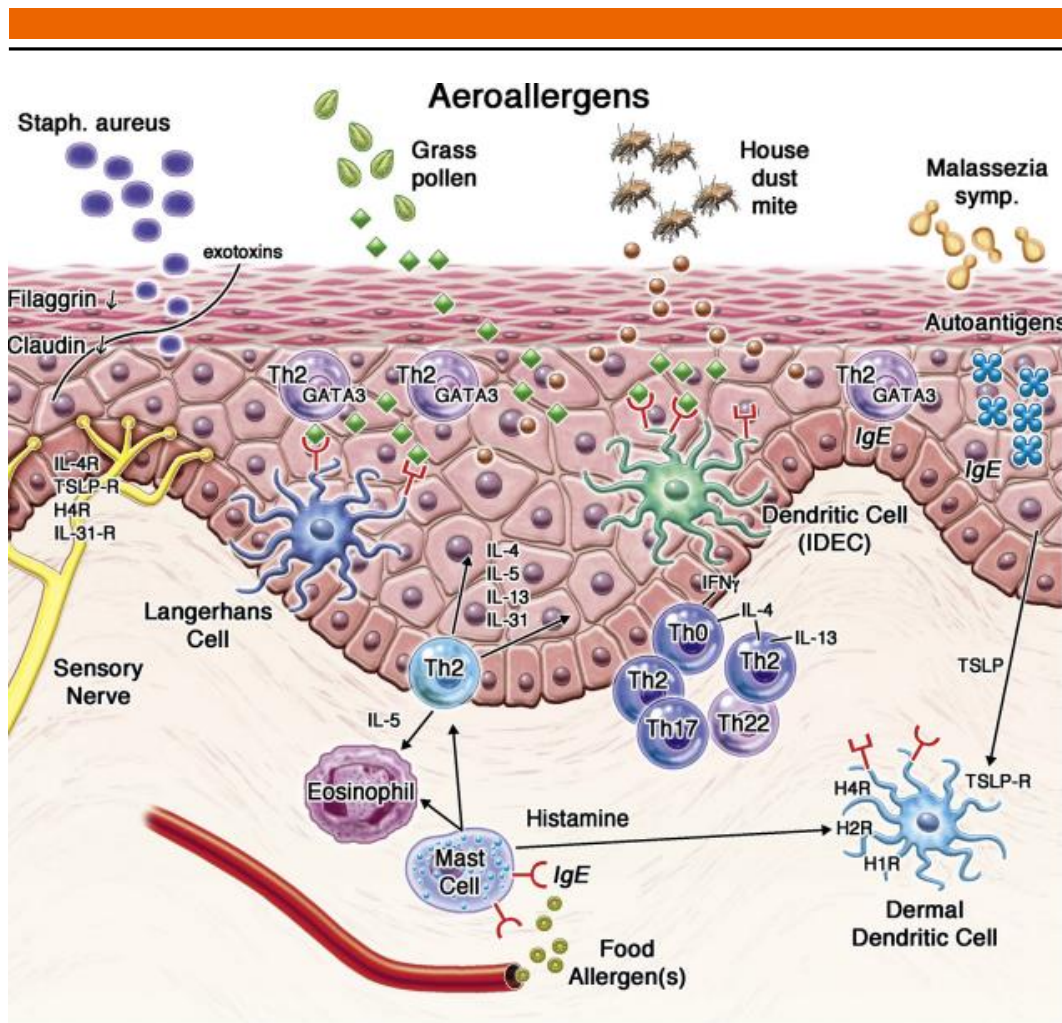


Figure 5: Causes of pro-inflammatory response (Werfel et al., 2016)

Concentration level of secreted pro-inflammatory cytokines are used to monitor inflammation in cells. Cytokines like CCL20 or IL-18 are secreted primarily from immune cells like macrophages and monocytes but also from cells like keratinocytes (Jenkins et al., 2011). These cytokines modulate the immune response and regulate further inflammatory cascades via signaling pathways (Hendrayani et al., 2016). Epithelial and endothelial cells like skin keratinocytes secrete mediators that trigger inflammatory signaling pathway with cytokines to recruit immune cells to the site of inflammation in the tissue (Henriquez-Olguin et al., 2015). Immune cells like monocytes and macrophages regulate immune response to tissue damage and injury by releasing more pro-inflammatory mediators like cytokines (Rayego-Mateos et al., 2020). Increasing levels of pro-inflammatory cytokines and recruited immune cells damage the tissue and build a negative inflammatory loop with more inflammation and more cytokine release (Pasparakis et al., 2014).

Itch

Itch, or pruritus, is a sensory disease that is characterized by an urge to scratch (Figure 6). It can be induced by inflammatory skin diseases or by systemic and neuropathic stimuli. The objective

scratch reflex is to remove the noxious stimulus but can also cause further skin damage with disrupting the skin barrier (Tivoli and Rubenstein 2009). Itching is a complex process including various pruritogenic substances and receptors can be subdivided into several different types induced by different mediators like histamine, proteases or peptides (Song et al., 2018).

Mast cells, basophils and keratinocytes release histamine after activation by immune and nonimmune mediators. The Histamine 1 (H1) and H4 receptors belong to the G-protein coupled receptors and triggers the activation of transient receptor potential vanilloid 1 (TRPV1) via the phospholipase system and increased Calcium (Ca^{2+}) concentration in the cell. The resulting release of neuropeptides such as substance P (SP) causes neurogenic inflammation (Kim and Yosipovitch 2020; Song et al., 2018).

Chronic itch is stimulated via the nonhistaminergic pathway stimulated which is activated by pruritogens such as cytokines, chemokines, peptides and proteases (Tivoli and Rubenstein 2009; Yosipovitch et al., 2018). SP is a neuropeptide released after inflammatory stimulation from sensory nerve endings and binds to the neurokinin 1 receptor (NK1R) (Tivoli and Rubenstein 2009; Song et al., 2018; Kim and Yosipovitch 2020). Various receptors are involved in this pathway and uses the phospholipase or kinase system to activate TRPV1 or TRPA1, which are both cation channels on the membrane of cells. The mechanisms of the sensitization of both ion channels are poorly understood (Luo et al., 2015; Bell et al., 2004).

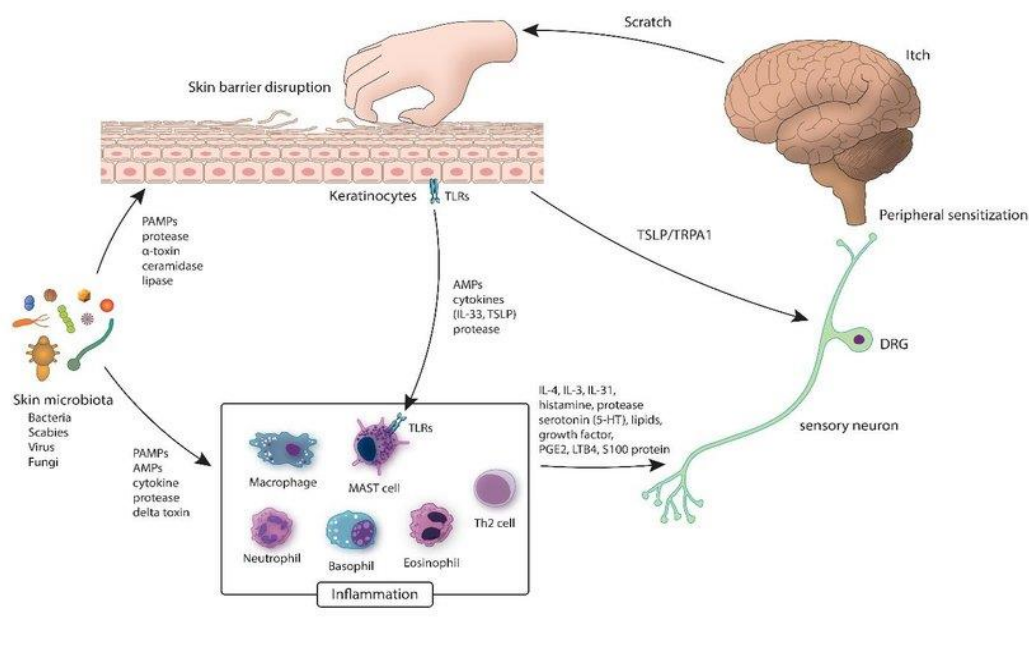


Figure 6: Itch cycle (Kim and Yosipovitch 2020)

Previous research has focused on cytokines, proteases, various receptors, SP, NK1R and mas-related G protein-coupled receptors. There is still more research to be done to fully understand the targets and involved pathways.

This secretion can be inhibited or mitigated by new chemical entities due to specific target binding (Soeberdt et al., 2020).

4.3 Targets

Inflammation and itch in skin processes consist of a complex network of targets and activated signaling pathways (Wong et al., 2017). Two targets in context of inflammation and itch are selected to identify potential therapy for itch. Small molecules in this study were pre-selected on structural binding characteristics to the related target. Due to their molecular weight and polarity these small molecules have promising treatment possibilities in topical applications (Gurevich and Gurevich 2014).

11 β HSD1 as molecular inflammation target

Glucocorticoids are important in different physiological functions like regulation of metabolism, blood pressure, stress, and immunological response in every specie. Glucocorticoids are a class of steroid hormones which affect cells by binding to the glucocorticoid receptor for further genomic effect (Timmermans et al., 2019). The activated complex upregulates or represses target gene expression for anti-inflammatory or pro-inflammatory proteins. The function of the activated glucocorticoid-receptor complex varies from upregulating anti-inflammatory proteins to downregulating pro-inflammatory proteins in the cytoplasm (Gustafsson 2016). An important human glucocorticoid is Cortisol, for regulation and supporting of a variety of central metabolic, cardiovascular, and homeostatic functions. The human skin is able to synthesize glucocorticoids through the steroidogenic pathway (Slominski and Manna 2017).

The release of Cortisol is regulated from the Hypothalamic-pituitary-adrenal axis (HDA). Through stimulation of the HDA-axis with stress, cortisol-releasing factor (CRF) is secreted and activates adrenocorticotrophic hormone (ACTH). ACTH promotes the release from Cortisol. Therefore, cortisol itself prevents further pro-inflammatory release by inhibiting CRH to activate ACTH (Spiga et al., 2011) (Figure 7).

Studies revealed high concentration of cortisone conversion in liver, placenta, and kidney but also in skin a conversion takes place (Kim et al., 2021; Lee et al., 2020). Therefore, in skin it has been detected in keratinocytes and fibroblasts and also in the outer root sheath of hair follicles (Terao et al., 2011). But the reduction and oxidation of cortisone or cortisol varies. Responsible for this

are two different enzymatic isoforms. For reduction a predominantly nicotinamide adenine dinucleotide (NAD) phosphate (NADPH) dependent type 1 and for oxidation a NAD dependent type 2 isozyme. The function of 11 β -hydroxy steroid dehydrogenase (HSD) type 2 is mainly to convert the glucocorticoid cortisol in its inactive form cortisone tissue specifically (Wyrwoll et al., 2011).

The dimeric enzyme 11 β HSD type 1 is a NADPH dependent dehydrogenase and activated through oxidation from cortisone to cortisol and acts primarily as an oxidoreductase (Rajan et al., 1996). However, 11 β HSD1 is an enzyme that catalyzes the conversion of the inactive form of cortisone to active cortisol and controls its local concentration (Chapman et al., 2013). The directionality of the enzyme 11 β HSD1 is dependent on the locality within the lumen of the ER. There, 11 β HSD1 colocalized with H6PDH, which is responsible for generating NADPH and permits the conversion of cortisone to cortisol (Dzyakanchuk et al., 2009).

Glucocorticoids have a wide spectrum of anti-inflammatory effects on cells of the immune system (Coutinho and Chapman 2011). They influence multiple signaling pathways including NF κ B and MAPK. 11 β HSD1 expression is upregulated by tumor necrosis factor α (TNF- α), UV-B exposure or interleukins like Il-1 β (Itoi et al., 2013). This mainly cytokine dependent upregulation lead to increasing expression of glucocorticoid regulating genes like IL-6 (Lee et al., 2020). Importantly, glucocorticoids act synergistically with pro-inflammatory cytokines to increase the expression of 11 β HSD1 (Lannan et al., 2012). 11 β HSD1 is researched in context of diabetes and obesity but is not sufficient investigated in context of skin (Morton and Seckl 2008; Kim et al., 2021).

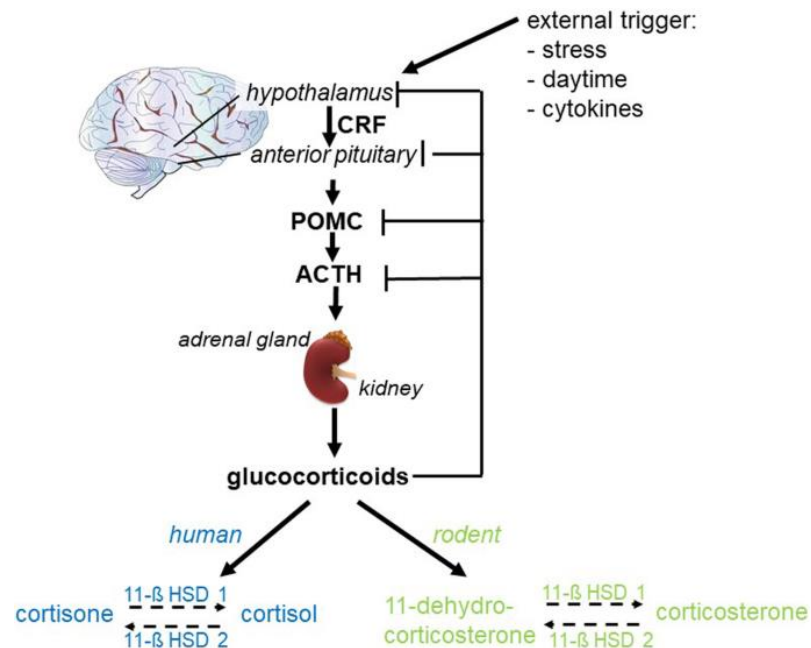


Figure 7: Activation of 11 β HSD1.

External trigger activate releasing of CRF and further secreting ACTH. This cascade activates production for corticosteroids in adrenal glands. (Wepler et al., 2020)

Thinning and disruption of the skin barrier promoting a skin inflammation and the expression of active glucocorticoids increases. However, excess glucocorticoids produce skin cell damage and lead to activation of surrounding immune cells and further pro-inflammatory signaling pathways with cytokine release (Oikarinen and Autio 1996; Niculet et al., 2020).

Synthetic glucocorticoids are widely used to treat mainly topical acute and chronic inflammation in skin to suppress inflammatory effects on keratinocytes and reduce the infiltration of inflammatory cells. INCB-13739 is a 11 β HSD1 specific inhibitor applied as supporting oral treatment in diabetes and obesity to control glucose concentration. (Gregory et al., 2020). Also, inhibitor PF-915275 was selected as potent systemic inhibitor with literature known pharmacokinetic properties (Siu et al., 2009).

Research is focusing on pre-receptor regulation of glucocorticoids by 11 β HSD1. Several dedicated efforts finding a selective 11 β HSD1 inhibitor as topical alternative for glucocorticoid treatment were reported. Further, different structural classes were profiled for inhibitory activity against 11 β HSD1 in intact cells and skin samples (Gathercole et al., 2013). Due to their properties in solubility, molecular weight and target affinity small molecules have efficient characteristics for treatment (Li & Kang 2020). For topical application the properties of the small molecules in molecular weight and lipophilic character are crucial for skin barrier penetration (Bos & Meinardi 2000). Topical application allows new chemical entities (NCEs) to penetrate the skin barrier and reduce biomarkers of skin inflammation and itch directly in affected tissue (Boudon et al., 2017).

NK1R as molecular itch target

The Neurokinin 1 receptor (NK1R) is a seven-transmembrane spanning G-protein coupled receptor encoded by the tachykinin receptor 1 (TACR1) gene (Schofield et al., 1990, Vasiliou et al., 2007). The receptor is found in the muscular wall of submucosal blood vessels, in epidermal keratinocytes and dermal fibroblasts (Liu et al., 2006). NK1R is involved in different physiological processes including pain and itch transmission (Pederson-Bjergaard et al., 1989), inflammation (McGillis et al., 1987), proliferation (Nilsson et al., 1985), and neurotransmitter release (Franck et al., 1989). SP is a well characterized neuropeptide and acts as agonist with high affinity and selectivity for NK1R (Eistetter et al., 1992). SP is a member of the tachykinin peptide family and distributed in the central and peripheral nervous system. SP belongs to the sensory neurotransmitter and neuromodulator in nociceptive pain pathways and regulates pathophysiological processes like pain, muscle contraction and intestinal secretion (Luger et al., 2002; O'Sullivan et al., 1998) (Figure 8). Further SP acts as inflammatory factor and is involved in itch signaling. SP is released from primary sensory nerve endings in the dermis into the surrounding tissue (Liu et al., 2006). The release of agonist SP from peripheral ends of neurons

play a major role in neurogenic inflammatory responses (Douglas and Leeman 2011). Research over the last decades linked the NK1R-SP system to different pathophysiological processes like skin inflammation, pruritus and immune responses (Agelopoulos et al., 2019). After SP binding on docking site of NK1R the activated receptor induces an activation of phospholipase C. This further activates the production of inositol triphosphate (IP3) resulting in elevation of intracellular calcium concentration as second messenger and phosphorylation of protein kinase c (PKC) (Douglas and Leeman 2011). Phosphorylated PKC activates MAPK including p38 and ERK1/2 and further activating NFκB (Jin et al., 2021). This process proceeds in different cell systems and is furthermore involved in proliferation, pain transmission and neuroimmune modulation (Douglas and Leeman 2011).

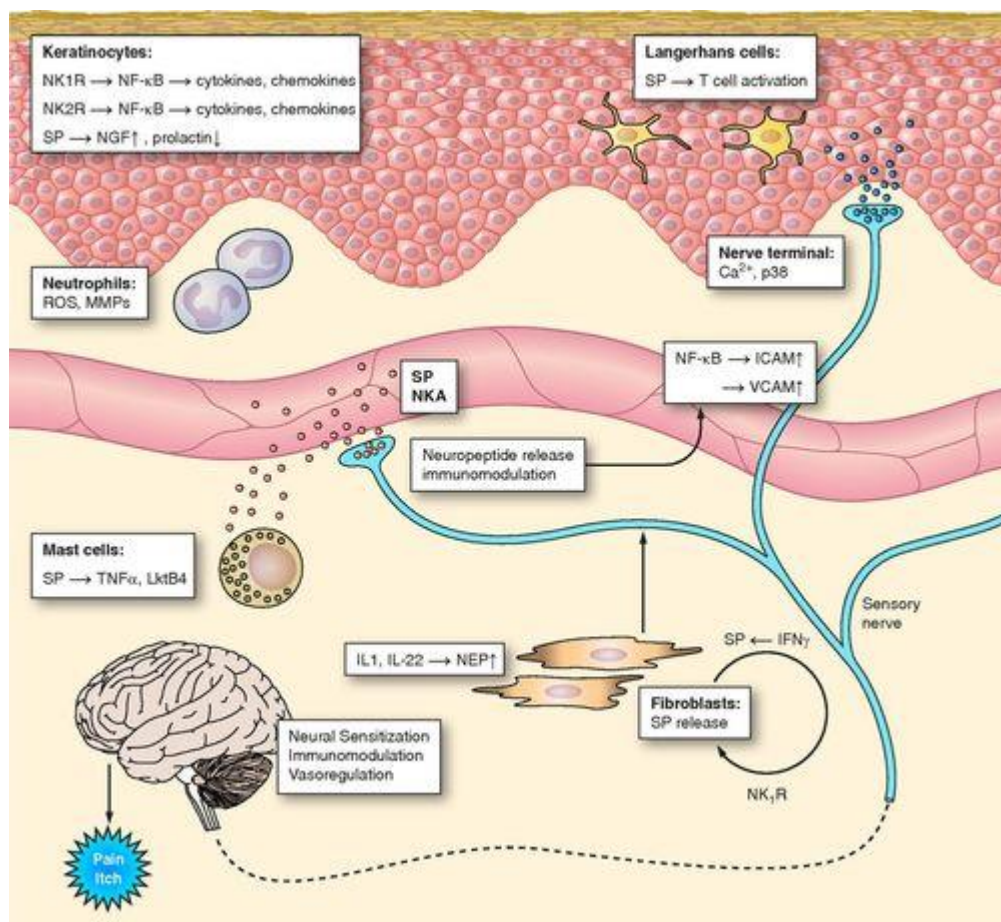


Figure 8: Function of NK1R in skin
 SP is released from peripheral primary sensory nerve endings in the skin. Binding on NK1R on keratinocytes activates signaling cascade and promotes pro-inflammatory cytokine and chemokine release which animates the immune response (Steinhoff et al., 2014).

Presence of SP promotes skin inflammation by enhancing the expression of neuronal growth factor (NGF) in keratinocytes and inducing the secretion of pro-inflammatory cytokines (Ständer and Luger 2015). Itch signaling is transmitted by sensory nerve fibers to the spinal cord where the synapses are connected with second order neurons. Therefore, itch activates numerous areas of the brain. Compared to nonpruritic skin, NK1R and release of SP are overexpressed and in elevated concentration in pruritic skin (Ständer and Yosipovitch 2019). Several NK1R antagonists are studied and have been investigated in a potential itch treatment. Aprepitant, an approved oral high affinity antagonist for NK1R, showed promising results in blocking nausea and vomiting after chemotherapy to NK1R in affected regions of the brain (Jin et al., 2021). Also, antagonist Fosaprepitant, a pro-drug of Aprepitant and Serlopitant showed results to cross the blood brain barrier (Frenkl et al., 2010). A small in vivo study showed reduced itch after treatment with Aprepitant or Serlopitant (Jin et al., 2021). Further in vivo studies have to be investigated to see significant results.

4.4 Skin diseases with the involvement of 11 β HSD1 and NK1R

NK1R belongs to GPCR family with investigated overexpression in inflammation site and promoting itch (McGillis et al., 1987). 11 β HSD1 is an enzyme with elevated activity and increased cortisone to cortisol conversion in context of inflammation (Chapman et al., 2013). Both these targets are relevant in context of multiple skin diseases like epidermolysis bullosa, atopic dermatitis or psoriasis. Due to inflammatory caused chronic condition, gene mutations or unknown causes, no effective treatment is developed yet for these three skin diseases and thus only symptomatic treatment as oral or systemic application is in clinical routine (Bieber et al., 2022; Prodingler et al., 2019; Balato et al., 2009). Epidermolysis bullosa (EB) is triggered by different mutations in keratinocyte specific keratin genes and intermediate filaments and are characterized by skin blistering and muscle dystrophy. EB is a skin disease with multiorgan involvement leading to a high lethality and morbidity (Bardhan et al., 2020). There are three different subtypes of EB and are distinguished by different mutations in the epidermis, dermis or the basement membrane zone (Sawamura et al., 2010). Analysis showed increased expression of IL-6 and IL-1 β in biopsies of EB affected skin beside elevated infiltration of immune cells triggering pro-inflammatory cytokine release and activation of transcription factors (Lu et al., 2007). Additionally, the most common symptom beside inflammation in EB is pruritus/itch (Kumar et al., 2016; Davila-Seijo et al., 2013). In recent studies treatment options for EB are investigated to treat symptomatic inflammation and itch to increase quality of life (Rognoni et al., 2016). Molecules like Rolipram or Apremilast are PDE4 antagonists to inhibit reduction of cAMP to AMP. Elevated cAMP level lead to a decreased expression of pro-inflammatory cytokines and

reduce itch (Koga et al., 2016). Further NK1R as cell surface receptor is focused for decreasing inflammation and itch in EB affected patients. Oral or topical treatment with Aprepitant and Serlopitant as NK1R antagonists showed antipruritic and decreased inflammation response (Chiou et al., 2020).

Related to the most common chronic inflammatory skin diseases atopic dermatitis (AD) belongs to atopic disorders involving allergic conditions (Tamagawa-Mineoka and Katoh 2020). Skin barrier dysfunction and impaired function of intercellular lipids of the SC are responsible for AD (Kim et al., 2019). Scratching of affected skin lesions further resulting in damaged skin barrier. A broken skin barrier result in penetration of pathogens, allergens and other pro-inflammatory stimuli (Egawa and Kabashima 2016). Interleukins which are released from activated keratinocytes through exposure to tissue damage, induce further immune reaction and secretion of cytokines (Hussein et al., 2014). Therapeutic approaches are topical treatment with glucocorticoids, calcineurin inhibitors or PDE4 inhibitor (Katoh et al., 2019). Studies with small molecules show therefore promising results for alternative treatment (Welsh et al., 2021).

Psoriasis is a chronic inflammatory skin disease with various subtypes. Uncontrolled keratinocyte proliferation and impaired differentiation leads to inflammation in Psoriasis (Rendon and Schäkel 2019). Triggered keratinocytes release pro-inflammatory cytokines and activate immune cells for further secretion of cytokines (Morizane et al., 2012). Itch signaling is transmitted by neurons and further initialize scratching and a broken skin barrier (Kim et al., 2017). Elevated cytokine concentration, released by keratinocytes, fibroblasts and immune cells in the skin damages skin tissue (Hänel et al., 2013). Long term therapy in psoriasis includes topical treatment with mainly glucocorticoids which can also lead to skin atrophy (Raharja et al., 2021). Further anti-itch treatments like Aprepitant as NK1R antagonist (Alam et al., 2021) or Apremilast as PDE4 inhibitor are used (Milakovic and Gooderham 2021). New therapies with small molecules are investigated as promising treatment (Torres and Filipe 2015).

Introduced skin diseases are related to inflammation and itch with overlapping target portfolio. Presented NK1-receptor plays a crucial role in itch and inflammation transmission and is targeted in multiple studies in context of skin diseases (Wercberger et al., 2021). 11 β HSD1 as cortisone converter plays also a crucial role in signal transduction of pro-inflammatory pathways (Itoi et al., 2013). Mechanisms of skin diseases are not fully understood, and an appropriate medication is not satisfactory for affected patients. Small molecules showed promising effects in recent studies and are investigated for reducing pro-inflammatory biomarkers (Hanke et al., 2016).

5 Materials & Methods

5.1 Materials

5.1.1 Reagents

TNF- α (Sigma, USA, #H8916/R&D Systems, USA, #10291),

INCB-13739 (ABCR, Germany, #350116)

PF-915275 (Sigma, USA, #PZ0400)

Aprepitant (Sigma, USA, #1041904) and

Forsaprepitant (Sigma, USA, #SML2228) were used for cell culture treatment.

The NCE candidates were selected for further experiments based on High throughput screening (HTS) campaigns (data not shown).

FPCM:[1-(4-Fluoro-phenyl)-cyclopropyl]-[3-(2-methyl-1H-pyrrolo[2,3-b]pyridin-3-yl)-pyrrolidin-1-yl]-methanone

TPCA: (S)-3-Trifluoromethyl-piperidine-1-carboxylic acid (5-hydroxy-adamantan-2-yl)-amide

DPAAM: 3,3-Dimethyl-pentanedioic acid adamantan-2-ylamide methylamide

MAPA:4-Methyl-2-[4-((S)-3-methyl-2-((S)-2-[2-(4-nitro-phenyl)-acetylamino]-3-phenyl-propionylamino)-butyryl)-2-oxo-piperazin-1-yl]-pentanoic acid ((S)-1-carbamoyl-3-methylsulfanyl-propyl)-amide

OPMA:5-Oxo-pyrrolidine-2-carboxylic acid {1-[1-({1-[1-(1-carbamoyl-3-methylsulfanyl-propylcarbamoyl)-3-methyl-butylcarbamoyl]-methyl}-carbamoyl)-2-methyl-propylcarbamoyl]-2-phenyl-ethyl}-amide

5.2 Methods

5.2.1 Cell culture

The HaCat Cell Line was cultured in DMEM (Thermo Fisher Scientific, USA, # 11500416) media with 10% FCS (Biochrom, Germany, #S0410). Primary keratinocytes were cultured with EpiLife Media (Thermo Scientific, USA, #MEPI500CA) and supplement HKGS (Thermo Scientific, USA, #S0015). THP1 cells were cultured with RPMI 1640 (ATTC modification; Gibco™, Thermo Fisher Scientific, USA, #11530586) media, 10% FCS and 0.05 mM 2-mercaptoethanol (Gibco™, Thermo Fisher Scientific, USA, #11528926). THP-1 cells were treated with 0.02 μ M PMA (Sigma, USA, #P8139) diluted in adjusted RPMI 1640 medium for 48 hours under standard cell culture conditions to induce macrophage differentiation making them adherent.

All cells were cultured at 37°C and 5% CO₂. For each condition the cells were harvested, homogenized and lysed in Cell Lytic M buffer (Sigma, USA, # C2978) and protease/phosphatase inhibitors (Roche, Switzerland, #4906837001/#11836153001) for Western Blot analysis.

5.2.2 Cell treatment

HaCat cells were treated with TNF- α with or without particular inhibitor in cell culture media. Primary keratinocytes were treated with TNF- α with or without an inhibitor in cell culture media. Different concentration and timepoints were estimated to stimulate the immune response.

5.2.3 ATP Quantification

The Cytotoxic effect of substances on cells were monitored using the ATPlite™ 1step Luminescence Assay System (PerkinElmer, USA, # 6016731) according to manufacturer's protocol. Briefly, cells were cultured in 96-well plates at 37°C and 5 % CO₂. After treatment with substances 100 μ L/well culture medium were removed and refilled with 100 μ L/well reconstituted reaction reagent (provided in the kit). Plates were subsequently shaken for 5 minutes at 700 rpm at room temperature, protected from light, using an orbital microplate shaker. Luminescence was detected using a Spark® 20M multiplate reader (TECAN, Switzerland). Untreated cells served as negative control. Cells treated with 7.5% Tween80 (G Biosciences, USA, #786-520) as positive control.

5.2.4 Interleukin 8 Quantification

For measuring natural and recombinant human Interleukin 8 were observed with the Human IL-8/CXCL8 Duo Set ELISA (R&D Systems, USA, #DY208-05) according to manufacturer's protocol. Before starting the ELISA, the microplate is coated with the capture antibody overnight at room temperature. After washing and blocking the microplate for 1h the samples and standards were added and incubated for 2h. Repeated washing steps between each stage and incubation with detection antibody for 2h and Streptavidin HRP for 20min. Finally, incubating substrate solution for 20min and stopping the reaction with stop solution before the determination at 450nm and 540nm as correction wavelength.

5.2.5 Interleukin 6 Quantification

To detect and quantify the level of human Interleukin 6 a Human Il-6 ELISA (Thermo Fisher Scientific, USA, #KHC0061C) was performed as described in the manufacturer's protocol. Therefore, samples and standards were added to the appropriate wells of the microplate with human Il-6 Biotin conjugate solution and incubated for 2h. Between each step a washing step was accomplished and afterwards a streptavidin HRP solution was added to the wells and incubated for 30min. After adding stabilized chromogen for 30min the stop solution was added and the absorbance at 450nm was detected.

5.2.6 CCL2/MCP-1 Quantification

To quantify the chemokine CCL2 a CCL2/MCP-1 Immunoassay (R&D Systems, USA, #DCP00) was performed according to the manufacturer's protocol. Therefore, samples and standards were added to the appropriate wells and incubated for 2h at room temperature. After washing the plate with washing buffer three times the human MCP-1/CCL2 conjugate was added to each well and also incubated at room temperature for 1h. Subsequently, a further washing step and incubation of the substrate solution for 30min in the dark. Afterwards the reaction was stopped with Stop Solution and determination at 450nm and 570nm as correction wavelength.

5.2.7 CCL20/MIP3 Quantification

For measuring natural and recombinant human Macrophage Interleukin Protein 3 (MIP3) observed with the Human CCL20/MIP3 Duo Set ELISA (R&D Systems, USA, #DY360-05) according to manufacturer's protocol. Before starting the ELISA, the microplate has to be coated with the capture antibody overnight at room temperature. After washing and blocking the microplate for 1h the samples and standards were added and incubated for 2h. Repeated washing steps between each stage and incubation with detection antibody for 2h and Streptavidin HRP for 20min. Finally, incubating substrate solution for 20min and stopping the reaction with stop solution before the determination at 450nm and 540nm as correction wavelength.

5.2.8 Interleukin 1 β Quantification

To quantify the Interleukin 1 β a human IL-1 β /IL-F2 Immunoassay (R&D Systems, USA, #DLB50) was performed according to the manufacturer's protocol. Therefore, samples and standards were added to the appropriate wells and incubated for 2h at room temperature. After washing the plate with washing buffer three times the human IL-1 β conjugate was added to each well and also

incubated at room temperature for 1h. Subsequently, a further washing step and incubation of the substrate solution for 20min in the dark. Afterwards the reaction was stopped with Stop Solution and determination at 450nm and 570nm as correction wavelength.

5.2.9 Interleukin 18 Quantification

For measuring natural and recombinant human total Interleukin 18 observed with the Human Total IL-18 Duo Set ELISA (R&D Systems, USA, #DY318-05) according to manufacturer's protocol. Before starting the ELISA, the microplate is coated with the capture antibody overnight at room temperature. After washing and blocking the microplate for 1h the samples and standards were added and incubated for 2h. Repeated washing steps between each stage and incubation with detection antibody for 2h and Streptavidin HRP for 20min. Finally, incubating substrate solution for 20min and stopping the reaction with stop solution before the determination at 450nm and 540nm as correction wavelength.

5.2.10 Caspase 1 Inflammasome Assay

The activity of caspase-1 was measured using the Caspase-Glo® 1 Inflammasome Assay (Promega GmbH, USA, #G9952) following the manufacturer's instructions. Monocytic THP-1 cells were seeded (5.0×10^5 /well) and differentiated with PMA for 48 hours in white 96-well plates. After the incubation, the plates were centrifuged at 1,500 rpm for 3 minutes and the supernatant was discarded. The blocking phase was started subsequently by adding either 100 μ L VX765 (BioVision, USA, #2781) (1 μ M), 100 μ L tested substances (see 6.3), or 100 μ L cell culture medium to the respective well. The setup was incubated at cell culture standards for 1 hour. Subsequently, the centrifugation step was repeated, and the supernatant was discarded. The treatment phase then began thereafter by adding either 100 μ L of cell culture medium to the blank reaction and negative control, or 100 μ L of α -hemolysin (Sigma, USA, #H9395) diluted in medium (2 μ g/mL) to the remaining conditions. The treated cells were incubated at cell culture standards for 3 hours. Meanwhile, the Caspase-Glo® 1 Reagent and the Caspase-Glo® 1 YVAD-CHO Reagent were prepared as described in the manufacturer's instructions and equilibrate to room temperature. After the incubation, the plates were equilibrated to room temperature for 5 minutes. Then, 100 μ L of Caspase-Glo® 1 Reagent were pipetted to half of the wells and 100 μ L of Caspase-Glo® 1 YVAD-CHO Reagent were added to the other half of the wells. The plates were covered and incubated at RT for 90 minutes. The luminescence was measured using a plate reader (Tecan Group, CHE).

5.2.11 Western Blot analysis

The total amount of protein was measured with BCA Assay (Thermo Scientific, USA, #A53225) following manufacturers protocol. Measurements were calculated with a Spark® 20M multiplate reader. To determine proteins of interest Western Blot analysis was used. 20µg of protein from cell lysates were mixed 1:4 with Laemmli buffer (BioRad, USA, #1610710) and were loaded on a 10% Midi Criterion TGX Stain-Free protein gel (BioRad, USA, #5678033) and run at 110 V for 1-1,5h. Afterwards, proteins were blotted onto PVDF membrane (BioRad, USA, #1704157) using the Trans-Blot Turbo Transfer system (BioRad, USA). The program for the high MW uses 2,5A for 10min. The membrane was blocked in 5% milk (Applichem, Darmstadt, Germany, #A0830) in washing buffer (BioRad, USA, #170-6435) for 2h at RT. The membranes were incubated overnight at 4°C with the indicated primary antibody (p44/42 MAPK (ERK 1/2) (#137F5) Rabbit mAb (ERK, 1:3000), Phospho-p44/42 MAPK (ERK 1/2) (Thr202/Tyr204) (#D13.14.4E) XP® Rabbit mAb (pERK, 1:2000), Akt Antibody (Akt, 1:5000), Phospho-Akt (Ser473) (#D9E) XP® Rabbit mAb (pAkt, 1:5000), p38 MAPK Antibody (p38, 1:5000), Phospho-p38 MAPK (Thr180/Tyr182) (#D3F9) XP® Rabbit mAb (pp38, 1:5000), NF-κB p65 (#D14E12) XP® Rabbit mAb (NF-κB, 1:5000), Phospho-NF-κB p65 (Ser536) (#93H1) Rabbit mAb (pNF-κB, 1:5000), Stat3 (#D1B2J) Rabbit mAb (Stat3, 1:5000) and Recombinant Anti-STAT3 (phospho S727) antibody (pStat3, 1:1000), all purchased from Cell Signaling Technology, USA) diluted in 5% milk with washing buffer. The membrane was washed twice with washing buffer before incubation with the secondary antibody (anti-rabbit, 1:2000, Sigma Aldrich, Darmstadt, Germany) diluted in 5% milk in washing buffer for 2h at RT. Unbound antibody was removed by washing twice in washing buffer. The protein bands were visualized by using AceGlow substrate solutions A and B (1:1) (VWR, International GmbH, Germany, #1B1583KIT). The signal was captured with the imaging system Fusion FX (Vilber Lourmat Deutschland GmbH, Germany). The signal intensities were quantified with the Bio-1D software version 15.07. As loading control, α-tubulin (1:2000 Cell Signaling Technology, USA, #11H10) was used. Western Blot pictures were manually edited to bring results in the right order, therefore unequal background intensity should be ignored.

5.2.12 Sample preparation for 2D-LC-MS/MS analysis

To analyze the proteome in treated and untreated cells a sample preparation and a quantitation by mass spectrometry was executed. Cells were harvested and the proteins were extracted, reduced and alkylated according to EasyPrep Mini MS Sample Prep Kit (Thermo Fisher Scientific, USA, #A40006) protocol. The alkylated protein was further digested and cleaned up in different washing steps. To compare multiple samples a TMT labeling was performed according to

TMTsixplex Isobaric Label Reagent Set (Thermo Fisher Scientific, USA, #PIER90066). To desalt the merged peptides the Pierce Peptide Desalting Spin Columns (Thermo Fisher Scientific, USA, #89851) according to the protocol were used. After Speed-Vac centrifugation the dry samples could be stored and further measured in MS.

5.2.13 2D-LC-MS/MS analysis

Mass spectrometry analysis of proteome was performed using a 2D-LC-MS/MS system and a TMTsixplex label quantification. Each condition was examined in three biological replicates. First the samples were separated sequentially using multidimensional chromatographic techniques. Analysis was performed using a TIMS-TOF mass spectrometer (Thermo Fisher Scientific, USA).

5.2.14 Gene set enrichment analysis

Gene set enrichment analysis was performed using g:Profiler (version e106_eg53_p16_65fcd97), Gene Ontology Biological Processes (GO:BP) and Reactome (REAC) databases. Correction was performed using Benjamini-Hochberg FDR multiple testing correction method with a significance threshold set to 0.05. Size of functional category was set between 5 (min) and 350 (max) genes (J. Reimand *et al.*, Nature protocols 2019). Resulting enrichment analysis data were exported in Cytoscape (version 3.7.2) and visualized using the EnrichmentMap application with a node cutoff Q-value of 0.04 and an edge cutoff (similarity) of 0.5.

5.2.15 In-silico molecular docking

The crystallized ligands of proteins from the Protein Data Bank (PDB) with $\geq 90\%$ sequence identity to 11-beta-dehydrogenase isozyme 1 were compared with molecules FPCM, TPCA and DPAAM. Compound similarity was calculated using the FragFp descriptor in the software DataWarrior (v5.5.0) (Sander and Freyss 2015). Ligand 8KD from crystal structure PDB 5PGZ (Ye *et al.*, 2017), was the most similar ligand to two of the hit compounds, TPCA and DPAAM, with 66% and 64% similarity respectively

Chains A and B of PDB 5PGX were used for the docking model, with the docking site centered on the A chain 8KD ligand. The NADP co-factor was retained in the active site. The Protein Preparation Wizard tool in the Schrödinger Maestro (v12.7) interface was used to prepare the model for docking. The Schrödinger Glide (v9.0) (Friesner *et al.*, 2006; Halgren *et al.*, 2004; Friesner *et al.*, 2004) grid was calculated using the OPLS 2005 forcefield (Jorgensen *et al.*, 1988). The compounds FPCM, TPCA and DPAAM were docked with XP precision.

The peptide-like hits MAPA and OPMA were manually modelled in the NK1R receptor site using the Chemical Computing Group software, Molecular Operating Environment (MOE, v2020.0901) (Molecular Operating Environment (MOE), 2020). The hits were modelled by modifying the SP ligand from model 1, chain A for each of the NMR structures 2ks9.pdb, 2ksa.pdb, and 2ksb.pdb (Gayen et al., 2011). Partial charges from the Amber10:EHT forcefield (Case et al., 2008) were applied to each system and the modeled hits were minimized with the receptor frozen and the ligand coordinates tethered.

5.2.16 Fluorescence Imaging Plate Reader (FLIPR) Assay

To determine transporter functionality a calcium flux activity assay (Molecular Devices, USA, # R8185) was performed with CHO-K1 and CHO-K1-NK1R cells. CHO-NK1R cells are stably transfected to overexpress NK1-receptor. Cells were cultured for 24h in 96-well plates under standard cell culture conditions. Afterwards 100µl Loading Buffer with 2,5mM probenecid was added per Well and incubated for 45min in the Incubator in the dark. Subsequently 25µl of HBSS buffer or tested substances (MAPA or OPMA) were added and incubated for additional 10min. After measuring the whole 96-well plate for 5min only the agonist SP with 10µM was added on one strip after another. In each strip was 25µl Agonist added and after another and measured in between for 2 min. The measurement was fluorescent based and detected using a Spark® 20M multiplate reader (TECAN, Switzerland).

5.2.17 Statistical analysis

All experiments were conducted with 6 biological replicates. For Western Blot and proteomic analysis 3 biological replicates were conducted. Statistical analysis was performed using GraphPad Prism 7 (GraphPad Software, USA). One-way ANOVA with $\alpha = 0.05$. Significances (****): $p < 0.0001$, (***): $p < 0.001$, (**): $p < 0.01$, (*): $p < 0.05$, (ns): $p \geq 0.05$. Means \pm SD are shown.

6 Results

For better clarity the tested NCEs were investigated related to their specific target. Therefore, the result part is grouped in investigations of FPCM, TPCA and DPAAM for 11 β HSD1 and MAPA and OPMA for NK1R. The tested NCEs were investigated for their docking ability, their effect on inflammation and itch in context of reducing known pro-inflammatory cytokines and phosphorylation levels of signalling pathways. Validation on primary cells confirmed results. A signal transfer model was evaluated to mimic signal transfer from skin cells to immune like cells to investigate transmission of pathway activation and cytokine secretion.

6.1 Results for 11 β HSD1

6.1.1 Molecular docking indicates target specific binding of three tested compounds

Three drug candidates (NCEs), identified from high throughput screening campaigns (data not shown), were evaluated in silico for their ability to dock into the binding pocket of 11 β HSD1. For this, a putative binding hypothesis was generated via molecular docking simulations in published X-ray structure (RCSB PDB 5PGX) (Figure 9). Comparing the hypothesized binding mode of compound FPCM with crystallized ligand 1EQ in published 11 β HSD1 X-ray structure (PDB 4IJW; Ye et al., 2017), the cyclopropyl-benzene groups align well. The pyrrole-pyridine was predicted to form a hydrogen bond with T124 while the carbonyl group forms a hydrogen bond with S170 (Figure 9A) (Li et al., 2014). The interaction with S170 and Y183 has been found to be one of the key interaction motifs for crystallized BMS inhibitors (e.g., ligand 8KD in PDB 5PGX, Ye et al., 2017). This interaction pattern was also determined for docked compounds DPAAM and TPCA which feature carbonyl groups in favorable positions close to the adamantane structure (Figure 9B+C).

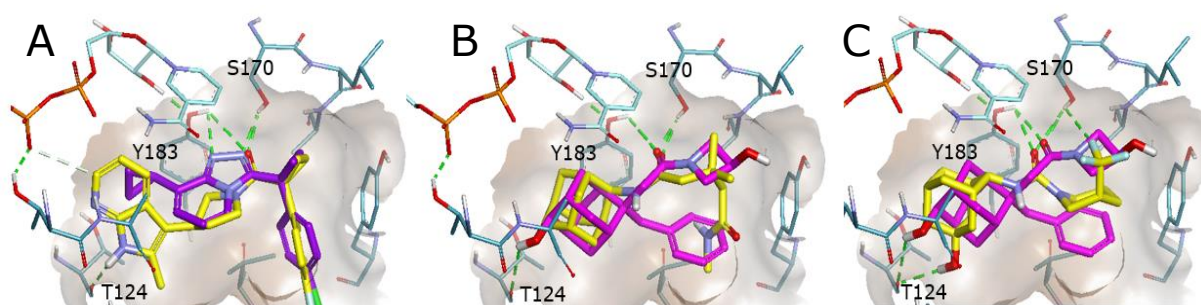


Figure 9: Compounds FPCM (A), TPCA (B), DPAAM (C) docked to the active site of 11 β -HSD1 (RCSB PDB 5PGX) [1]. Hydrogen bonds are shown as green dashed lines. Control compound (purple) compared with tested compounds (yellow).

In summary, all three investigated molecules appear to dock into the binding pocket of 11 β HSD1 interacting with similar side chain residues and thus show a potential of inhibiting this enzyme. TPCA and DPAAM align well with control inhibitor (purple) due to similarities in structure. Compound FPCM was compared with a different control inhibitor due to structural variances in adamantane structure of the molecule but showed equal performance in hydrogen bonding. To elucidate the influence of tested novel compounds on enzyme performance additional perception has to be analyzed.

6.1.2 Proteome analysis of pro-inflammatory induced HaCat cells by 2D-LC-MS/MS labeling-assisted proteomics

To gain further insights on how these three novel compounds alter the effect of 11 β HSD1 after binding, we performed a proteome analysis on HaCat cells after treatment with these compounds. First, we evaluated the cytotoxicity of the compounds of interest in an ATP dependent viability assay and used controls that have been established in the literature. This was done individually and in combination with TNF- α (Figure S1 + S2) as inflammatory induction. A viability of 80% was set as a limit for this assay. The resulting concentration was selected as working concentration for further experiments.

Here, we used the human keratinocyte like cell line, HaCat, as a model to investigate changes in cellular up- and downregulated proteins (Stokes et al., 2015) when induced by TNF- α and induction in presence of the inhibitors. The significantly regulated proteins were further examined with a Gene set enrichment analysis (GSEA) to gain further insight into the signaling pathway and biological processes (BPs) involved. Results were mapped with cytoscape to visualize correlations.

After FPCM treatment a total of 2017 proteins were identified through functional enrichment analysis. After data pre-processing 128 proteins were found to be significantly regulated compared to the control ($p < 0.05$). Of these, 44 proteins were downregulated, and 84 proteins were upregulated. On performing a GSEA the dataset obtained from the downregulated proteins showed significant gene ontology clusters in activation of immune response (A1), IL-6 production (A2) and IL-12 production (A3) and upregulation in protein folding (B1). The downregulated clusters associated with purine nucleotide metabolic process and translation from this dataset were also noteworthy (Figure 10, S3).

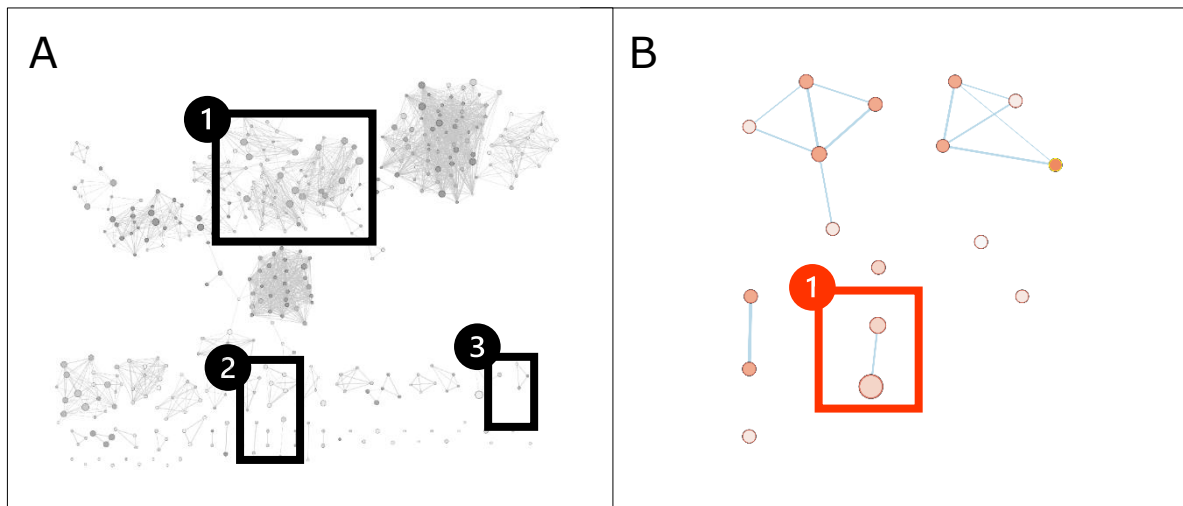


Figure 10: Enrichment of down (black) and upregulated (red) proteins after FPCM treatment. All BPs and pathways enriched in inflammation induced HaCat cells due to down and upregulated proteins were mapped and arranged according to function similarities. Each node (circle) represents a distinct biological process (GO:BP) or pathway (REAC) involving between 5 and 350 genes. Color gradient describes statistic linked to the identification of the biological process and pathways. Edges (lines) represent the number of genes overlapping between biological processes or pathways, determined using the similarity coefficient. (node cutoff = 0.04 and an edge cutoff = 0.5) Numbers represent cluster of similar biological process or pathway. A1: activation of immune response, A2: IL-6 production, A3: IL-12 production; B1: protein folding.

A total of 2017 proteins were identified after TPCA treatment through over-representation analysis (ORA). After pre-calculating the dataset, 211 proteins were found to be significant compared to the control ($p < 0.05$). Of these resulting proteins, 88 were downregulated and 113 proteins were upregulated analyzed using GSEA. The dataset obtained grouped clusters in downregulation of immune effector process regulation (A1), IL-12 regulation (A2) and NF κ B signaling (A3) and upregulation in regulation of protein kinase activity (B1). Proteins clustered in translation, WNT signaling, and DNA repair were downregulated after TPCA treatment. Upregulated protein cluster include negative regulation of proteolysis and nucleocytoplasmic transport were also noteworthy but were not further analyzed (Figure 11, S4).

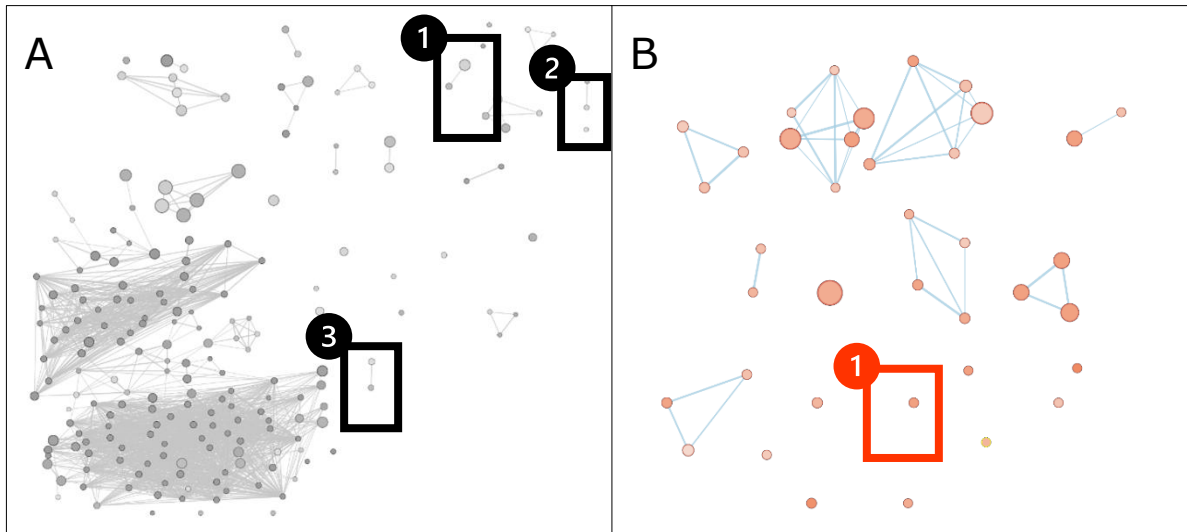


Figure 11: Enrichment of down (black) and upregulated (red) proteins after TPCA treatment. All BPs and pathways enriched in inflammation induced HaCat cells due to down and upregulated proteins were mapped and arranged according to function similarities. Each node (circle) represents a distinct biological process (GO:BP) or pathway (REAC) involving between 5 and 350 genes. Color gradient describes statistic linked to the identification of the biological process and pathways. Edges (lines) represent the number of genes overlapping between biological processes or pathways, determined using the similarity coefficient. (node cutoff = 0.04 and an edge cutoff = 0.5) Numbers represent cluster of similar biological process or pathway. A1: immune effector process regulation, A2: IL-12 regulation, A3: NFκB signaling, B1: regulation of protein kinase activity.

Further, treatment with compound DPAAM identified a total of 2167 proteins using ORA. Behind the calculated criteria of significance ($p < 0.05$) 74 proteins compared to control were analyzed. Of these remaining proteins, 14 proteins were downregulated, and 60 proteins were upregulated. After mapping the significant proteins with cytoscape the dataset showed grouped clusters of downregulation in G-protein beta:gamma signaling (A1) and upregulation in epidermal growth factor (B1) (Figure 12, S5).

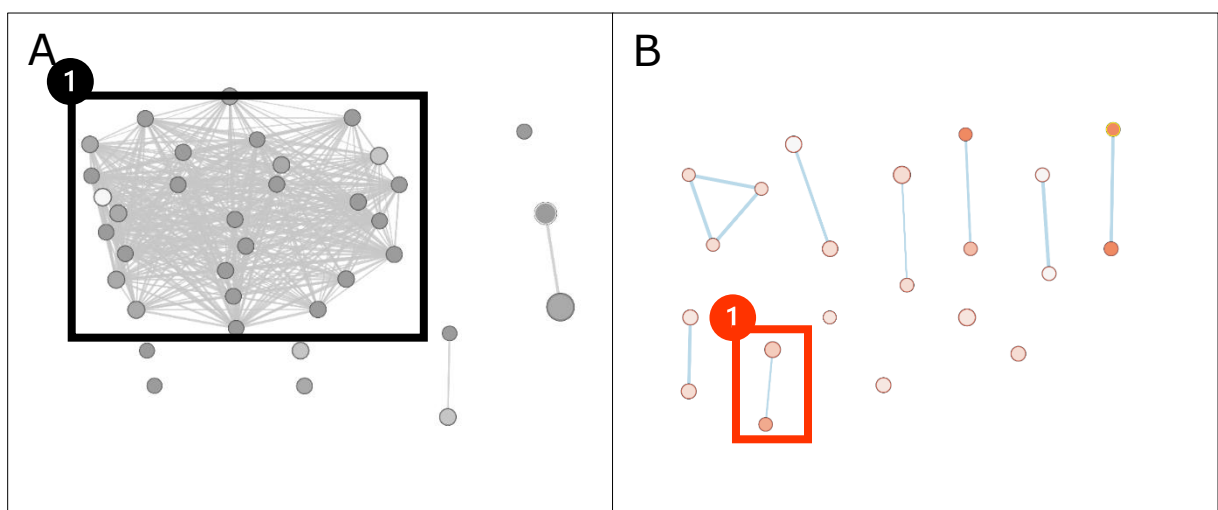


Figure 12: Enrichment of down (black) and upregulated (red) proteins after DPAAM treatment. All BPs and pathways enriched in inflammation induced HaCat cells due to down and upregulated proteins were mapped and arranged according to function similarities. Each node (circle) represents a distinct biological process (GO:BP) or pathway (REAC) involving between 5 and 350 genes. Color gradient describes statistic linked to the

identification of the biological process and pathways. Edges (lines) represent the number of genes overlapping between biological processes or pathways, determined using the similarity coefficient. (node cutoff = 0.04 and an edge cutoff = 0.5) Numbers represent cluster of similar biological process or pathway. A1: G-protein beta:gamma signaling, B1: epidermal growth factor.

GSEA data compared showed similar quantity of total protein with a huge variance in up- and downregulated proteins. Even though more upregulated proteins were calculated in GSEA after mapping these datasets, more correlation networks were obtained in downregulated proteins. After FPCM and TPCA treatment many smaller protein networks could be observed in downregulated proteins compared to one major network after DPAAM treatment. Upregulated protein networks were only loose linked after each treatment. Proteomic analysis revealed that pro-inflammatory associated proteins and the immune response are more likely downregulated after treatment with FPCM, TPCA and DPAAM in HaCat cells. For further investigation in downregulation of pro-inflammatory cytokines a quantification analysis of IL-6, IL-8 and CCL2 as literature known downstream targets of 11 β HSD1 was performed (Xing et al., 1998).

6.1.3 Decreasing inflammatory response after treatment with FPCM, TPCA and DPAAM in HaCat cells

Impact of cytokine secretion in HaCat cells after compound treatment can provide further insights about effects on anti-inflammatory influence. Therefore, the secretion of prominent pro-inflammatory cytokines in HaCat cells were quantified after TNF- α induction compared to inhibitor treatment. After TNF- α induction and inhibitor treatment with novel compounds FPCM, TPCA and DPAAM the IL-6 secretion of HaCat cells showed significant reduction. Compound FPCM reduced IL-6 secretion by 84%, TPCA by 65% and DPAAM by 85% compared to induced secretion by TNF- α . The control INCB-13739 and PF-915275 are known 11 β HSD1 inhibitor and reduced stimulation by 45% and PF-915275 by 34%. After each NCE treatment the secreted IL-6 concentration decreased significantly (Figure 13A). The measured concentrations after NCE treatment are lower as the selected inhibitors though on 10-fold higher working concentration.

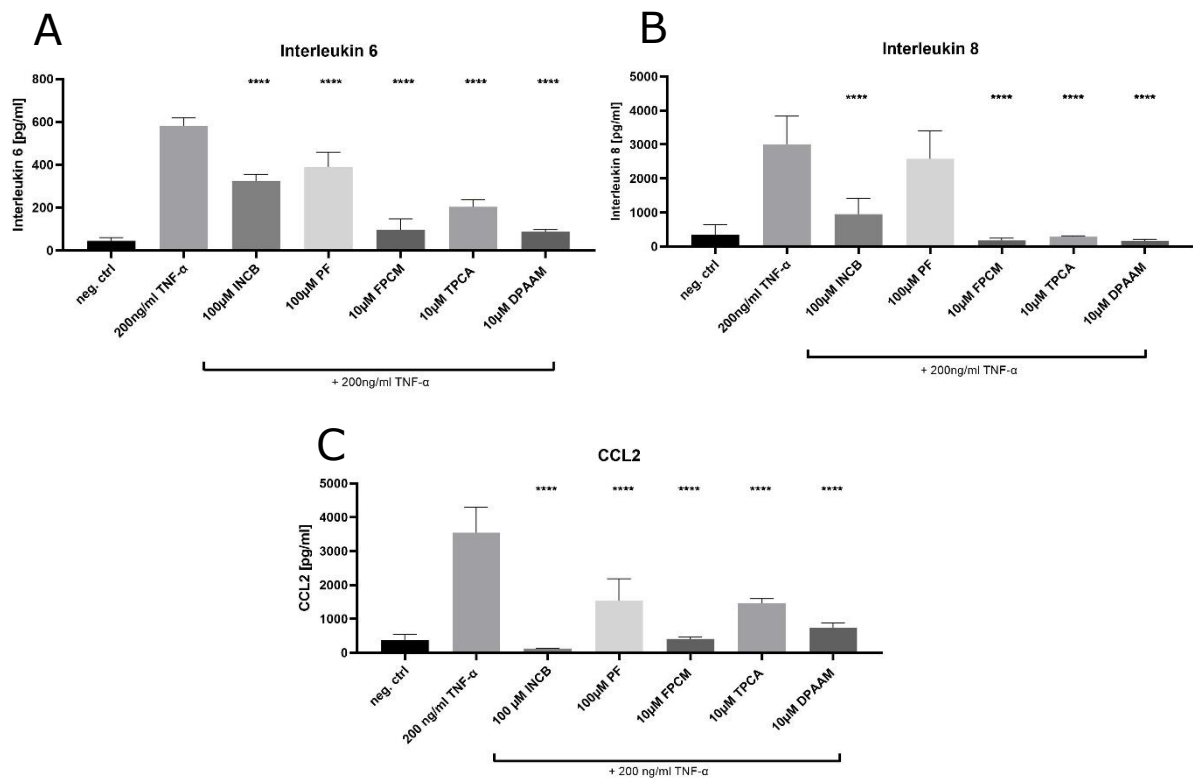


Figure 13: Reduction of pro-inflammatory biomarkers after pre-treatment using FPCM, TPCA and DPAAM after stimulation with TNF- α .

A: Reduction of IL-6 after treatment with FPCM, TPCA and DPAAM B: Reduction of IL-8 after treatment with FPCM, TPCA and DPAAM C: Reduction of CCL2 after treatment with FPCM, TPCA and DPAAM. NCE's reduced the stimulated inflammatory effect significantly. HaCat cells were seeded in 96well and treated for 48h with substances in humidified atmosphere at 37°C and 5% CO₂. neg. ctrl served as solvent control of 0,2% DMSO. INCB served as abbreviation for INCB-13739. PF served as abbreviation for PF-915275. Supernatant was further used for Elisa analysis (n=6, One-way ANOVA followed by $\alpha = 0.05$. Significances (****): $p < 0.0001$, (***) : $p < 0.001$, (**) : $p < 0.01$, (*) : $p < 0.05$, (ns): $p \geq 0.05$). Means \pm SD are shown.

To enhance the perspective of altered cytokine secretion after inhibitor treatment after pro-inflammatory induction, the NCEs were further tested on the reduction of IL-8 secretion. Results showed a significant reduced IL-8 secreted concentration after compound treatment compared to induction. FPCM decreased IL-8 secretion by 95%, TPCA by 92% and DPAAM by 95% compared to TNF- α induced secretion. Inhibitors were used with 10-fold higher use concentration and decreased the IL-8 secretion by 72% with INCB-13739 and 23% with PF-915275 treatment (Figure 13B).

In addition to efficient significant reduction of IL-6 and IL-8 secretion CCL2 concentration were quantified to broaden up the signaling cascade. The different cytokines are expressed after activation of different signaling pathways. But nevertheless, a cross-activation of different signaling pathways lead also to elevated expression and secretion of tested cytokines (Tang et al., 2016; Hillmer et al., 2017). Reduction of CCL2 concentration were analyzed after treatment with FPCM by 89%, TPCA by 59% and DPAAM by 79% compared with induction by TNF- α . Control

inhibitor INCB-13739 reduced the CCL2 secretion by 97% and PF-915275 by 57% significantly ($p < 0.0001$) (Figure 13C).

In conclusion, TPCA, FPCM and DPAAM compounds were identified as novel NCEs that significantly decrease three inflammatory downstream targets from 11 β HSD1. To understand the impact of structural based effects. DPAAM as potent compound for inhibiting pro-inflammatory cytokine secretion was further analyzed on structural analogies and differences with five compounds from DPAAM series.

6.1.4 Differences in chemical analogue structure influence effectivity in modulating downstream targets

Five compounds with analog structures to DPAAM were identified using Tanimoto similarities between 1-0,9 and tested on the reduction of pro-inflammatory interleukins after induction with TNF- α where none of the tested substances showed a significant reduction of IL-6 or CCL2 concentration compared to the TNF- α stimulation and treatment with DPAAM from the 11 β HSD1 series (Figure S8).

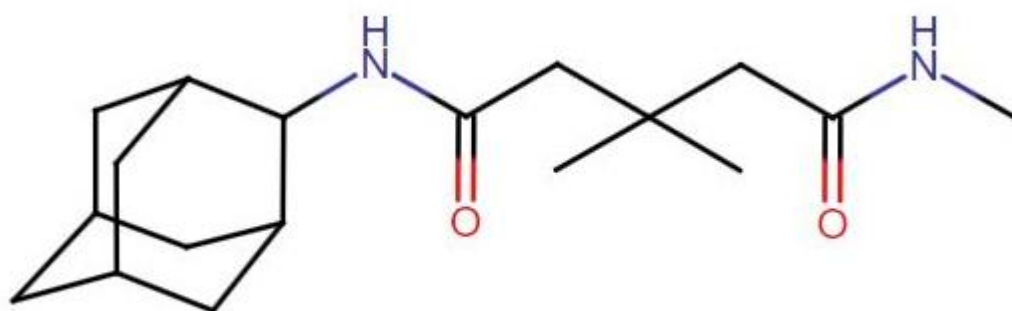


Figure 14: Chemical structure of DPAAM

An analogue structure element of the five selected compounds and DPAAM is an adamantane moiety at the side chain of the chemical structure (Figure 14). The second side chain differs from DPAAM with an additional cyclopropan or methyl-piperidin moiety compared to a planar structure which suggests an influence in effectivity on inhibition of pro-inflammatory cytokines downstream 11 β HSD1.

The additional methyl-piperidin moiety could lead to steric inhibition (Pedersen et al., 2017) of the activity and also the cyclopropane suggests decreasing activity of the molecule. In summary, five tested similar structured compounds to DPAAM showed no reduction in cytokine release.

Further insights of the three compounds TPCA, FPCM and DPAAM were investigated through phosphorylation activity of signaling related proteins.

6.1.5 Decreased phosphorylated protein of ERK after treatment with NCEs

Mitogen activated protein kinases (MAPKs; p38, ERK), Protein Kinase B (PKB; Akt) or transcription factors (TFs; NFκB, Stat3) are signaling pathways activated by stimuli including pro-inflammatory cytokines like TNF-α. Cell treatment with TNF-α increase phosphorylation of MAPKs, PKB and TF and elevate activation. Activated MAPKs, PKB and TFs are involved in upregulating pro-inflammatory cytokines including IL-6, IL-8 or CCL2. Therefore, the compounds FPCM, TPCA and DPAAM were investigated on their potential effects on phosphorylation to determine its influence on signaling pathways and its activation as mediators to inhibit pro-inflammatory signaling in context of 11βHSD1. The treatment of FPCM, TPCA and DPAAM did not show any significant effect on the change of phosphorylation level of MAPKs, PKB or TFs but a decreasing effect is mentioned. However, FPCM decreased the phosphorylation level of ERK by 30%, TPCA by 71% and DPAAM by 74% in HaCat cells compared to TNF-α treatment (Figure 15).

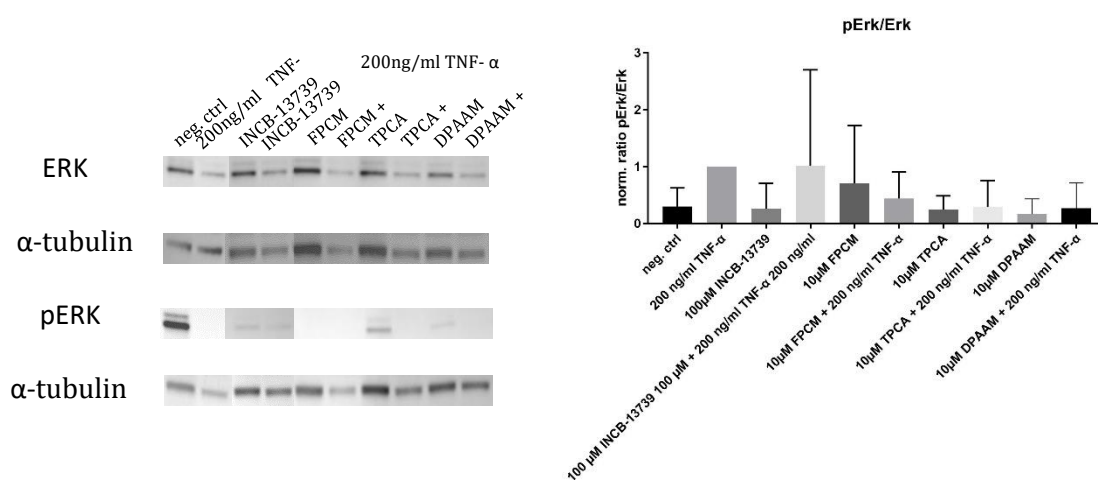


Figure 15: Quantification of ERK and phosphorylated ERK after treatment with FPCM, TPCA and DPAAM
HaCat cells were seeded in 6-well plate and treated for 48h with substances in humidified atmosphere at 37°C and 5% CO₂ afterwards harvested and lysed in Lysis Buffer. Cell lysates were further used for Western Blot analysis. neg. ctrl served as solvent control of 0,2% DMSO. 20μg protein lysate were used to assess the expression of ERK. Blotting results were manually edited to bring compounds in the right order, therefore unequal background intensity should be ignored. (n=3, One-way ANOVA followed by α = 0.05. Significances (****): p < 0.0001, (***) : p < 0.001, (**): p < 0.01, (*): p < 0.05, (ns): p ≥ 0.05). Means ± SD are shown.

These data suggest that the compounds FPCM, TPCA and DPAAM suppress phosphorylation of ERK in TNF-α treated HaCat cells. To consider metabolic and biological differences in cell lines the experiments were further elucidated on primary keratinocytes to verify the results.

6.1.6 Proteome analysis of pro-inflammatory induced primary keratinocytes by 2D-LC-MS/MS labeling-assisted proteomics

Metabolic response and biological variants of primary cells differentiate from cell lines (Pastor et al., 2010). Due to differences in biochemical signaling further investigations in the context of inhibition and stimulation need to be done to resemble the in vivo system. The proteome of pro-inflammatory induced primary keratinocytes was analyzed by 2D-LC-MS/MS labeling-assisted proteomics to investigate the influence of compound treatment.

Calculating significance ($p < 0.05$) obtained 178 proteins out of 2304 proteins in total after FPCM treatment. Of the resulting proteins, 92 were downregulated and 86 were upregulated. Enrichment analysis of the dataset and mapping accordingly to function similarities obtained downregulated proteins clustered by IL-27 signaling pathway (A1) and upregulation of IL-12 signaling pathway (B1), NF κ B signaling (B2) and ERK pathway related proteins (B3). Downregulated cluster in tissue morphogenesis and lipid catabolic processes and upregulated protein cluster in organic acid transport, ion transmembrane transport and regulation of chromosome organization were notable but not further analyzed (Figure 16, S11).

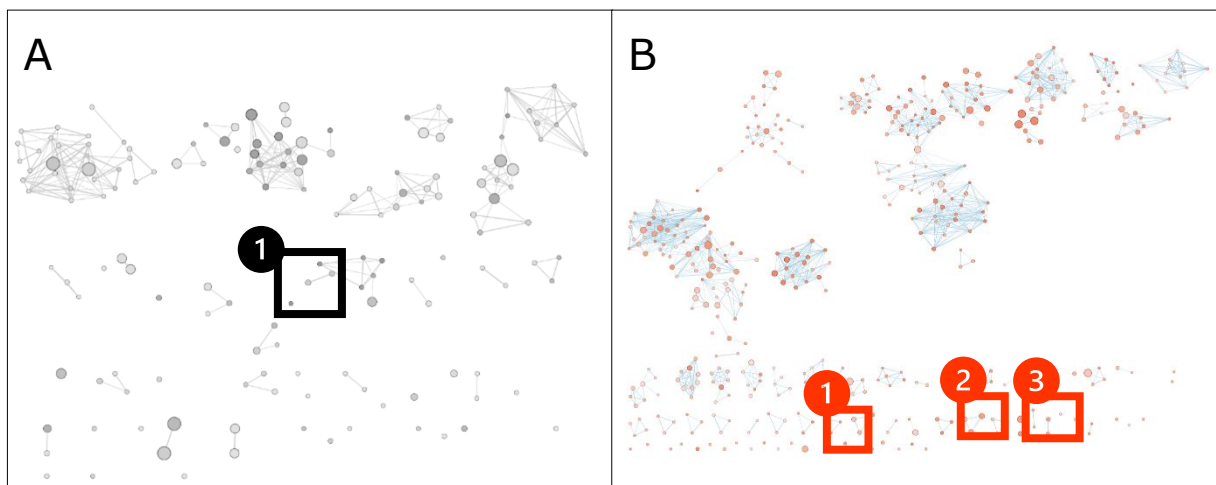


Figure 16: Enrichment of down (black) and upregulated (red) proteins after FPCM treatment

All BPs and pathways enriched in inflammation induced primary keratinocytes due to down and upregulated proteins were mapped according to function similarities. Each node (circle) represents a distinct biological process (GO:BP) or pathway (REAC) involving between 5 and 350 genes. Color gradient describes statistic linked to the identification of the biological process and pathways. Edges (lines) represent the number of genes overlapping between to biological processes or pathways, determined using the similarity coefficient. Numbers represent cluster of similar biological process or pathway. A1: IL-27 signaling pathway B1: IL-12 signaling pathway, B2: NF κ B signaling B3: ERK pathway related proteins.

In total, 2304 proteins were identified after TPCA treatment, and 92 proteins fulfilled the criteria of significant ($p < 0.05$) regulation. Of the remaining proteins, 29 were downregulated and 63 were upregulated. Gene analysis procured downregulated clusters in keratinocyte differentiation (A1)

and epidermis development (A2) and upregulation in MAPK signaling (B1) and IL-1 signaling (B2). Downregulated proteins in mitochondrial transport, fatty acid metabolic processes and formation of apoptosome and upregulated protein cluster in translation and respiration were noticeable but were not further analyzed (Figure 17, S12).

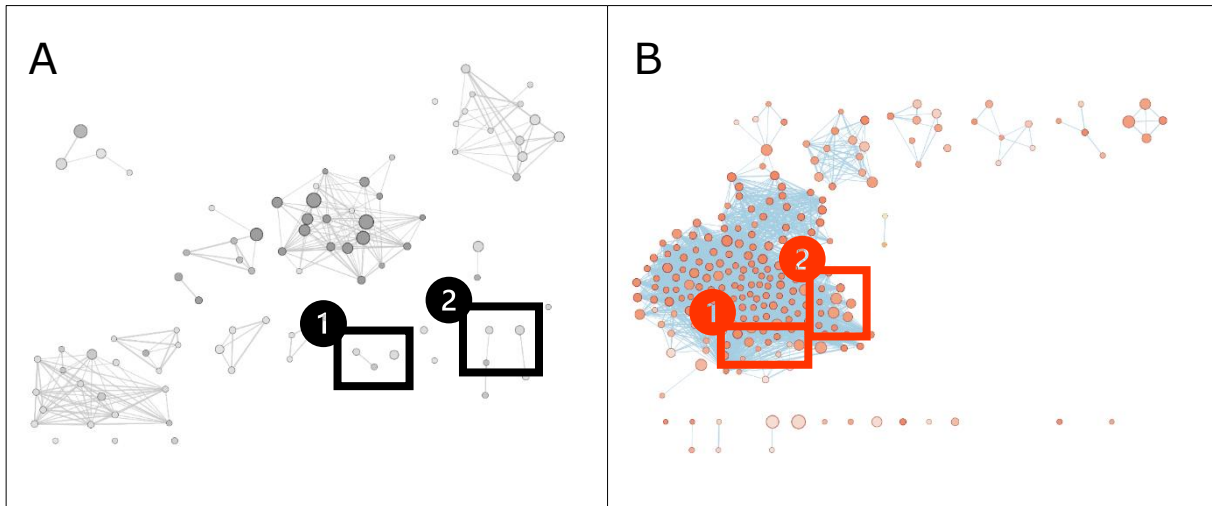


Figure 17: Enrichment of down (black) and upregulated (red) proteins after TPCA treatment. All BPs and pathways enriched in inflammation induced primary keratinocytes due to down and upregulated proteins were mapped according to function similarities. Each node (circle) represents a distinct biological process (GO:BP) or pathway (REAC) involving between 5 and 350 genes. Color gradient describes statistic linked to the identification of the biological process and pathways. Edges (lines) represent the number of genes overlapping between to biological processes or pathways, determined using the similarity coefficient. Numbers represent cluster of similar biological process or pathway. A1: keratinocyte differentiation, A2: epidermis development; B1: MAPK signaling, B2: IL-1 signaling.

After DPAAM treatment 2349 proteins in total were identified and 366 were found to be significantly regulated in comparison to the control ($p > 0,05$). Of these proteins, 152 were downregulated and 214 were upregulated. After performing enrichment analysis, the dataset was clustered by downregulated proteins of Toll like receptor signaling pathway (A1) and upregulation of IL-1 β signaling pathway (B1), Jak/STAT signaling (B2) and MAPK signaling. Downregulated protein cluster in ribosome biogenesis, ATP metabolic processes and heart contraction and upregulated protein cluster in metabolic processes and translation were noteworthy but not further analyzed (Figure 18, S13).

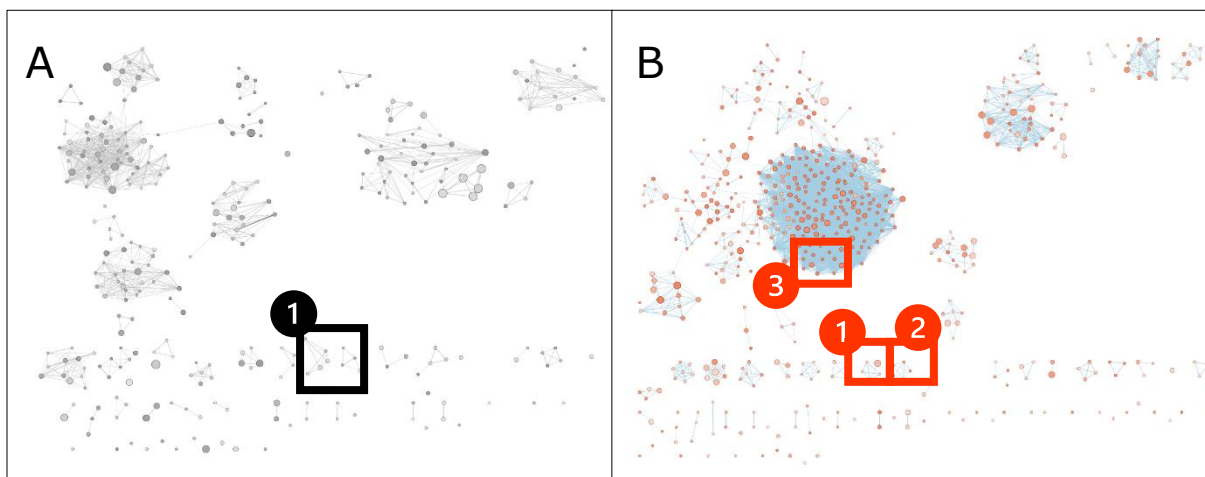


Figure 18: Enrichment of down (black) and upregulated (red) proteins after DPAAM treatment. All BPs and pathways enriched in inflammation induced primary keratinocytes due to down and upregulated proteins were mapped according to function similarities. Each node (circle) represents a distinct biological process (GO:BP) or pathway (REAC) involving between 5 and 350 genes. Color gradient describes statistic linked to the identification of the biological process and pathways. Edges (lines) represent the number of genes overlapping between to biological processes or pathways, determined using the similarity coefficient. Numbers represent cluster of similar biological process or pathway. A1: Toll-like receptor signaling pathway; B1: IL-1 β signaling pathway B2: Jak/STAT signaling, B3: MAPK signaling.

As expected GSEA data of primary keratinocytes showed similar protein enrichment compared to HaCat cells. In contrast to HaCat cells the total protein identified in primary keratinocytes is higher and more significant proteins could be analyzed. In addition, more pathway and biological processes are mapped, and bigger networks could be observed in upregulated proteins after treatment. Proteomic analysis revealed that processes and pathways related to pro-inflammation in NCE treated primary keratinocytes are downregulated. To investigate the impact of compound treatment on downstream cytokines IL-6, IL-8 and CCL2 from target 11 β HSD1 in primary keratinocytes a quantification analysis was performed.

6.1.7 Confirmation of three significant 11 β HSD1 inhibitors significantly affect downstream targets in primary keratinocytes

Testing the determined three NCEs from prior testing with HaCat cells, on primary cells on reduction of IL-6 compared to control inhibitor, showed a significant decrease in secretion of pro-inflammatory cytokine IL-6. Cytokine secretion concentration levels of IL-6 decreased after FPCM treatment by 58%, after TPCA by 45% and after DPAAM treatment by 79%. Control inhibitor INCB-13739 decreased IL-6 secretion by 40% (1 μ M) and 43% (0,1 μ M) (Figure 19A).

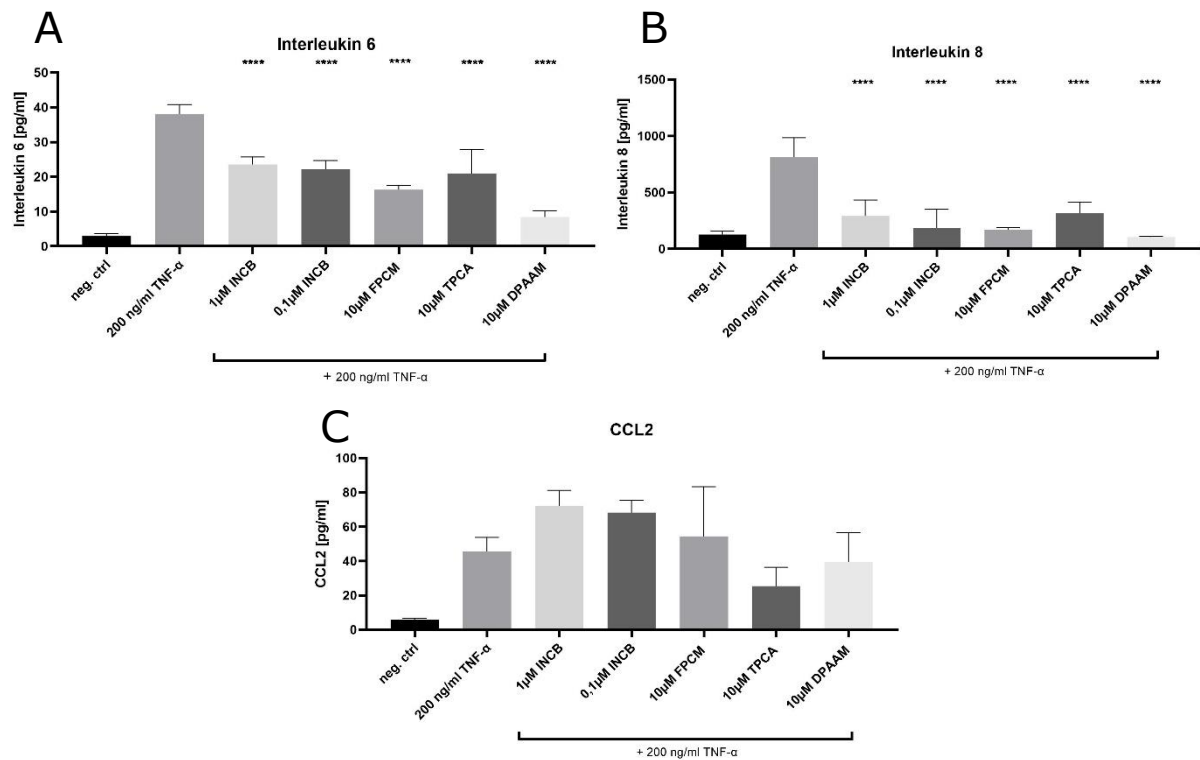


Figure 19: FPCM, TPCA, DPAAM treatment reduced the downstream 11 β HSD1 effector targets IL-6, IL-8 and CCL2. A: Reduction of IL-6 after treatment with FPCM, TPCA, DPAAM B: Reduction of IL-8 after treatment with FPCM, TPCA, DPAAM C: Reduction of CCL2 after treatment with FPCM, TPCA, DPAAM. Primary keratinocytes were seeded in 96well and treated for 48h with substances in humidified atmosphere at 37°C and 5% CO₂. neg. ctrl served as solvent control of 0,2% DMSO. INCB served as abbreviation for INCB-13739. Supernatant was further used for IL-6 Elisa analysis. (n=6, One-way ANOVA followed by $\alpha = 0.05$. Significances (****): $p < 0.0001$, (**): $p < 0.001$, (*): $p < 0.01$, (*): $p < 0.05$, (ns): $p \geq 0.05$). Means \pm SD are shown.

Testing the FPCM, TPCA and DPAAM compounds on reduction of IL-8 compared to selected inhibitors showed a significant decrease in secretion. Cytokine secretion levels of IL-8 after treatment with FPCM decreased by 80%, after TPCA treatment by 62% and after DPAAM treatment by 88%. Control inhibitor decreased secreted IL-8 concentration by 34% (1 μ M) and 35% (0,1 μ M) respectively (Figure 19B).

Testing the identified putative inhibitors on reduction of CCL2 compared to selected inhibitors showed no decrease in secretion. Neither the inhibitor nor the tested NCEs could reduce the increased CCL2 secretion after TNF- α stimulation significantly. However, after TPCA treatment a reduction by 75%, could be observed. (Figure 19C).

Primary keratinocytes are a great option for building further perceptions in cellular and molecular processes beside metabolic and biological variants compared to HaCat as keratinocyte like cell line. In vivo, signaling is transferred within different cells related to immune response. To gain further insights in signaling between cells a signal transfer model was conducted.

6.1.8 Proteome analysis of pro-inflammatory induced THP-1 cells by signal transfer from treated HaCat cells by 2D-LC-MS/MS labeling-assisted proteomics

To investigate the signal transfer from keratinocyte like cells to immune cells in cell culture the supernatant of treated HaCat cells were transferred to differentiated THP-1 cells. THP1 cells are of a leukemic monocyte lineage. Inflammation and itch are implemented through signal transfer from transmitter through receiver until a sensory neuron triggers itch in the central nervous system. To mimic this signal transfer in cell culture the supernatant of inhibitor treated HaCat cells was transferred on differentiated THP-1 cells. Treatment time of THP-1 cells were elucidated in prior analysis (Figure S16) and were optimized to 24h. After treatment of FPCM 3388 proteins in total were identified and 508 were determined with a significant p-value ($p < 0.05$). Of the resulting proteins, 221 were downregulated and 287 were upregulated. After performing an enrichment analysis, the dataset obtained clusters in downregulated proteins in regulation of G-protein-coupled receptor signaling pathway (A1), DNA replication (A2), apoptosis (A3), and IL-12 signaling with JAK-STAT signaling activation (A4) and upregulation of cellular matrix interactions (B1) and interferon signaling (B2) (Figure 20, S17).

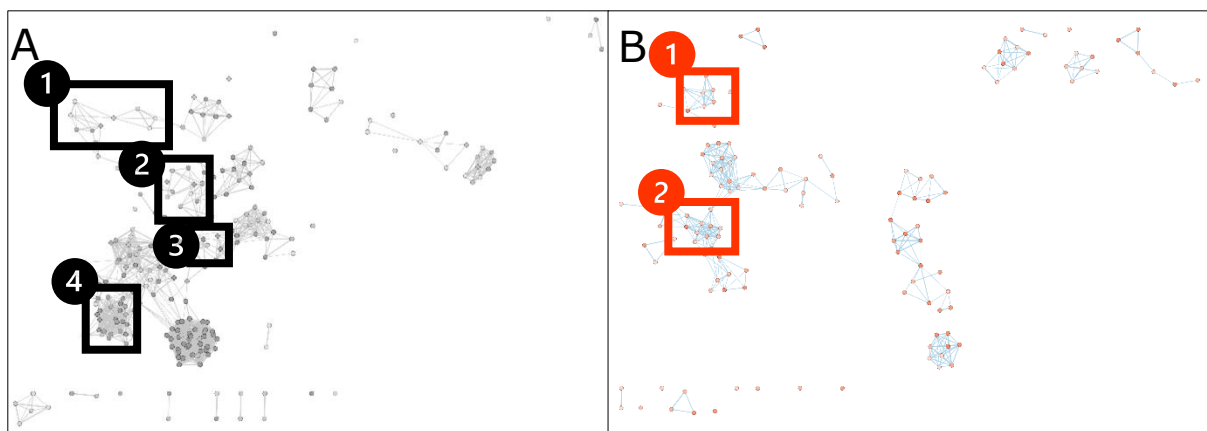


Figure 20: Enrichment of down (black) and upregulated (red) proteins in pro inflammatory induced THP-1 macrophages after treatment with secretom from HaCat cells treated with compound FPCM.

All BPs and pathways enriched in inflammation induced THP-1 cells were clustered according to their function similarities using Cytoscape. Each node (circle) represents a distinct biological process (GO:BP) or pathway (REAC) involving between 5 and 350 genes. Color gradient describes the statistic linked to the identification of the biological processes or pathways, determined by the similarity coefficient. Numbers represents clusters of similar biological processes or pathway. A1: regulation of G-protein-coupled receptor signaling pathway; A2: DNA replication; A3: apoptosis; A4: IL-12 signaling with JAK-STAT signaling activation, B1: cellular matrix interactions; B2: interferon signaling.

After the treatment with TPCA, 3388 proteins could be investigated in total in differentiated pro-inflammatory induced THP-1 cells. From these 685 proteins were significant ($p < 0.05$) regulated compared to induction. So, 304 proteins were analyzed with GSEA to be downregulated and 381 to be upregulated. Downregulated proteins were mapped in clusters accordingly to function

similarities in IL-1 production (A1), immune and inflammation response (A2), regulation of hormone secretion and activation of Janus kinase activity (A3), apoptosis (A4) and Wnt signaling pathway (A5). Upregulated proteins were clustered in translation (B1), interferon signaling (B2) and negative regulation of MAPK and ERK1/2 cascade (B3) (Figure 21, S18).

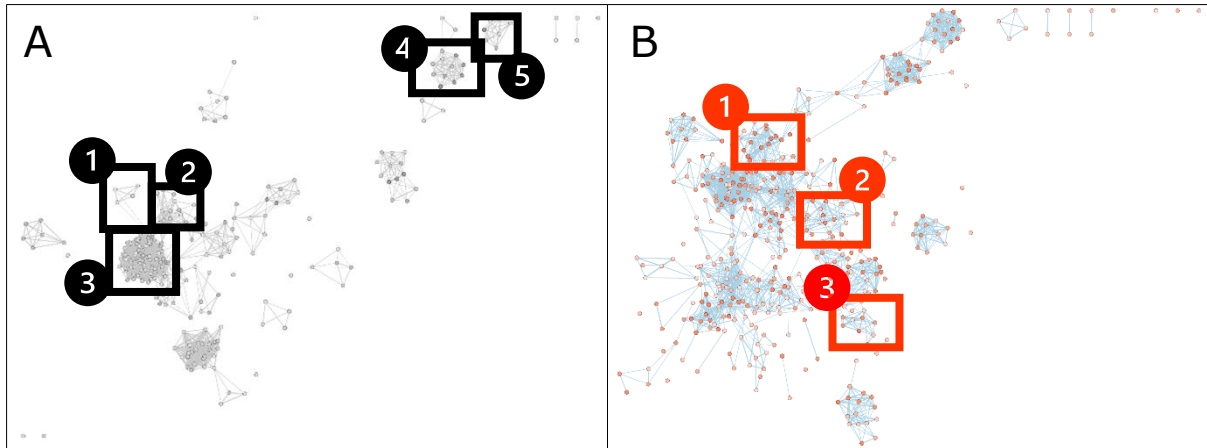


Figure 21: Enrichment of down (black) and upregulated (red) proteins in pro inflammatory induced THP-1 macrophages after treatment with secretom from HaCat cells treated with compound TPCA. All BPs and pathways enriched in inflammation induced THP-1 cells were clustered according to their function similarities using Cytoscape. Each node (circle) represents a distinct biological process (GO:BP) or pathway (REAC) involving between 5 and 350 genes. Color gradient describes the statistic linked to the identification of the biological processes or pathways. Numbers represents clusters of similar biological processes or pathway. A1: IL-1 production; A2: immune and inflammation response; A3: regulation of hormone secretion and activation of JAK activity; A4: apoptosis; A5: Wnt signaling pathway, B1: translation; B2: interferon signaling; B3: negative regulation of MAPK and ERK1/2 cascade.

After the treatment with compound DPAAM resulted in a total number of 3302 proteins identified in pro-inflammatory induced THP-1 macrophage-like cells and 719 proteins fulfilled the criterium of $p < 0.05$. Of these remaining proteins, 302 were downregulated and 417 proteins were upregulated analyzed using GESA and followed by clustering using Cytoscape. Among the downregulated proteins, clusters of regulation of inflammatory and immune response (A1), IL-12 JAK-STAT signaling (A2) and G-protein beta:gamma signaling (A3) could be assayed. Upregulated proteins were clustered of NFkB signaling (B1), haemostasis (B2), epidermal growth factor receptor signaling pathway (B3) (Figure 22, S19).

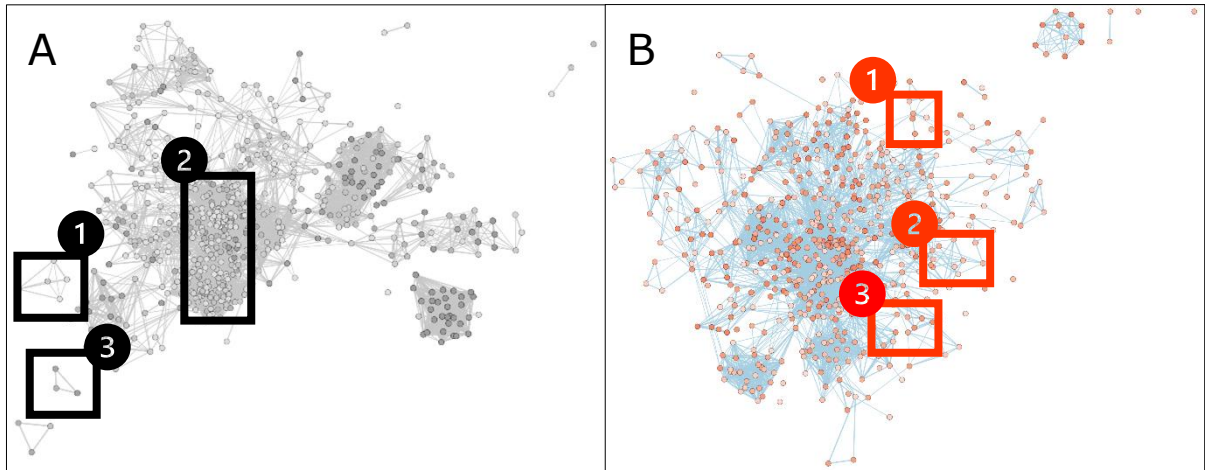


Figure 22: Enrichment of down (black) and upregulated (red) proteins in pro inflammatory induced THP-1 macrophages after treatment with secretom from HaCat cells treated with compound DPAAM. All BPs and pathways enriched in inflammation induced THP-1 cells were clustered according to their function similarities using Cytoscape. Each node (circle) represents a distinct biological process (GO:BP) or pathway (REAC) involving between 5 and 350 genes. Color gradient describes the statistic linked to the identification of the biological processes or pathways. Numbers represents clusters of similar biological processes or pathway. A1: regulation of inflammatory and immune response; A2: JAK-STAT signaling; A3: G-protein beta:gamma signaling, B1: NFkB signaling; B2: haemostasis; B3: epidermal growth factor receptor signaling pathway.

Proteomic analysis showed similar amounts of total protein after THP-1 treatment with different inhibitors. Also, similar significant proteins could be observed and balanced proportion of up- and downregulated proteins. Smaller protein cluster were mapped after FPCM and TPCA treatment but after DPAAM treatment on THP-1 cells one major network could be detected. Proteomic analysis of pro-inflammatory induced THP-1 cells after secretome transfer from treated HaCat cells determined the downregulation of related pro-inflammatory processes and upregulated immune response. To investigate downstream target specific cytokines a quantification with known cytokines IL-18, IL-1 β and CCL20 were investigated.

6.1.9 Secretome of treated HaCat cells significantly reduced inflammatory response of THP-1 cells

The concentration of known secreted cytokines were quantified and showed that control inhibitor INCB-13739 reduced significantly the concentration of CCL20 by 18% compared to FPCM also by 18%, TPCA by 41% and DPAAM by 38% (Figure 23A). Compound TPCA decreased IL-1 β significantly by 58% compared to FPCM by 21%, DPAAM by 45% in contrast of decreasing secretion by control inhibitor INCB-13739 by 51% (Figure 23B). The transfer of NCE treated HaCat supernatant on THP-1 cells lead to a significant reduction of secreted IL-18 cytokine concentration of 73% by FPCM, 77% by TPCA and 62% by DPAAM compared to control inhibitor with 68% reduction. The level of secreted cytokine decreased to control level (Figure 23C).

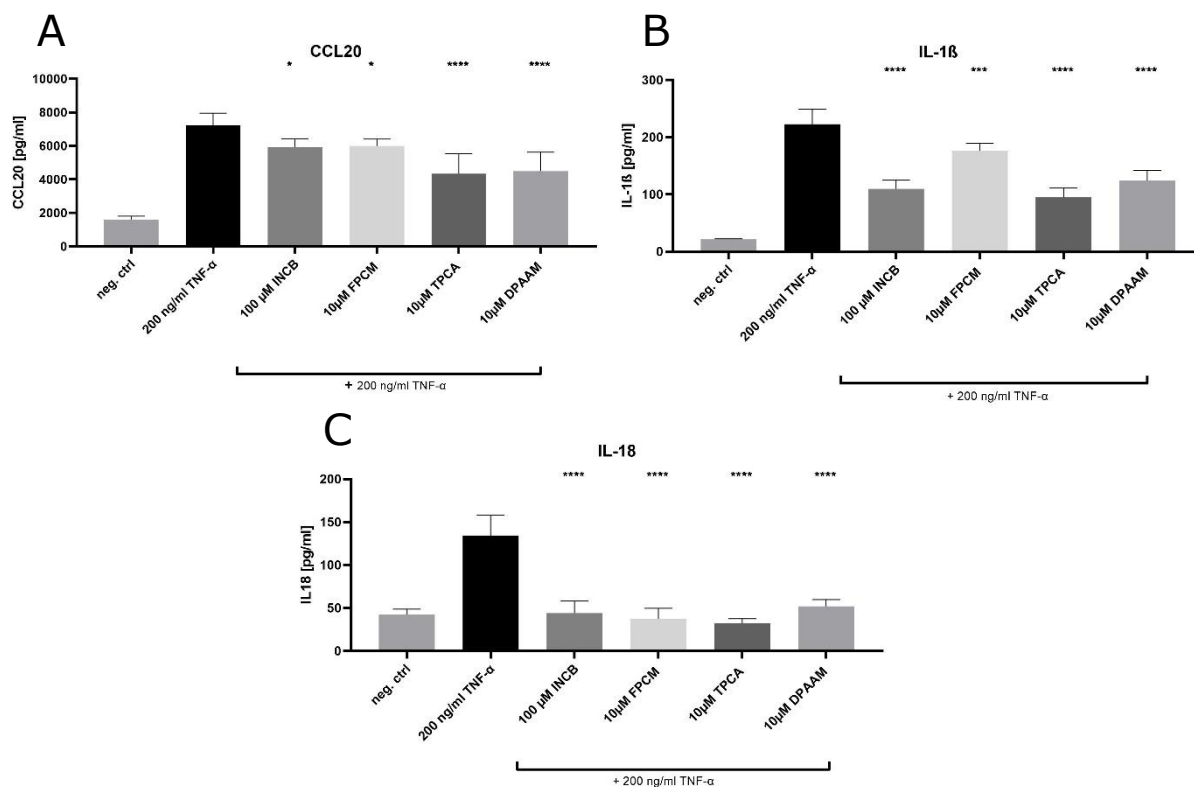


Figure 23: Treatment with FPCM, TPCA and DPAAM cell culture media from HaCat cells to THP-1 cells result in decreased secretion.

A: CCL20; B IL-1 β ; C: IL-18 comparable of controls. THP-1 were seeded in 96well and treated for 24h with supernatant from 48h treated HaCat cells in humidified atmosphere at 37°C and 5% CO₂. neg. ctrl served as solvent control of 0,2% DMSO. INCB served as abbreviation for INCB-13739. Supernatant was further used for Elisa analysis. (n=6, One-way ANOVA followed by $\alpha = 0.05$. Significances (****): $p < 0.0001$, (***) : $p < 0.001$, (**) : $p < 0.01$, (*) : $p < 0.05$, (ns): $p \geq 0.05$). Means \pm SD are shown.

Investigated pro- inflammatory cytokines downstream 11 β HSD1 showed significant reduced concentration level after signal transferred HaCat secretome to induced THP-1 cells. Cytokines are responsible for several activation of further cytokines or enzymes. Pro-inflammatory IL-1 β secretion is related to activation of Caspase 1. To investigate the context of tested compounds to inflammatory relation between cytokine and enzyme further examination was conducted.

6.1.10 Confirmation of involvement of caspase 1 in processing IL-1 β

Pro-inflammatory stimulation triggers caspase 1 activation and IL-1 β maturation in monocytes like THP-1 cells (Broz and Monack 2011; Qu et al., 2007). Pro-IL-1 β polypeptide must be post-translationally processed by caspase 1 to mature pro-inflammatory cytokine IL-1 β (Sutterwalla et al., 2006). This suggests that activation of caspase 1 and release of IL-1 β are closely related and the three identified inhibitors were tested to demonstrate the relation of reducing the caspase 1 activity to inhibit IL-1 β release.

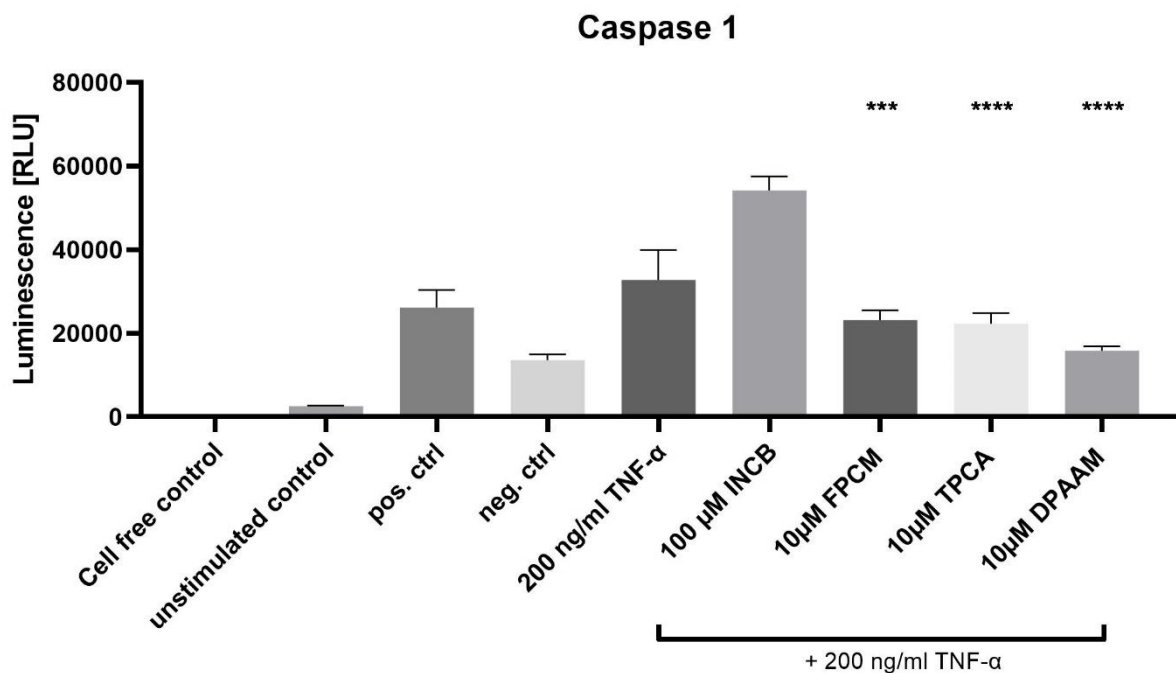


Figure 24: FPCM, TPCA and DPAAM result in decreased activity of caspase 1 in THP-1 cells comparable to controls. THP-1 were seeded in 96well and differentiated for 48h. Treated for 3h with compounds and the activity of caspase 1 measured afterwards. 2μg/ml Alpha Hemolysin acts as positive control and 1μM VX765 acts as caspase 1 inhibitor (neg. ctrl). INCB served as abbreviation for INCB-13739. (n=6, One-way ANOVA followed by $\alpha = 0.05$. Significances (****): $p < 0.0001$, (***): $p < 0.001$, (**): $p < 0.01$, (*): $p < 0.05$, (ns): $p \geq 0.05$). Means \pm SD are shown.

As pro-inflammatory stimulation TNF- α increased the activity of caspase 1 more potent compared to alpha-hemolysin (positive control). The known inhibitor INCB-13739 also increased the activity of caspase 1 significantly higher than positive control. The three identified inhibitors FPCM, TPCA and DPAAM significantly reduced the caspase 1 activity (Figure 24). DPAAM significantly decreased the activity of caspase 1 to negative control level. Results show that inhibition of cytokine secretion and connected caspase 1 activity of tested novel compounds were significantly effective. Further investigations of tested novel inhibitors reducing phosphorylation level after secretome transfer of treated HaCat cells to THP-1 cells have to be elucidated to research their impact on signaling pathways.

6.1.11 Phosphorylation analysis of key inflammatory kinases after supernatant transfer of treated HaCat to THP-1 cells

Activated MAPKs, PKB and TFs are involved in upregulating pro-inflammatory cytokines including IL-1 β , IL-18 or CCL20. Therefore, compounds FPCM, TPCA and DPAAM were investigated on their potential effects on reducing phosphorylation levels to determine its influence on signaling pathways after signal transfer from treated HaCat cells on THP-1 cells. Accordingly, FPCM (61%), TPCA (34%) and DPAAM (66%) decreased the phosphorylation level of ERK in THP-1 cells after signal transfer from treated HaCat cells significantly (Figure 25A). These data suggest that the compounds FPCM, TPCA and DPAAM are likely to suppress phosphorylation of ERK in THP-1 cells after TNF- α treatment on HaCat cells. The known 11 β HSD1 inhibitor INCB-13739 showed a significantly decreased phosphorylation of ERK by 74% and suggesting that inhibitor and NCEs suppress the same signaling pathway. DPAAM decreased the phosphorylation of Stat3 in THP-1 cells after signal transfer from treated HaCat cells by 76% significantly (Figure 25B).

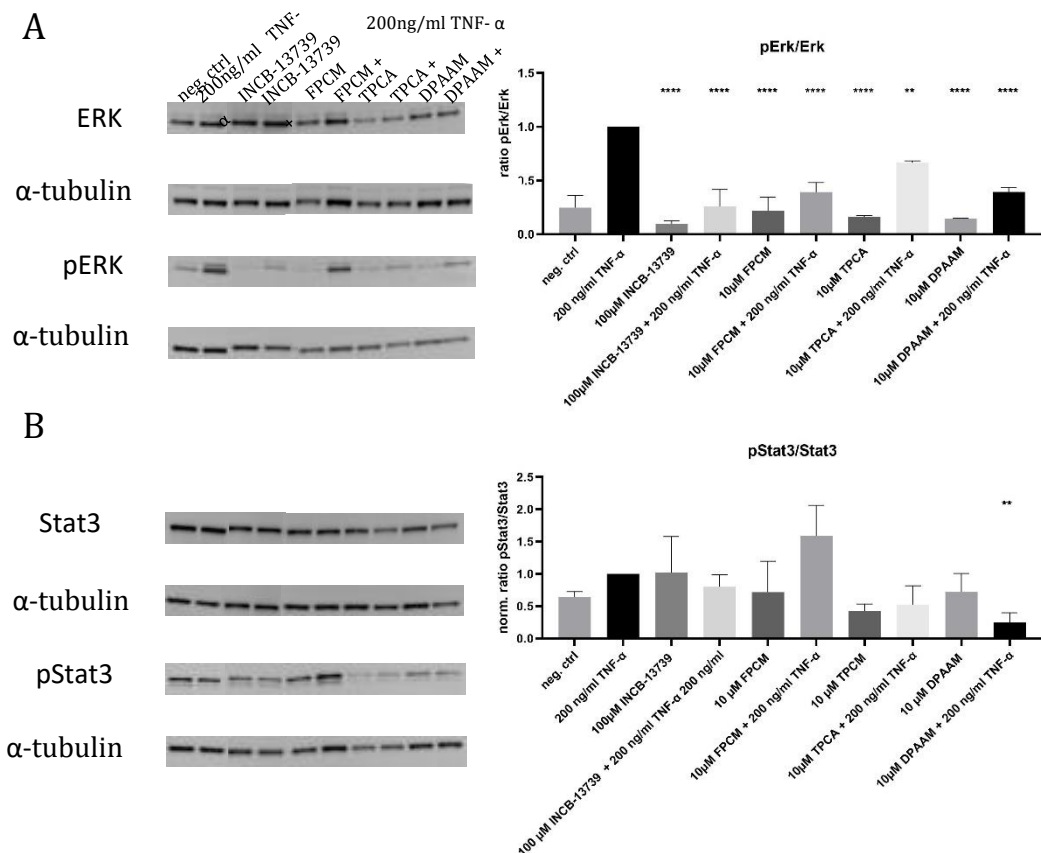


Figure 25: Quantification of A: ERK and phosphorylated protein and B: Stat3 and phosphorylated Stat3 after treatment with FPCM, TPCA and DPAAM in THP-1 cells. THP-1 were seeded in 6well plates and treated for 24h with supernatant from 48h treated HaCat cells in humidified atmosphere at 37°C and 5% CO₂. Afterwards harvested and lysed in Lysis Buffer. Cell lysis were further used for protein

concentration and Western Blot analysis. neg. ctrl served as solvent control of 0,2% DMSO. 20µg protein concentration were used to assess the expression of ERK and Stat3. Blotting results were manually edited to bring compounds in the right order, therefore unequal background intensity should be ignored. (n=3, One-way ANOVA followed by $\alpha = 0.05$. Significances (****): $p < 0.0001$, (***) : $p < 0.001$, (**) : $p < 0.01$, (*) : $p < 0.05$, (ns): $p \geq 0.05$). Means \pm SD are shown.

Protein phosphorylation regulates function and signaling through conformational changes in the affected phosphorylated protein. Thus, activated protein are critical for signal transduction. Treatment of FPCM, TPCA and DPAAM affect phosphorylation level of ERK significantly after signal transfer from HaCat to THP-1 cells. DPAAM showed also significant reduction of phosphorylated Stat3 level after treatment compared to FPCM and TPCA.

6.2 Results for NK1R

6.2.1 Molecular docking supports hypothesis of target specific binding of two tested compounds

To elucidate potential binding confirmations of two prescreened hits from library with structural characteristics for binding NK1R in silico docking experiment were conducted. Due to the high number of degrees of freedom, binding hypotheses of peptide- like hits have been determined via manual modeling with reference compound SP (high-affinity peptide) using NMR structures of NK1R (RCSB PDB 2KS9, 2KSA, 2KSB (Gayen et al., 2011)) (Figure 25 top).

Molecules were tethered to SP while keeping the receptor rigid. Overall, modelled binding hypotheses of the two compounds resemble the binding of SP: the methyl-sulfonyl, isobutyl, and phenyl moieties align well with equivalent moieties on SP. In addition, the nitrobenzene group was predicted to form salt bridge interactions with E172 and E186 in NK1 structure 2KSB (Figure 25 center (MAPA) and bottom (OPMA)).

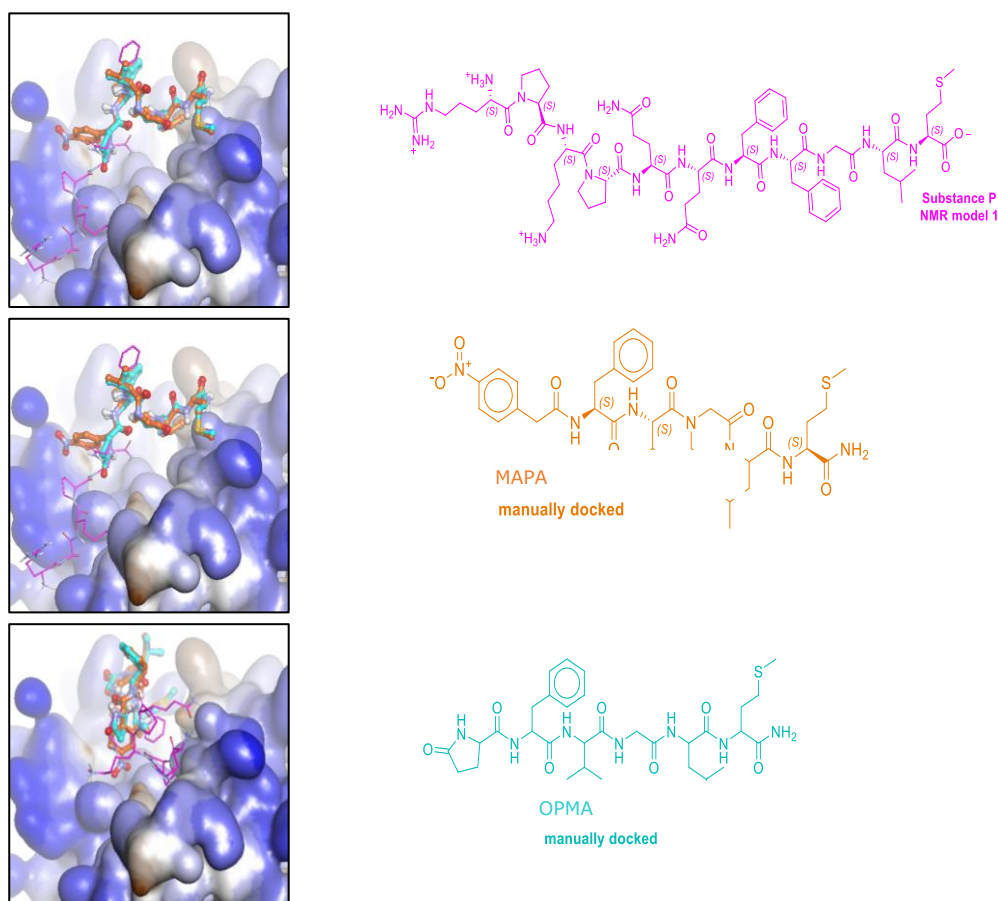


Figure 26: Manually modelled binding hypotheses of hit molecules MAPA and OPMA (orange, cyan) to NMR models of the NK1 receptor with reference to Substance P (magenta). (RCSB PDB entries 2KS9, 2KSA, 2KSB (Gayen et al., 2011))

In conclusion, in silico docking experiments support the hypothesis of MAPA and OPMA adopting a similar binding pose to NK1R compared to SP.

6.2.2 Ca²⁺ influx after activation of NK1R in CHO-K1 and CHO-K1-NK1R cells

The influence of the novel inhibitors on the specific NK1R activation was measured based on Ca²⁺ influx. The distributed Ca²⁺ concentration in CHO-K1 and CHO-K1-NK1R with overexpression of NK1R were compared. For CHO-K1 cells overexpressing NK1R a faster Ca²⁺ flux could be determined after treatment using the agonist SP, and a dose dependent inhibition of the tested inhibitors was measured (Figure S22). The IC₅₀ of MAPA measured after treatment on CHO-K1 was $1,59 \cdot 10^{-10}$ M compared to IC₅₀ measured on NK1R overexpressed on CHO-K1-NK1R $1,078 \cdot 10^{-5}$ M. Computed IC₅₀ of OPMA after treatment on CHO-K1 cells was $9,59 \cdot 10^{-5}$ M compared to IC₅₀ after treatment on CHO-K1-NK1R with $4,70 \cdot 10^{-8}$ M (Figure 27).

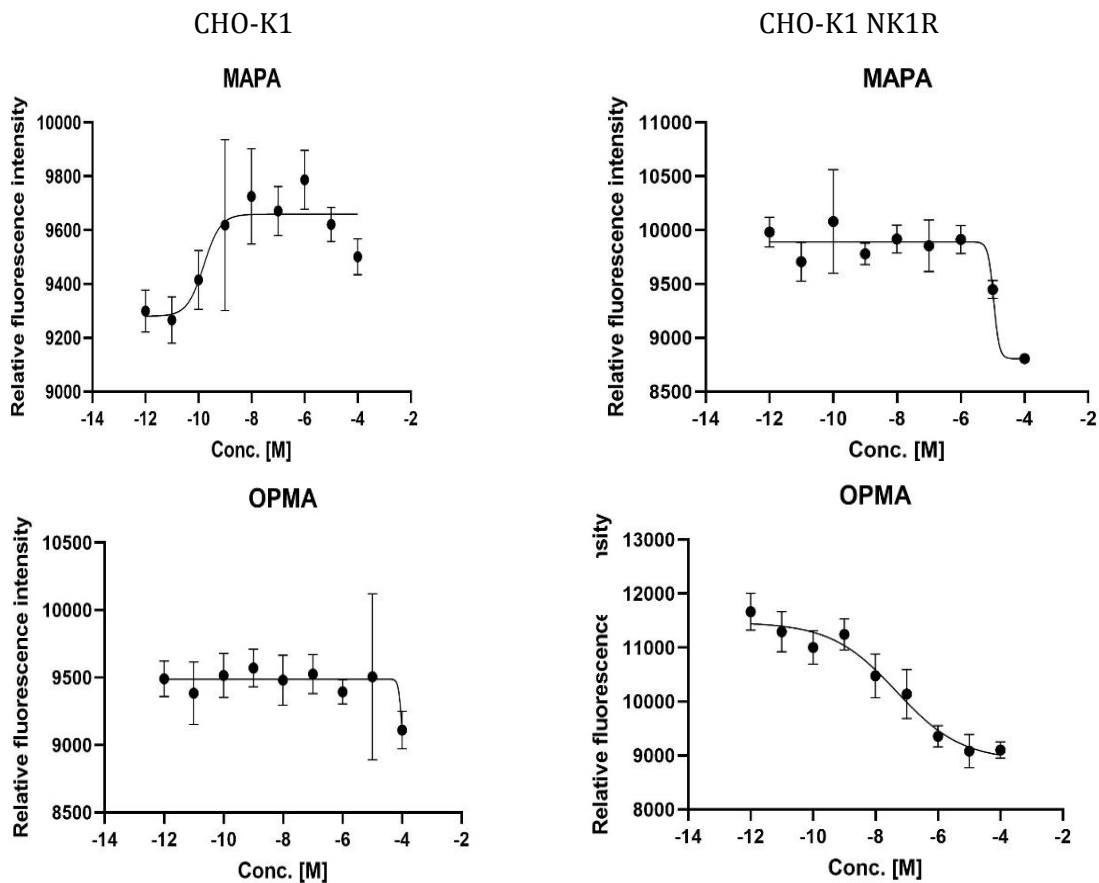


Figure 27: IC₅₀ of MAPA and OPMA calculated based on the Ca²⁺ concentration after NK1R activation. CHO-K1 or CHO-K1-NK1R cells were seeded in 96well plates overnight in humidified atmosphere at 37°C and 5% CO₂. Treatment for 10min and after treatment with agonist (SP) subsequently measured. (n=6, transformed data to log followed by non-linear regression. Means ± SD are shown.)

For CHO-K1 no Ca²⁺ flux changes were observed, and the measured inhibitors had no effect on the flux base level but in CHO-K1 overexpressing NK1R Ca²⁺ decreased after treatment with MAPA and OPMA (data not shown).

6.2.3 Proteome analysis of pro-inflammatory induced HaCat cells by 2D-LC-MS/MS labeling-assisted proteomics

At first, we elucidated cytotoxicity of the used compounds in an ATP viability assay and set a limit viability of 80% as threshold for further experiments (Figure S20+S21). In addition, TNF- α and SP was compared regarding their induction of elevated levels of secreted IL-6 level. Stimulation with TNF- α lead to a significant increased secretion of IL-6 and was further used as inducer.

The proteome of pro-inflammatory induced HaCat cells was analysed by 2D-LC-MS/MS labeling-assisted proteomics. Inflammation was induced in HaCat cells using 200ng/ml TNF- α . As previously described, cells were treated for 48h with TNF- α with or without inhibitor to induce stable inhibition of induced inflammation. The examination of HaCat proteome was performed by Gene set enrichment analysis (GSEA) to cluster up- and downregulated proteins.

In total 2167 proteins for MAPA were identified of which 172 proteins were found to be significant (p-value below 0,05). The resulting proteins, where 85 were downregulated and 87 proteins were upregulated were used to perform a GSEA and showed characteristic cluster in downregulation of protein ubiquitination (A1) and upregulation in regulation of cilium assembly (B1), signaling by ALK (B2) and Interleukin-1 processing (B3) (Figure 28, S23).

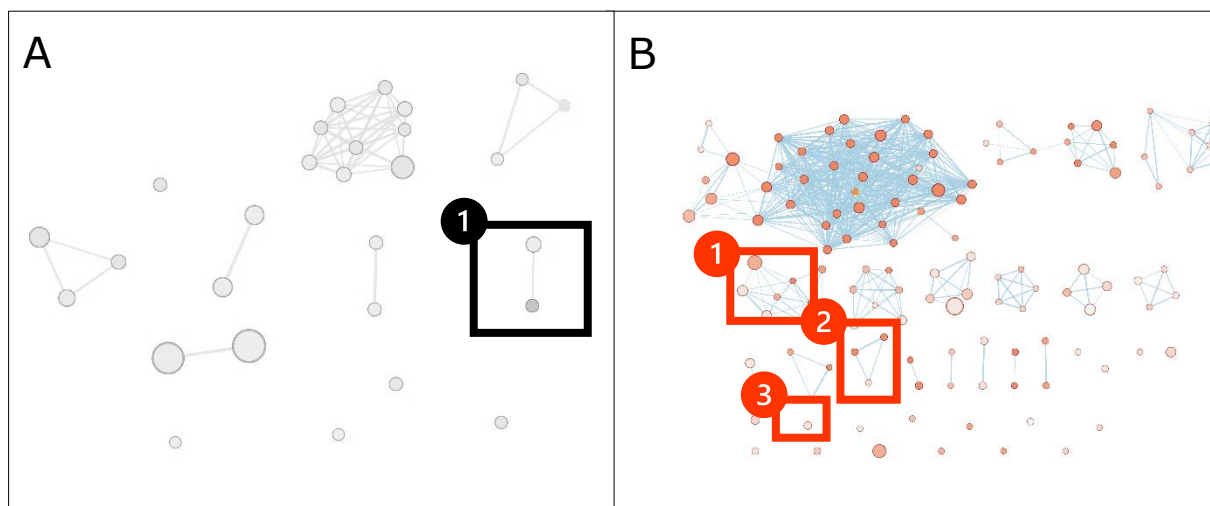


Figure 28: Enrichment of down (black) and upregulated (red) proteins after MAPA treatment. All BPs and pathways enriched in inflammation induced HaCat cells due to down- and upregulated proteins were arranged according to function similarities. Each node (circle) represents a distinct biological process (GO:BP) or pathway (REAC) involving between 5 and 350 genes. Color gradient describes statistic linked to the identification of the biological process and pathways. Edges (lines) represent the number of genes overlapping between to biological processes or pathways, determined using the similarity coefficient. Numbers represent cluster of similar biological

process or pathway. A1: protein ubiquitination, B1: regulation of cilium assembly, B2: signaling by ALK, B3: Interleukin-1 processing.

In total 2167 proteins for OPMA were identified and 177 proteins had the criteria of a p-value lower than 0,05. The resulting proteins, where 90 were downregulated and 87 proteins were upregulated were exported for a GSEA and showed grouped cluster in downregulation in protein modification and ubiquitination (A1), Protein ubiquitination (A2) and upregulation in signaling by ALK (B1) and regulation of NFκB signaling (B2) (Figure 29, S24).

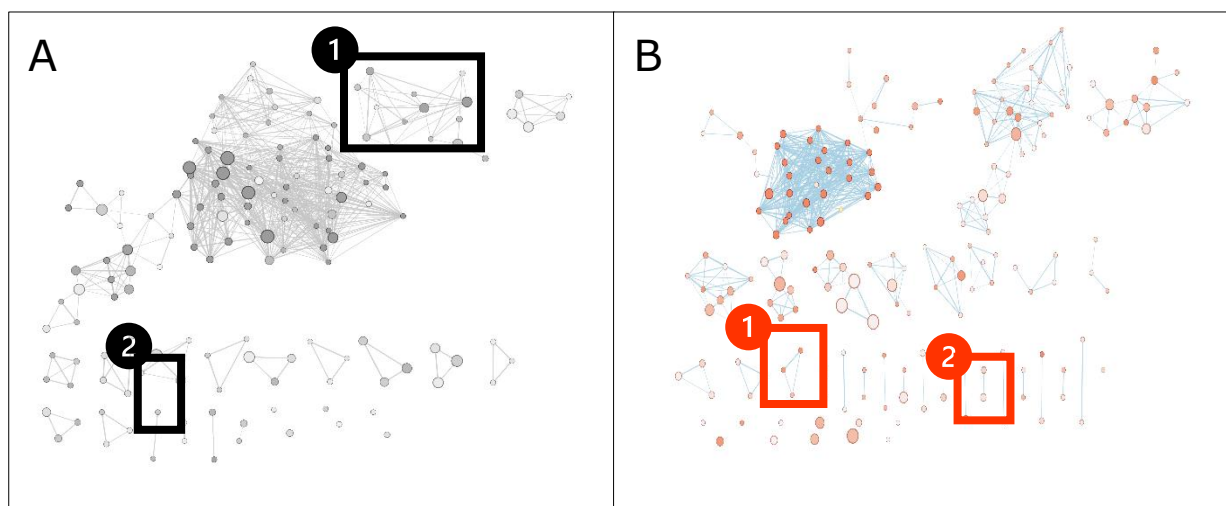


Figure 29: Enrichment of down (black) and upregulated (red) proteins after OPMA treatment. All BPs and pathways enriched in inflammation induced HaCat cells due to down and upregulated proteins were arranged according to function similarities. Each node (circle) represents a distinct biological process (GO:BP) or pathway (REAC) involving between 5 and 350 genes. Color gradient describes statistic linked to the identification of the biological process and pathways. Edges (lines) represent the number of genes overlapping between to biological processes or pathways, determined using the similarity coefficient. Numbers represent cluster of similar biological process or pathway. A1: protein modification and ubiquitination, A2: protein ubiquitination, B1: signaling by ALK, B2: regulation of NFκB signaling.

With proteomics analysis it could be observed that pro-inflammatory related processes are more likely downregulated after MAPA and OPMA treatment. For deeper understanding in downregulation of pro-inflammatory cytokines a quantification analysis of IL-6, IL-8 and CCL2 as literature known cytokines after TNF-α induction was performed (Xing et al., 1998).

6.2.4 Decreasing pro-inflammatory cytokine concentration after treatment with MAPA and OPMA in HaCat cells

Tested compound MAPA reduced the increased IL-6 secretion by TNF-α by 79% compared to the reference compounds Aprepitant and Fosaprepitant (both 69%). OPMA decreased the TNF-α induced secretion of IL-6 by 58% (Figure 30A). The measured concentrations after NCE treatment are lower as the selected inhibitors though on 10-fold higher use concentration.

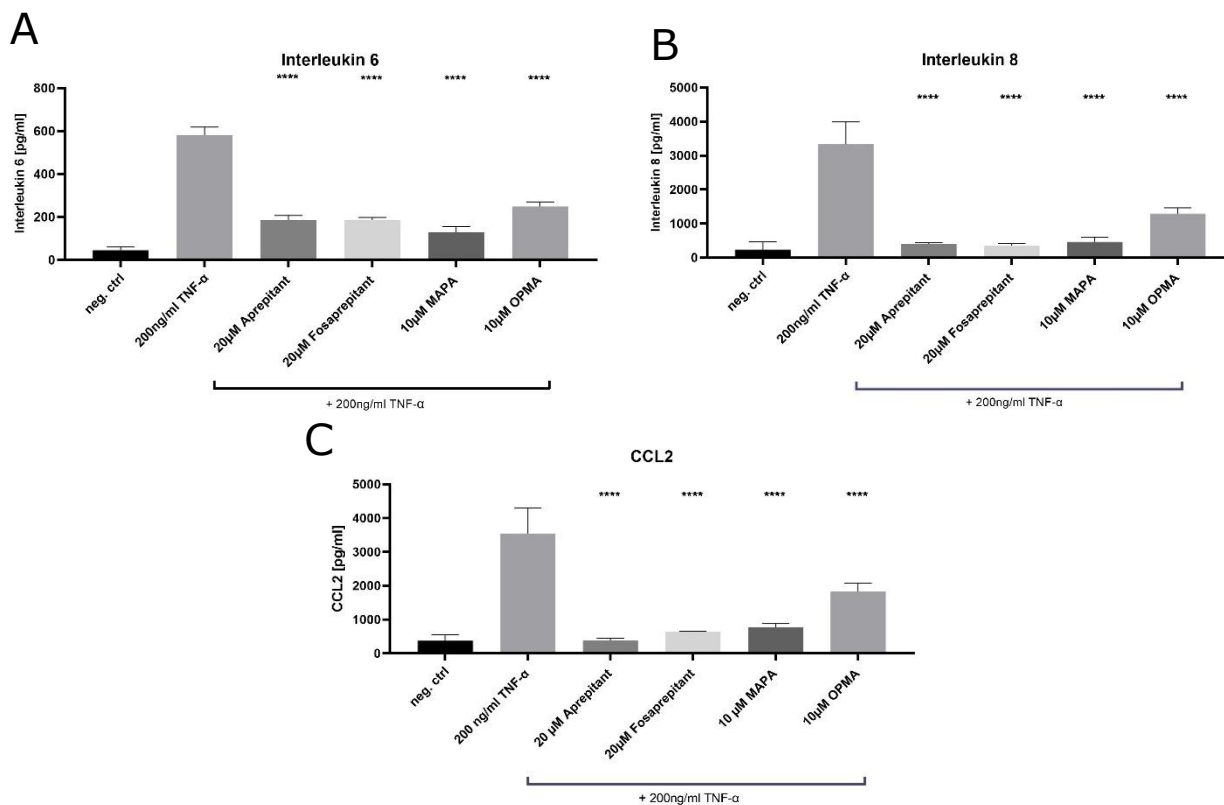


Figure 30: Reduction of pro-inflammatory biomarkers after pre-treatment using MAPA and OPMA after stimulation with TNF- α .

A: Reduction of IL-6 after treatment with MAPA and OPMA B: Reduction of IL-8 after treatment with MAPA and OPMA C: Reduction of CCL2 after treatment with MAPA and OPMA. NCEs reduced the stimulated inflammatory effect significantly. neg. ctrl served as solvent control of 0,2% DMSO. HaCat cells were seeded in 96well and treated for 48h with substances in humidified atmosphere at 37°C and 5% CO₂. Supernatant was further used for Elisa analysis (n=6, One way ANOVA followed by $\alpha=0.05$. Significances (****): $p < 0.0001$, (***): $p < 0.001$, (**): $p < 0.01$, (*): $p < 0.05$, (ns): $p \geq 0.05$). Means \pm SD are shown.

Additionally, the NCEs were tested for their reduction of the secretion of IL-8 and showed significant reduced IL-8 secreted concentration. MAPA decreased IL-8 secretion by 87% and OPMA by 62% compared to induced secretion by TNF- α . Literature known inhibitors decreased IL-8 secretion by 89% for Aprepitant and 90% by Fosaprepitant with 10-fold higher working concentration compared to MAPA and OPMA (Figure 30B). Compound MAPA decreased secretion of CCL2 by 79% and OPMA by 49% compared to TNF- α induced secretion (Figure 30C). MAPA and OPMA showed in all three measured NK1R downstream biomarkers significantly reduced secreted concentration.

In conclusion MAPA and OPMA were identified as novel NCEs that significantly decrease the secretion of pro-inflammatory downstream interleukins from NK1R. OPMA as potent compound for inhibiting pro-inflammatory cytokine secretion were further investigated for analogies and differences in structure and in their ability and the efficacy in binding process with compounds from OPMA series.

6.2.5 Differences in chemical analogue structure influence effectivity in modulating downstream targets

To investigate analogies of the chemical structure and their effect on the inhibition of the target receptor, five molecules with a similarity between 1-0,9 using Tanimoto similarities were analyzed for compound OPMA of NK1R series. Confirmed interleukin secretion were analyzed to compare the effectivity of the similar compounds where none of the compound's analogue by structure to OPMA from the NK1R series showed significant reduction of IL-6 or CCL2 concentration compared to the TNF- α stimulated control (Figure S27-see Supplement sheet). Differences of the five tested compounds for OPMA are the presence of two to three additional benzyl rings in the chemical structure of the five tested compounds. This could lead to steric inhibition and therefore to a reduced reactivity compared to the original structure (Majerz and Dziembowska 2010). This suggests that the additional Benzyl rings lead to decreased docking effectivity and therefore to no effect on inhibiting pro-inflammatory secretion induced by TNF- α . Two tested compounds showed large side chains which suggests to doesn't fit in binding pocket.

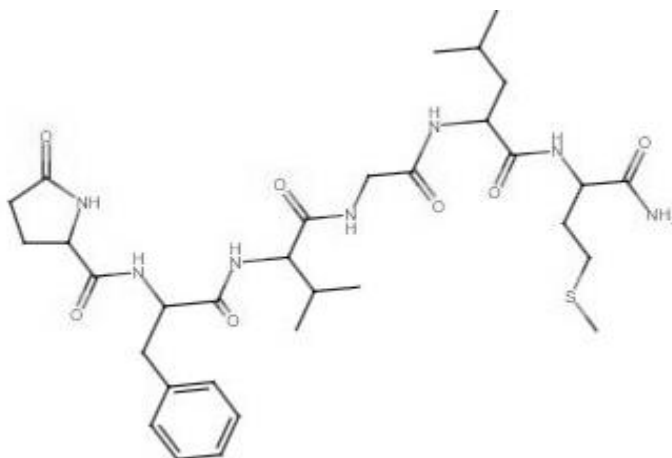


Figure 31: Chemical structure of OPMA

The additional benzyl rings are located in the middle of the molecule structure (data not shown); therefore, the middle of the structure is suggested to have a higher impact on the receptor docking than the structure endings with more matching structure properties (Figure 31).

6.2.6 Decreased phosphorylation protein after treatment with MAPA and OPMA

Mitogen activated protein kinases (MAPKs; p38, ERK), Protein Kinase B (PKB; Akt) or transcription factors (TFs; NF κ B, Stat3) belong to signaling pathways and are activated by stimuli including pro-inflammatory cytokines like TNF- α . Cell treatment with TNF- α increases

phosphorylation of MAPKs, PKB and TF and elevates their activation. Activated MAPKs, PKB and TFs are involved in upregulating pro-inflammatory cytokines including IL-6, IL-8 or CCL2. Therefore, the identified compounds MAPA and OPMA were investigated on their potential effects on downstream target phosphorylation. The treatment of MAPA and OPMA decreased the phosphorylation level of ERK and NFκB in HaCat cells not significantly but by 13% and 25% for NFκB and 62% and 69% for ERK respectively.

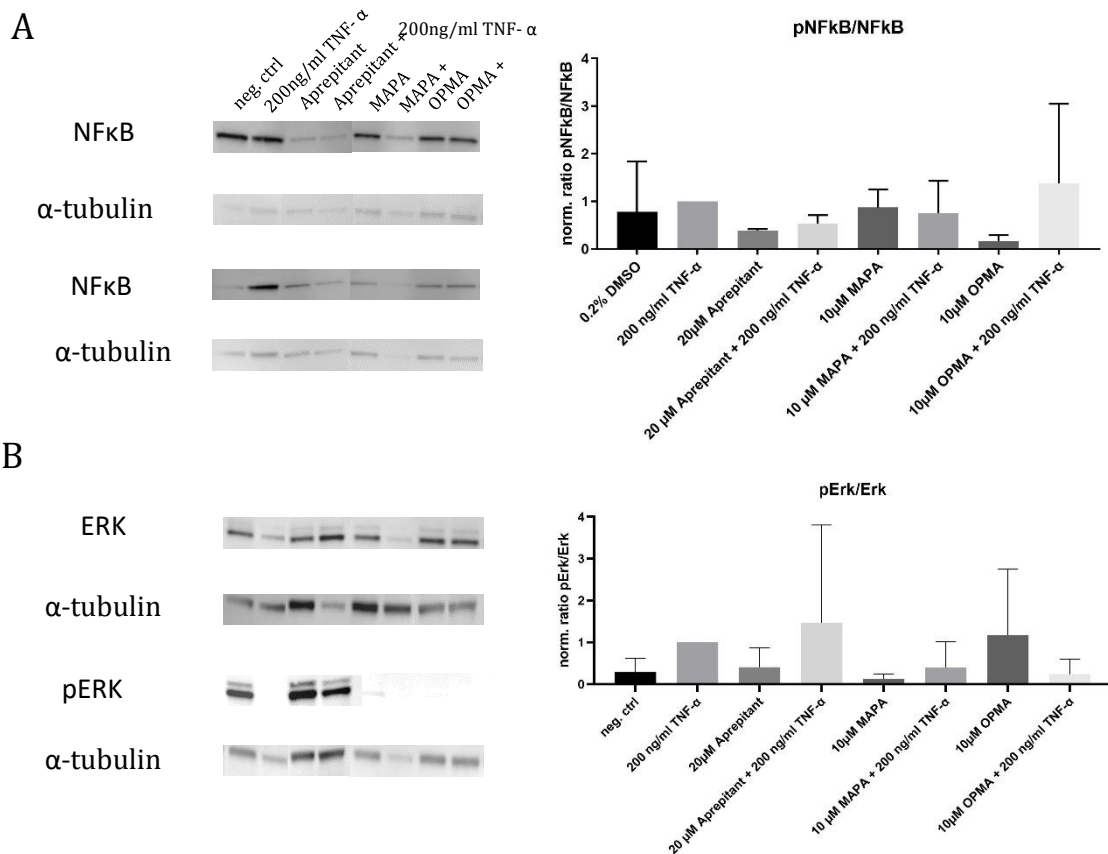


Figure 32: Quantification of A: NFκB and phosphorylated protein and B: ERK and phosphorylated protein after treatment with MAPA and OPMA.

HaCat cells were seeded in 6well plates and treated for 48h with substances in humidified atmosphere at 37°C and 5% CO₂ afterwards harvested and lysed in Lysis Buffer. Cell lysates were further used for protein concentration and Western Blot analysis. 20µg protein concentration were used. (n=3, One-way ANOVA followed by $\alpha = 0.05$. Significances (***): $p < 0.0001$, (**): $p < 0.001$, (*): $p < 0.01$, (*): $p < 0.05$, (ns): $p \geq 0.05$). Means \pm SD are shown. Representative picture of 3 biological replicates are shown.

These data suggest that the compounds MAPA and OPMA are likely to suppress phosphorylation of ERK and NFκB in TNF-α treated HaCat cells (Figure 32). NCE MAPA and OPMA reduced phosphorylation level of ERK to control level and prevent phosphorylation level of NFκB to increase above positive control.

6.2.7 Proteome analysis of pro-inflammatory induced primary keratinocytes by 2D-LC-MS/MS labeling-assisted proteomics

Metabolic response and biological variants of primary cells differ from cell lines (Pastor et al., 2010). Differences in proteome were further investigated in context of inhibition and stimulation after MAPA and OPMA treatment. The proteome of pro-inflammatory induced primary keratinocytes was analyzed by 2D-LC-MS/MS labeling-assisted proteomics.

For MAPA 2227 proteins in total were identified and 286 proteins implemented the criteria of a p-value beneath 0,05. The residual proteins, where 158 were upregulated and 128 proteins were downregulated were calculated in GSEA and clustered with downregulation of epidermis development (A1), keratinization and wound healing (A2) and upregulation of cell junction assembly (B1), regulation of inflammatory response (B2) and JAK-STAT and IL-12 signaling (B3) (Figure 33, S30).

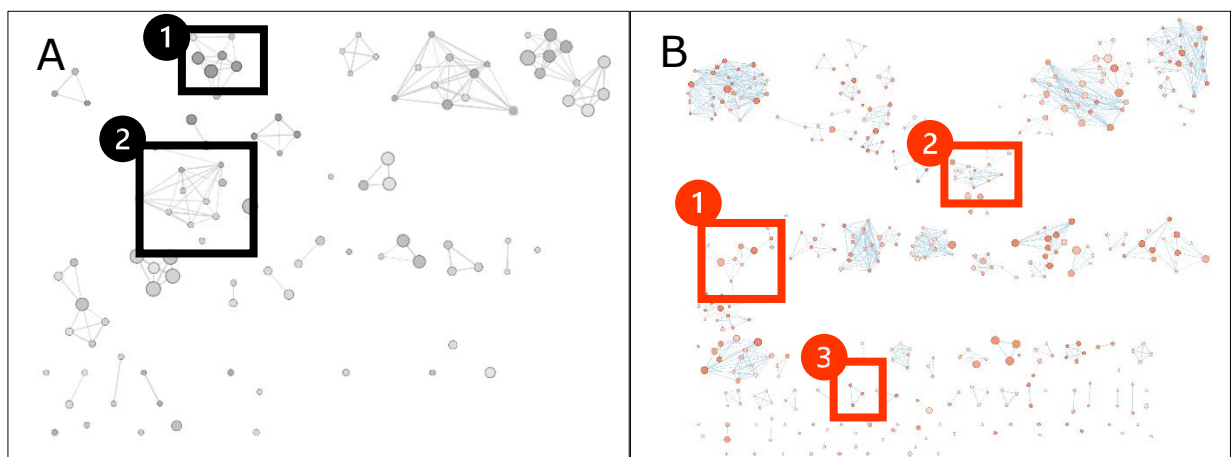


Figure 33: Enrichment of down (black) and upregulated (red) proteins after MAPA treatment.

All BPs and pathways enriched in inflammation induced primary keratinocytes due to down and upregulated proteins were arranged according to function similarities. Each node (circle) represents a distinct biological process (GO:BP) or pathway (REAC) involving between 5 and 350 genes. Color gradient describes statistic linked to the identification of the biological process and pathways. Edges (lines) represent the number of genes overlapping between biological processes or pathways, determined using the similarity coefficient. Numbers represent cluster of similar biological process or pathway. A1: epidermis development, A2: keratinization and wound healing B1: cell junction assembly B2: regulation of inflammatory response, B3: JAK-STAT and IL-12 signaling.

For OPMA 2227 proteins in total were identified and 196 proteins fulfill the condition of a p-value lower than 0,05. Remaining proteins, where 51 were downregulated and 145 proteins were upregulated were clustered in gene set enrichment analysis with downregulation in interferon production (A1) and cell junction assembly (A2), and upregulation of regulation of JNK and MAPK pathways (B1), regulation MAPK and Wnt signaling (B2) and inflammatory response (B3) (Figure 34, S31).

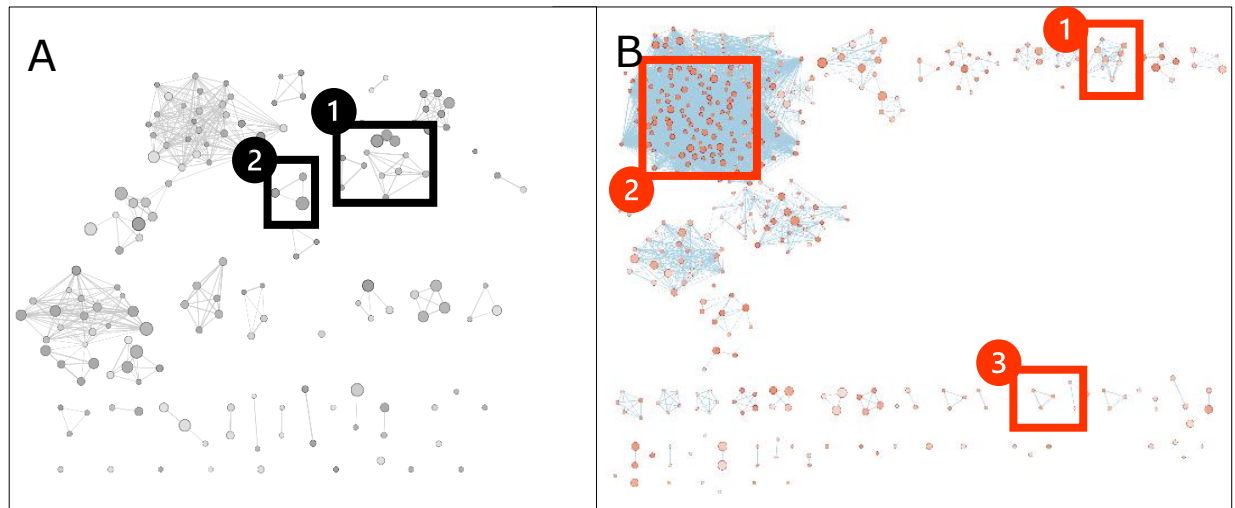


Figure 34: Enrichment of down and upregulated proteins after OPMA treatment.

All BPs and pathways enriched in inflammation induced primary keratinocytes due to down and upregulated proteins were arranged according to function similarities. Each node (circle) represents a distinct biological process (GO:BP) or pathway (REAC) involving between 5 and 350 genes. Color gradient describes statistic linked to the identification of the biological process and pathways. Edges (lines) represent the number of genes overlapping between to biological processes or pathways, determined using the similarity coefficient. Numbers represent cluster of similar biological process or pathway. A1: interferon production, A2: cell junction assembly B1: regulation of JNK and MAPK signaling B2: regulation of MAPK and Wnt signaling, B3: inflammatory response.

Proteomic analysis of primary keratinocytes revealed increased immune response and decreased cell regulation and apoptotic signaling after treatment of MAPA and OPMA as inhibitors for NK1R. To investigate regulation of downstream target pro-inflammatory cytokines on primary keratinocytes an Elisa quantification was performed.

6.2.8 Confirmation of two significant NK1R inhibitors on downstream targets

To determine the efficacy of used inhibitors on primary keratinocytes the secretion of IL-6, IL-8 and CCL2 were evaluated after stimulation with TNF- α . Aprepitant and Fosaprepitant decreased the secretion of IL-6 in different concentrations (Aprepitant 1 μ M-8%; Fosaprepitant 1 μ M-19%, 0,1%-22%) after inducing with TNF- α with dominant reduction of Fosaprepitant (Figure 35A). For secretion of IL-8 Aprepitant (Aprepitant 1 μ M-72%, 0,1 μ M-81%) has significant reduction of the pro inflammatory cytokine compared to Fosaprepitant (Fosaprepitant 1 μ M-2%) (Figure 35B). For CCL2 no significant reduction could be determined after treatment (Figure 35C).

Testing compounds MAPA and OPMA on primary cells reduction of IL-6 compared to control inhibitors showed a significant decrease (MAPA 19%; OPMA 56%) in secretion of pro-inflammatory cytokine (Figure 35A). The level of released IL-6 with OPMA is lower compared to control inhibitors. In case of MAPA the level of IL-6 concentration resembles with inhibitors. The working concentration of inhibitors were adjusted on keratinocyte viability whereas MAPA and OPMA were tested with working concentration elucidated from prior HaCat analysis.

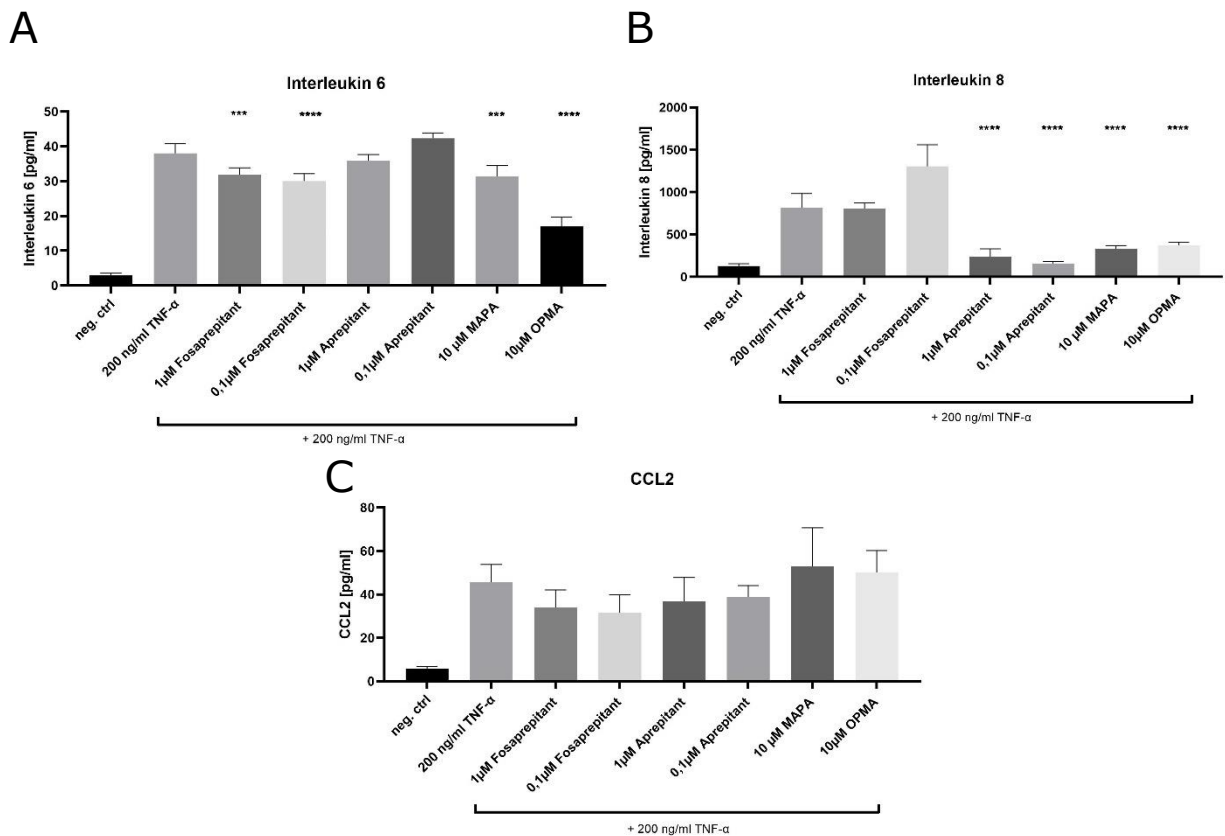


Figure 35: Decreasing secretion of biomarkers through treatment with MAPA and OPMA. A: Reduction of IL-6 after treatment with MAPA and OPMA B: Reduction of IL-8 after treatment with MAPA and OPMA C: Reduction of CCL2 after treatment with MAPA and OPMA. neg. ctrl served as solvent control of 0,2% DMSO. Primary keratinocytes were seeded in 96well and treated for 48h with substances in humidified atmosphere at 37°C and 5% CO₂. Supernatant was further used for IL-6 Elisa analysis. (n=6, One-way ANOVA followed by $\alpha = 0.05$. Significances (****): $p < 0.0001$, (***): $p < 0.001$, (**): $p < 0.01$, (*): $p < 0.05$, (ns): $p \geq 0.05$). Means \pm SD are shown.

Compound MAPA and OPMA testing on reduction of IL-8 compared to control inhibitors showed a significant decrease in secretion. Cytokine concentration levels of IL-8 after treatment with Aprepitant and NCEs (MAPA 60%; OPMA 55% reduction) decreased to control level (Figure 35B). Neither the inhibitor nor the tested NCEs could reduce the increased CCL2 secretion after TNF- α stimulation (Figure 35C).

6.2.9 Proteome analysis of secretome of pro-inflammatory induced HaCat cells transferred to THP-1 cells y 2D-LC-MS/MS labeling-assisted proteomics

To investigate the signal transfer from treated HaCat cells, supernatant was transferred to differentiated THP-1 cells. THP-1 are isolated leukemic monocytes and act like immune cells (Bosshart und Heinzelmann 2016). Treatment time of THP-1 cells were determined prior analysis and elucidated to 24h (Figure S16). To identify up- and downregulated biological processes and pathways related to inflammation and itch after secretome of treated HaCat cells were transferred to THP-1 cells a proteome analysis was performed.

After treatment with the MAPA, 3074 proteins were detected in total in pro-inflammatory induced THP-1 macrophages, with 395 proteins showing a p-value of less than 0.05. Resulting proteins where 146 proteins were downregulated, and 249 proteins were upregulated were analyzed using GESA and clustered afterwards by Cytoscape. Downregulated proteins were clustered in regulation of G-protein-coupled receptor signaling pathway (A1), the regulation of IL-1 β production and cellular defense response (A2), regulation of inflammatory response with e.g. ERK1/2 cascade, negative regulation of MAPK cascade and NF κ B signaling, cytokine production, cell migration and Toll-like receptor signaling pathway (A3). Upregulated protein clusters were interferon signaling (B1), cellular response to chemical and oxidative stress (B2) activation of p38 MAPK cascade and NF κ B signaling (B3) (Figure 36, S34).

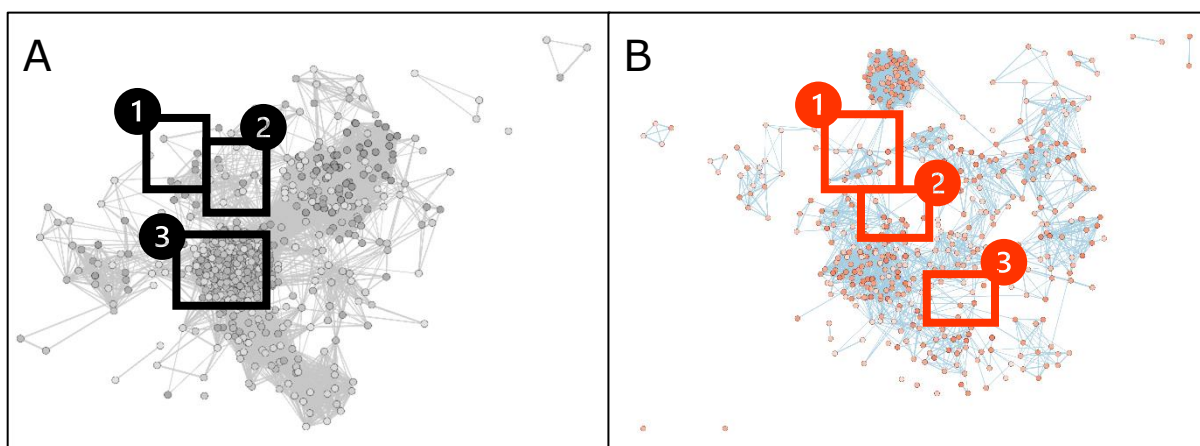


Figure 36: Enrichment map of downregulated (black) and upregulated (red) proteins in pro inflammatory induced THP-1 macrophages after treatment with secretome from HaCat cells treated with compound MAPA. All BPs and pathways enriched in inflammation induced THP-1 cells were clustered according to their function similarities using Cytoscape. Each node (circle) represents a distinct biological process (GO:BP) or pathway (REAC) involving between 5 and 350 genes. Color gradient describes the statistic linked to the identification of the biological processes or pathways. Numbers represents clusters of similar biological processes or pathway. A1: regulation of G-protein-coupled receptor signaling pathway; A2: regulation of IL-1 β production and cellular defense response; A3: regulation of inflammatory response; B1: interferon signaling; B2: cellular response to chemical and oxidative stress; B3: activation of p38 MAPK cascade and NF κ B signaling

In total, 3074 proteins were screened in differentiated THP-1 cells for the treatment with compound OPMA transfer, and 414 proteins fulfil the condition of $p < 0.05$. Of these, 181 downregulated and 233 upregulated proteins could be investigated and cluster of different processes of down and upregulated proteins could be analyzed. A downregulation of regulation with histamine secretion involved in inflammatory response (A1), Wnt signaling (A2) and cell cycle initiation (A3) could be investigated. Further, an upregulation of metabolic processes response (B1) and translation (B2) (Figure 37, S35). A closer look at the cluster of metabolic processes response revealed, for example, the upregulation of p38 MAPK cascade, apoptotic process, cell migration and hemostasis.

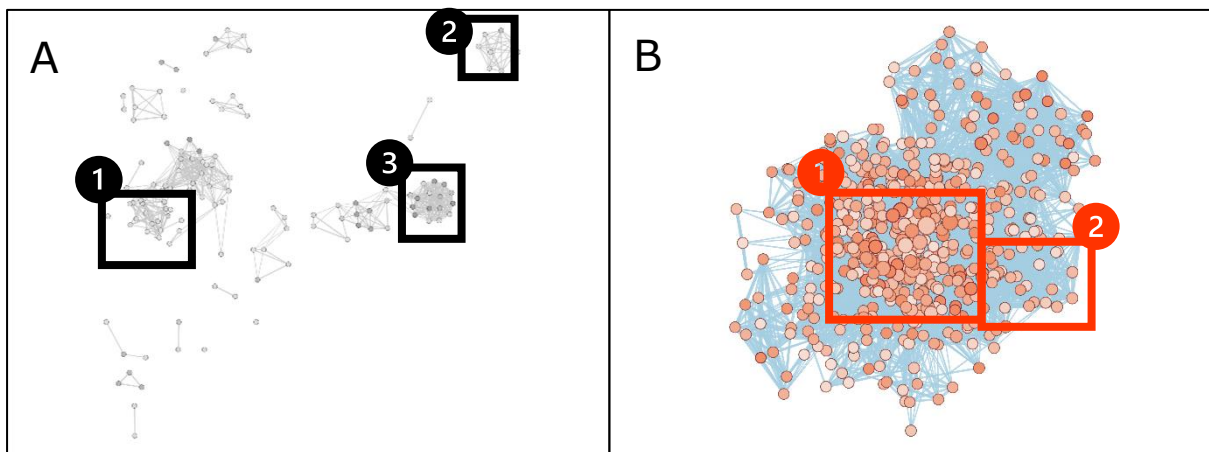


Figure 37: Enrichment map of downregulated (black) and upregulated (red) proteins in pro inflammatory induced THP-1 macrophages after treatment with secretome from HaCat cells treated with compound OPMA. All BPs and pathways enriched in inflammation induced THP-1 cells were clustered according to their function similarities using Cytoscape. Each node (circle) represents a distinct biological process (GO:BP) or pathway (REAC) involving between 5 and 350 genes. Color gradient describes the statistic linked to the identification of the biological processes or pathways. A1: regulation with histamine secretion involved in inflammatory response; A2: Wnt signaling; A3: cell cycle initiation. Upregulated protein clusters (red numbers) B1: metabolic process response; B2: translation. All mapped proteins fulfil the criterium of $p < 0.05$.

Proteome analysis of THP-1 cells after signal transfer of secretome of treated HaCat cells with MAPA and OPMA showed downregulated inflammatory response suggesting anti-inflammatory effect through treatment with MAPA and OPMA on THP-1 cells.

6.2.10 Secretome of treated HaCat cells significantly reduce inflammation response of THP-1 cells

Aprepitant and Fosaprepitant showed significant inhibition of secreted THP-1 downstream targets CCL20, IL-1 β and IL-18 after cell culture media transfer from HaCat cells and 24h treatment on THP-1 cells. Aprepitant reduced IL-1 β secretion by 28% and Fosaprepitant by 47% (Figure 38A) and CCL20 by 18% (Figure 38B). The secretion of IL-18 was reduced by Aprepitant by 48% and by Fosaprepitant by 71% (Figure 38C). The effect of MAPA and OPMA treated HaCat supernatant on THP-1 cells result in reduction of secreted IL-1 β cytokine concentration by 30% (Figure 38A). Reduced CCL20 secretion by 11% for MAPA and 10% by OPMA treatment (Figure 38B) compared to TNF- α induction. The transfer of NCE treated HaCat supernatant on THP-1 cells lead to a significant reduction of secreted IL-18 cytokine concentration by 79% by MAPA and 84% by OPMA compared to induction (Figure 38C).

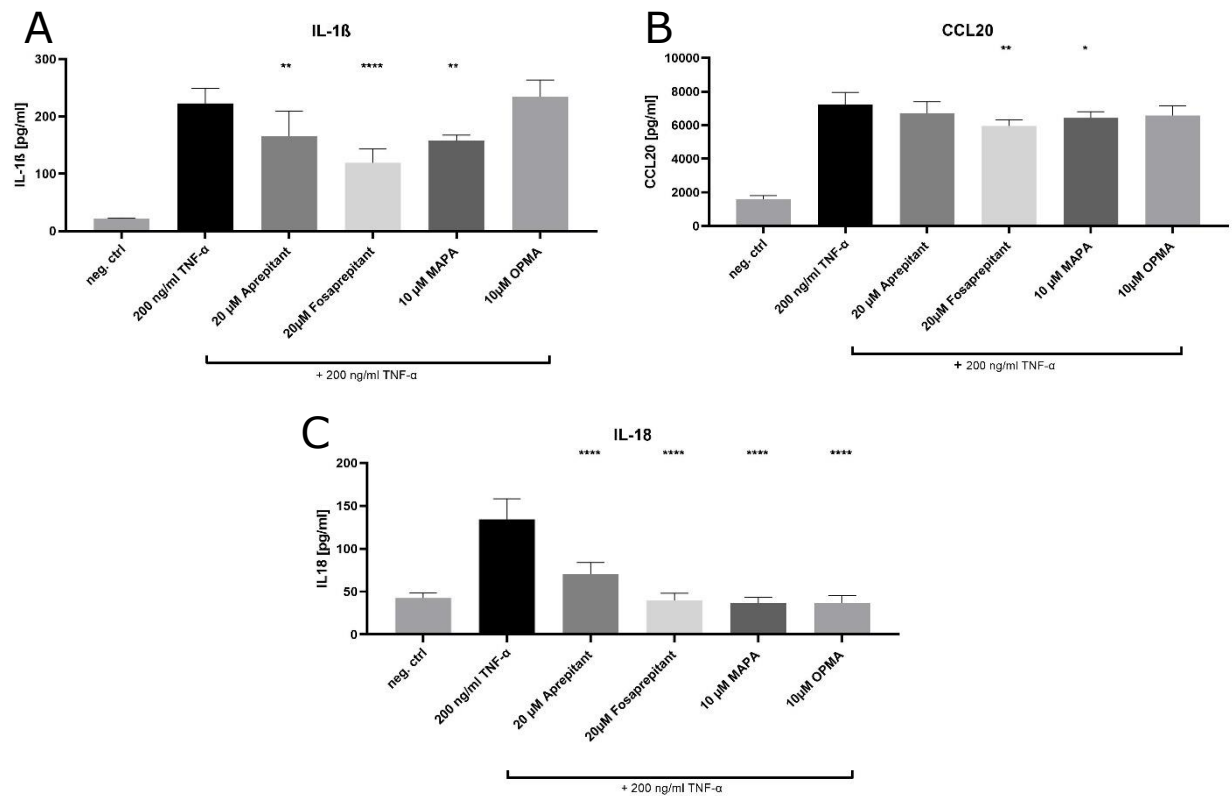


Figure 38: MAPA and OPMA treatment in cell culture media from HaCat cells inhibits the secretion. A: IL-1 β ; B: CCL20; C: IL-18. THP-1 were seeded in 96well plates and treated for 24h with supernatant from 48h treated HaCat cells in humidified atmosphere at 37°C and 5% CO₂. neg. ctrl served as solvent control of 0,2% DMSO. Supernatant was further used for Elisa analysis. (n=6, One-way ANOVA followed by $\alpha = 0.05$. Significances (****): $p < 0.0001$, (**): $p < 0.001$, (*): $p < 0.01$, (*) : $p < 0.05$, (ns): $p \geq 0.05$). Means \pm SD are shown.

Transferred secretome from treated HaCat cells to THP-1 cells indicates significantly reduced IL-1 β , IL-18 and CCL20 level suggesting a reduced pro-inflammatory cytokine secretion. Investigations in involvement of IL-1 β signaling in activation of caspase 1 activity were tested.

6.2.11 Confirmation of involvement of caspase 1 in processing IL-1 β

Activated monocytes like THP-1 cells release IL-1 β and caspase 1 after pro-inflammatory stimulation (Qu et al., 2007). Pro-inflammatory stimulation triggers caspase 1 activation and IL-1 β maturation (Broz and Monack 2011). Pro-IL-1 β polypeptide is post-translationally processed by caspase 1 to activate pro-inflammatory cytokine IL-1 β (Sutterwalla et al., 2006). This suggests that activation of caspase 1 and release of IL-1 β are closely related and here two NCEs were tested to demonstrate the relation of blocking caspase 1 activity to inhibit IL-1 β release.

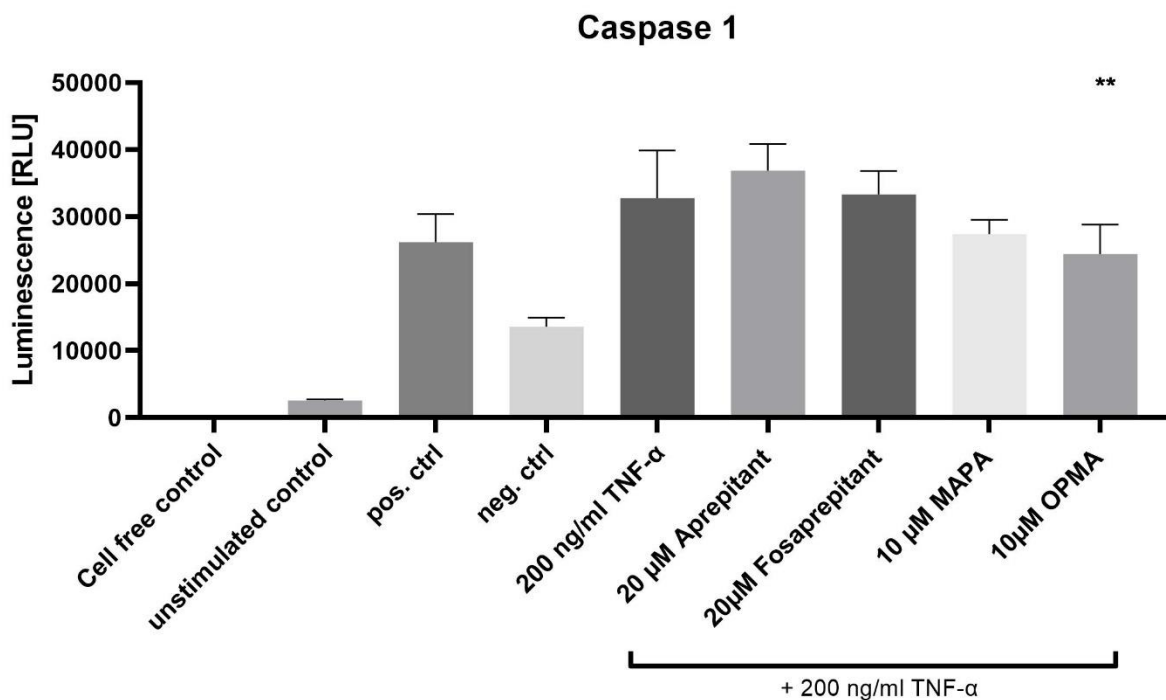


Figure 39: FPCM, TPCA and DPAAM result in decreased activity of caspase 1 comparable to controls. THP1 were seeded in 96well and differentiated for 48h. Treated for 3h with compounds and the activity of caspase 1 measured afterwards. 2μg/ml Alpha Hemolysin acts as positive control and 1μM VX765 acts as caspase 1 inhibitor (neg. ctrl). (n=6, One-way ANOVA followed by $\alpha = 0.05$. Significances (***): $p < 0.0001$, (**): $p < 0.001$, (*): $p < 0.05$, (ns): $p \geq 0.05$). Means \pm SD are shown.

As pro-inflammatory stimulation TNF- α increased activity of caspase 1 more than positive control alpha-hemolysin. Literature known control inhibitor Aprepitant and Fosaprepitant also increased activity of caspase 1. The two tested NCEs MAPA and OPMA reduced caspase 1 activity. OPMA showed significant decreased caspase 1 activity by 26% (Figure 39).

6.2.12 Elucidation of phosphorylated protein after supernatant transfer of treated HaCat cells to THP-1 cells

Activated MAPKs, PKB and TFs are involved in upregulating pro-inflammatory cytokines including Il-1 β , Il-18 or CCL20. Therefore, compounds like MAPA and OPMA were investigated on their potential effects on phosphorylation to determine its influence on signaling pathways after signal transfer from treated HaCat cells on THP-1 cells. MAPA and OPMA decreased the phosphorylation level of ERK in THP-1 cells after signal transfer from treated HaCat cells significantly by 62% with MAPA and 69% with OPMA treatment (Figure 40). These data suggest that the compounds MAPA and OPMA are likely to suppress phosphorylation of ERK in THP-1 cells after TNF- α treatment on HaCat cells. The literature known inhibitor Aprepitant showed a

significantly decreased phosphorylation of ERK by 73% and is suggesting that inhibitor and NCEs suppress the same signaling pathway.

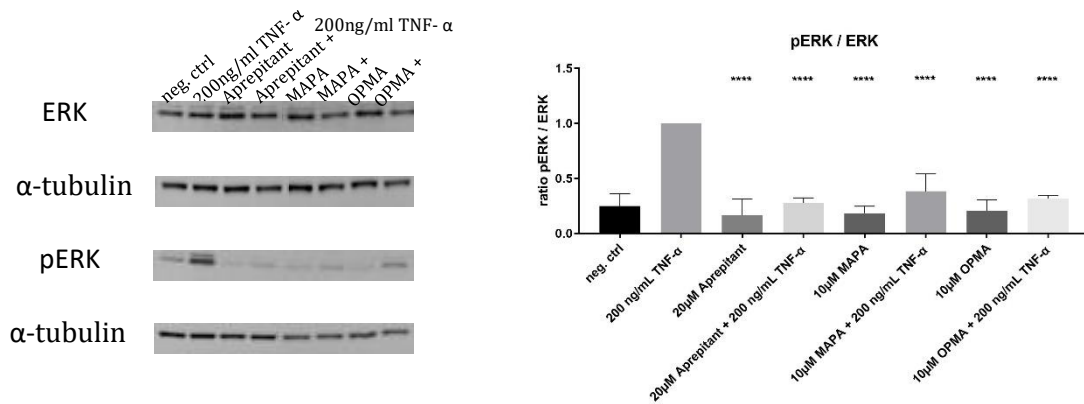


Figure 40: Quantification of ERK signaling pathway through treatment with inhibitors or NCEs MAPA and OPMA. THP-1 were seeded in 6well and treated for 24h with supernatant from 48h treated HaCat cells in humidified atmosphere at 37°C and 5% CO₂. Afterwards harvested and lysed in Lysis Buffer. Cell lysis were further used for protein concentration and Western Blot analysis. neg. ctrl served as solvent control of 0,2% DMSO. 20μg protein concentration were loaded. (n=3, One-way ANOVA followed by $\alpha = 0.05$. Significances (****): $p < 0.0001$, (***) : $p < 0.001$, (**): $p < 0.01$, (*) : $p < 0.05$, (ns): $p \geq 0.05$). Means \pm SD are shown.

Treated HaCat cell secretome transferred to THP-1 cells showed significantly reduced ERK phosphorylation level suggesting reduced pro-inflammatory signaling and further decreased cytokine secretion after MAPA and OPMA treatment.

7 Discussion

7.1.1 11 β HSD1 as molecular inflammatory target

In the present study we demonstrated three inhibitors FPCM, TPCA and DPAAM of 11 β HSD1 which significantly reduce pro-inflammatory downstream markers on skin cells. A multidisciplinary approach, including in silico binding experiments, proteomic analysis and quantification of phosphorylation level of signaling pathway proteins, was applied to the analysis of HaCat cells, primary keratinocytes and the signal transfer to immune like THP1 cells. The conversion from inactive cortisone to active cortisol is the main function of 11 β HSD1 (Koska et al., 2006; Gregory et al., 2020) and plays a crucial role in skin inflammation (Frick et al., 2004). Elevated activity leads to increased conversion of active cortisol and further to pro-inflammatory damaging effects on the surrounding tissue cells (Hardy et al., 2018; Bieber 1972; Gregory et al., 2020). Topical application as treatment of inflamed skin like psoriasis, atopic dermatitis or epidermolysis bullosa result in less side effects due to direct treatment with less metabolization (Thornton 2011). Small molecules as NCEs are a treatment strategy for skin barrier penetration due to their small and lipophilic characteristic (Bos and Meinardi 2000).

In silico experiments obtain insights in docking of small molecules on the protein target (Moro et al., 2016). Crystal structures include important information about the orientation and confirmation for inhibitor development (Thomas and Potter 2014). Several research groups have identified different classes and structures of potential 11 β HSD1 inhibitors with promising pharmacokinetic data (Sun et al., 2021). The in silico docking experiments in this study with FPCM, TPCA and DPAAM demonstrate the docking position compared to control inhibitor. The chemical structure of all three inhibitors point out a promising binding on the enzyme 11 β HSD1 (Figure 9) and therefore show a potential for inhibiting 11 β HSD1. To investigate further inhibitory effects of tested compound after binding additional analysis of proteome was conducted in context of inflammatory induction with TNF- α .

Induction of TNF- α has been used as a model to study inflammation signaling mechanisms and application for treatment of immune diseases (Jang et al., 2021, Page et al., 2018). Activation of TNFR1 as receptor for TNF- α can trigger different signaling complexes resulting in activation of NF κ B and MAPKs (Haas et al., 2009, Gerlach et al., 2011). The downstream function of this signaling is known to induce inflammation and immune defense against pathogens (Aggarwal et al., 2012, Brenner et al., 2015). Elevated expression of 11 β HSD1 in cells after TNF- α induced inflammation lead to increased levels of pro-inflammatory cytokine secretion downstream 11 β HSD1 (Hardy et al., 2016, Stegk et al., 2009, Hardy et al., 2008). To systemically identify and

quantify from the myriad of proteins in cells, the specific proteins and their temporal involvement in these processes (Yu et al., 2010) a proteomics analysis was performed with HaCat cells and primary keratinocytes induced with TNF- α and treated with FPCM, TPCA and DPAAM. After treatment with FPCM an upregulation in protein folding in HaCat cells was analyzed (Figure 10). Due to inflammatory stress inside the cell network of maintaining the homeostasis increasing unfolded proteins assemble and a transcriptional upregulation of folding proteins is regulated (Liu et al., 2012). In primary keratinocytes an upregulation of pro-inflammatory cytokines like IL-12 and pathway proteins like NF κ B and ERK were analyzed and is attributed to TNF- α induced inflammation (Figure 16) (Luo and Zhang 2017; Zhang and An 2009). Analyzed downregulated protein cluster in immune response, IL-27, IL-12 and IL-6 production effects an anti-inflammatory response to FPCM treatment in HaCat cells and primary keratinocytes (Bosmann and Ward 2013). Also, upregulation of kinase activity is associated with increased activity for MAPKs and NF κ B activity in inflammation (Karin 2005). After TPCA treatment an upregulation in kinase activity was analyzed in HaCat cells and primary keratinocytes which confirms an induction of induced inflammation with TNF- α . This increased NF κ B activity fits with the analyzed increased proteolysis activity which is involved in NF κ B regulation (Rothschild et al., 2019). Downregulation of immune effector processes, IL-12 production and NF κ B signaling assume an inhibitory effect after TPCA treatment (Figure 17). The epidermal growth factor is known for regulating signaling pathways and increased activity in inflammation (Choi et al., 2018; Pastore et al., 2008). Besides the downregulation of inflammatory beta:gamma signaling could be observed after treatment with DPAAM in HaCat cells (Figure 12). In primary keratinocytes a downregulation of toll like receptors assumes an inflammatory inhibition by DPAAM (Figure 18) (Liew et al., 2005). Tested inhibitors showed downregulating evidence in immune response and processes (Figure 10,11,12 + 16,17,18). To better understand 11 β HSD1 downstream effects after FPCM, TPCA and DPAAM treatment a quantification of literature known pro-inflammatory cytokines secreted by keratinocytes were analyzed. IL-6, IL-8 and CCL2 are highly expressed cytokines on inflammation side (Tomlinson et al., 2010; Wang et al., 2009). In this report, we showed that FPCM, TPCA and DPAAM are highly potent compounds for significantly reducing IL-6, IL-8 and CCL2 secretion as pro-inflammatory cytokines downstream 11 β HSD1 (Figure 13). Confirmation analysis in primary keratinocytes verifies the significant reduction in quantification of cytokines IL-6 and IL-8 (Figure 18). This confirms further the potent anti-inflammatory effect of tested inhibitors. To understand the chemical structure of tested inhibitors, molecules with analogue structure and similarity to DPAAM were investigated to inhibit downstream 11 β HSD1 cytokines. None of the analogue structures could decrease IL-6, IL-8 and CCL2 as pro-inflammatory cytokines. The adamantane structure of the molecule is thought to play a crucial role in effectivity. Beside DPAAM also TPCA

have an adamantane structure implemented. FPCM showed potent results even no adamantane, but an aromatic structure is implemented. The second side chain differed from planar structure by DPAAM compared to structural similar molecules. But compared to FPCM and TPCA no planar structural side chain is present. The minimum analog structure potentially assuring the efficacy is the center part of the molecules. Involved residues in the active site of 11 β HSD1 are Y183 and Ser170 (Yan et al., 2016; Thomas and Potter 2014). All three tested NCEs bind with their center oxygen double bond with Ser170. At the amino acid Y183 the adamantane structure of DPAAM and TPCA and the aromatic structure of FPCM bond (Figure 14) on the docking side of 11 β HSD1. However, the center parts and the second site chain of similar tested compounds from DPAAM series differ compared to DPAAM structure, suggesting a different binding. To examine the inhibition of tested compounds FPCM, TPCA and DPAAM on phosphorylation level of signaling proteins additional investigations in pathway analysis was performed.

The inhibition of central kinases in the signaling context of inflammatory pathway were Akt, Stat3, NF κ B or MAPKs like ERK and p38 (Kataoka 2009; Hodge et al., 2005; Cianciulli et al., 2016). Activation of Akt phosphorylates and additionally activates NF κ B (Tang et al., 2016) when induced by TNF- α . Activated NF κ B is known for promoting the activation of ERK and p38 (Tang et al., 2016). Elevated inflammation markers trigger the activation and phosphorylation of Stat3 and lead to the activation of the MAPK (Hillmer et al., 2017). In skin diseases like atopic dermatitis and psoriasis signaling via MAPKs, Akt, Stat3 an NF κ B are directly or indirectly involved in the regulation of cytokines (Tan et al., 2017; Zeze et al., 2022). In psoriasis Akt, Stat3, p38, ERK and NF κ B signaling pathways are described as central mediators involved (Zhang and Zhang 2018; Abdallah et al., 2021; Johansen et al., 2005) as well as in atopic dermatitis (Ko et al., 2022; Bao et al., 2013; Xiao et al., 2017; Tan et al., 2017). The activation of signaling pathways activate transcription factors and second messenger to further cascade the stimulation (Kataoka 2009). Due to connected pathways, inhibiting one pathway would suggest a measurable decreased inflammatory outcome. After treatment with FPCM, TPCA and DPAAM it is observed that ERK phosphorylation was downregulated (Figure 15). In fact, significantly decreased inflammatory cytokines involved in triggering inflammation in skin disorders like psoriasis and atopic dermatitis it could be assumed that these novel inhibitors reduce the inflammation by inhibiting the ERK pathway. Studies showed that inhibition of the ERK pathway restored decreased expression of filaggrin, alleviated epidermal thickness and decreased inflammatory cytokine release (Zeze et al., 2022; Huang et al., 2019). Combined, these data together with the results of this study inhibition of ERK pathway indicates the potential as a therapeutic target in skin diseases. The literature known inhibitor INCB-13739 showed a decreased phosphorylation of p38 suggesting that control and NCEs suppress different signaling pathways (Figure S38). Inhibition

of p38 pathway is involved in improvement of skin barrier function and decreased pro-inflammatory cytokine release (Tan et al., 2017). Both signaling pathways belong to MAPK (Roux and Blenis 2004) and inhibition leads to decreased cytokine expression and further improvement of skin barrier and inflammation (de Souza et al., 2014). For further information INCB-13739 together with one of the three novel inhibitors could be investigated for synergistic inhibition.

To transmit signaling from keratinocytes to immune cells in skin a method for mimicking this signaling transfer was elucidated to analyze secreted immune response. The secretome of treated HaCat cells were transferred on differentiated immune like cells to analyze the immune response. Used THP-1 cells are immortalized monocyte like cells and represent possibilities to investigate behavior in immune response (Bosshart and Heinzelmann 2016). It is known that immune cells like THP-1 cells express increased numbers of G-protein coupled receptors in inflammation for cytokine attraction (Sun and Ye 2012). In proteome analysis of transferred FPCM treated THP-1 cells a downregulation in G-protein coupled receptor regulation was investigated. An inhibitory impact of FPCM to inflammatory regulation is seen in downregulation of IL-12 expression and JAK-STAT pathway regulation (Figure 20).

Inflammatory trigger like induction with TNF- α lead to increased cytokine secretion and immune response (Jang et al., 2021). After TPCA transferred treatment to THP-1 cells a downregulation of IL-1 expression, immune and inflammatory response could be determined. Suggesting anti-inflammatory properties of TPCA in transferred triggered THP-1 cells (Figure 21). The main function of target 11 β HSD1 is to convert the hormone cortisone to cortisol which plays a crucial role in inflammation in elevated levels (Koska et al., 2006; Gregory et al., 2020). Upregulation of hormone secretion with treatment transfer to THP-1 cells suggests a possible treatment to reduce conversion of cortisone to reduce cortisol levels and further decrease inflammation in cells. Upregulation in interferon signaling and negative regulation of MAPK after transferred TPCA treatment suggesting an increased pro-inflammatory interferon signaling (Kopitar-Jerala 2017) and decreased regulation of MAPK signaling thus an anti-inflammatory impact. Similar to FPCM after transferred DPAAM treatment on THP-1 cells a downregulation in G-protein coupled regulation and IL-12 secretion was analyzed (Figure 22). Suggesting similar effect of both tested NCEs in context of regulation of inflammatory response. Upregulation in NF κ B signaling and epidermal growth receptor signaling leads to the assumption for pro-inflammatory response after transferred induction of TNF- α .

Downregulated inflammatory response after transferring secretome with tested compounds an analysis of literature known cytokines secreted from THP-1 cells were investigated. THP-1 cells secrete CCL20, IL-1 β and IL-18 after inflammatory activation (Heo et al., 2020; Gritsenko et al., 2020; Piccini et al., 2008) and as seen in Figure 23 novel inhibitors significantly decrease secreted

pro-inflammatory cytokines. Underpinning decreased Caspase 1 activity after treatment with tested inhibitors confirm decreased levels of IL-1 β and IL-18 (Figure 24) (Dinarello 2006). In this recent study we showed that inhibitors FPCM, TPCA and DPAAM are highly potent molecules due to significant decreased cytokines after signal transfer from keratinocytes to immune like THP-1 cells. ERK, p38, Akt, Stat3 and NF κ B signaling mediate induction of inflammatory cytokines in monocyte like THP-1 cells (Kurosawa et al., 2000; Liu et al., 2003; Chen et al., 2016; Kuuliala et al., 2016).

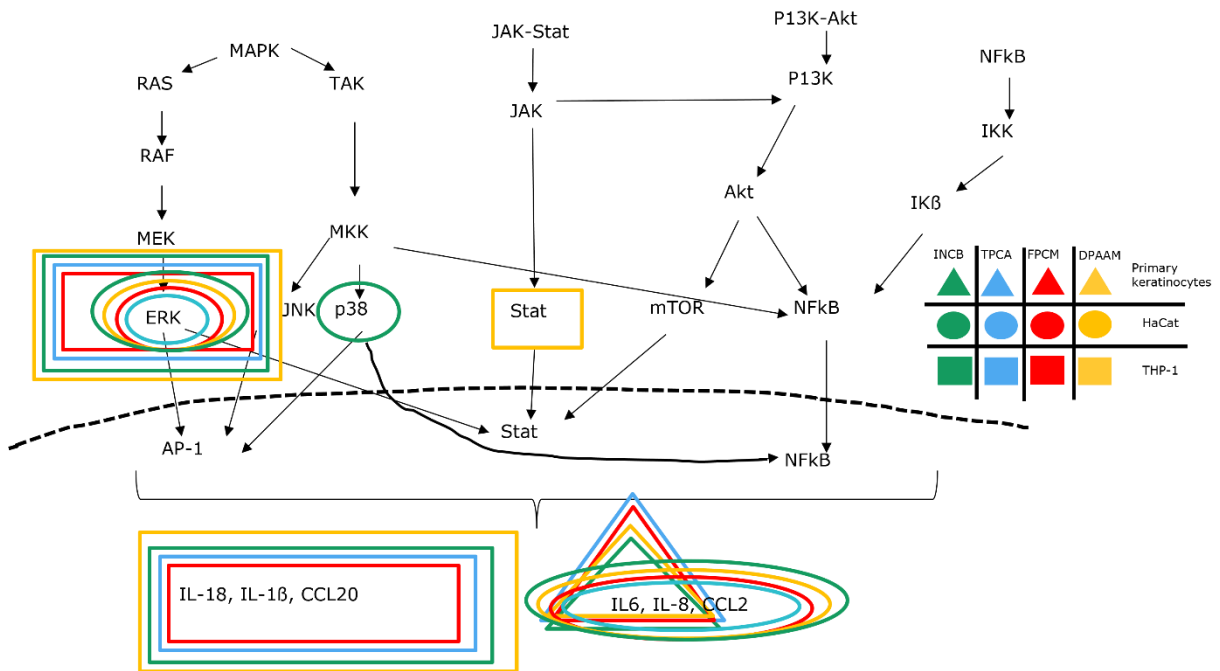


Figure 41: Schematic overview of different effect sides on pathway proteins and cytokines related to 11 β HSD1. Colors describe different compounds and shapes describe different cell type. Outlined proteins are downregulated in different cell types after compound treatment.

Skin diseases like psoriasis and atopic dermatitis have similarities to inflamed skin but there is no cure and only symptom treatment in systemic or oral application form studied (Bieber et al., 2022; Balato et al., 2009). Pathogenesis of atopic dermatitis is skin barrier dysfunction, neuroinflammation and dysregulation of the immune system and is related to the most common chronic skin diseases (Silverberg 2019; Cabanillas et al., 2017). An infringed skin barrier caused by scratching lead to pathogen infiltration and promotion of inflammation. Activation of immune cells trigger cytokine release and activate further cells for pro-inflammatory mediator secretion (Welsh et al., 2021). As topical treatment mainly glucocorticoids are used to treat inflammation (Bieber 2022; Welsh et al., 2021). Besides antibody treatments glucocorticoids are used for topical treatment in pro-inflammatory skin diseases like psoriasis (Balato et al., 2009). Glucocorticoids bind to glucocorticoid receptors (GR) which are expressed in most cell types and activate anti-inflammatory signaling. GR itself can bind to transcription factors and interact and suppress pro-

inflammatory gene expression. Also, glucocorticoid showed anti-inflammatory effects by modulating cytokine secretion by inhibiting p38 (Busillo et al., 2013; Bhattacharyya et al., 2007). GR interacts with NFkB and AP-1 and can block complex formation leading to repressing cytokine expression (Reily et al., 2006). High dose and long-term treatment of glucocorticoids have several negative side effects like muscle atrophy, growth retardation or diabetes (Rhen et al., 2005; Miner et al., 2005). Long-term treatment can lead to glucocorticoid resistance with loss of effectiveness in the affected tissue (Barnes et al., 2009; Cruz-Topete and Cidlowski 2014). Therefore, development of novel therapies for topical treatment of inflamed skin tissue may reduce side effects (Cruz-Topete and Cidlowski 2014).

The study showed the inhibition of different signaling proteins in several signaling pathways by small molecules (Figure 41). In this report we confirm the significant decrease of phosphorylation of ERK after FPCM, TPCA and DPAAM and Stat3 after DPAAM treatment in skin cells (Figure 25). Summarizing all tested novel NCEs showed potent and significant reduction of pro-inflammation in skin cells. Nevertheless, DPAAM showed more potent inhibition of phosphorylated signaling proteins after transferred to THP-1 cells (Figure 25B) and overall, a decreased cytokine concentration. But regardless all tested compounds showed potent inhibition and should be further investigated. The benefit of 11 β HSD1 potent inhibitors in skin inflammation linked with skin disorders like psoriasis and atopic dermatitis were investigated. We showed that treatment of 11 β HSD1 specific inhibitors impact activation and reduce secreted pro-inflammatory cytokines from HaCat and primary keratinocytes and further inhibit signal transfer to activate immune cells. These collected data support the progression of NCEs FPCM, TPCA and DPAAM as a key milestone in drug development for treatment of skin inflammation.

7.1.2 NK1R as molecular itch target

Itching and inflammation are common skin diseases associated with an unpleasant feeling that causes a desire to scratch (Song et al., 2018). There are numerous external and internal factors including pathogens or allergologic causes which lead to itch and inflammation (Olek-Hrab et al., 2016). A treatment most skin diseases like psoriasis, atopic dermatitis or epidermolysis bullosa are yet not matching the medical need for affected patients.

Small molecules are common in latest research for treating itch and inflammation in topic application (Soeberdt et al., 2020; Bieber et al., 2022). The tested small molecules from this study were preselected from an internal database through structural characteristics in affinity related to NK1R in different tissue but were not further investigated due to metabolic and toxicological limitation when delivered systemically. Due to their properties in solubility, molecular weight

and target affinity small molecules have efficient characteristics for treatment (Li & Kang 2020). For topical application the properties of the small molecules in molecular weight and lipophilic character are crucial for skin barrier penetration (Bos & Meinardi 2000). Topical application allow NCEs to penetrate the skin barrier and reduce biomarkers of skin inflammation and itch directly in affected tissue. The pathophysiology of inflammatory and itchy tissue involved in different skin disorders like psoriasis, epidermolysis bullosa or atopic dermatitis in the context of NK1R could prove an effective treatment for patients (Alam et al., 2021; Chiou et al., 2020). In this study, we show that the compounds MAPA and OPMA are highly potent and selective for NK1R that inhibits activation, signaling of downstream cytokines and signal transfer in cell-based assays.

NK1R is a key regulating receptor in pain (Iversen 1998), immune response (Mantyh 1991) and neurodegenerative diseases (Quartara and Maggi 1998). Missing data in structure and biochemistry are limiting factors in new drug development of targeting this receptor (Chen et al., 2019). An accomplished in silico experiment supports the hypothesis of target specific binding of the two tested compounds. Due to peptide characteristics of MAPA and OPMA binding was compared to agonist SP (Figure 26). After freezing the receptor model rotation, the tested compounds fit in the active site. This selectivity was confirmed in further investigations of the inhibition of activation of NK1R downstream Ca^{2+} flux after treatment with agonist SP. Influx of Ca^{2+} after binding of the receptor indicates specific downstream signaling activity (Morelli et al., 2020; Evans and Falke 2007). Observing a decreased Ca^{2+} flux after treatment with MAPA and OPMA (Figure 27) leads to confirmation of binding specific to NK1R and suggesting an inhibition of downstream signaling.

Activation of TNF- α downstream signaling cascade has usually been used as an inflammation model for investigating signaling mechanisms and treatment of immune diseases (Jang et al., 2021, Page et al., 2018). TNF- α belongs to the cytokine family and is a key mediator of inflammatory cascades (Chu 2013) and can trigger different signaling pathways like MAPKs and NF κ B (Haas et al., 2009, Gerlach et al., 2011). Inhibitor treatment for NK1R showed decreased inflammatory secretion suggesting a regulation of pro-inflammatory signaling (Chernova et al., 2009; Zhao et al., 2020). A proteome analysis to analyze systemic identification and quantification of the complement of proteins (Yu et al., 2010) was performed with HaCat cells and primary keratinocytes with induced inflammation by TNF- α and treatment with MAPA and OPMA. After treatment with MAPA an upregulation in Anaplastic lymphoma kinase (ALK) signaling, IL-1 processing and regulation of cilium assembly in HaCat cells was analyzed (Figure 28). Cilium is associated with signal transduction due to microtubule organization for cellular signaling. Upregulated cilium assembly indicates increased internal signaling as it is during inflammatory response (Fie et al., 2020). Cilium structure and transfer changes during inflammation and

upregulation after MAPA treatment suggests an increasing intracellular signaling transfer (Dinsmore and Reiter 2016). ALK signaling is known for increased activation during pro-inflammatory responses (Zeng et al., 2017) just as increasing IL-1 processing (Dinarello 2018). In primary keratinocytes an upregulation of cell junctions assembly, inflammatory response and regulation of JAK-STAT and IL-12 after treatment with MAPA could be detected (Figure 33). Cell junctions are a multi-protein complex maintaining a barrier while regulating permeability (Edelblum and Turner 2009). During itch and inflammation, the skin barrier is damaged, and the tight barrier protection and permeability is lost (Yang et al., 2020). The upregulation of cell junction assembly in primary keratinocytes after MAPA treatment suggests an increasing repair mechanism to build up the skin barrier (Brandner 2016). Detected upregulation of JAK-STAT signaling (Banerjee et al., 2017), IL-12 expression (Gee et al., 2009) and increased inflammatory response are resulting evidence to triggered inflammation in primary keratinocytes. Downregulation of protein ubiquitination after MAPA and OPMA treatment in HaCat cells indicates reduced inflammatory response and decreased TNF signaling pathways. Protein ubiquitination regulates activity of the inflammasome and controls activation of signaling pathways (Cockram et al., 2020). In primary keratinocytes upregulated epidermis development and keratinization after MAPA treatment suggest activated recovery mechanisms for damaged skin barrier and wound healing (Segre 2006; Takeo et al., 2015). After OPMA treatment in primary keratinocytes an increased MAPK/JNK activation, regulation of Wnt signaling and organelle organization could be determined (Figure 34). Upregulated MAPK/JNK and Wnt signaling confirm induced inflammation due to TNF- α treatment and reflect a signaling activation (Moens et al., 2013; Jridi et al., 2020). An increased organelle organization suggests an autophagy activation due to inflammation (Yao et al., 2021). In primary keratinocytes a downregulation in interferon production, cell junction assembly and keratinization was analyzed. Different to after treatment with MAPA cell junction assembly is downregulated suggesting decreasing recovery responses (Brandner 2016). Interferons are molecules which influence functions and activate immune response (Kopitar-Jerala 2017). Due to downregulating the interferon production an anti-inflammatory effect of OPMA could be suggested. Both tested novel compounds reduce induced inflammation in HaCat and primary keratinocytes lead to alteration in inflammatory related processes suggesting an impact in decreasing pro-inflammatory signaling.

To better understand of NK1R downstream effects after binding of MAPA and OPMA a quantification of literature known increased cytokines after induced inflammation were analyzed. Cytokines are soluble factors produced by cells to communicate with target cells about functions for instance in inflammation (Dinarello 2007). IL-6, IL-8 and CCL2 are highly expressed cytokines on inflammation side (Tomlinson et al., 2010; Wang et al., 2009). To examine the signaling of NK1R

the downstream cytokines IL-6, IL-8 and CCL2 were measured after treatment with MAPA and OPMA and showed significant reduction in HaCat cells (Figure 30). Also, after treatment of primary keratinocytes a significant decrease of IL-6 and IL-8 could be confirmed (Figure 35). Decreasing cytokine concentration confirms the inhibitory effect (Taherkhani et al., 2020) of novel inhibitors elucidated in binding specificity and proteome analysis. To find out more about the chemical structure of novel inhibitors MAPA and OPMA five similar molecules to OPMA were tested on their efficacy to decrease pro-inflammatory cytokines. OPMA showed in cell-based assays a more potent inhibitory effect of reduction in pro-inflammatory cytokines and phosphorylation level of proteins. Due to additional benzyl rings in the similar structures, it is suggesting that these may negatively influence the binding on these molecules. Due to large side chains and different stereocenter of two tested similar molecules it is suggested to not fit in the binding pocket and are unable to bind properly (Stank et al., 2016) (Figure 31).

To investigate signaling pathways downstream NK1R which lead to decreased inflammatory cytokine secretion phosphorylation levels of signaling pathway proteins were evaluated. Signaling pathways Akt, Stat3, NFκB or MAPKs like ERK and p38 are literature known for their phosphorylation at inflammation side (Kataoka 2009; Hodge et al., 2005; Cianciulli et al., 2016) and their cross-activation (Tang et al., 2016; Hillmer et al., 2017). Signaling pathways like MAPKs, Akt, Stat3 and NFκB are directly or indirectly involved in cytokine secretion of skin diseases like atopic dermatitis and psoriasis (Tan et al., 2017; Zeze et al., 2022). In skin disease like epidermolysis bullosa MAPKs p38 and ERK and NFκB are involved (Uitto et al., 2010, Russell et al., 2010; Ludwig 2017). In skin disease psoriasis Akt, Stat3, p38, ERK and NFκB signaling pathways are involved (Zhang and Zhang 2018; Abdallah et al., 2021; Johansen et al., 2005) as in atopic dermatitis (Ko et al., 2022; Bao et al., 2013; Xiao et al., 2017; Tan et al., 2017). An accomplished clinical trial published 2020 from Chiou et al., showed an epidermolysis bullosa related itch improvement after oral intake of NK1R inhibitor Serlopitant (Chiou et al., 2020). Serlopitant is a NK1R-antagonist, originally developed for chronic use in treatment of overactive bladder and showed significantly reduced itch in patients after Aprepitant treatment (Pariser et al., 2020, Ständer et al., 2019). Structural analogies of Aprepitant and Serlopitant on chemical side chain and similar molecular weight makes them compare well (Pojawa-Golab et al., 2019). Further they implement a new clinical trial with increased patient number to achieve statistical significance (NCT03836001). In this study, after MAPA and OPMA treatment decreased phosphorylated levels of ERK and NFκB could be observed (Figure 30). Based on cross-activation of different signaling pathways it could be suggested that a decrease in phosphorylation of NFκB and ERK lead to measured inhibited inflammatory signaling cascades and a decreased secretion of downstream pro-inflammatory cytokines IL-6, IL-8 and CCL2 like analyzed. Although Chiou et

al., (2020) showed itch improvement after oral treatment, systemic treatment in this study showed decreased pro-inflammatory cytokine secretion and decreased phosphorylation levels. Since itch and inflammation act together (Wong et al., 2017) an itch improvement could be suggested after treatment with MAPA and OPMA. Further investigations of topic treatment in in vivo studies should confirm recent results in improvement of itch and inflammation.

To mimic the signal transfer from cells from the epidermis to immune cells located in the dermis, we developed a model for signal transfer from treated HaCat cells to THP-1 cells in cell culture. After treatment with elucidated novel inhibitors the supernatant of HaCat cells were transferred to differentiated THP-1 cells to analyze up- and downregulation of inflammatory processes and signaling. To get an overview of involved cellular processes related to inflammation a proteome analysis with treated THP-1 cells. After MAPA treatment a downregulation in G-protein coupled receptor regulation, IL-1 β regulation and inflammation response of ERK, MAPK and NF κ B. G-protein coupled receptors are known for their affiliation to inflammatory response (Stevenson et al., 2014). Due to the downregulation of G-protein coupled receptor regulation it is suggested that G-protein coupled receptor NK1R is also downregulated. Further downregulated stimuli in IL-1 β production and inflammatory response of ERK, MAPK and NF κ B fits with downregulation in NK1R signaling (Park et al., 1999; Yu et al., 2002; Okabe et al., 2000). Investigated upregulation of interferon signaling, chemical and oxidative stress response and activation of p38 and NF κ B after MAPA treatment is suggested to be triggered by induction of inflammation through TNF- α treatment (Haas et al., 2009, Gerlach et al., 2011; Yarilina and Ivashkiv 2011). OPMA treatment leads to analyzed downregulation of histamine secretion in inflammatory response, Wnt signaling and cell cycle initiation suggesting decreased inflammatory signaling response. Histamine is a known modulator for pro-inflammatory response with variation of G-protein coupled receptors related to itch and inflammation (Branco et al., 2018). Downregulation of Wnt signaling is also related to histamine secretion (Diks et al., 2003) as well as cell cycle initiation as inflammatory response (Baselet et al., 2017). Baselet et al., 2017 compared X-ray with IR triggered inflammation in epithelial cells and showed increased IL-6 and CCL2 concentrations with cell cycle arrest in dose dependency. Compared with TNF- α induced inflammation an increased level of IL-6 and CCL2 could be determined in HaCat cells suggesting an impact on signal transferred THP-1 cells. Upregulated translation and metabolic process response including p38, apoptosis and cell migration after OPMA treatment are potentially related to TNF- α induced inflammation in secretome transferred THP1 cells (Mazumder et al., 2010; Chu 2013). Gene expression of cytokines is elevated after pro-inflammatory induction (Chu 2013) and is also analyzed in this proteome analysis.

The pro-inflammatory biomarkers CCL20, IL-18 and IL-1 β were analyzed as downstream targets secreted from THP-1 cells (Heo et al., 2020; Gritsenko et al., 2020; Piccini et al., 2008). Treatment with MAPA and OPMA showed a significant reduced secreted pro inflammatory biomarker concentration (Figure 38). MAPA showed decreased secretion of CCL20, IL-18 and IL-1 β compared to OPMA with significant decreasing IL-1 β secretion. Underpinning the significant decrease of Caspase 1 activity after OPMA treatment confirm levels of IL-1 β and IL-18 (Dinarello 2006) (Figure 39). This study showed that novel inhibitors MAPA and OPMA are highly potent molecules to significantly decrease cytokines after transferred and mimicked signal transfer downstream NK1R, ERK, p38, Akt, Stat3 and NF κ B signaling mediate induction of inflammatory cytokines in monocyte like THP-1 cells (Kurosawa et al., 2000; Liu et al., 2003; Chen et al., 2016; Kuuliala et al., 2016). In this study the signaling pathway ERK was significantly reduced in phosphorylation level after signal transfer of MAPA and OPMA treatment (Figure 40). Even THP-1 cells act only limited as immune cells the resulting downregulation of immune response after transferred MAPA and OPMA treatment proceed as first indicator for reducing pro-inflammatory and itch evidence.

Chronic itch can be transmitted by histaminergic and/or non-histaminergic nerve fibers. Histamine plays a crucial role in histamine-1 and histamine-4 receptor mediated itch. Both histamine receptors regulate immunomodulatory activities (Cataldi et al., 2014; Bieber et al., 2022). Keratinocytes and immune cells express a variety of receptors like G-protein coupled receptor or cytokine receptor for numerous itch mediators like proteases, neuropeptides and cytokines. The activation of receptors lead the cells to increased release of pro-inflammatory cytokines and enhanced itch response (Papanikolaou et al., 2021).

Psoriasis, atopic dermatitis and epidermolysis bullosa are common skin diseases with similarities in inflamed skin tissue and scratching behavior due to itch. In all three skin diseases is no completely cure and only symptom treatment in systemic or oral application form researched (Bieber et al., 2022; Prodinge et al., 2019; Balato et al., 2009).

Epidermolysis bullosa is caused by different mutations in the components of the cytoskeletal keratin intermediate filaments with multiorgan involvement affecting most epithelialized tissue (Prodinge et al., 2019; Bruckner-Tuderman et al., 2013). Leading to a high lethality and morbidity in numerous subvariants and only symptomatic treatment therefore causative treatment options are urgently required (Murell 2010). Little is known in signal transduction of epidermolysis bullosa. Increased phosphorylation of ERK, Akt and p38 have been noted in affected patient skin samples (Hellberg et al., 2013). In addition, inflammation solving mechanisms in myeloid cells have been identified to be essential for inflammation (Kim et al., 2011). Besides, corticosteroids are still the main symptom treatment. A promising target is the inhibition of, the in EB skin

increased esterase, PDE4 with substances like Rolipram, Roflumilast or Apremilast. PDE4 degrades cAMP in inflammatory cells or keratinocytes and supports pro-inflammatory mechanisms (Figure 40). Inhibition of PDE4 increases the intracellular second messenger concentration of cAMP following activation and phosphorylation of transcription factor resulting in a decrease of pro-inflammatory cytokines (Koga et al., 2016). Furthermore, concentration of matrix metalloproteinase 9 decreased and anti-inflammatory mediators increased by PDE4 inhibition (Oger et al., 2005; Kwak et al., 2005). Also, activation of NFκB and phosphorylation of MAPK are hindered through PDE4 inhibition (Sousa et al., 2010).

Atopic dermatitis is related to the most common chronic skin diseases and belongs to atopic disorders including allergic circumstances (Silverberg 2019). Pathogenesis of atopic dermatitis is a combination of skin barrier dysfunction, neuroinflammation and dysregulation of the immune system (Cabanillas et al., 2017; Welsh et al., 2021). Scratching damages the skin barrier and pathogens can penetrate easier and promote enhanced inflammation. Activated immune cells release more cytokines and activate further cells to release increased pro-inflammatory mediators and neuropeptides which promotes inflammation and barrier damage (Bieber 2022; Welsh et al., 2021). Topical therapies include glucocorticoids, calcineurin inhibitors and PDE4 inhibitor (Figure 42). More recently small molecules for inhibition of Janus-kinase have provided first promising results (Welsh et al., 2021).

A main characteristic in psoriasis is an inflammation leading to dysfunctional differentiation and uncontrolled keratinocyte proliferation. Alterations in immune responses lead to development of psoriatic inflammation (Balato et al., 2009). Also, activation of the innate immune system with autoimmune reactions lead to increased autoimmune inflammation, potentiating inflammatory mechanisms (Liang et al., 2017). Studies revealed that Stat3 and NFκB are highly elevated in psoriatic inflammation, involved in the production of pro-inflammatory cytokines (Gaffen 2009). Antibody treatments like Guselkumab or Brodalumab for Immunglobulin-G treatment against different pro-inflammatory cytokines, Apremilast as PDE4 inhibitor or Acitretin by receptor binding of retinoids for normalization of differentiation and proliferation of keratinocytes are new tested treatments in context of psoriasis (Balato et al., 2009) (Figure 42).

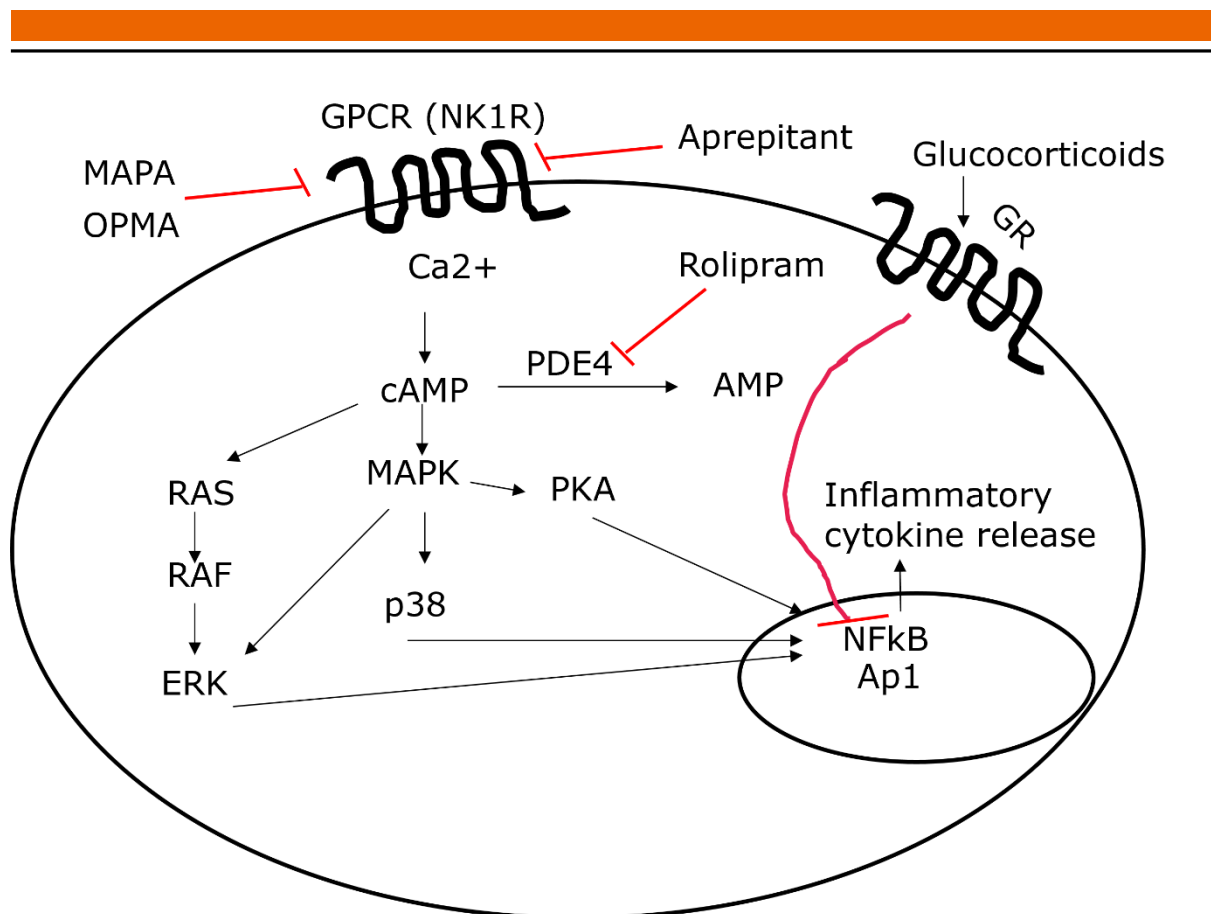


Figure 42: Schematic overview of compound effects related to NK1R. Aprepitant and Rolipram as literature described drugs for epidermolysis bullosa and itch treatment compared to tested novel compounds MAPA and OPMA and standard treatment with glucocorticoids.

In all three skin diseases the mentioned and investigated signaling pathways play a crucial role in activating cytokine release or phosphorylation of further signaling pathways. Studying the significantly reduced secretion of pro-inflammatory cytokines and phosphorylation of pro-inflammatory signaling pathways show possible treatments aspects for skin disorders. In this study NCEs MAPA and OPMA showed significant reduction of pro-inflammatory cytokines in HaCat, primary keratinocytes and after signal transfer in THP-1 like immune cells. In addition, phosphorylation level of pro-inflammatory cytokines are decreased which leads to suggest of an anti-inflammatory characteristic. Summarizing the effects of MAPA and OPMA treatment on reduction of pro-inflammatory and itch response, OPMA showed promising data related to cytokine reduction and downregulation of inflammatory response on all three tested cell types. Further efforts are underway to quantify and confirm the reduced pro-inflammatory signaling of NK1R after MAPA and OPMA treatment in an in vivo atopic dermatitis mouse model. Topical application of formulated compounds alternative to corticosteroids and unspecific molecules might improve treatment of inflammation and itch in effected mice directly on an effected target site. This study is the first demonstration of skin cell-based assay investigation of MAPA and OPMA in context of skin inflammation and itch.

We hypothesize that topical treatment of NK1R specific inhibitors impact activation and reduce secreted pro-inflammatory cytokines from keratinocytes and further inhibit signal transfer to activate immune cells and improve itch. These data support the evaluation of MAPA and OPMA as potential drug candidates for treatment of skin inflammation and itch.

8 Executive summary

The aim of this study was to identify inhibitor compounds for target 11 β HSD1 and NK1R and understand the mode of action and the characteristic of these compounds by analyzing signaling pathways, effects in primary cells and signal transfer to immune like cells. Signaling pathways and secreted biomarkers are of interest to determine the efficacy of inhibitor compounds and to understand signaling transfer in detail. First, docking analysis of tested compounds were elucidated and showed promising binding of compounds to 11 β HSD1 or NK1R. Accordingly, a quantitative proteome analysis was conducted to get an overview about up and down regulated proteins after compound treatment in combination with inflammatory induction. Proteome analysis indicated downregulated proteins related to inflammation and itch in keratinocyte like HaCat cells and primary cells evenly. For detailed analysis in known pro-inflammatory cytokines, keratinocyte like HaCat cells and primary cells were investigated on their pro-inflammatory biomarker secretion after induction with TNF- α and treatment with compounds. Compound treatment showed significant inhibited secretion of IL-6, IL-8 and CCL2 downstream target as known pro-inflammatory biomarkers in HaCat cells and primary keratinocytes. Further, phosphorylation level of known inflammatory signaling pathways were elucidated and showed also decreased activation. Even though no significance could be determined a clear downregulation of phosphorylated ERK levels were analyzed.

To mimic the signal transfer with different involved skin cells, a model for signaling transfer was elucidated and secretome of treated HaCat cells were transferred to immune like THP-1 cells. Proteome analysis indicated downregulated proteins related to inflammation and itch after treatment with identified 11 β HSD1 and NK1R inhibitors. Further, transmitted inhibitory signaling from compound treated HaCat cells showed downstream 11 β HSD1 and NK1R significant reduction of IL-1 β , IL18 and CCL20 as pro-inflammatory biomarkers in immune cells. Phosphorylation level of signaling pathways showed significant decreased activation of ERK phosphorylation and with DPAAM treatment decreased phosphorylated Stat3 level, suggesting a downregulation in inflammation and itch related cytokine secretion and signaling transmission. Summarizing this study, results show that identified compounds have a significant impact in downregulation of pro-inflammatory cytokine release and phosphorylation of signaling proteins downstream 11 β HSD1 and NK1R. The two compounds MAPA and OPMA related to NK1R, and the three compounds FPCM, TPCA and DPAAM related to 11 β HSD1 showed promising binding data and significant reduction of pro-inflammatory related processes. Further analysis showed transmitted inhibition of pro-inflammatory cytokine secretion and phosphorylated signal proteins demonstrating a potential inhibition of inflammation and itch related processes.

9 Outlook

For a deeper understanding of how the signaling from triggered keratinocytes influence neuronal cells, a model for signal transfer from induced keratinocytes to neuronal cells need to be tested. Currently, compound efficacy testing as a proof of principle is accomplished by each cell type in 2D cell culture independently. To mimic a signaling transfer more cell types beside keratinocytes need to be evaluated in context of inflammation and itch. Signal transfer from inhibitor treated keratinocytes to immune like cells showed a substantial impact on transmitted inflammatory biomarkers. To confirm inhibitory signaling effects investigations on neuronal like cells need to be accomplished. In vivo peripheral neuronal cells play a crucial role in signal transfer of pain and itch and further signal transmission to the brain. Results of signal transfer model can provide evidence on efficacy and biological response related to identified compounds in a more in vivo related context.

Initially to an in vivo study, compounds were tested on the penetration ability on different skin types like artificial skin membrane, mouse skin and human skin transplants. Different skin types differ in their resorption due to their percutaneous penetration ability. Further, results on ex vivo skin types indicate penetration ability for in vivo skin experiments. In vivo studies with identified inhibitors need to investigate penetration, metabolic effects and efficacy on pathogenic skin. To test the efficacy of the identified inhibitors an in vivo study on atopic dermatitis mice is ongoing. Target NK1R is related to itch and inflammation in skin diseases and known inhibitors are used for treatment in different skin pathologies. In the context of former penetration results identified NK1R compounds are formulated and applied topically on atrophic skin lesions. Scratching behavior, wound healing, blood cytokine concentration and overall health and side effects are analyzed and evaluated. Expecting positive results of identified compounds independently more investigations related to synergistic effects could be determined. Result dependent further in vivo experiments could be planned with synergistic compounds. Promising data from this study about DPAAM as 11 β HSD1 inhibitor and OPMA as NK1R inhibitor could formulated and combined applied on pathogenic skin lesions to analyze synergistic effects. Also, compound combinations with known inhibitor from literature together with new identified compounds could be tested dependent on further penetration results.

10 Appendix

10.1 Abbreviations

µg	Microgram
µL	Microliter
nm	Nanometer
µm	Micrometer
mm	Millimetre
kDa	Kilodalton
min	Minute
h	Hour
PBS	Phosphate buffered saline
SC	Stratum Corneum
SD	Standard Deviation
UV	Ultra-Violet
ECM	Extracellular-Matrix
AD	Atopic Dermatitis
CA ²⁺	Calcium
TLR	Toll like receptor
TF	Transcription factor
IL	Interleukin
CCL	CC-Chemokine-Ligand
SP	Substance P
NK1R	Neurokinin Receptor 1
11βHSD	11β-Hydroxysteroid Dehydrogenase
CHO	Chinese Hamster Ovary cells
HRP	Horseradish peroxidase
rpm	Rounds per minute
mM	Milli Mol
ATP	Adenosine Triphosphate

CO ₂	Carbon Dioxide
ELISA	Enzyme-linked Immunosorbent-Assay
MIP3	Macrophage inflammatory protein 3
TMT	Tandem Mass Tag
NMR	Nuclear Magnetic Resonance
HBSS	Hank's Balanced Salt Solution
ANOVA	Analysis of Variants
MOE	Molecular Operating Environment
REAC	Reactome
GO:BP	Gene Ontology: Biological Processes
°C	Celcius
RPMI	Roswell Park Memorial Institute
DMEM	Dulbecco's Modified Eagle's Medium
FCS	Fetal Calf Serum
cAMP	Cyclic adenosinmonophosphate
PDE4	Phosphodiesterase-4
NGF	Neuronal growth factor
PKC	Proteinkinase C
IP3	Inositoltriphosphate
NCE	New Chemical Entity
TNF- α	Tumor necrosis factor alpha
ER	Endoplasmatic reticulum
H6PDH	Hexose6 Dehydrogenase
NADPH	Nicotinaminde adenine dinucleotide phosphate
ACTH	Adenocorticotropic hormone
CRH	Cortisol releasing hormone
TRPA1	transient receptor potential ankyrin 1
ERK	Extracellular-signal regulated kinases
STAT	Signal transducers and activators of transcription

JAK	Januskinases
MAPK	Mitogen activated protein kinases
NFkB	Nuclear Factor kappa B
AP-1	Actiavator protein 1
TLR	Toll like receptor
PRR	Pattern recognition receptor
PAMP	Pathogen associated molecular pattern
DAMP	Danger associated molecular pattern
PMA	Phorbol 12-myristate 13-acetate
2D	Two dimensional
LC	Liquid Chromatography
MS	Mass spectrometry
RT	Room temperature
V	Volt
MW	Mega Watt
BP	Biological Process
TACR1	Tachikinin receptor 1

10.2 List of figures

Figure 1: Morphology of the skin with epidermis, dermis and hypodermis.....	4
Figure 2: Morphology of the epidermis.....	5
Figure 3: Symptoms and mediators in inflammation.....	8
Figure 4: Schematic overview of pro-inflammatory signaling pathways.....	9
Figure 5: Causes of pro-inflammatory response.....	10
Figure 6: Itch cycle	11
Figure 7: Activation of 11 β HSD1.....	13
Figure 8: Function of NK1R in skin.....	15
Figure 9: Compounds FPCM (A), TPCA (B), DPAAM (C) docked to the active site of 11 β -HSD1...	25
Figure 10: Enrichment of down (black) and upregulated (red) proteins after FPCM treatment..	27
Figure 11: Enrichment of down (black) and upregulated (red) proteins after TPCA treatment. .	28
Figure 12: Enrichment of down (black) and upregulated (red) proteins after DPAAM treatment	28
Figure 13: Reduction of pro-inflammatory biomarkers after pre-treatment using FPCM, TPCA and DPAAM after stimulation with TNF- α	30
Figure 14: Quantification of ERK and phosphorylated ERK after treatment with FPCM, TPCA and DPAAM.....	32
Figure 15: Enrichment of down (black) and upregulated (red) proteins after FPCM treatment..	33
Figure 16: Enrichment of down (black) and upregulated (red) proteins after TPCA treatment. .	34
Figure 17: Enrichment of down (black) and upregulated (red) proteins after DPAAM treatment.	35
Figure 18: FPCM, TPCA, DPAAM treatment reduced the downstream 11 β HSD1 effector targets Il- 6, Il-8 and CCL2.....	36
Figure 19: Enrichment of down (black) and upregulated (red) proteins in pro inflammatory induced THP-1 macrophages after treatment with secretom from HaCat cells treated with compound FPCM.....	37
Figure 20: Enrichment of down (black) and upregulated (red) proteins in pro inflammatory induced THP-1 macrophages after treatment with secretom from HaCat cells treated with compound TPCA.	38

Figure 21: Enrichment of down (black) and upregulated (red) proteins in pro inflammatory induced THP-1 macrophages after treatment with secretom from HaCat cells treated with compound DPAAM.....	39
Figure 22: Treatment with FPCM, TPCA and DPAAM cell culture media from HaCat cells to THP-1 cells result in decreased secretion.	40
Figure 23: FPCM, TPCA and DPAAM result in decreased activity of caspase 1 in THP-1 cells comparable to controls.....	41
Figure 24: Quantification of A: ERK and phosphorylated protein and B: Stat3 and phosphorylated Stat3 after treatment with FPCM, TPCA and DPAAM in THP-1 cells.	42
Figure 25: Manually modelled binding hypotheses of hit molecules MAPA and OPMA (center, bottom) to NMR models of the NK1 receptor with reference to Substance P (top).....	44
Figure 26: IC50 of MAPA and OPMA calculated based on the Ca ²⁺ concentration after NK1R activation.	45
Figure 27: Enrichment of down (black) and upregulated (red) proteins after MAPA treatment.	46
Figure 28: Enrichment of down (black) and upregulated (red) proteins after OPMA treatment.	47
Figure 29: Reduction of pro-inflammatory biomarkers after pre-treatment using MAPA and OPMA after stimulation with TNF- α	48
Figure 30: Quantification of A: NF κ B and phosphorylated protein and B: ERK and phosphorylated protein after treatment with MAPA and OPMA.....	50
Figure 31: Enrichment of down (black) and upregulated (red) proteins after MAPA treatment.	51
Figure 32: Enrichment of down and upregulated proteins after OPMA treatment.	52
Figure 33: Decreasing secretion of biomarkers through treatment with MAPA and OPMA.....	53
Figure 34: Enrichment map of downregulated (black) and upregulated (red) proteins in pro inflammatory induced THP-1 macrophages after treatment with secretome from HaCat cells treated with compound MAPA.	55
Figure 35: Enrichment map of downregulated (black) and upregulated (red) proteins in pro inflammatory induced THP-1 macrophages after treatment with secretome from HaCat cells treated with compound OPMA.....	56
Figure 36: MAPA and OPMA treatment in cell culture media from HaCat cells inhibits the secretion.	57
Figure 37: FPCM, TPCA and DPAAM result in decreased activity of caspase 1 comparable to controls.....	58



Figure 38: Quantification of ERK signaling pathway through treatment with inhibitors or NCEs
MAPA and OPMA. 59

Figure 39: Schematic overview of different effect sides on pathway proteins and cytokines related
to 11 β HSD1..... 64

Figure 40: Schematic overview of compound effects related to NK1R. 72

10.3 References

1. Abdallah, H. B., Johansen, C., & Iversen, L. (2021). Key Signaling Pathways in Psoriasis: Recent Insights from Antipsoriatic Therapeutics. *Psoriasis: Targets and Therapy*, 11, 83.
2. Agelopoulos, K., Rüländer, F., Dangelmaier, J., Lotts, T., Osada, N., Metzke, D., ... & Ständer, S. (2019). Neurokinin 1 receptor antagonists exhibit peripheral effects in prurigo nodularis including reduced ERK 1/2 activation. *Journal of the European Academy of Dermatology and Venereology*, 33(12), 2371-2379.
3. Aggarwal, B. B., Gupta, S. C., & Kim, J. H. (2012). Historical perspectives on tumor necrosis factor and its superfamily: 25 years later, a golden journey. *Blood, The Journal of the American Society of Hematology*, 119(3), 651-665.
4. Alam, M., Buddenkotte, J., Ahmad, F., & Steinhoff, M. (2021). Neurokinin 1 receptor antagonists for pruritus. *Drugs*, 81(6), 621-634.
5. Alan, I. S., & Alan, B. (2018). Side effects of glucocorticoids. *Pharmacokinetics and adverse effects of drugs-mechanisms and risks Factors*, 93-115.
6. Anderson, E. D., Sastalla, I., Earland, N. J., Mahnaz, M., Moore, I. N., Otaizo-Carrasquero, F., ... & Myles, I. A. (2018). Prolonging culture of primary human keratinocytes isolated from suction blisters with the Rho kinase inhibitor Y-27632. *PLoS One*, 13(9), e0198862.
7. Ansar, W., & Ghosh, S. (2016). Inflammation and inflammatory diseases, markers, and mediators: Role of CRP in some inflammatory diseases. In *Biology of C reactive protein in health and disease* (pp. 67-107). Springer, New Delhi.
8. Balato, N., Di Costanzo, L., & Balato, A. (2009). Differential diagnosis of psoriasis. *The Journal of Rheumatology Supplement*, 83, 24-25.
9. Banerjee, S., Biehl, A., Gadina, M., Hasni, S., & Schwartz, D. M. (2017). JAK-STAT signaling as a target for inflammatory and autoimmune diseases: current and future prospects. *Drugs*, 77(5), 521-546.
10. Bao, L., Zhang, H., & Chan, L. S. (2013). The involvement of the JAK-STAT signaling pathway in chronic inflammatory skin disease atopic dermatitis. *Jak-Stat*, 2(3), e24137.
11. Bardhan, A., Bruckner-Tuderman, L., Chapple, I. L., Fine, J. D., Harper, N., Has, C., ... & Heagerty, A. H. (2020). Epidermolysis bullosa. *Nature Reviews Disease Primers*, 6(1), 1-27.
12. Barnes PJ, Adcock IM: Glucocorticoid resistance in inflammatory diseases. *Lancet* 2009; 373:1905–1917
13. Baselet, B., Belmans, N., Coninx, E., Lowe, D., Janssen, A., Michaux, A., ... & Aerts, A. (2017). Functional gene analysis reveals cell cycle changes and inflammation in endothelial cells irradiated with a single X-ray dose. *Frontiers in pharmacology*, 8, 213.
14. Bell, J. K., McQueen, D. S., & Rees, J. L. (2004). Involvement of histamine H4 and H1 receptors in scratching induced by histamine receptor agonists in BalbC mice. *British journal of pharmacology*, 142(2), 374-380.
15. Bieber, J. B. (1972). Cortisone. Memoirs of a Hormone Hunter Edward C. Kendall. *Isis*, 63(2).
16. Bieber, T. (2022). Atopic dermatitis: an expanding therapeutic pipeline for a complex disease. *Nature Reviews Drug Discovery*, 21(1), 21-40.
17. Bikle, D. D., Xie, Z., & Tu, C. L. (2012). Calcium regulation of keratinocyte differentiation. *Expert review of endocrinology & metabolism*, 7(4), 461-472.
18. Bloom, W., Jensch, R. P., & Fawcett, D. W. (2002). *Bloom & Fawcett's Concise Histology*. Arnoldpublishers.

19. BOER, M., & DUCHNIK, E. (2016). Romuald MALESZKA a Mariola MARCHLEWICZ. Structural and biophysical characteristics of human skin in maintaining proper epidermal barrier function. *Advances in Dermatology and Allergology*, 1, 1-5.
20. Bos, J. D., & Meinardi, M. M. (2000). The 500 Dalton rule for the skin penetration of chemical compounds and drugs. *Experimental Dermatology: Viewpoint*, 9(3), 165-169.
21. Bosmann, M., & Ward, P. A. (2013). Modulation of inflammation by interleukin-27. *Journal of leukocyte biology*, 94(6), 1159-1165.
22. Bosshart, H., & Heinzlmann, M. (2016). THP-1 cells as a model for human monocytes. *Annals of translational medicine*, 4(21).
23. Boudon, S. M., Vuorinen, A., Geotti-Bianchini, P., Wandeler, E., Kratschmar, D. V., Heidl, M., ... & Odermatt, A. (2017). Novel 11 β -hydroxysteroid dehydrogenase 1 inhibitors reduce cortisol levels in keratinocytes and improve dermal collagen content in human ex vivo skin after exposure to cortisone and UV. *PLoS One*, 12(2), e0171079.
24. Branco, A. C. C. C., Yoshikawa, F. S. Y., Pietrobon, A. J., & Sato, M. N. (2018). Role of histamine in modulating the immune response and inflammation. *Mediators of inflammation*, 2018.
25. Brandner, J. M. (2016). Importance of tight junctions in relation to skin barrier function. *Skin Barrier Function*, 49, 27-37.
26. Brenner, D., Blaser, H., & Mak, T. W. (2015). Regulation of tumour necrosis factor signalling: live or let die. *Nature Reviews Immunology*, 15(6), 362-374.
27. Broz, P., & Monack, D. M. (2011). Molecular mechanisms of inflammasome activation during microbial infections. *Immunological reviews*, 243(1), 174-190.
28. Bruckner-Tuderman, L., McGrath, J. A., Robinson, E. C., & Uitto, J. (2013). Progress in epidermolysis bullosa research: Summary of DEBRA International Research Conference 2012. *Journal of Investigative Dermatology*, 133(9), 2121-2126.
29. Cabanillas, B., Brehler, A. C., & Novak, N. (2017). Atopic dermatitis phenotypes and the need for personalized medicine. *Current Opinion in Allergy and Clinical Immunology*, 17(4), 309.
30. Case, D. A., Darden, T. A., Cheatham, T. E., Simmerling, C. L., Wang, J., Duke, R. E., ... & Kollman, P. A. (2008). *Amber 10* (No. BOOK). University of California.
31. Cataldi, M., Borriello, F., Granata, F., Annunziato, L., & Marone, G. (2014). Histamine receptors and antihistamines: from discovery to clinical applications. *History of Allergy*, 100, 214-226.
32. Chanput, W., Mes, J., Vreeburg, R. A., Savelkoul, H. F., & Wichers, H. J. (2010). Transcription profiles of LPS-stimulated THP-1 monocytes and macrophages: a tool to study inflammation modulating effects of food-derived compounds. *Food & function*, 1(3), 254-261.
33. Chapman, K., Holmes, M., & Seckl, J. (2013). 11 β -hydroxysteroid dehydrogenases: intracellular gate-keepers of tissue glucocorticoid action. *Physiological reviews*, 93(3), 1139-1206.
34. Chen, L., Deng, H., Cui, H., Fang, J., Zuo, Z., Deng, J., ... & Wang, X. & Zhao, L. (2018). Inflammatory responses and inflammation-associated diseases in organs.
35. Chen, M., Lechner, J., Zhao, J., Toth, L., Hogg, R., Silvestri, G., ... & Xu, H. (2016). STAT3 activation in circulating monocytes contributes to neovascular age-related macular degeneration. *Current molecular medicine*, 16(4), 412-423.
36. Chen, S., Lu, M., Liu, D., Yang, L., Yi, C., Ma, L., ... & Zhao, Q. (2019). Human substance P receptor binding mode of the antagonist drug aprepitant by NMR and crystallography. *Nature communications*, 10(1), 1-8.
37. Chernova, I., Lai, J. P., Li, H., Schwartz, L., Tuluc, F., Korchak, H. M., ... & Kilpatrick, L. E. (2009). Substance P (SP) enhances CCL5-induced chemotaxis and intracellular

- signaling in human monocytes, which express the truncated neurokinin-1 receptor (NK1R). *Journal of leukocyte biology*, 85(1), 154-164.
38. Chiou, A. S., Choi, S., Barriga, M., Dutt-Singh, Y., Solis, D. C., Nazarov, J., ... & Tang, J. Y. (2020). Phase 2 trial of a neurokinin-1 receptor antagonist for the treatment of chronic itch in patients with epidermolysis bullosa: a randomized clinical trial. *Journal of the American Academy of Dermatology*, 82(6), 1415-1421.
 39. Choi, S. Y., Lee, Y. J., Kim, J. M., Kang, H. J., Cho, S. H., & Chang, S. E. (2018). Epidermal growth factor relieves inflammatory signals in staphylococcus aureus-treated human epidermal keratinocytes and atopic dermatitis-like skin lesions in Nc/Nga mice. *BioMed research international*, 2018.
 40. Chu, W. M. (2013). Tumor necrosis factor. *Cancer letters*, 328(2), 222-225.
 41. Chung, B. Y., Um, J. Y., Kim, J. C., Kang, S. Y., Park, C. W., & Kim, H. O. (2020). Pathophysiology and treatment of pruritus in elderly. *International Journal of Molecular Sciences*, 22(1), 174.
 42. Cockram, P. E., Kist, M., Prakash, S., Chen, S. H., Wertz, I. E., & Vucic, D. (2021). Ubiquitination in the regulation of inflammatory cell death and cancer. *Cell Death & Differentiation*, 28(2), 591-605.
 43. Colombo, I., Sangiovanni, E., Maggio, R., Mattozzi, C., Zava, S., Corbett, Y., ... & Dell'Agli, M. (2017). HaCaT cells as a reliable in vitro differentiation model to dissect the inflammatory/repair response of human keratinocytes. *Mediators of inflammation*, 2017.
 44. Coutinho, A. E., & Chapman, K. E. (2011). The anti-inflammatory and immunosuppressive effects of glucocorticoids, recent developments and mechanistic insights. *Molecular and cellular endocrinology*, 335(1), 2-13.
 45. Cruz-Topete, D., & Cidowski, J. A. (2015). One hormone, two actions: anti-and pro-inflammatory effects of glucocorticoids. *Neuroimmunomodulation*, 22(1-2), 20-32.
 46. D. Yonova, "Pruritus in certain internal diseases," Hippokratia, vol. 11, no. 2, pp. 67-71, 2007.
 47. D.A. Case, T.A. Darden, T.E. Cheatham, III, C.L. Simmerling, J. Wang, R.E. Duke, R. Luo, M. Crowley, R.C. Walker, W. Zhang, K.M. Merz, B. Wang, S. Hayik, A. Roitberg, G. Seabra, I. Kolossváry, K.F. Wong, F. Paesani, J. Vanicek, X. Wu, S.R. Brozell, T. Steinbrecher, H. Gohlke, L. Yang, C. Tan, J. Mongan, V. Hornak, G. Cui, D.H. Mathews, M.G. Seetin, C. Sagui, V. Babin, and P.A. Kollman (2008), AMBER 10, University of California, San Francisco
 48. Davila-Seijo, P., Hernández-Martín, A., Morcillo-Makow, E., Lucas, R., Domínguez, E., Romero, N., ... & García-Doval, I. (2013). Prioritization of therapy uncertainties in dystrophic epidermolysis bullosa: where should research direct to? An example of priority setting partnership in very rare disorders. *Orphanet Journal of Rare Diseases*, 8(1), 1-8.
 49. de Souza, A. P., Vale, V. L. C., Silva, M. D. C., de Oliveira Araújo, I. B., Trindade, S. C., Moura-Costa, L. F. D., ... & Meyer, R. (2014). MAPK involvement in cytokine production in response to Corynebacterium pseudotuberculosis infection. *BMC microbiology*, 14(1), 1-9.
 50. Diks, S. H., Hardwick, J. C., Diab, R. M., van Santen, M. M., Versteeg, H. H., van Deventer, S. J., ... & Peppelenbosch, M. P. (2003). Activation of the canonical β -catenin pathway by histamine. *Journal of Biological Chemistry*, 278(52), 52491-52496.
 51. Dinarello, C. A. (2006). Interleukin 1 and interleukin 18 as mediators of inflammation and the aging process. *The American journal of clinical nutrition*, 83(2), 447S-455S.
 52. Dinarello, C. A. (2007). Historical insights into cytokines. *European journal of immunology*, 37(S1), S34-S45.
 53. Dinarello, C. A. (2018). Overview of the IL-1 family in innate inflammation and acquired immunity. *Immunological reviews*, 281(1), 8-27.

54. Dinsmore, C., & Reiter, J. F. (2016). Endothelial primary cilia inhibit atherosclerosis. *EMBO reports*, 17(2), 156-166.
55. Douglas, S. D., & Leeman, S. E. (2011). Neurokinin-1 receptor: functional significance in the immune system in reference to selected infections and inflammation. *Annals of the New York Academy of Sciences*, 1217(1), 83-95.
56. Driskell, R. R., Jahoda, C. A., Chuong, C. M., Watt, F. M., & Horsley, V. (2014). Defining dermal adipose tissue. *Experimental dermatology*, 23(9), 629-631.
57. Dzyakanchuk, A. A., Balázs, Z., Nashev, L. G., Amrein, K. E., & Odermatt, A. (2009). 11 β -Hydroxysteroid dehydrogenase 1 reductase activity is dependent on a high ratio of NADPH/NADP⁺ and is stimulated by extracellular glucose. *Molecular and cellular endocrinology*, 301(1-2), 137-141.
58. Edelblum, K. L., & Turner, J. R. (2009). The tight junction in inflammatory disease: communication breakdown. *Current opinion in pharmacology*, 9(6), 715-720.
59. Egawa, G., & Kabashima, K. (2016). Multifactorial skin barrier deficiency and atopic dermatitis: Essential topics to prevent the atopic march. *Journal of Allergy and Clinical Immunology*, 138(2), 350-358.
60. Eistetter, H. R., Mills, A., Brewster, R., Alouani, S., Rambosson, C., & Kawashima, E. (1992). Functional characterization of neurokinin-1 receptors on human U373MG astrocytoma cells. *Glia*, 6(2), 89-95.
61. Elias, P. M. (2007, April). The skin barrier as an innate immune element. In *Seminars in immunopathology* (Vol. 29, No. 1, pp. 3-14). Springer-Verlag.
62. Erickson, S., Ver Heul, A., & Kim, B. S. (2021). New and emerging treatments for inflammatory itch. *Annals of Allergy, Asthma & Immunology*, 126(1), 13-20.
63. Franck, J., Fried, G., and Brodin, E. (1989) Substance P enhances release of endogenous serotonin from rat ventral spinal cord. *Eur. J. Pharmacol.*, 174:85-90.
64. Frenkl, T. L., Zhu, H., Reiss, T., Seltzer, O., Rosenberg, E., & Green, S. (2010). A multicenter, double-blind, randomized, placebo controlled trial of a neurokinin-1 receptor antagonist for overactive bladder. *The Journal of urology*, 184(2), 616-622.
65. Frick, C., Atanasov, A. G., Arnold, P., Ozols, J., & Odermatt, A. (2004). Appropriate function of 11 β -hydroxysteroid dehydrogenase type 1 in the endoplasmic reticulum lumen is dependent on its N-terminal region sharing similar topological determinants with 50-kDa esterase. *Journal of Biological Chemistry*, 279(30), 31131-31138.
66. Friesner, R. A., Banks, J. L., Murphy, R. B., Halgren, T. A., & Klicic, J. J. JL (2004). Glide: A New Approach for Rapid, Accurate Docking and Scoring. 1. Method and Assessment of Docking Accuracy. *J. Med. Chem*, 47(7).
67. Gaffen, S. L. (2009). Structure and signalling in the IL-17 receptor family. *Nature Reviews Immunology*, 9(8), 556-567.
68. Gathercole, L. L., Lavery, G. G., Morgan, S. A., Cooper, M. S., Sinclair, A. J., Tomlinson, J. W., & Stewart, P. M. (2013). 11 β -Hydroxysteroid dehydrogenase 1: translational and therapeutic aspects. *Endocrine reviews*, 34(4), 525-555.
69. Gayen, A., Goswami, S. K., & Mukhopadhyay, C. (2011). NMR evidence of GM1-induced conformational change of Substance P using isotropic bicelles. *Biochimica et Biophysica Acta (BBA)-Biomembranes*, 1808(1), 127-139.
70. Gee, K., Guzzo, C., Che Mat, N. F., Ma, W., & Kumar, A. (2009). The IL-12 family of cytokines in infection, inflammation and autoimmune disorders. *Inflammation & Allergy-Drug Targets (Formerly Current Drug Targets-Inflammation & Allergy)(Discontinued)*, 8(1), 40-52.
71. Gerlach, B., Cordier, S. M., Schmukle, A. C., Emmerich, C. H., Rieser, E., Haas, T. L., ... & Walczak, H. (2011). Linear ubiquitination prevents inflammation and regulates immune signalling. *Nature*, 471(7340), 591-596.

72. Gregory, S., Hill, D., Grey, B., Ketelbey, W., Miller, T., Muniz-Terrera, G., & Ritchie, C. W. (2020). 11 β -hydroxysteroid dehydrogenase type 1 inhibitor use in human disease—a systematic review and narrative synthesis. *Metabolism*, *108*, 154246.
73. Gritsenko, A., Yu, S., Martin-Sanchez, F., Diaz-del-Olmo, I., Nichols, E. M., Davis, D. M., ... & Lopez-Castejon, G. (2020). Priming is dispensable for NLRP3 inflammasome activation in human monocytes in vitro. *Frontiers in immunology*, *11*, 565924.
74. Gurevich, E. V., & Gurevich, V. V. (2014). Therapeutic potential of small molecules and engineered proteins. In *Arrestins-Pharmacology and Therapeutic Potential* (pp. 1-12). Springer, Berlin, Heidelberg.
75. Gustafsson, J. A. (2016). Historical overview of nuclear receptors. *The Journal of Steroid Biochemistry and Molecular Biology*, *157*, 3-6.
76. Haas, T. L., Emmerich, C. H., Gerlach, B., Schmukle, A. C., Cordier, S. M., Rieser, E., ... & Walczak, H. (2009). Recruitment of the linear ubiquitin chain assembly complex stabilizes the TNF-R1 signaling complex and is required for TNF-mediated gene induction. *Molecular cell*, *36*(5), 831-844.
77. Halgren, T. A., Murphy, R. B., Friesner, R. A., Beard, H. S., & Frye, L. L. W. Thomas Pollard, A., & Banks, J. L. (2004). *Glide: A new approach for rapid, accurate docking and scoring*, *2*, 1750-1759.
78. Han, L., & Dong, X. (2014). Itch mechanisms and circuits. *Annual review of biophysics*, *43*, 331.
79. Hänel, K. H., Cornelissen, C., Lüscher, B., & Baron, J. M. (2013). Cytokines and the skin barrier. *International journal of molecular sciences*, *14*(4), 6720-6745.
80. Hanke, T., Merk, D., Steinhilber, D., Geisslinger, G., & Schubert-Zsilavecz, M. (2016). Small molecules with anti-inflammatory properties in clinical development. *Pharmacology & therapeutics*, *157*, 163-187.
81. Hardy R, Rabbitt EH, Filer A, et al. Local and systemic glucocorticoid metabolism in inflammatory arthritis. *Ann Rheum Dis* 2008; *67*: 1204-1210.
82. Hardy, R. S., Doig, C. L., Hussain, Z., O'Leary, M., Morgan, S. A., Pearson, M. J., ... & Raza, K. (2016). 11 β -Hydroxysteroid dehydrogenase type 1 within muscle protects against the adverse effects of local inflammation. *The Journal of pathology*, *240*(4), 472-483.
83. Hardy, R. S., Fenton, C., Croft, A. P., Naylor, A. J., Begum, R., Desanti, G., ... & Raza, K. (2018). 11 Beta-hydroxysteroid dehydrogenase type 1 regulates synovitis, joint destruction, and systemic bone loss in chronic polyarthritis. *Journal of autoimmunity*, *92*, 104-113.
84. Hellberg, L., Samavedam, U. K., Holdorf, K., Hänsel, M., Recke, A., Beckmann, T., ... & Laskay, T. (2013). Methylprednisolone blocks autoantibody-induced tissue damage in experimental models of bullous pemphigoid and epidermolysis bullosa acquisita through inhibition of neutrophil activation. *Journal of Investigative Dermatology*, *133*(10), 2390-2399.
85. Hendrayani, S. F., Al-Harbi, B., Al-Ansari, M. M., Silva, G., & Aboussekhra, A. (2016). The inflammatory/cancer-related IL-6/STAT3/NF- κ B positive feedback loop includes AUF1 and maintains the active state of breast myofibroblasts. *Oncotarget*, *7*(27), 41974.
86. Henríquez-Olguín, C., Altamirano, F., Valladares, D., López, J. R., Allen, P. D., & Jaimovich, E. (2015). Altered ROS production, NF- κ B activation and interleukin-6 gene expression induced by electrical stimulation in dystrophic mdx skeletal muscle cells. *Biochimica et Biophysica Acta (BBA)-Molecular Basis of Disease*, *1852*(7), 1410-1419.
87. Heo, Y. J., Choi, S. E., Lee, N., Jeon, J. Y., Han, S. J., Kim, D. J., ... & Kim, H. J. (2020). CCL20 induced by visfatin in macrophages via the NF- κ B and MKK3/6-p38 signaling pathways contributes to hepatic stellate cell activation. *Molecular Biology Reports*, *47*(6), 4285-4293.

88. Hillmer, E. J., Zhang, H., Li, H. S., & Watowich, S. S. (2016). STAT3 signaling in immunity. *Cytokine & growth factor reviews*, 31, 1-15.
89. Hodge, D. R., Hurt, E. M., & Farrar, W. L. (2005). The role of IL-6 and STAT3 in inflammation and cancer. *European journal of cancer*, 41(16), 2502-2512.
90. Hu, X., Fu, M., Zhao, X., & Wang, W. (2021). The JAK/STAT signaling pathway: From bench to clinic. *Signal Transduction and Targeted Therapy*, 6(1), 1-33.
91. Huang, X., Yu, P., Liu, M., Deng, Y., Dong, Y., Liu, Q., ... & Wu, T. (2019). ERK inhibitor JSI287 alleviates imiquimod-induced mice skin lesions by ERK/IL-17 signaling pathway. *International immunopharmacology*, 66, 236-241.
92. Hussein, Y. M., Shalaby, S. M., Nassar, A., Alzahrani, S. S., Alharbi, A. S., & Nouh, M. (2014). Association between genes encoding components of the IL-4/IL-4 receptor pathway and dermatitis in children. *Gene*, 545(2), 276-281.
93. Ip, C. K., & Wong, A. S. (2012). p70 S6 kinase and actin dynamics: a perspective. *Spermatogenesis*, 2(1), 44-52.
94. Itoi, S., Terao, M., Murota, H., & Katayama, I. (2013). 11 β -Hydroxysteroid dehydrogenase 1 contributes to the pro-inflammatory response of keratinocytes. *Biochemical and biophysical research communications*, 440(2), 265-270.
95. Iversen, L. (1998). Substance P equals pain substance?. *Nature*, 392(6674), 334-335.
96. Jang, D. I., Lee, A. H., Shin, H. Y., Song, H. R., Park, J. H., Kang, T. B., ... & Yang, S. H. (2021). The role of tumor necrosis factor alpha (TNF- α) in autoimmune disease and current TNF- α inhibitors in therapeutics. *International journal of molecular sciences*, 22(5), 2719.
97. Jenkins, S. J., Ruckerl, D., Cook, P. C., Jones, L. H., Finkelman, F. D., Van Rooijen, N., ... & Allen, J. E. (2011). Local macrophage proliferation, rather than recruitment from the blood, is a signature of TH2 inflammation. *science*, 332(6035), 1284-1288.
98. Jin, P., Deng, S., Sherchan, P., Cui, Y., Huang, L., Li, G., ... & Tang, J. (2021). Neurokinin receptor 1 (NK1R) antagonist aprepitant enhances hematoma clearance by regulating microglial polarization via PKC/p38MAPK/NF κ B pathway after experimental intracerebral hemorrhage in mice. *Neurotherapeutics*, 18(3), 1922-1938.
99. Johansen, C., Kragballe, K., Westergaard, M., Henningsen, J., Kristiansen, K., & Iversen, L. (2005). The mitogen-activated protein kinases p38 and ERK1/2 are increased in lesional psoriatic skin. *British Journal of Dermatology*, 152(1), 37-42.
100. Jorgensen, W. L., & Tirado-Rives, J. (1988). The OPLS [optimized potentials for liquid simulations] potential functions potential functions for proteins, energy minimizations for crystals of cyclic peptides and crambin. *J Am Chem Soc*, 110, 1657-1666.
101. Jridi, I., Canté-Barrett, K., Pike-Overzet, K., & Staal, F. J. (2021). Inflammation and Wnt signaling: target for immunomodulatory therapy?. *Frontiers in Cell and Developmental Biology*, 8, 615131.
102. K. Olek-Hrab, M. Hrab, J. Szyfer-Harris, and Z. Adamski, "Pruritus in selected dermatoses," *European Review for Medical and Pharmacological Sciences*, vol. 20, no. 17, pp. 3628–3641, 2016.
103. Karin, M. (2005). Inflammation-activated protein kinases as targets for drug development. *Proceedings of the American Thoracic Society*, 2(4), 386-390.
104. Kataoka, T. (2009). Chemical biology of inflammatory cytokine signaling. *The Journal of Antibiotics*, 62(12), 655-667.
105. Katoh, N., Ohya, Y., Ikeda, M., Ebihara, T., Katayama, I., Saeki, H., ... & Yamamoto-Hanada, K. (2019). Clinical practice guidelines for the management of atopic dermatitis 2018. *The Journal of dermatology*, 46(12), 1053-1101.
106. Kim, B. J., Lee, N. R., Lee, C. H., Lee, Y. B., Choe, S. J., Lee, S., ... & Choi, E. H. (2021). Increased expression of 11 β -hydroxysteroid dehydrogenase type 1 contributes to

- epidermal permeability barrier dysfunction in aged skin. *International journal of molecular sciences*, 22(11), 5750.
107. Kim, E. K., & Choi, E. J. (2010). Pathological roles of MAPK signaling pathways in human diseases. *Biochimica et Biophysica Acta (BBA)-Molecular Basis of Disease*, 1802(4), 396-405.
 108. Kim, H. S., & Yosipovitch, G. (2020). The skin microbiota and itch: is there a link?. *Journal of clinical medicine*, 9(4), 1190.
 109. Kim, J. H., Kim, Y. H., & Kim, S. C. (2011). Epidermolysis bullosa acquisita: a retrospective clinical analysis of 30 cases.
 110. Kim, J., Kim, B. E., & Leung, D. Y. (2019, March). Pathophysiology of atopic dermatitis: Clinical implications. In *Allergy and asthma proceedings* (Vol. 40, No. 2, p. 84). OceanSide Publications.
 111. Kim, W. B., Jerome, D., & Yeung, J. (2017). Diagnosis and management of psoriasis. *Canadian Family Physician*, 63(4), 278-285.
 112. Ko, K. I., Merlet, J. J., DerGarabedian, B. P., Zhen, H., Suzuki-Horiuchi, Y., Hedberg, M. L., ... & Graves, D. T. (2022). NF- κ B perturbation reveals unique immunomodulatory functions in Prx1+ fibroblasts that promote development of atopic dermatitis. *Science translational medicine*, 14(630), eabj0324.
 113. Köckerling, F., Köckerling, D., & Lomas, C. (2013). Cornelius Celsus—ancient encyclopedist, surgeon–scientist, or master of surgery?. *Langenbeck's Archives of Surgery*, 398(4), 609-616.
 114. Koga, H., Recke, A., Vidarsson, G., Pas, H. H., Jonkman, M. F., Hashimoto, T., ... & Ludwig, R. J. (2016). PDE4 inhibition as potential treatment of epidermolysis bullosa acquisita. *Journal of Investigative Dermatology*, 136(11), 2211-2220.
 115. Kopitar-Jerala, N. (2017). The role of interferons in inflammation and inflammasome activation. *Front Immunol.* 2017; 8: 873.
 116. Koska, J., De Courten, B., Wake, D. J., Nair, S., Walker, B. R., Bunt, J. C., ... & Tataranni, P. A. (2006). 11 β -Hydroxysteroid Dehydrogenase Type 1 in Adipose Tissue and Prospective Changes in Body Weight and Insulin Resistance. *Obesity*, 14(9), 1515-1522.
 117. Kumar, V., Behr, M., Kiritsi, D., Scheffschick, A., Grahner, A., Homberg, M., ... & Magin, T. M. (2016). Keratin-dependent thymic stromal lymphopoietin expression suggests a link between skin blistering and atopic disease. *Journal of Allergy and Clinical Immunology*, 138(5), 1461-1464.
 118. Kuuliala, K., Kuuliala, A., Hämäläinen, M., Koivuniemi, R., Kautiainen, H., Moilanen, E., ... & Leirisalo-Repo, M. (2017). Impaired Akt phosphorylation in monocytes of patients with rheumatoid arthritis. *Scandinavian journal of immunology*, 85(2), 155-161.
 119. Kwak, H. J., Song, J. S., Heo, J. Y., Yang, S. D., Nam, J. Y., & Cheon, H. G. (2005). Roflumilast inhibits lipopolysaccharide-induced inflammatory mediators via suppression of nuclear factor- κ B, p38 mitogen-activated protein kinase, and c-Jun NH2-terminal kinase activation. *Journal of Pharmacology and Experimental Therapeutics*, 315(3), 1188-1195.
 120. Lannan, E. A., Galliher-Beckley, A. J., Scoltock, A. B., & Cidlowski, J. A. (2012). Proinflammatory actions of glucocorticoids: glucocorticoids and TNF α coregulate gene expression in vitro and in vivo. *Endocrinology*, 153(8), 3701-3712.
 121. Lee, N. R., Kim, B. J., Lee, C. H., Lee, Y. B., Lee, S., Hwang, H. J., ... & Choi, E. H. (2020). Role of 11 β -hydroxysteroid dehydrogenase type 1 in the development of atopic dermatitis. *Scientific reports*, 10(1), 1-12.
 122. Li, J., Kennedy, L. J., Wang, H., Li, J. J., Walker, S. J., Hong, Z., ... & Robl, J. A. (2014). Optimization of 1, 2, 4-triazolopyridines as inhibitors of human 11 β -hydroxysteroid dehydrogenase type 1 (11 β -HSD-1). *ACS medicinal chemistry letters*, 5(7), 803-808.

123. Liang, Y., Sarkar, M. K., Tsoi, L. C., & Gudjonsson, J. E. (2017). Psoriasis: a mixed autoimmune and autoinflammatory disease. *Current opinion in immunology*, 49, 1-8.
124. Liew, F. Y., Patel, M., & Xu, D. (2005). Toll-like receptor 2 signalling and inflammation. *Annals of the rheumatic diseases*, 64(suppl 4), iv104-iv105.
125. Liu, H. S., Pan, C. E., Liu, Q. G., Yang, W., & Liu, X. M. (2003). Effect of NF- κ B and p38 MAPK in activated monocytes/macrophages on pro-inflammatory cytokines of rats with acute pancreatitis. *World Journal of Gastroenterology*, 9(11), 2513.
126. Liu, J. Y., Hu, J. H., Zhu, Q. G., Li, F. Q., & Sun, H. J. (2006). Substance P receptor expression in human skin keratinocytes and fibroblasts. *British Journal of Dermatology*, 155(4), 657-662.
127. Liu, X. D., Ko, S., Xu, Y., Fattah, E. A., Xiang, Q., Jagannath, C., ... & Eissa, N. T. (2012). Transient aggregation of ubiquitinated proteins is a cytosolic unfolded protein response to inflammation and endoplasmic reticulum stress. *Journal of Biological Chemistry*, 287(23), 19687-19698.
128. Lu, H., Chen, J., Planko, L., Zigrino, P., Klein-Hitpass, L., & Magin, T. M. (2007). Induction of inflammatory cytokines by a keratin mutation and their repression by a small molecule in a mouse model for EBS. *Journal of Investigative Dermatology*, 127(12), 2781-2789.
129. Ludwig, R. J. (2017). Signalling and targeted therapy of inflammatory cells in epidermolysis bullosa acquisita. *Experimental dermatology*, 26(12), 1179-1186.
130. Luger, T. A. (2002). Neuromediators—a crucial component of the skin immune system. *Journal of dermatological science*, 30(2), 87-93.
131. Luo, C., & Zhang, H. (2017). The role of proinflammatory pathways in the pathogenesis of colitis-associated colorectal cancer. *Mediators of inflammation*, 2017.
132. Luo, J., Feng, J., Liu, S., Walters, E. T., & Hu, H. (2015). Molecular and cellular mechanisms that initiate pain and itch. *Cellular and molecular life sciences*, 72(17), 3201-3223.
133. Majerz, I., & Dziembowska, T. (2011). Geometric Aspects of Aromaticity: Interrelations between Intramolecular Hydrogen Bonds, Steric Effects and π -Electron Delocalisation in Nitroanilines.
134. Mantyh, P. W. (1991). Substance P and the inflammatory and immune response. *Annals of the New York Academy of Sciences*, 632, 263-271.
135. Matejuk, A. (2018). Skin immunity. *Archivum immunologiae et therapiae experimentalis*, 66(1), 45-54.
136. Mazumder, B., Li, X., & Barik, S. (2010). Translation control: a multifaceted regulator of inflammatory response. *The Journal of Immunology*, 184(7), 3311-3319.
137. Milakovic, M., & Gooderham, M. J. (2021). Phosphodiesterase-4 inhibition in psoriasis. *Psoriasis: Targets and Therapy*, 11, 21.
138. Miner JN, Hong MH, Negro-Vilar A: New and improved glucocorticoid receptor ligands. *Expert Opin Investig Drugs* 2005;14: 1527–1545
139. Moens, U., Kostenko, S., & Sveinbjörnsson, B. (2013). The role of mitogen-activated protein kinase-activated protein kinases (MAPKAPKs) in inflammation. *Genes* 4, 101–133.
140. Molecular Operating Environment (MOE), 2020.09 Chemical Computing Group ULC, 1010 Sherbooke St. West, Suite #910, Montreal, QC, Canada, H3A 2R7, 2022.
141. Morelli, A. E., Sumpster, T. L., Rojas-Canales, D. M., Bandyopadhyay, M., Chen, Z., Tkacheva, O., ... & Larregina, A. T. (2020). Neurokinin-1 receptor signaling is required for efficient Ca²⁺ flux in T-cell-receptor-activated T cells. *Cell reports*, 30(10), 3448-3465.
142. Morizane, S., Yamasaki, K., Mühleisen, B., Kotol, P. F., Murakami, M., Aoyama, Y., ... & Gallo, R. L. (2012). Cathelicidin antimicrobial peptide LL-37 in psoriasis enables

-
- keratinocyte reactivity against TLR9 ligands. *Journal of Investigative Dermatology*, 132(1), 135-143.
143. Moro, S., Sturlese, M., Ciancetta, A., & Floris, M. (2016). In silico 3D modeling of binding activities. In *In silico methods for predicting drug toxicity* (pp. 23-35). Humana Press, New York, NY.
144. Morton, N. M., & Seckl, J. R. (2008). 11 β -hydroxysteroid dehydrogenase type 1 and obesity. *Obesity and Metabolism*, 36, 146-164.
145. MP, F. R. M. R. R. (2006). Frye LL Greenwood JR Extra precision glide: docking and scoring incorporating a model of hydrophobic enclosure for protein-ligand complexes. *Journal of Medicinal Chemistry*, 49, 6177-6196.
146. Nguyen, A. V., & Soulika, A. M. (2019). The dynamics of the skin's immune system. *International journal of molecular sciences*, 20(8), 1811.
147. Niculet, E., Bobeica, C., & Tatu, A. L. (2020). Glucocorticoid-induced skin atrophy: the old and the new. *Clinical, Cosmetic and Investigational Dermatology*, 13, 1041.
148. Nilsson, J., von Euler, A.M., and Daalsgard, C.-J. (1985) Stimulation of connective tissue cell growth by substance P and substance K. *Nature*, 315:6143
149. Oger, S., Méhats, C., Dallot, E., Cabrol, D., & Leroy, M. J. (2005). Evidence for a role of phosphodiesterase 4 in lipopolysaccharide-stimulated prostaglandin E2 production and matrix metalloproteinase-9 activity in human amniochorionic membranes. *The Journal of Immunology*, 174(12), 8082-8089.
150. OIKARINEN, A., & AUTIO, P. (1991). New aspects of the mechanism of corticosteroid-induced dermal atrophy. *Clinical and experimental dermatology*, 16(6), 416-419.
151. Okabe, T., Hide, M., Koro, O., & Yamamoto, S. (2000). Substance P induces tumor necrosis factor- α release from human skin via mitogen-activated protein kinase. *European journal of pharmacology*, 398(2), 309-315.
152. Olek-Hrab, K., Hrab, M., Szyfter-Harris, J., & Adamski, Z. (2016). Pruritus in selected dermatoses. *European Review for Medical and Pharmacological Sciences*, 20(17), 3628-3641.
153. O'Sullivan, R. L., Lipper, G., & Lerner, E. A. (1998). The neuro-immuno-cutaneous-endocrine network: relationship of mind and skin. *Archives of Dermatology*, 134(11), 1431-1435.
154. Page, M. J., Bester, J., & Pretorius, E. (2018). The inflammatory effects of TNF- α and complement component 3 on coagulation. *Scientific reports*, 8(1), 1-9.
155. Papanikolaou, M., Onoufriadis, A., Mellerio, J. E., Nattkemper, L. A., Yosipovitch, G., Steinhoff, M., & McGrath, J. A. (2021). Prevalence, pathophysiology and management of itch in epidermolysis bullosa. *British Journal of Dermatology*, 184(5), 816-825.
156. Pariser, D. M., Bagel, J., Lebwohl, M., Yosipovitch, G., Chien, E., & Spellman, M. C. (2020). Serlopitant for psoriatic pruritus: a phase 2 randomized, double-blind, placebo-controlled clinical trial. *Journal of the American Academy of Dermatology*, 82(6), 1314-1320.
157. Park, Y. M., & Kim, C. W. (1999). The effects of substance P and vasoactive intestinal peptide on interleukin-6 synthesis in cultured human keratinocytes. *Journal of dermatological science*, 22(1), 17-23.
158. Pasparakis, M., Haase, I., & Nestle, F. O. (2014). Mechanisms regulating skin immunity and inflammation. *Nature reviews immunology*, 14(5), 289-301.
159. Pastor, D. M., Poritz, L. S., Olson, T. L., Kline, C. L., Harris, L. R., Koltun, W. A., Chinchilli, V. M., & Irby, R. B. (2010). Primary cell lines: false representation or model system? a comparison of four human colorectal tumors and their coordinately established cell lines. *International journal of clinical and experimental medicine*, 3(1), 69-83..

160. Pastore, S., Mascia, F., Mariani, V., & Girolomoni, G. (2008). The epidermal growth factor receptor system in skin repair and inflammation. *Journal of Investigative Dermatology*, 128(6), 1365-1374.
161. Pearson, G., Robinson, F., Beers Gibson, T., Xu, B. E., Karandikar, M., Berman, K., & Cobb, M. H. (2001). Mitogen-activated protein (MAP) kinase pathways: regulation and physiological functions. *Endocrine reviews*, 22(2), 153-183.
162. Pedersen, C. M., & Bols, M. (2017). On the nature of the electronic effect of multiple hydroxyl groups in the 6-membered ring—the effects are additive but steric hindrance plays a role too. *Organic & Biomolecular Chemistry*, 15(5), 1164-1173.
163. Pedersen, L., & Jemec, G. B. (2006). Mechanical properties and barrier function of healthy human skin. *Acta dermato-venereologica*, 86(4).
164. Pederson-Bjergaard, U., Bogeskov-Nielsen, L., Jensen, K., Edvinsson, L., Jansen, I., and Olesen, J. (1989) Algesia and local responses induced by neurokinin A and substance P in human skin and tempo- ral muscle. *Peptides*, 10:1147-1152.
165. Piccini, A., Carta, S., Tassi, S., Lasiglié, D., Fossati, G., & Rubartelli, A. (2008). ATP is released by monocytes stimulated with pathogen-sensing receptor ligands and induces IL-1 β and IL-18 secretion in an autocrine way. *Proceedings of the National Academy of Sciences*, 105(23), 8067-8072.
166. Pojawa-Gołab, M., Jaworecka, K., & Reich, A. (2019). NK-1 receptor antagonists and pruritus: review of current literature. *Dermatology and therapy*, 9(3), 391-405.
167. Prodinger, C., Reichelt, J., Bauer, J. W., & Laimer, M. (2019). Epidermolysis bullosa: advances in research and treatment. *Experimental dermatology*, 28(10), 1176-1189.
168. Qu, Y., Franchi, L., Nunez, G., & Dubyak, G. R. (2007). Nonclassical IL-1 β secretion stimulated by P2X7 receptors is dependent on inflammasome activation and correlated with exosome release in murine macrophages. *The Journal of Immunology*, 179(3), 1913-1925.
169. Quartara, L., & Maggi, C. A. (1998). The tachykinin NK1 receptor. Part II: Distribution and pathophysiological roles. *Neuropeptides*, 32(1), 1-49.
170. Raharja, A., Mahil, S. K., & Barker, J. N. (2021). Psoriasis: A brief overview. *Clinical Medicine*, 21(3), 170.
171. Raingeaud, J., Whitmarsh, A. J., Barrett, T., Derijard, B., & Davis, R. J. (1996). MKK3-and MKK6-regulated gene expression is mediated by the p38 mitogen-activated protein kinase signal transduction pathway. *Molecular and cellular biology*, 16(3), 1247-1255.
172. Rajan, V., Edwards, C. R., & Seckl, J. R. (1996). 11 beta-Hydroxysteroid dehydrogenase in cultured hippocampal cells reactivates inert 11-dehydrocorticosterone, potentiating neurotoxicity. *Journal of Neuroscience*, 16(1), 65-70.
173. Randall, M. J., Jüngel, A., Rimann, M., & Wuertz-Kozak, K. (2018). Advances in the Biofabrication of 3D Skin in vitro: Healthy and Pathological Models. *Frontiers in bioengineering and biotechnology*, 6, 154.
174. Rayego-Mateos, S., Morgado-Pascual, J. L., Opazo-Ríos, L., Guerrero-Hue, M., García-Caballero, C., Vázquez-Carballo, C., ... & Egido, J. (2020). Pathogenic pathways and therapeutic approaches targeting inflammation in diabetic nephropathy. *International Journal of Molecular Sciences*, 21(11), 3798.
175. Rendon, A., & Schäkel, K. (2019). Psoriasis pathogenesis and treatment. *International journal of molecular sciences*, 20(6), 1475.
176. Rhen T, Cidlowski JA: Antiinflammatory action of glucocorticoids – new mechanisms for old drugs. *N Engl J Med* 2005;353:1711–1723
177. Richardson, M. (2003). Understanding the structure and function of the skin. *Nursing times*, 99(31), 46-48.
178. Richter, E., Ventz, K., Harms, M., Mostertz, J., & Hochgräfe, F. (2016). Induction of macrophage function in human THP-1 cells is associated with rewiring of MAPK

- signaling and activation of MAP3K7 (TAK1) protein kinase. *Frontiers in cell and developmental biology*, 4, 21.
179. Rodrigues, M., Kosaric, N., Bonham, C. A., & Gurtner, G. C. (2019). Wound healing: a cellular perspective. *Physiological reviews*, 99(1), 665-706.
 180. Rognoni, E., Ruppert, R., & Fässler, R. (2016). The kindlin family: functions, signaling properties and implications for human disease. *Journal of cell science*, 129(1), 17-27.
 181. Rothschild, D. E., McDaniel, D. K., Ringel-Scaia, V. M., & Allen, I. C. (2018). Modulating inflammation through the negative regulation of NF-κB signaling. *Journal of leukocyte biology*, 103(6), 1131-1150.
 182. Roux, P. P., & Blenis, J. (2004). ERK and p38 MAPK-activated protein kinases: a family of protein kinases with diverse biological functions. *Microbiology and molecular biology reviews*, 68(2), 320-344. S. Stander, M. Steinhof, M. Schmelz, E. Weisshaar, D. Metz, " and T. Luger, "Neurophysiology of pruritus: cutaneous elicitation of itch," *JAMA Dermatology*, vol. 139, no. 11, pp. 1463-1470, 2003.
 183. Sabio, G., & Davis, R. J. (2014, June). TNF and MAP kinase signalling pathways. In *Seminars in immunology* (Vol. 26, No. 3, pp. 237-245). Academic Press.
 184. Sander, T., & Freyss, J. (2015). Mütevazı von Korff, Christian Rufener. DataWarrior: Kimya İçin Veri Görselleştirme ve Analizini Destekleyen Açık Kaynaklı Bir Program. *J Chem Inf Model*, 55, 460-473.
 185. Sawamura, D., Nakano, H., & Matsuzaki, Y. (2010). Overview of epidermolysis bullosa. *The Journal of dermatology*, 37(3), 214-219.
 186. Schofield, P.R., Shivers, B.D., and Seeburg, P.H. (1990) The role of receptor subtype diversity in the CNS. *Trends Neurosci.*, 13:11.
 187. Schöppe, J., Ehrenmann, J., Klenk, C., Rucktooa, P., Schütz, M., Doré, A. S., & Plücker, A. (2019). Crystal structures of the human neurokinin 1 receptor in complex with clinically used antagonists. *Nature communications*, 10(1), 1-11.
 188. Schroecksnadel, S., Jenny, M., & Fuchs, D. (2011). Myelomonocytic THP-1 cells for in vitro testing of immunomodulatory properties of nanoparticles. *Journal of Biomedical Nanotechnology*, 7(1), 209-210.
 189. Segre, J. A. (2006). Epidermal barrier formation and recovery in skin disorders. *The Journal of clinical investigation*, 116(5), 1150-1158.
 190. Shin, J. W., Kwon, S. H., Choi, J. Y., Na, J. I., Huh, C. H., Choi, H. R., & Park, K. C. (2019). Molecular mechanisms of dermal aging and antiaging approaches. *International journal of molecular sciences*, 20(9), 2126.
 191. Silverberg, J. I. (2019). Comorbidities and the impact of atopic dermatitis. *Annals of Allergy, Asthma & Immunology*, 123(2), 144-151.
 192. Siu, M., Johnson, T. O., Wang, Y., Nair, S. K., Taylor, W. D., Cripps, S. J., ... & Vogel, J. E. (2009). N-(Pyridin-2-yl) arylsulfonamide inhibitors of 11β-hydroxysteroid dehydrogenase type 1: Discovery of PF-915275. *Bioorganic & medicinal chemistry letters*, 19(13), 3493-3497.
 193. Slominski, A. T., & Manna, P. R. (2017). On the role of skin in the regulation of local and systemic steroidogenic activities 2015; 103: 72-88. DOI: 10.1016/j.steroids.2015.04.006 Steroids. 7. Slominski AT, Brożyna AA, Tuckey RC Cutaneous Glucocorticoidogenesis and Cortisol Signaling Are Defective in Psoriasis. *Journal of Investigative Dermatology*, 137(8), 1609-1611.
 194. Soeberdt, M., Kilic, A., & Abels, C. (2020). Small molecule drugs for the treatment of pruritus in patients with atopic dermatitis. *European Journal of Pharmacology*, 881, 173242.
 195. Song, J., Xian, D., Yang, L., Xiong, X., Lai, R., & Zhong, J. (2018). Pruritus: progress toward pathogenesis and treatment. *BioMed research international*, 2018.
 196. Sousa, L. P., Lopes, F., Silva, D. M., Tavares, L. P., Vieira, A. T., Rezende, B. M., ... & Teixeira, M. M. (2010). PDE4 inhibition drives resolution of neutrophilic

- inflammation by inducing apoptosis in a PKA-PI3K/Akt-dependent and NF- κ B-independent manner. *Journal of leukocyte biology*, 87(5), 895-904.
197. Spiga, F., Walker, J. J., Terry, J. R., & Lightman, S. L. (2011). HPA axis-rhythms. *Comprehensive physiology*, 4(3), 1273-1298.
198. Ständer, S., & Luger, T. A. (2015). NK-1 antagonists and itch. *Pharmacology of Itch*, 237-255.
199. Ständer, S., & Yosipovitch, G. (2019). Substance P and neurokinin 1 receptor are new targets for the treatment of chronic pruritus. *British Journal of Dermatology*, 181(5), 932-938.
200. Ständer, S., Kwon, P., Hirman, J., Perlman, A. J., Weisshaar, E., Metz, M., ... & TCP-102 Study Group. (2019). Serlopitant reduced pruritus in patients with prurigo nodularis in a phase 2, randomized, placebo-controlled trial. *Journal of the American Academy of Dermatology*, 80(5), 1395-1402.
201. Stegk, J. P., Ebert, B., Martin, H. J., & Maser, E. (2009). Expression profiles of human 11 β -hydroxysteroid dehydrogenases type 1 and type 2 in inflammatory bowel diseases. *Molecular and cellular endocrinology*, 301(1-2), 104-108.
202. Steinhoff, M. S., von Mentzer, B., Geppetti, P., Pothoulakis, C., & Bunnett, N. W. (2014). Tachykinins and their receptors: contributions to physiological control and the mechanisms of disease. *Physiological reviews*, 94(1), 265-301.
203. Stevenson, N. L., Martin-Martin, B., Freeman, J., Kriston-Vizi, J., Ketteler, R., & Cutler, D. F. (2014). G protein-coupled receptor kinase 2 moderates recruitment of THP-1 cells to the endothelium by limiting histamine-invoked W eibel-P alade body exocytosis. *Journal of Thrombosis and Haemostasis*, 12(2), 261-272.
204. Stokes, M. P., Farnsworth, C. L., Gu, H., Jia, X., Worsfold, C. R., Yang, V., ... & Silva, J. C. (2015). Complementary PTM profiling of drug response in human gastric carcinoma by immunoaffinity and IMAC methods with total proteome analysis. *Proteomes*, 3(3), 160-183
205. Sun, H. L., Wu, Y. W., Bian, H. G., Yang, H., Wang, H., Meng, X. M., & Jin, J. (2021). Function of uric acid transporters and their inhibitors in hyperuricaemia. *Frontiers in pharmacology*, 12, 667753.
206. Sun, L., & Ye, R. D. (2012). Role of G protein-coupled receptors in inflammation. *Acta pharmacologica Sinica*, 33(3), 342-350.
207. Taherkhani, S., Suzuki, K., & Castell, L. (2020). A short overview of changes in inflammatory cytokines and oxidative stress in response to physical activity and antioxidant supplementation. *Antioxidants*, 9(9), 886.
208. Takeo, M., Lee, W., & Ito, M. (2015). Wound healing and skin regeneration. *Cold Spring Harbor perspectives in medicine*, 5(1), a023267.
209. Tamagawa-Mineoka, R., & Katoh, N. (2020). Atopic dermatitis: identification and management of complicating factors. *International Journal of Molecular Sciences*, 21(8), 2671.
210. Tan, Q., Yang, H., Liu, E., & Wang, H. (2017). P38/ERK MAPK signaling pathways are involved in the regulation of filaggrin and involucrin by IL-17. *Molecular Medicine Reports*, 16(6), 8863-8867.
211. Tang, B., Tang, F., Wang, Z., Qi, G., Liang, X., Li, B., ... & He, S. (2016). Upregulation of Akt/NF- κ B-regulated inflammation and Akt/Bad-related apoptosis signaling pathway involved in hepatic carcinoma process: suppression by carnosic acid nanoparticle. *International Journal of Nanomedicine*, 11, 6401.
212. Terao, M., Murota, H., Kimura, A., Kato, A., Ishikawa, A., Igawa, K., ... & Katayama, I. (2011). 11 β -Hydroxysteroid dehydrogenase-1 is a novel regulator of skin homeostasis and a candidate target for promoting tissue repair. *PloS one*, 6(9), e25039.
213. Thornton, K., Parrish, F., & Swords, C. (2011). Topical vs. Systemic Treatments For Acute Otitis Media. *Pediatric Nursing*, 37(5).

214. Timmermans, S., Souffriau, J., & Libert, C. (2019). A general introduction to glucocorticoid biology. *Frontiers in immunology*, 10, 1545.
215. Tivoli, Y. A., & Rubenstein, R. M. (2009). Pruritus: An updated look at an old problem. *The Journal of clinical and aesthetic dermatology*, 2(7), 30.
216. Tomlinson, J. W., Durrani, O. M., Bujalska, I. J., Gathercole, L. L., Tomlins, P. J., Reuser, T. T., ... & Rauz, S. (2010). The Role of 11 β -Hydroxysteroid Dehydrogenase 1 in Adipogenesis in Thyroid-Associated Ophthalmopathy. *The Journal of Clinical Endocrinology & Metabolism*, 95(1), 398-406.
217. Torres, T., & Filipe, P. (2015). Small molecules in the treatment of psoriasis. *Drug development research*, 76(5), 215-227.
218. Uitto, J., McGrath, J. A., Rodeck, U., Bruckner-Tuderman, L., & Robinson, E. C. (2010). Progress in epidermolysis bullosa research: toward treatment and cure. *Journal of Investigative Dermatology*, 130(7), 1778-1784.
219. Vasiliou, A. S., MacKenzie, A., Morris, R., McLaughlin, L., Bubb, V. J., Haddley, K., & Quinn, J. P. (2007). Generation of a transgenic model to address regulation and function of the human neurokinin 1 receptor (NK1R). *Neuropeptides*, 41(4), 195-205.
220. Wang, X. M., Hamza, M., Wu, T. X., & Dionne, R. A. (2009). Upregulation of IL-6, IL-8 and CCL2 gene expression after acute inflammation: Correlation to clinical pain. *PAIN@*, 142(3), 275-283.
221. Weiss, H. J., & Angiari, S. (2020). Metabolite transporters as regulators of immunity. *Metabolites*, 10(10), 418.
222. Welsh, S. E., Xiao, C., Kaden, A. R., Brzezynski, J. L., Mohrman, M. A., Wang, J., ... & Polymeropoulos, M. H. (2021). Neurokinin-1 receptor antagonist tradipitant has mixed effects on itch in atopic dermatitis: results from EPIONE, a randomized clinical trial. *Journal of the European Academy of Dermatology and Venereology*, 35(5), e338.
223. Wepler, M., Preuss, J. M., Merz, T., McCook, O., Radermacher, P., Tuckermann, J. P., & Vettorazzi, S. (2020). Impact of downstream effects of glucocorticoid receptor dysfunction on organ function in critical illness-associated systemic inflammation. *Intensive Care Medicine Experimental*, 8(1), 1-13.
224. Werberger, R., Braz, J. M., Weinrich, J. A., & Basbaum, A. I. (2021). Pain and itch processing by subpopulations of molecularly diverse spinal and trigeminal projection neurons. *Proceedings of the National Academy of Sciences*, 118(28), e2105732118.
225. Werfel, T., Allam, J. P., Biedermann, T., Eyerich, K., Gilles, S., Guttman-Yassky, E., ... & Akdis, C. A. (2016). Cellular and molecular immunologic mechanisms in patients with atopic dermatitis. *Journal of allergy and clinical immunology*, 138(2), 336-349.
226. Wilson, V. G. (2013). Growth and differentiation of HaCaT keratinocytes. In *Epidermal cells* (pp. 33-41). Springer, New York, NY.
227. Wong, L. S., Wu, T., & Lee, C. H. (2017). Inflammatory and noninflammatory itch: implications in pathophysiology-directed treatments. *International journal of molecular sciences*, 18(7), 1485.
228. Wyrwoll, C. S., Holmes, M. C., & Seckl, J. R. (2011). 11 β -hydroxysteroid dehydrogenases and the brain: from zero to hero, a decade of progress. *Frontiers in neuroendocrinology*, 32(3), 265-286.
229. Xiao, D. Q., Xu, P. H., Deng, H., Chen, L. S., Ding, X. A., Bai, M., ... & Yuan, D. F. (2017). The characterization and clinical significance of PI3K/Akt signaling pathway activation in the peripheral T cells of pediatric patients with atopic dermatitis. *International Journal of Clinical and Experimental Medicine*, 10, 2904-2910.
230. Xing, Z., Gauldie, J., Cox, G., Baumann, H., Jordana, M., Lei, X. F., & Achong, M. K. (1998). IL-6 is an antiinflammatory cytokine required for controlling local or

-
- systemic acute inflammatory responses. *The Journal of clinical investigation*, 101(2), 311-320.
231. Yang, G., Seok, J. K., Kang, H. C., Cho, Y. Y., Lee, H. S., & Lee, J. Y. (2020). Skin barrier abnormalities and immune dysfunction in atopic dermatitis. *International journal of molecular sciences*, 21(8), 2867.
232. Yao, R. Q., Ren, C., Xia, Z. F., & Yao, Y. M. (2021). Organelle-specific autophagy in inflammatory diseases: a potential therapeutic target underlying the quality control of multiple organelles. *Autophagy*, 17(2), 385-401.
233. Yarilina, A., & Ivashkiv, L. B. (2010). Type I interferon: a new player in TNF signaling. *TNF Pathophysiology*, 11, 94-104.
234. Ye, X. Y., Chen, S. Y., Wu, S., Yoon, D. S., Wang, H., Hong, Z., ... & Robl, J. A. (2017). Discovery of clinical candidate 2-((2 S, 6 S)-2-phenyl-6-hydroxyadamantan-2-yl)-1-(3'-hydroxyazetid-1-yl) ethanone [BMS-816336], an orally active novel selective 11 β -hydroxysteroid dehydrogenase type 1 inhibitor. *Journal of Medicinal Chemistry*, 60(12), 4932-4948.
235. Yosipovitch, G., Rosen, J. D., & Hashimoto, T. (2018). Itch: from mechanism to (novel) therapeutic approaches. *Journal of allergy and clinical immunology*, 142(5), 1375-1390.
236. Yousef, H., Alhajj, M., & Sharma, S. (2017). *Anatomy, skin (integument), epidermis*.
237. Yu, B., Koga, T., Urabe, K., Moroi, Y., Maeda, S., Yanagihara, Y., & Furue, M. (2002). Differential regulation of thymus- and activation-regulated chemokine induced by IL-4, IL-13, TNF- α and IFN- γ in human keratinocyte and fibroblast. *Journal of dermatological science*, 30(1), 29-36.
238. Yu, L. R., Stewart, N. A., & Veenstra, T. D. (2010). Proteomics: the deciphering of the functional genome. In *Essentials of genomic and personalized medicine* (pp. 89-96). Academic Press.
239. Zeng, L., Kang, R., Zhu, S., Wang, X., Cao, L., Wang, H., ... & Tang, D. (2017). ALK is a therapeutic target for lethal sepsis. *Science translational medicine*, 9(412), ean5689.
240. Zeze, N., Kido-Nakahara, M., Tsuji, G., Maehara, E., Sato, Y., Sakai, S., ... & Nakahara, T. (2022). Role of ERK Pathway in the Pathogenesis of Atopic Dermatitis and Its Potential as a Therapeutic Target. *International journal of molecular sciences*, 23(7), 3467.
241. Zhang, J. M., & An, J. (2009). *Int Anesthesiol Clin*. Author manuscript, 27-37.
242. Zhang, M., & Zhang, X. (2019). The role of PI3K/AKT/FOXO signaling in psoriasis. *Archives of Dermatological Research*, 311(2), 83-91.
243. Zhao, X. N., Bai, Z. Z., Li, C. H., Sheng, C. L., & Li, H. Y. (2020). The NK-1R antagonist aprepitant prevents LPS-induced oxidative stress and inflammation in RAW264. 7 macrophages. *Drug design, development and therapy*, 14, 1943.

10.4 Appendix

Supplemental Data 11HSD1

Viability testing for the determination of use levels

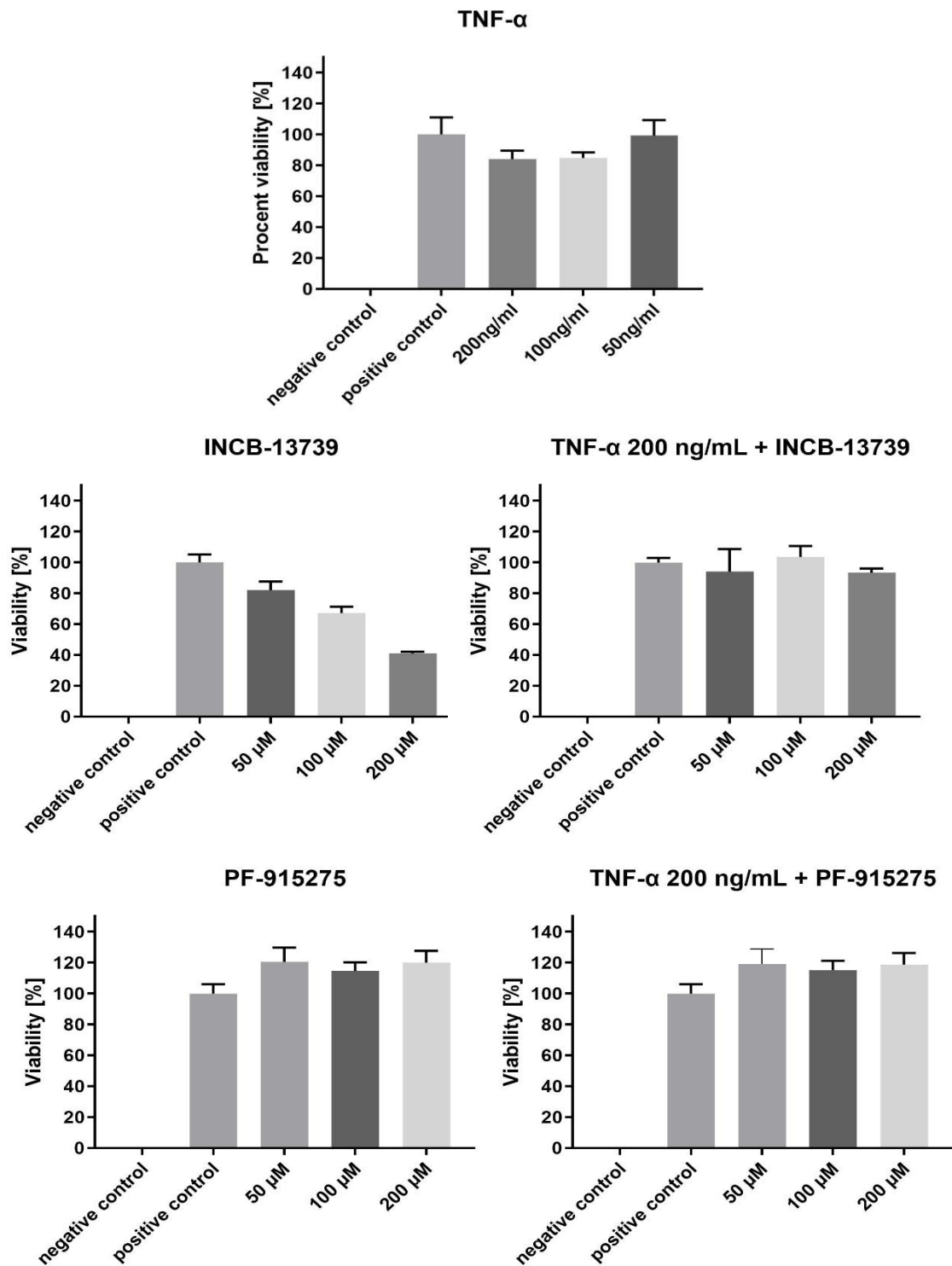


Figure S1: Viability testing of Inhibitors and inducer and in combination of both to determine use level on HaCat cells. A viability of 80% was set as a limit for this assay. The resulting concentration was selected as working concentration for further experiments. neg. ctrl served as solvent control of 0,2% DMSO.

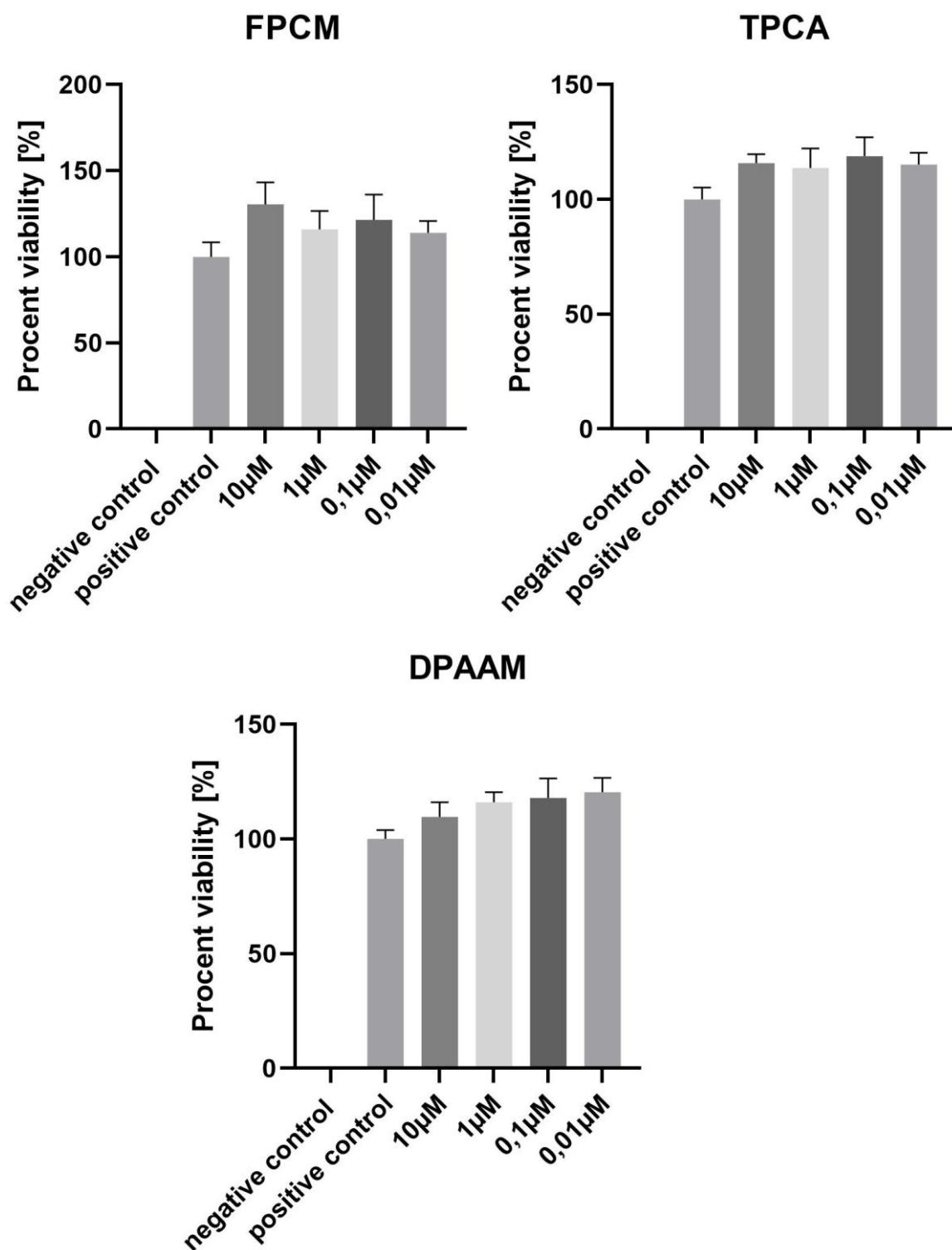


Figure S2: Viability testing of tested NCEs to determine use level. A viability of 80% was set as a limit for this assay. The resulting concentration was selected as working concentration for further experiments. neg. ctrl served as solvent control of 0,2% DMSO.

Proteomic Data of FPCM treatment on HaCat cells

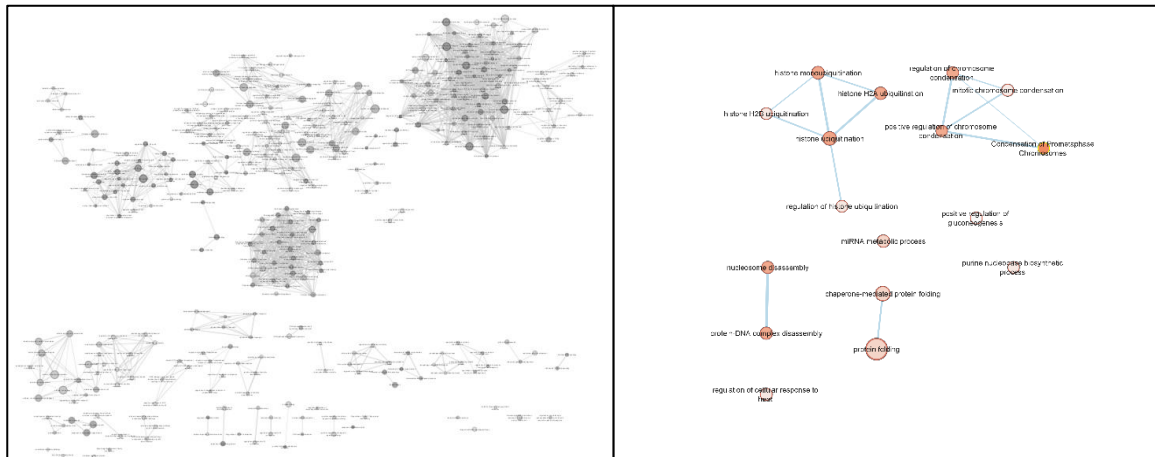


Figure S3: Enrichment of down (black) and upregulated (red) proteins after FPCM treatment in HaCat cells. All BPs and pathways enriched in inflammation induced HaCat cells due to down and upregulated proteins were arranged according to function similarities. Each node (circle) represents a distinct biological process (GO:BP) or pathway (REAC) involving between 5 and 350 genes. Color gradient describes statistic linked to the identification of the biological process and pathways. Edges (lines) represent the number of genes overlapping between to biological processes or pathways, determined using the similarity coefficient. (node cutoff = 0.04 and an edge cutoff = 0.5)

Proteomic Data of TPCA treatment on HaCat cells

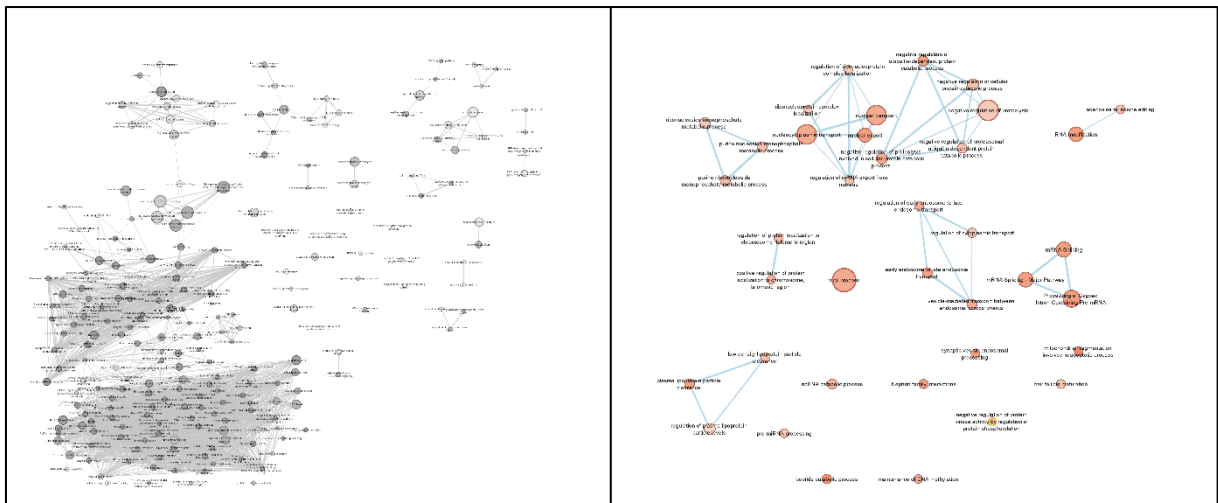


Figure S4: Enrichment of down (black) and upregulated (red) proteins after TPCA treatment in HaCat cells. All BPs and pathways enriched in inflammation induced HaCat cells due to down and upregulated proteins were arranged according to function similarities. Each node (circle) represents a distinct biological process (GO:BP) or pathway (REAC) involving between 5 and 350 genes. Color gradient describes statistic linked to the identification of the biological process and pathways. Edges (lines) represent the number of genes overlapping between to biological processes or pathways, determined using the similarity coefficient. (node cutoff = 0.04 and an edge cutoff = 0.5)

Proteomic Data of DPAAM treatment on HaCat cells

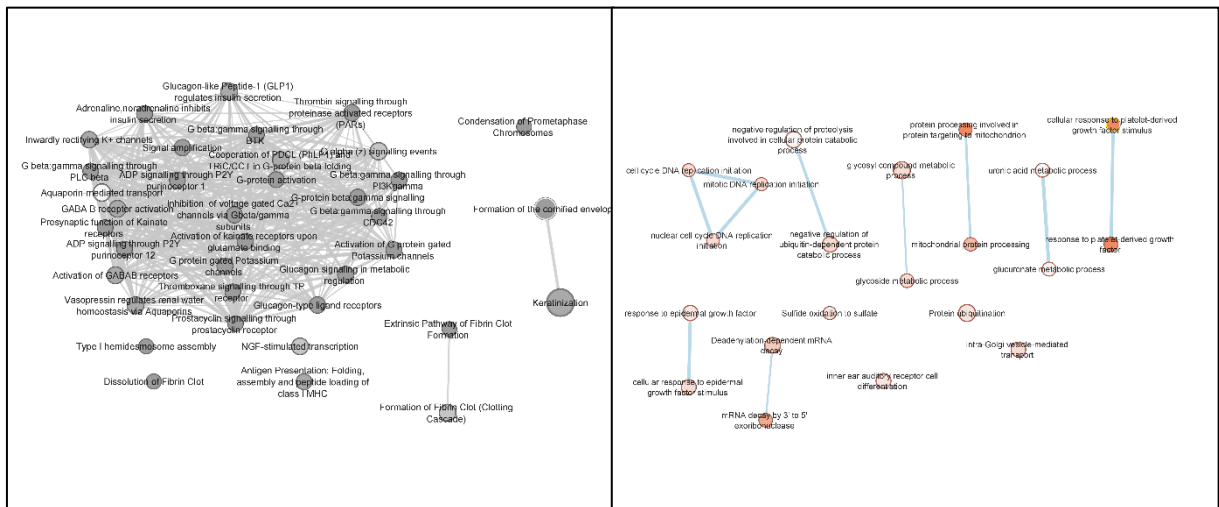


Figure S5: Enrichment of down (black) and upregulated (red) proteins after DPAAM treatment in HaCat cells. All BPs and pathways enriched in inflammation induced HaCat cells due to down and upregulated proteins were arranged according to function similarities. Each node (circle) represents a distinct biological process (GO:BP) or pathway (REAC) involving between 5 and 350 genes. Color gradient describes statistic linked to the identification of the biological process and pathways. Edges (lines) represent the number of genes overlapping between to biological processes or pathways, determined using the similarity coefficient. (node cutoff = 0.04 and an edge cutoff = 0.5)

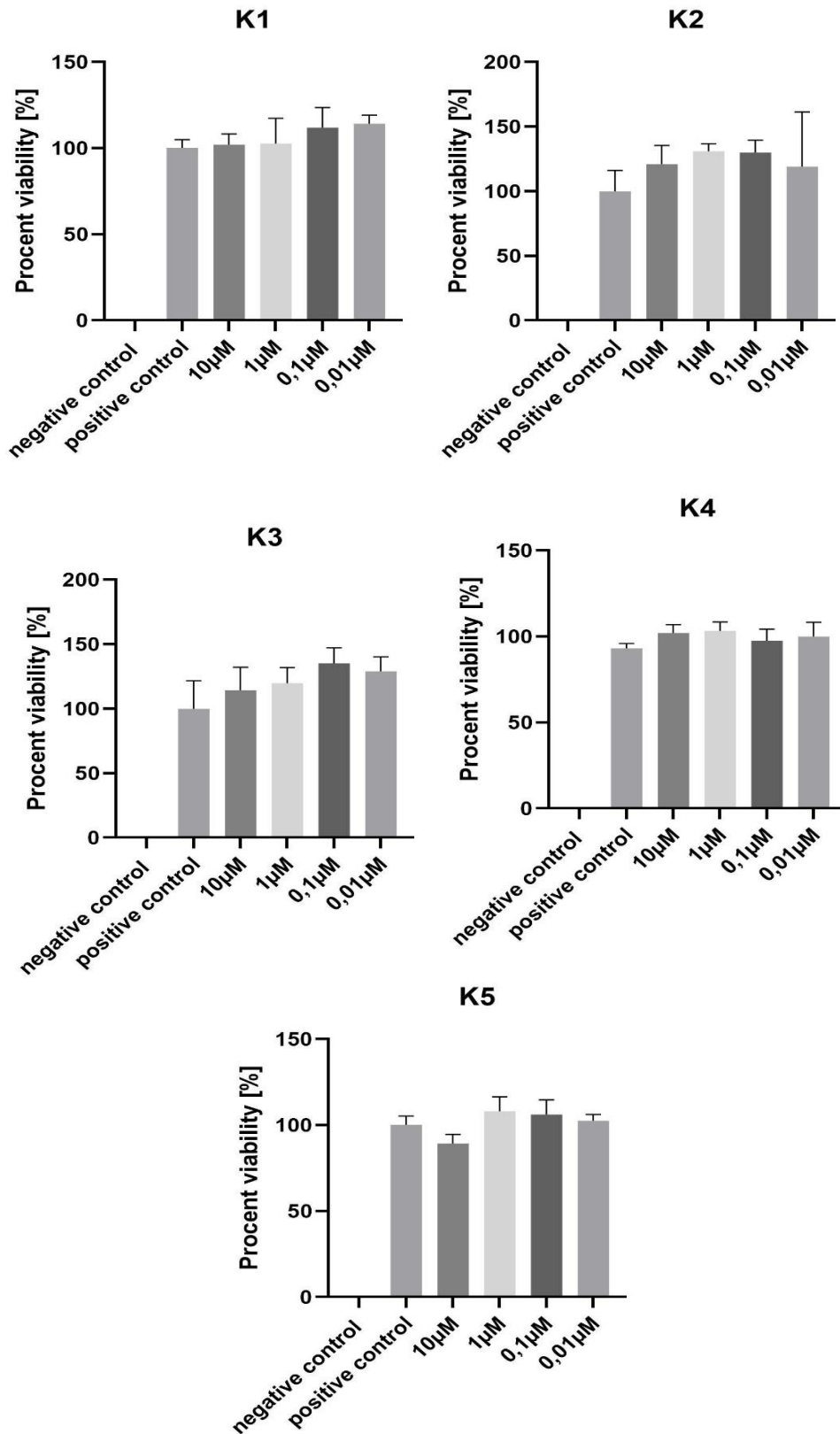


Figure S7: Viability testing of analogue compounds to DPAAM to determine use level. A viability of 80% was set as a limit for this assay. The resulting concentration was selected as working concentration for further experiments. neg. ctrl served as solvent control of 0,2% DMSO.

Inflammatory response after treatment with analogue compounds to DPAAM

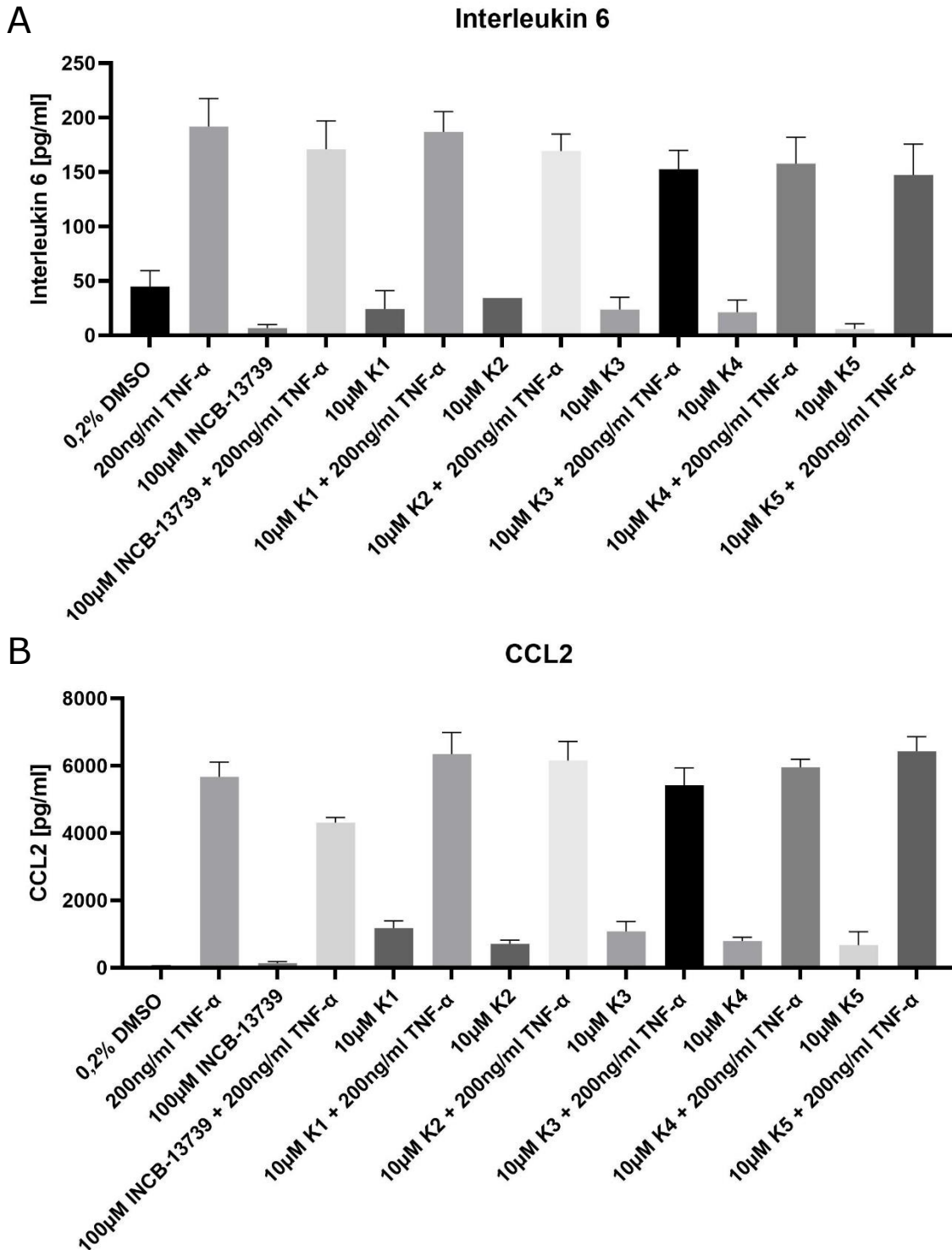


Figure S8: Response of pro-inflammatory biomarkers IL-6 and CCL2. A: Secretion response of IL-6 after five analogue compounds to DPAAM. B: Secretion response of CCL2 after five analogue compounds to DPAAM. HaCat cells were seeded in 96well and treated for 48h with substances in humidified atmosphere at 37°C and 5% CO₂. 0.2% DMSO served as negative control. Supernatant was further used for Elisa analysis (n=6, One-way ANOVA followed by $\alpha = 0.05$. Significances (****): $p < 0.0001$, (***): $p < 0.001$, (**): $p < 0.01$, (*): $p < 0.05$, (ns): $p \geq 0.05$). Means \pm SD are shown.

Keratinocytes
Viability testing for the determination of use level

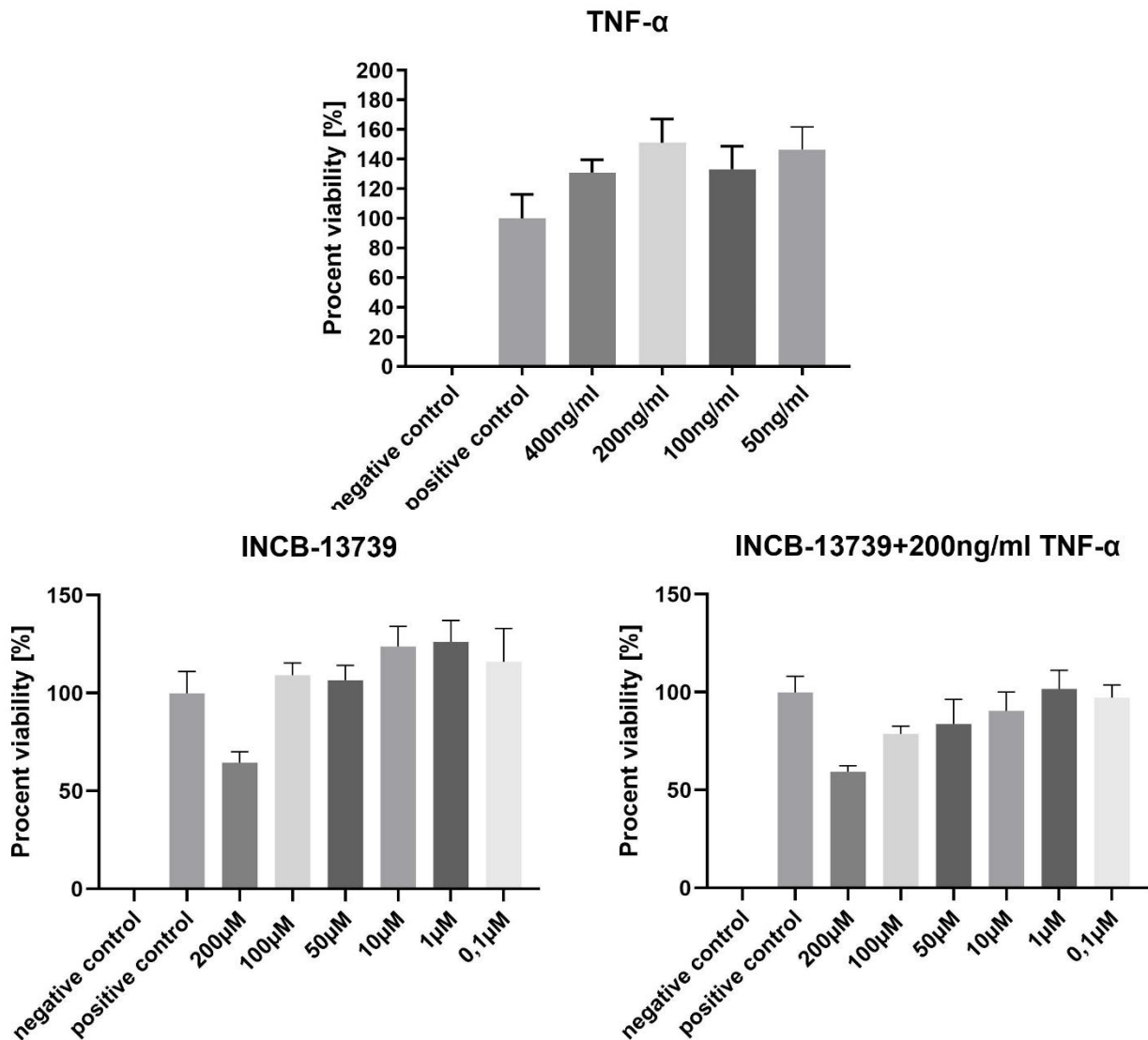


Figure S9: Viability testing of Inhibitor and inducer and in combination of both to determine use level on primary keratinocytes. A viability of 80% was set as a limit for this assay. The resulting concentration was selected as working concentration for further experiments. neg. ctrl served as solvent control of 0,2% DMSO.

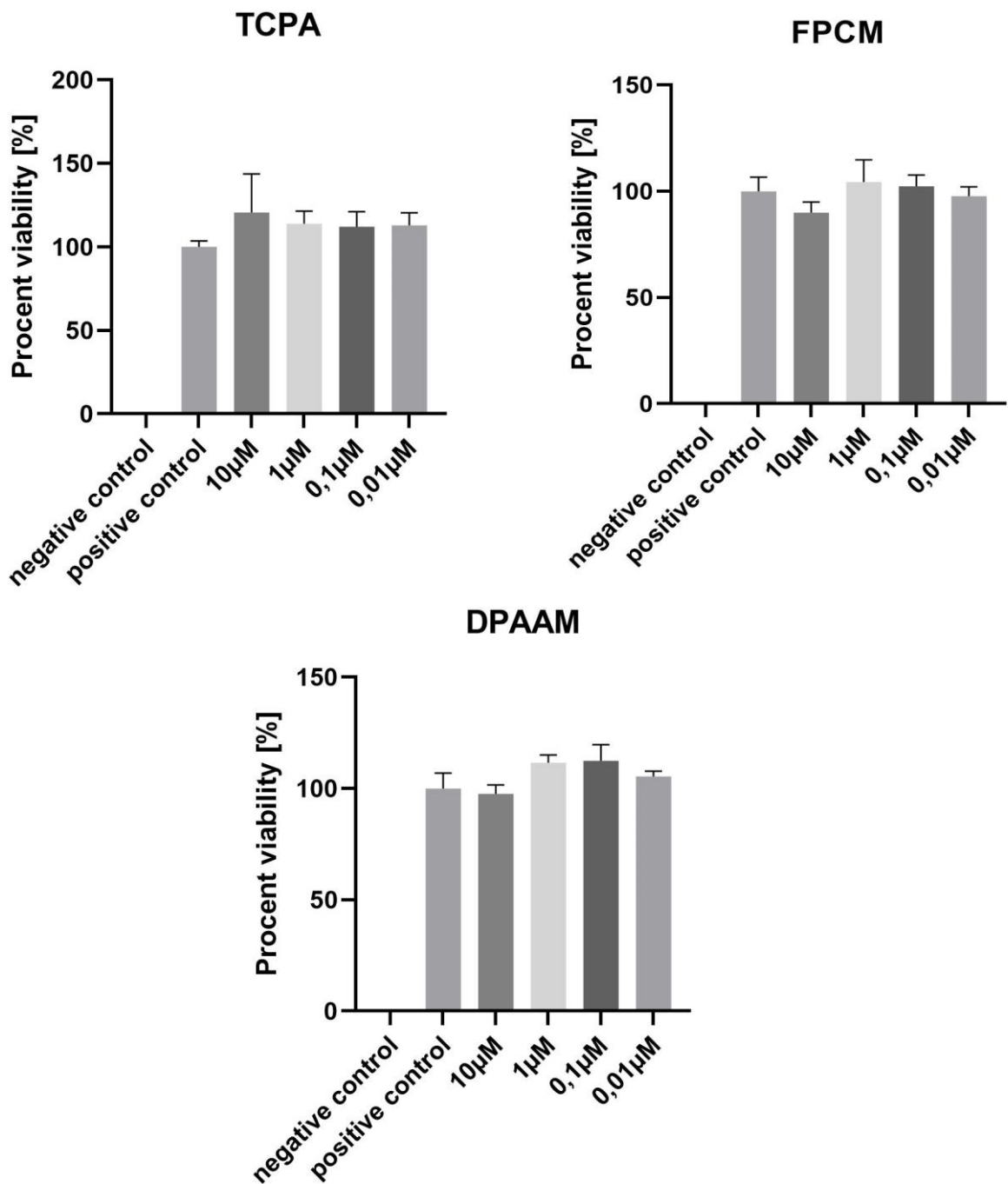


Figure S10: Viability testing of tested NCEs to determine use level on primary keratinocytes. A viability of 80% was set as a limit for this assay. The resulting concentration was selected as working concentration for further experiments. neg. ctrl served as solvent control of 0,2% DMSO.

Proteomic Data of FPCM treatment on primary keratinocytes

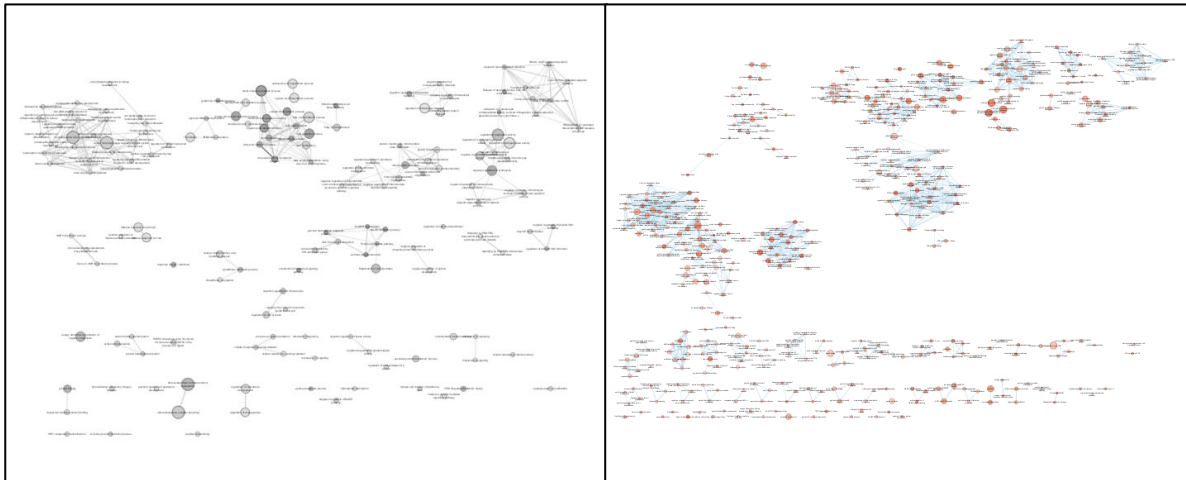


Figure S11: Enrichment of down (black) and upregulated (red) proteins after FPCM treatment in primary keratinocytes. All BPs and pathways enriched in inflammation induced HaCat cells due to down and upregulated proteins were arranged according to function similarities. Each node (circle) represents a distinct biological process (GO:BP) or pathway (REAC) involving between 5 and 350 genes. Color gradient describes statistic linked to the identification of the biological process and pathways. Edges (lines) represent the number of genes overlapping between to biological processes or pathways, determined using the similarity coefficient. (node cutoff = 0.04 and an edge cutoff = 0.5)

Proteomic Data of TPCA treatment on primary keratinocytes

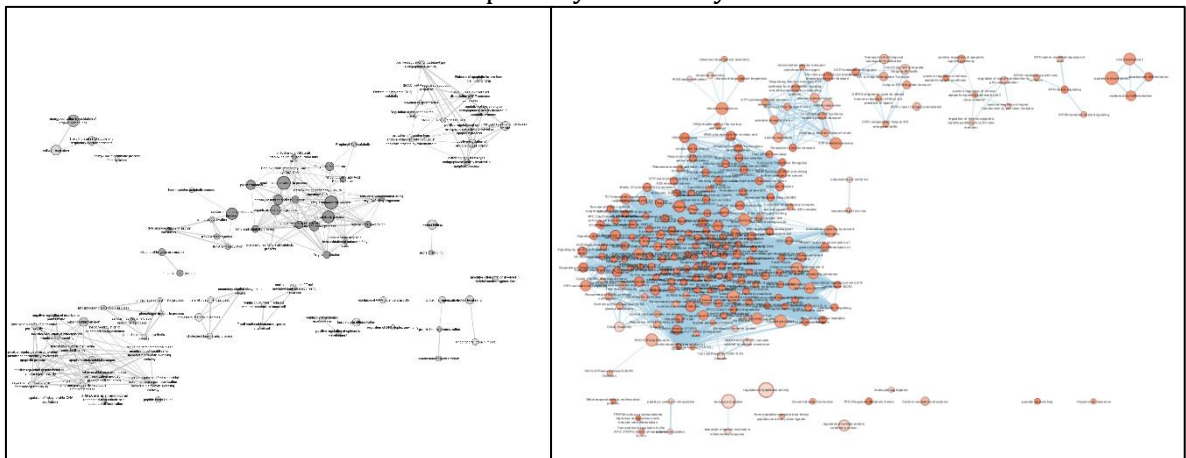


Figure S12: Enrichment of down (black) and upregulated (red) proteins after TPCA treatment in primary keratinocytes. All BPs and pathways enriched in inflammation induced HaCat cells due to down and upregulated proteins were arranged according to function similarities. Each node (circle) represents a distinct biological process (GO:BP) or pathway (REAC) involving between 5 and 350 genes. Color gradient describes statistic linked to the identification of the biological process and pathways. Edges (lines) represent the number of genes overlapping between to biological processes or pathways, determined using the similarity coefficient. (node cutoff = 0.04 and an edge cutoff = 0.5)

Proteomic Data of DPAAM treatment on primary keratinocytes

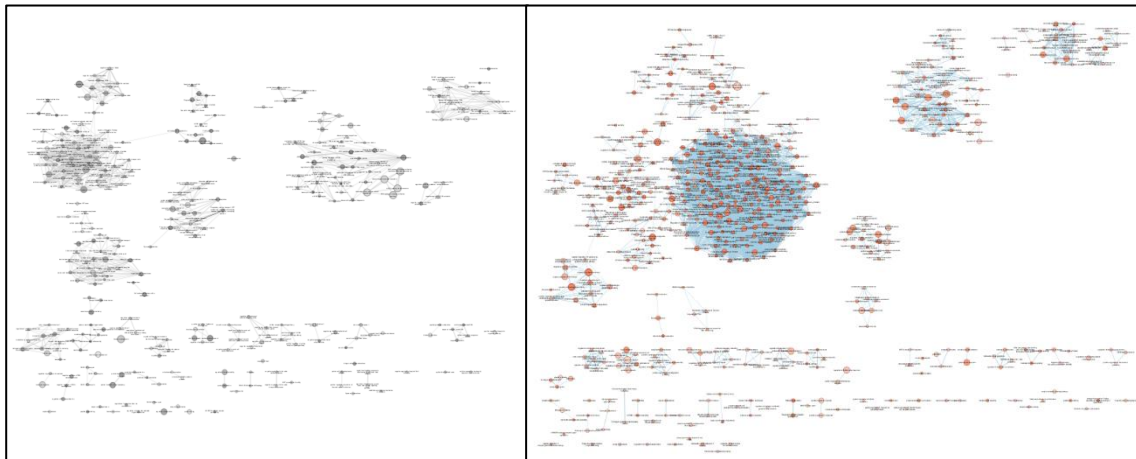


Figure S13: Enrichment of down (black) and upregulated (red) proteins after DPAAM treatment in primary keratinocytes. All BPs and pathways enriched in inflammation induced HaCat cells due to down and upregulated proteins were arranged according to function similarities. Each node (circle) represents a distinct biological process (GO:BP) or pathway (REAC) involving between 5 and 350 genes. Color gradient describes statistic linked to the identification of the biological process and pathways. Edges (lines) represent the number of genes overlapping between to biological processes or pathways, determined using the similarity coefficient. (node cutoff = 0.04 and an edge cutoff = 0.5)

THP1 cells
Viability testing for the determination of use level

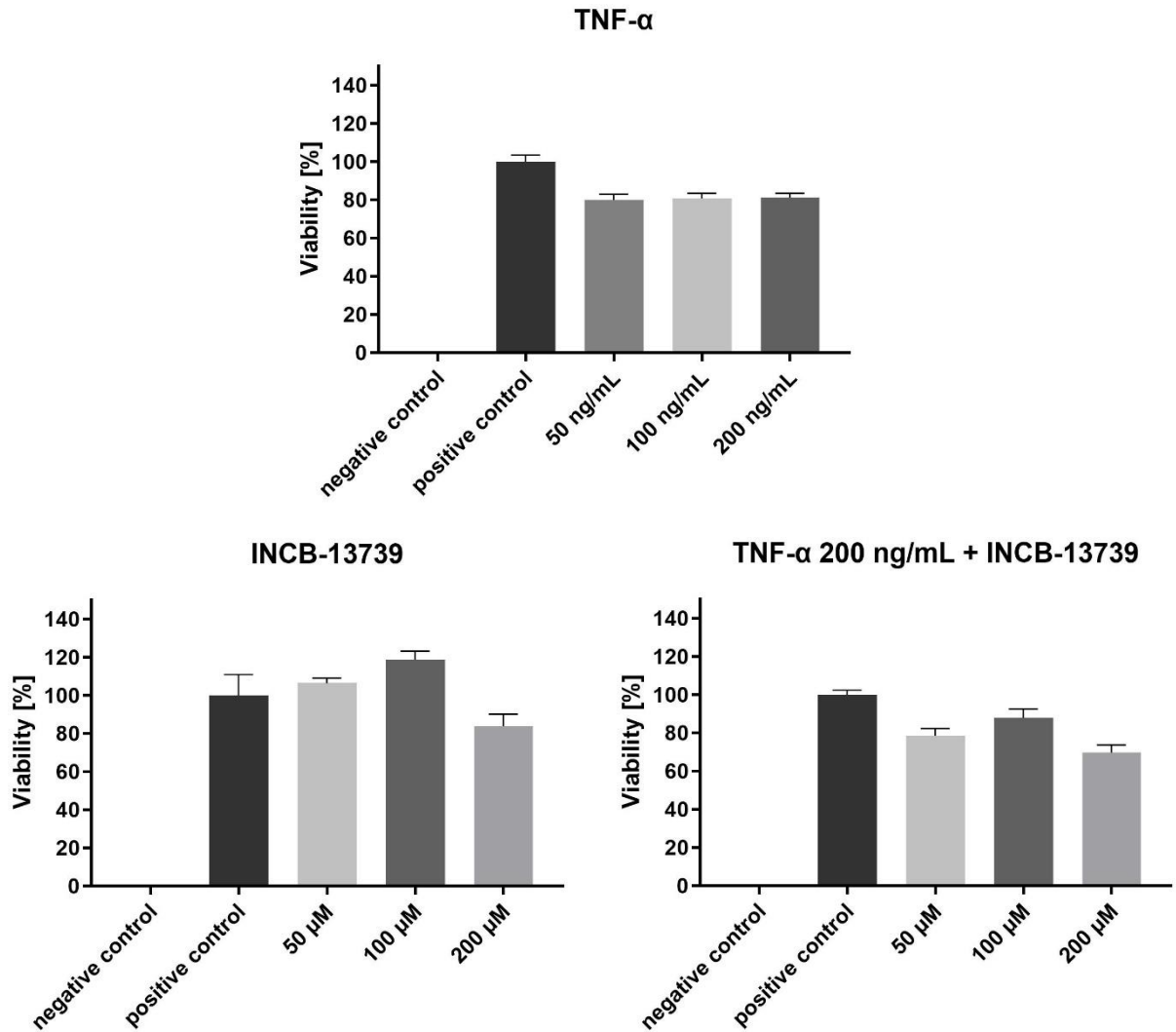


Figure S14: Viability testing of Inhibitor and inducer and in combination of both to determine use level on THP-1 cells. A viability of 80% was set as a limit for this assay. The resulting concentration was selected as working concentration for further experiments. neg. ctrl served as solvent control of 0,2% DMSO.

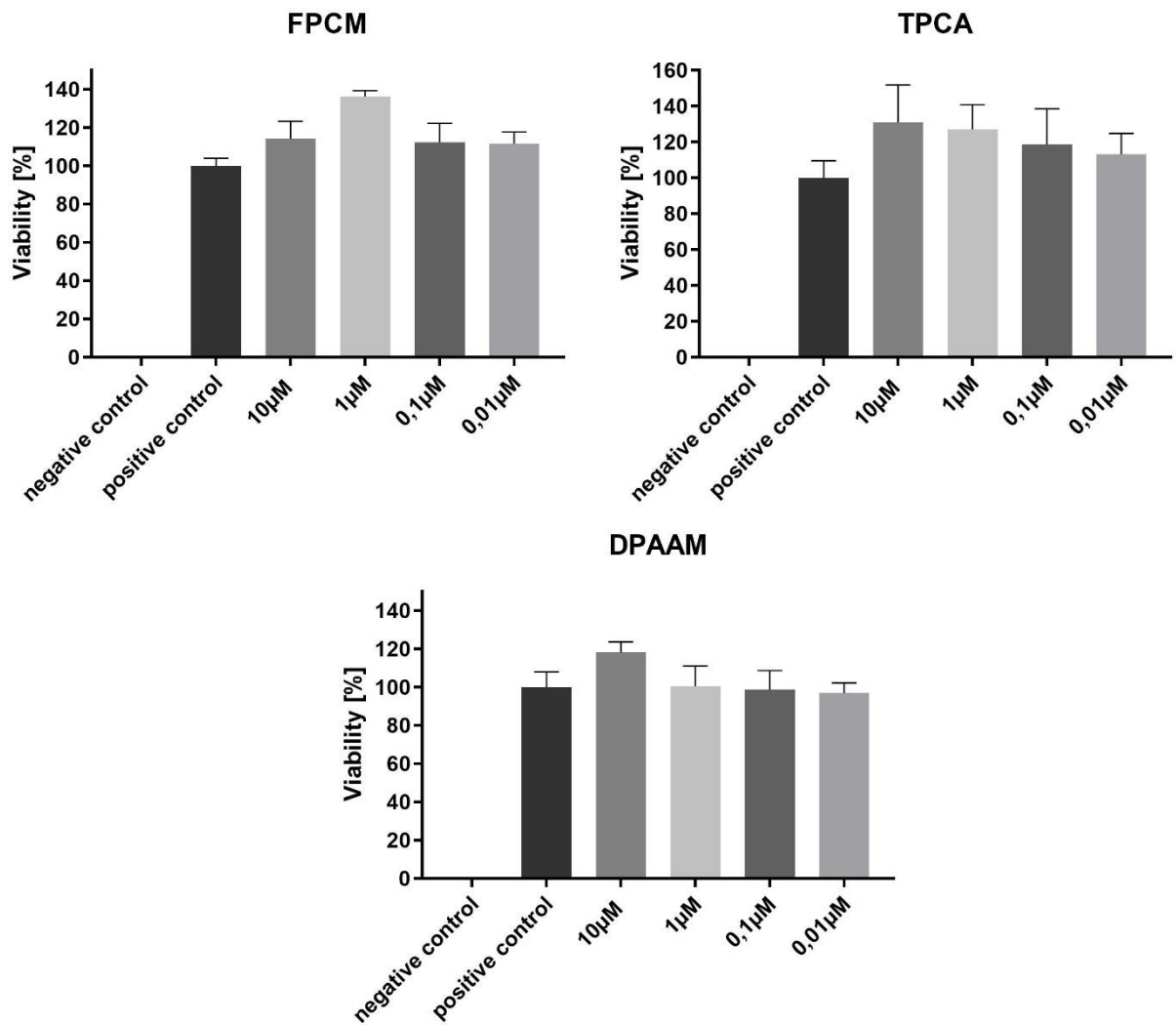
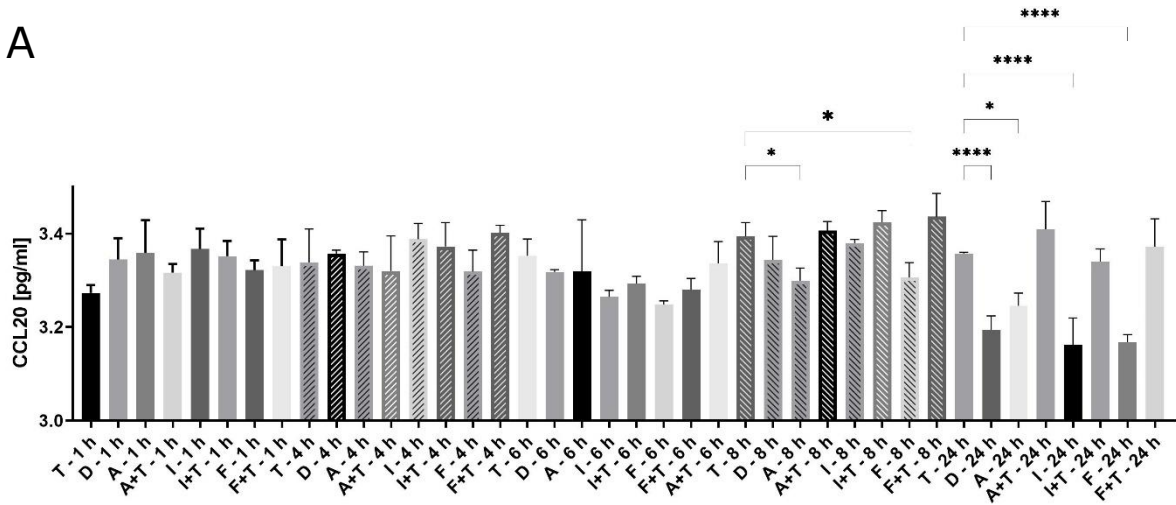


Figure S15: Viability testing of tested NCEs to determine use level on THP-1 cells. A viability of 80% was set as a limit for this assay. The resulting concentration was selected as working concentration for further experiments. neg. ctrl served as solvent control of 0,2% DMSO.

Treatment time

A



B

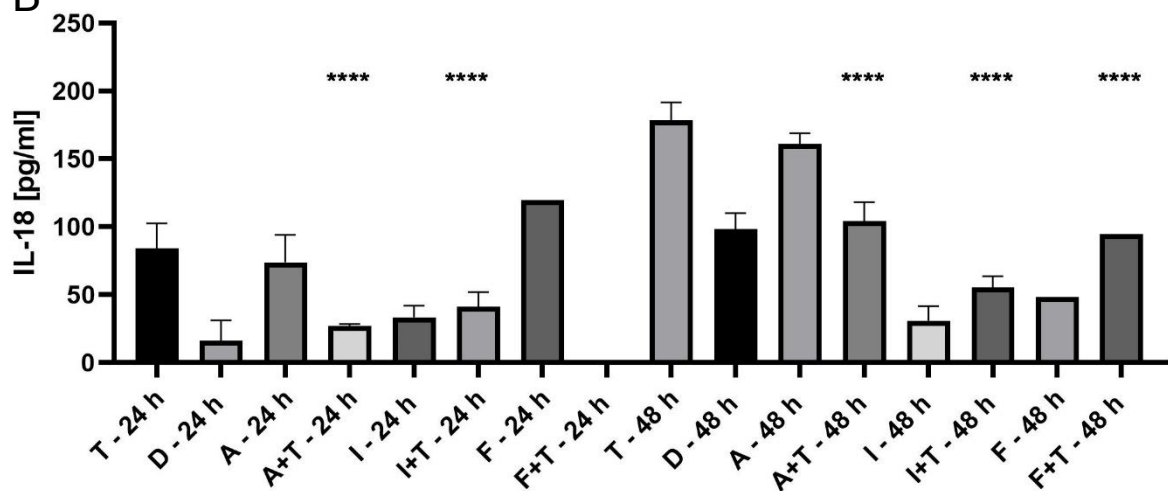


Figure S16: Response of pro-inflammatory biomarkers CCL20 and IL-18. A: Secretion response of CCL20 after different treatment time. B: Secretion response of IL-18 after different treatment time. HaCat cells were seeded in 96well and treated for 48h with substances in humidified atmosphere at 37°C and 5% CO₂. Supernatant was transferred to differentiated THP-1 cells and incubated. T= TNF- α , D= DMSO 0,2%, A=Aprepitant, I= INCB-13739, F= Fosaprepitant. Supernatant was further used for Elisa analysis (n=6, One-way ANOVA followed by $\alpha = 0.05$. Significances (****): $p < 0.0001$, (***): $p < 0.001$, (**): $p < 0.01$, (*): $p < 0.05$, (ns): $p \geq 0.05$). Means \pm SD are shown.



Proteomic Data of FPCM treatment on THP-1 cells

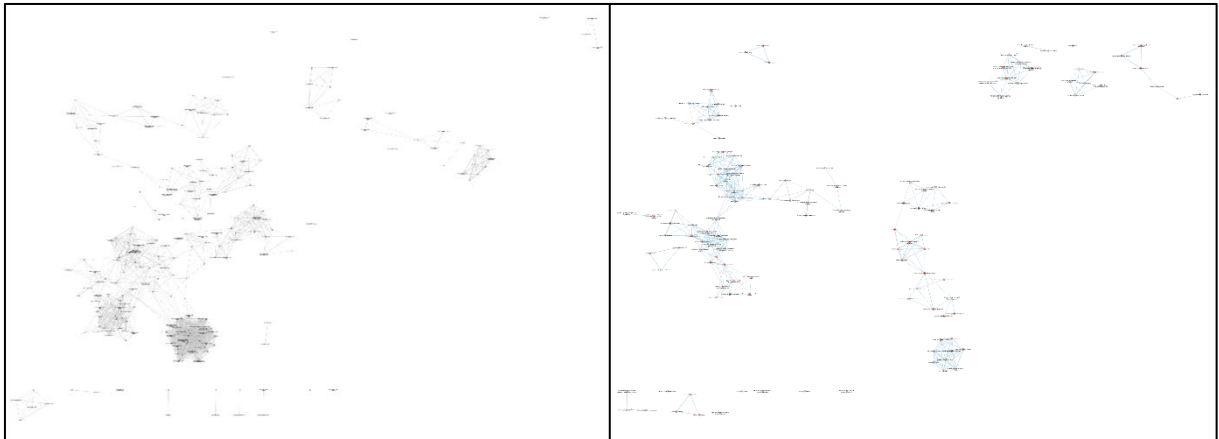


Figure S17: Enrichment of down (black) and upregulated (red) proteins in pro inflammatory induced THP-1 macrophages after treatment with secretom from HaCat cells treated with compound FPCM.

All BPs and pathways enriched in inflammation induced THP-1 cells were clustered according to their function similarities using Cytoscape. Each node (circle) represents a distinct biological process (GO:BP) or pathway (REAC) involving between 5 and 350 genes. Color gradient describes statistic linked to the identification of the biological process and pathways. Edges (lines) represent the number of genes overlapping between to biological processes or pathways, determined using the similarity coefficient.

Proteomic Data of TPCA treatment on THP-1 cells

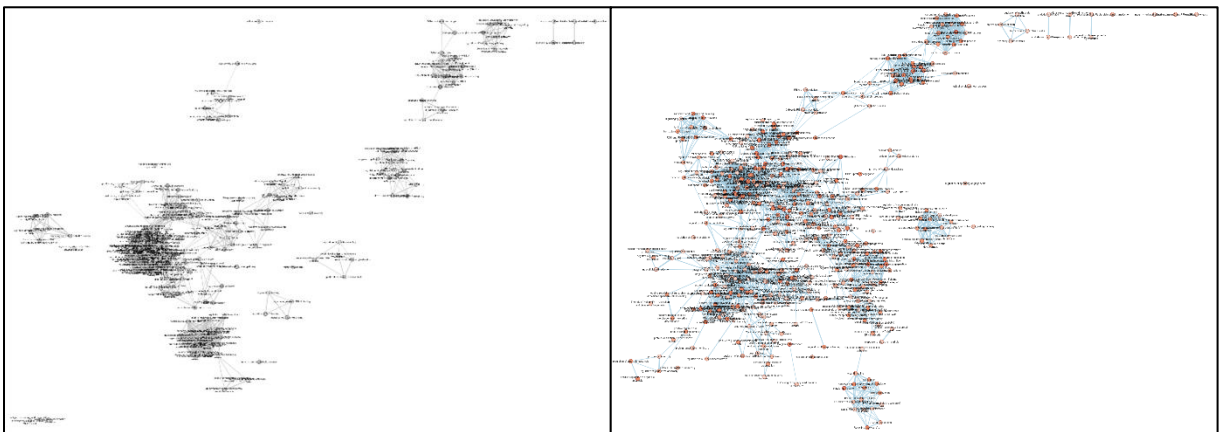


Figure S18: Enrichment of down (black) and upregulated (red) proteins in pro inflammatory induced THP-1 macrophages after treatment with secretom from HaCat cells treated with compound TPCA.

All BPs and pathways enriched in inflammation induced THP-1 cells were clustered according to their function similarities using Cytoscape. Each node (circle) represents a distinct biological process (GO:BP) or pathway (REAC) involving between 5 and 350 genes. Color gradient describes statistic linked to the identification of the biological process and pathways. Edges (lines) represent the number of genes overlapping between to biological processes or pathways, determined using the similarity coefficient.

Proteomic Data of DPAAM treatment on THP-1 cells

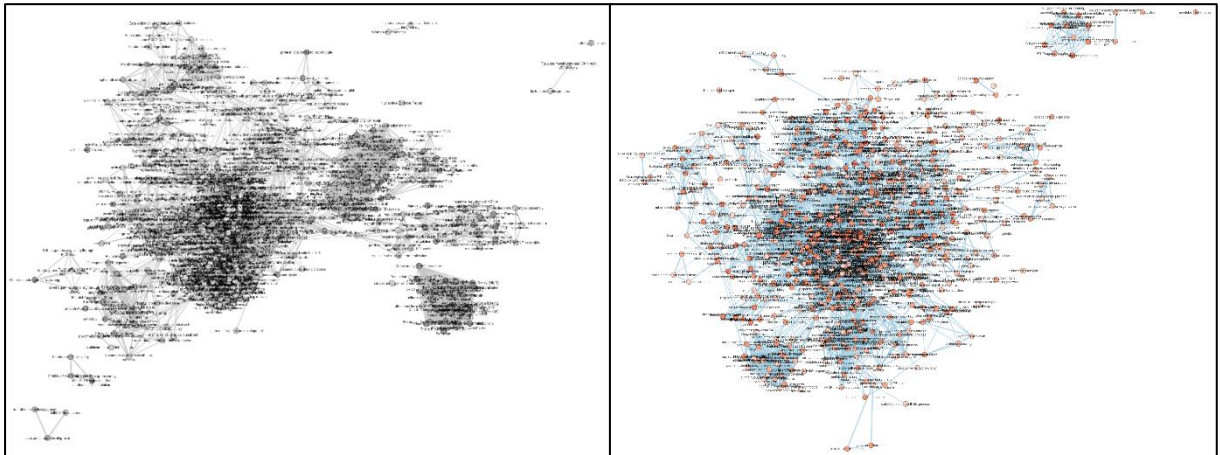


Figure S19: Enrichment of down (black) and upregulated (red) proteins in pro inflammatory induced THP-1 macrophages after treatment with secretom from HaCat cells treated with compound DPAAM.

All BPs and pathways enriched in inflammation induced THP-1 cells were clustered according to their function similarities using Cytoscape. Each node (circle) represents a distinct biological process (GO:BP) or pathway (REAC) involving between 5 and 350 genes. Color gradient describes statistic linked to the identification of the biological process and pathways. Edges (lines) represent the number of genes overlapping between to biological processes or pathways, determined using the similarity coefficient.

Supplemental Data NK1R
Viability testing for the determination of use level

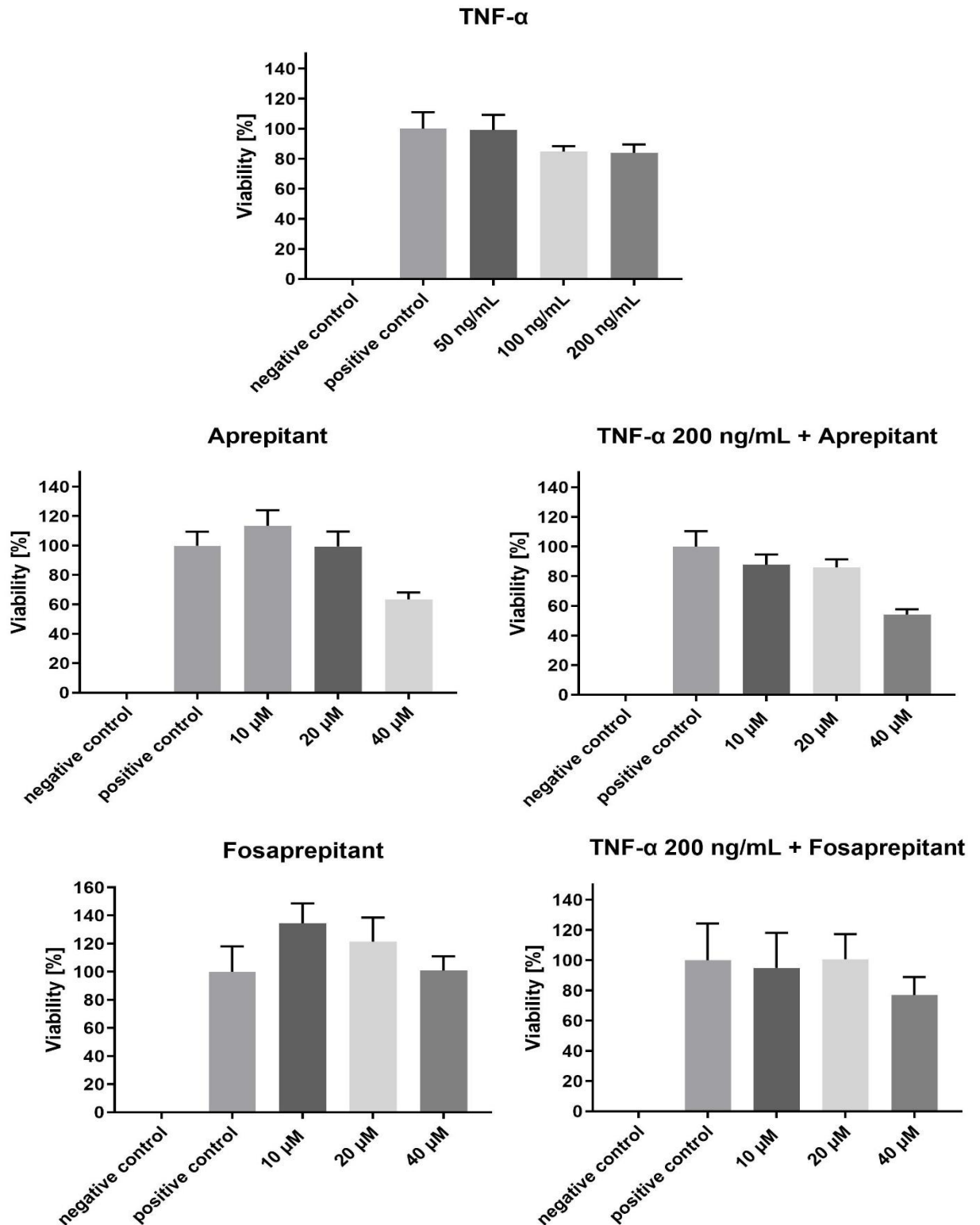


Figure S20: Viability testing of Inhibitor and inducer and in combination of both to determine use level on HaCat cells. A viability of 80% was set as a limit for this assay. The resulting concentration was selected as working concentration for further experiments. neg. ctrl served as solvent control of 0,2% DMSO.

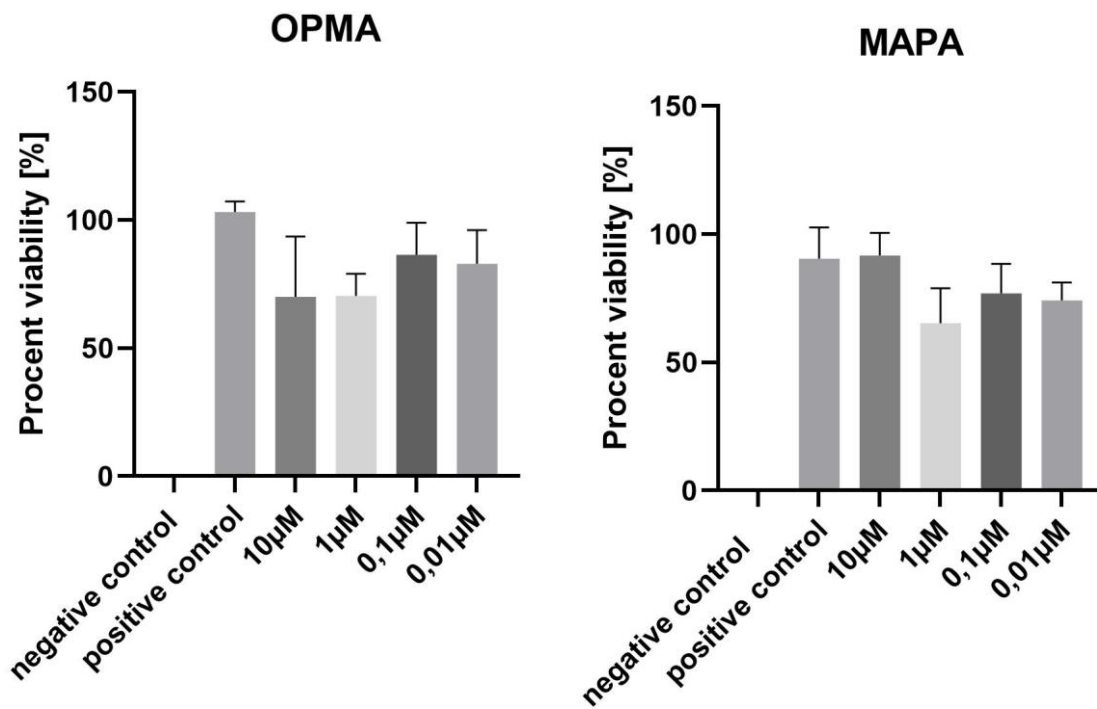


Figure S21: Viability testing of tested NCEs to determine use level on HaCat cells. A viability of 80% was set as a limit for this assay. The resulting concentration was selected as working concentration for further experiments. neg. ctrl served as solvent control of 0,2% DMSO.

Calcium Influx Data of compounds in CHO-K1 and CHO-K1-NK1R cells

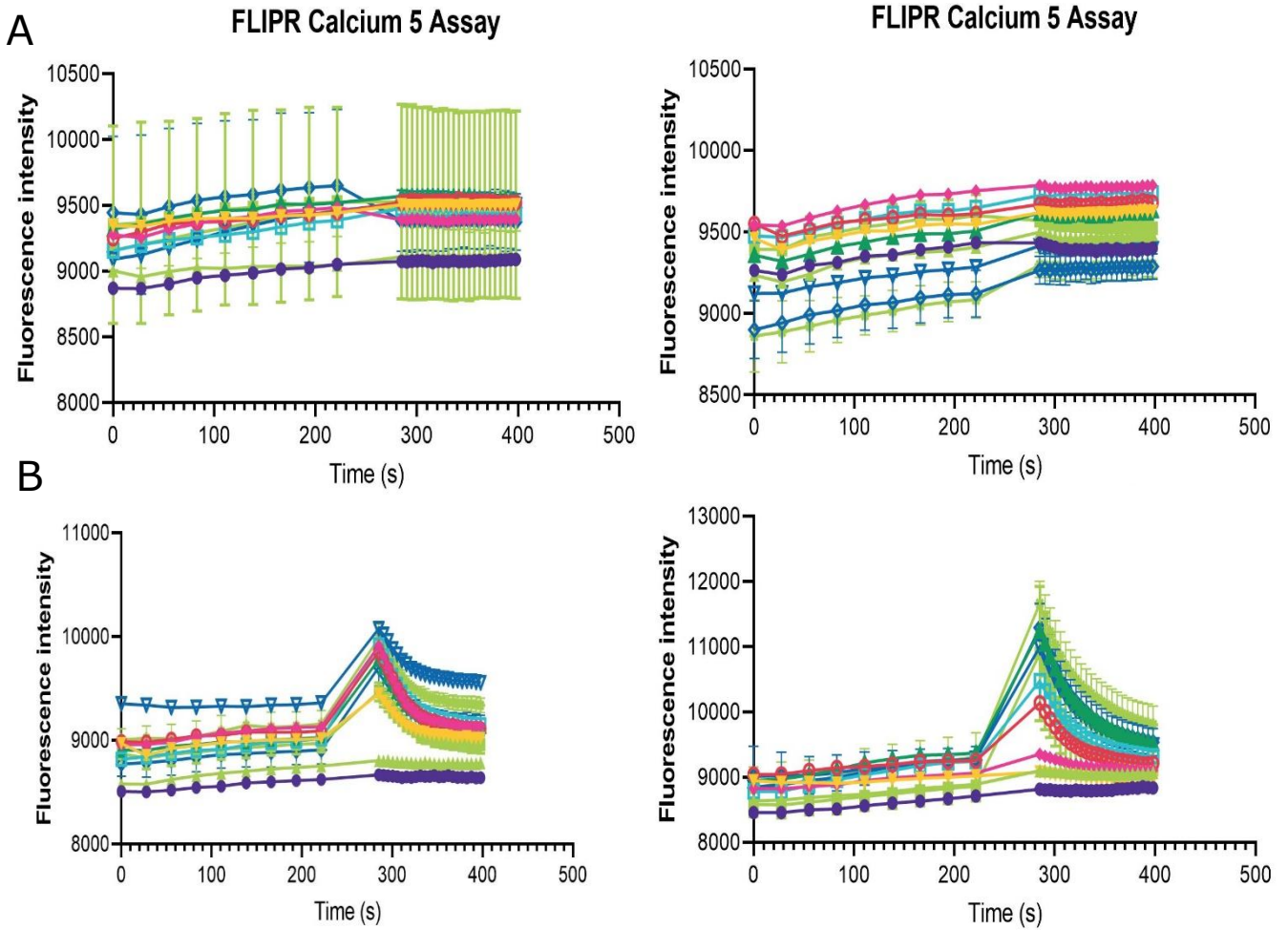


Figure S22: Ca²⁺ influx after NK1R activation after treatment with MAPA and OPMA on A: CHO-K1 cells and B: CHO-K1-NK1R cells

CHO-K1 or CHO-K1-NK1R cells were seeded in 96well plates overnight in humidified atmosphere at 37°C and 5% CO₂. Treatment for 10min and after treatment with agonist (SP) subsequently measured. (n=6, transformed data to log followed by non-linear regression. Means ± SD are shown.)

Proteomic Data on HaCat cells after MAPA treatment

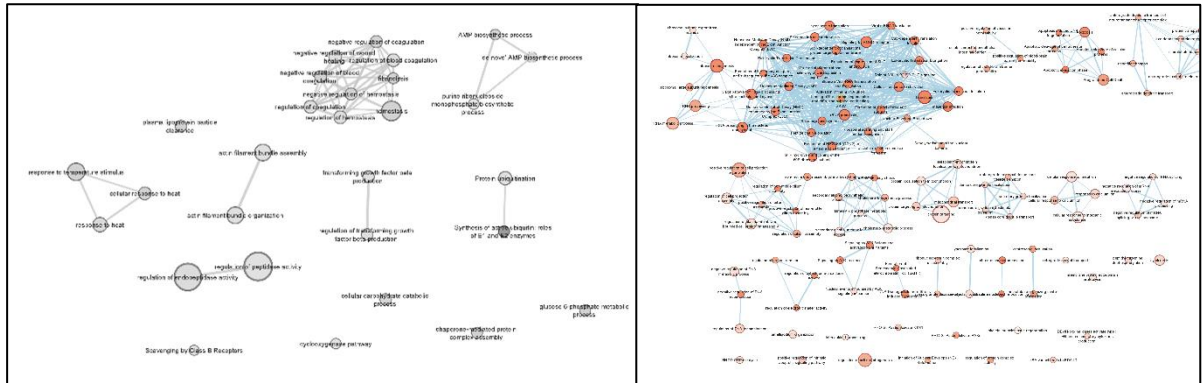


Figure S23: Enrichment of down (black) and upregulated (red) proteins after MAPA treatment. All BPs and pathways enriched in inflammation induced HaCat cells due to down and upregulated proteins were arranged according to function similarities. Each node (circle) represents a distinct biological process (GO:BP) or pathway (REAC) involving between 5 and 350 genes. Color gradient describes statistic linked to the identification of the biological process and pathways. Edges (lines) represent the number of genes overlapping between to biological processes or pathways, determined using the similarity coefficient.

Proteomic Data on HaCat cells after OPMA treatment

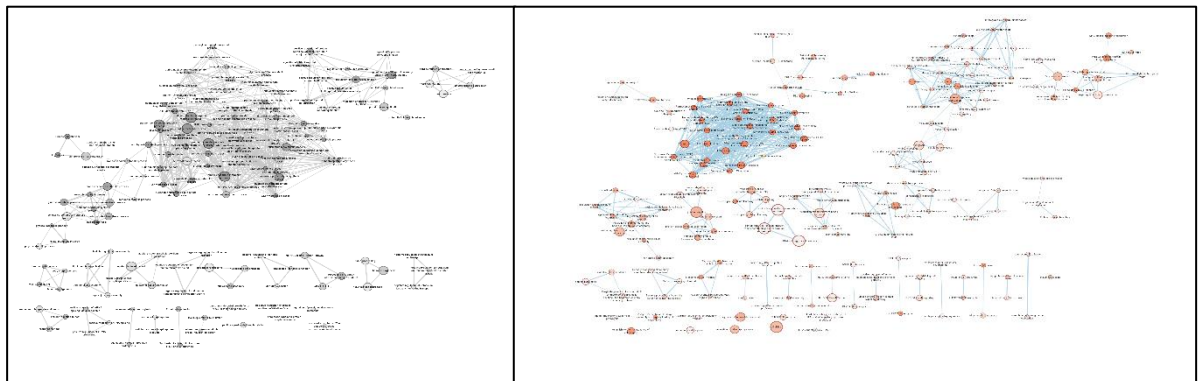


Figure S24: Enrichment of down (black) and upregulated (red) proteins after OPMA treatment. All BPs and pathways enriched in inflammation induced HaCat cells due to down and upregulated proteins were arranged according to function similarities. Each node (circle) represents a distinct biological process (GO:BP) or pathway (REAC) involving between 5 and 350 genes. Color gradient describes statistic linked to the identification of the biological process and pathways. Edges (lines) represent the number of genes overlapping between to biological processes or pathways, determined using the similarity coefficient.

Differences in chemical analogue structure influence effectivity in modulating downstream targets

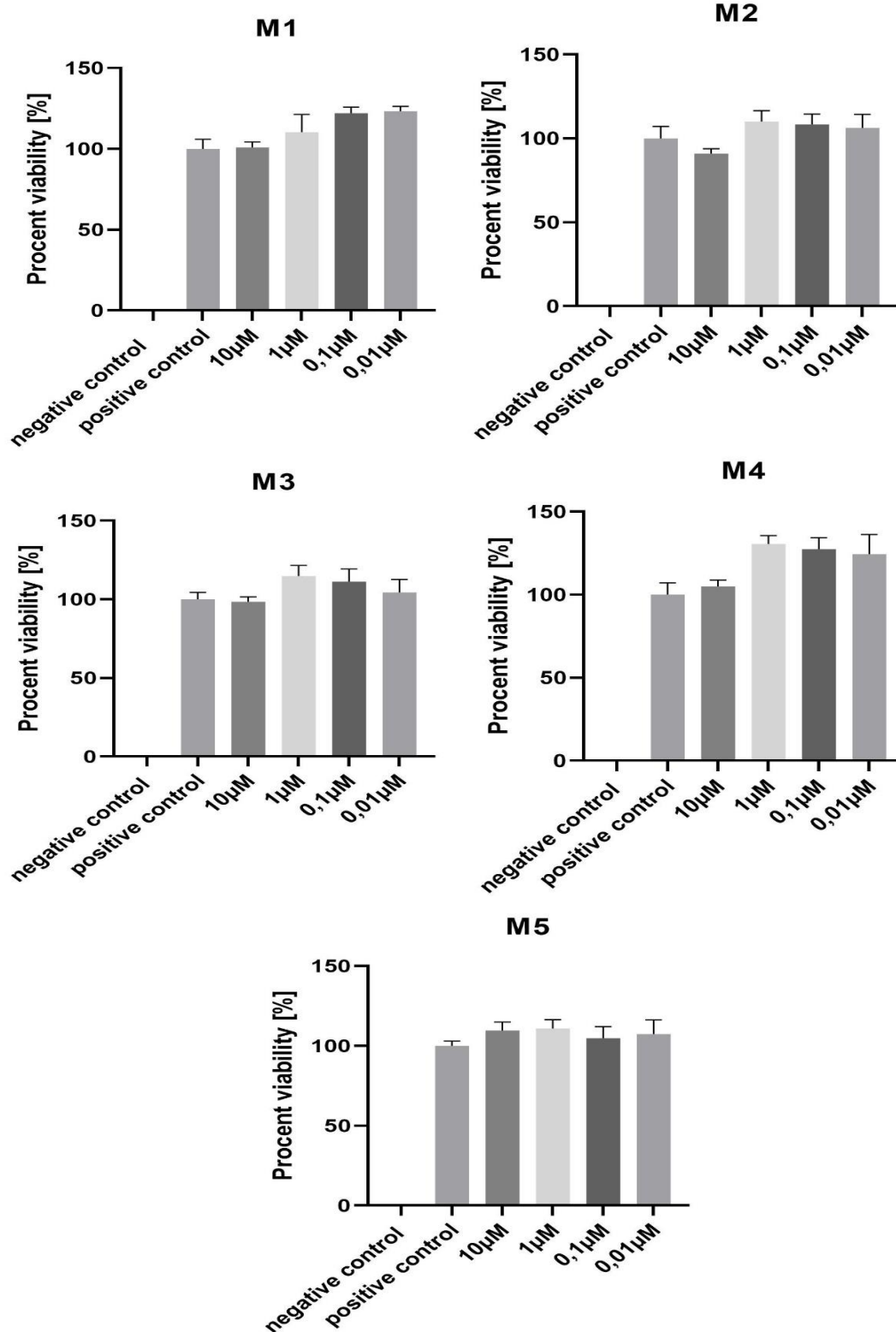


Figure S26: Viability testing of analogue compounds to DPAAM to determine use level. A viability of 80% was set as a limit for this assay. The resulting concentration was selected as working concentration for further experiments. neg. ctrl served as solvent control of 0,2% DMSO.

Inflammatory response after treatment with analogue compounds to DPAAM

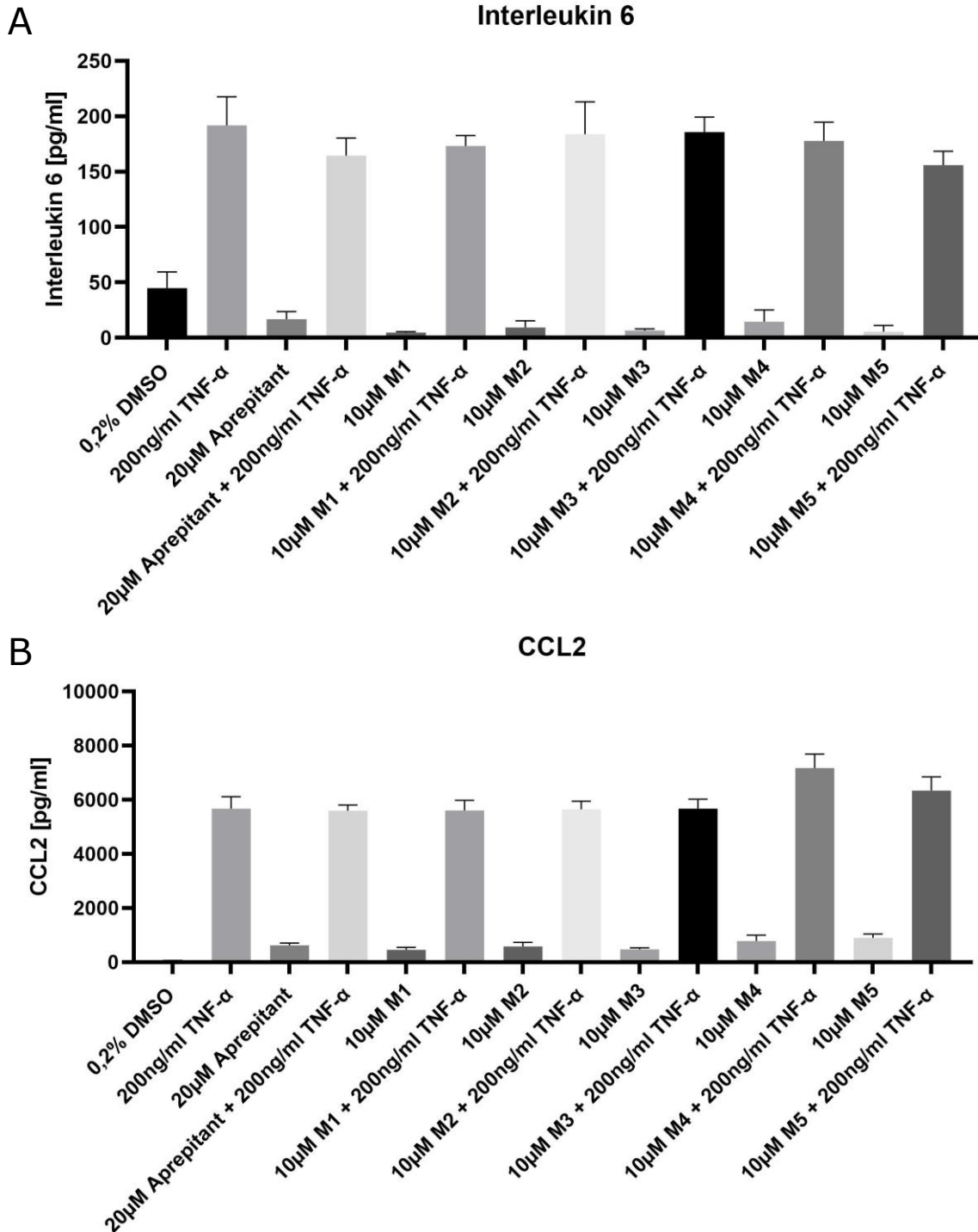


Figure S27: Response of pro-inflammatory biomarkers IL-6 and CCL2. A: Secretion response of IL-6 after five analogue compounds to DPAAM. B: Secretion response of CCL2 after five analogue compounds to DPAAM. HaCat cells were seeded in 96well and treated for 48h with substances in humidified atmosphere at 37°C and 5% CO₂. 0.2% DMSO served as negative control. Supernatant was further used for Elisa analysis (n=6, One-way ANOVA followed by $\alpha = 0.05$. Significances (****): $p < 0.0001$, (***) : $p < 0.001$, (**) : $p < 0.01$, (*) : $p < 0.05$, (ns): $p \geq 0.05$). Means \pm SD are shown.

Keratinocytes NK1R
Viability testing for the determination of use level

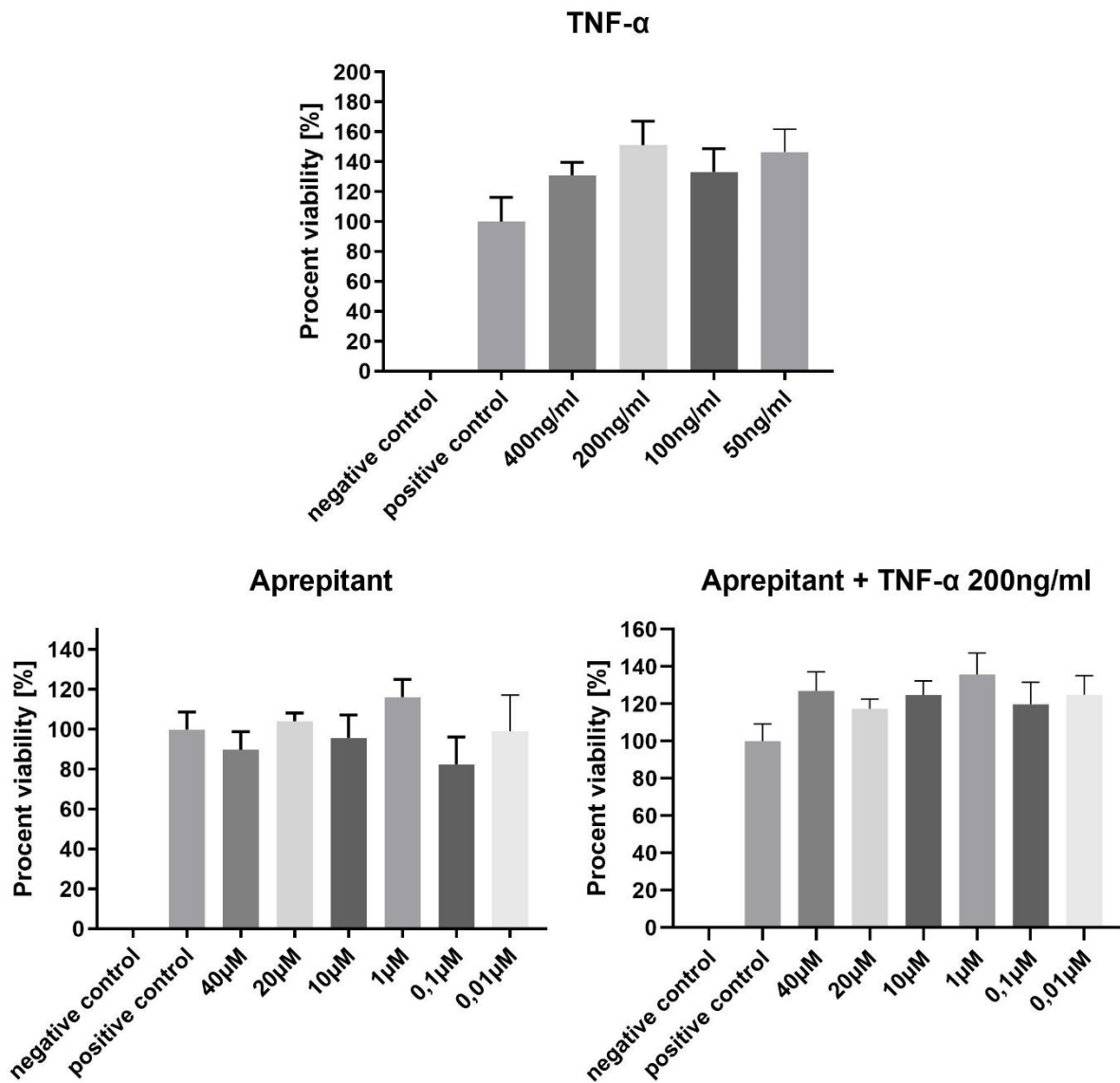


Figure S28: Viability testing of Inhibitor and inducer and in combination of both to determine use level on primary keratinocytes. A viability of 80% was set as a limit for this assay. The resulting concentration was selected as working concentration for further experiments. neg. ctrl served as solvent control of 0,2% DMSO.

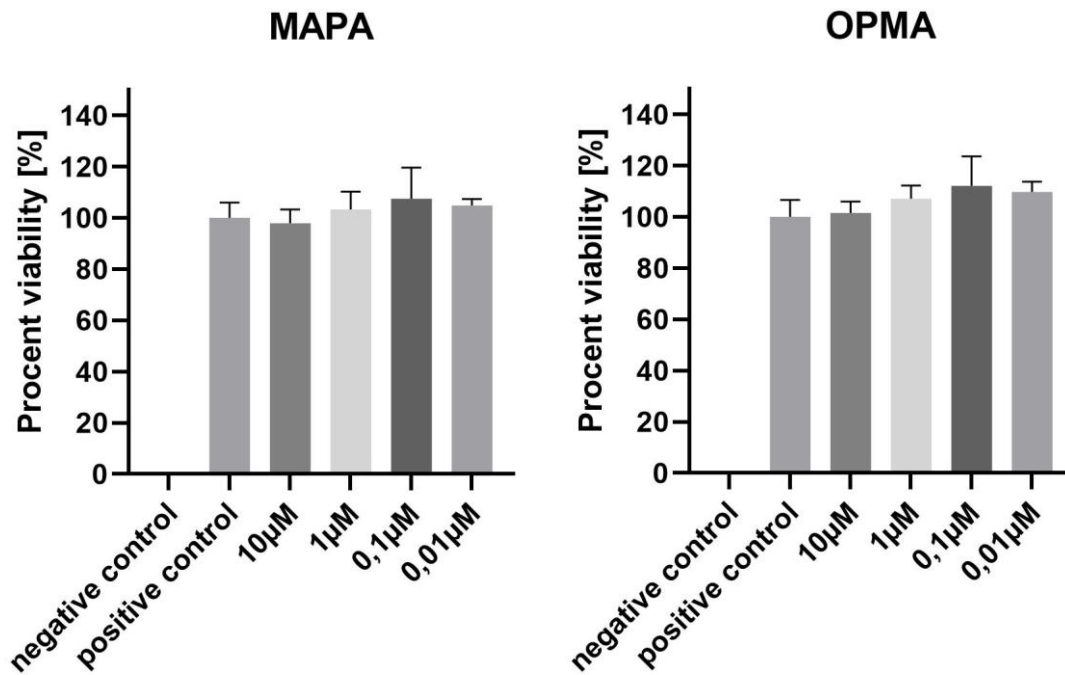


Figure S29: Viability testing of tested NCEs to determine use level on primary keratinocytes. A viability of 80% was set as a limit for this assay. The resulting concentration was selected as working concentration for further experiments. neg. ctrl served as solvent control of 0,2% DMSO.

Proteomic Data on primary keratinocytes cells after MAPA treatment

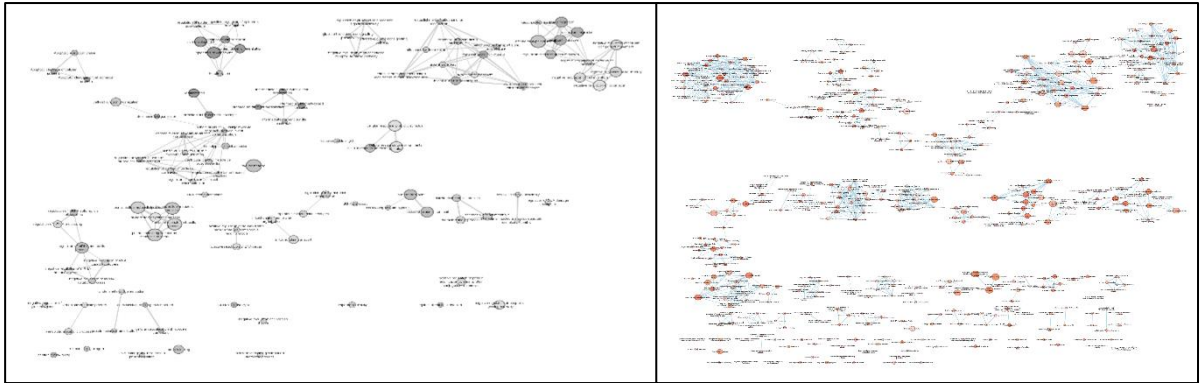


Figure S30: Enrichment of down (black) and upregulated (red) proteins after MAPA treatment. All BPs and pathways enriched in inflammation induced primary keratinocytes due to down and upregulated proteins were arranged according to function similarities. Each node (circle) represents a distinct biological process (GO:BP) or pathway (REAC) involving between 5 and 350 genes. Color gradient describes statistic linked to the identification of the biological process and pathways. Edges (lines) represent the number of genes overlapping between to biological processes or pathways, determined using the similarity coefficient.

Proteomic Data on primary keratinocytes cells after OPMA treatment

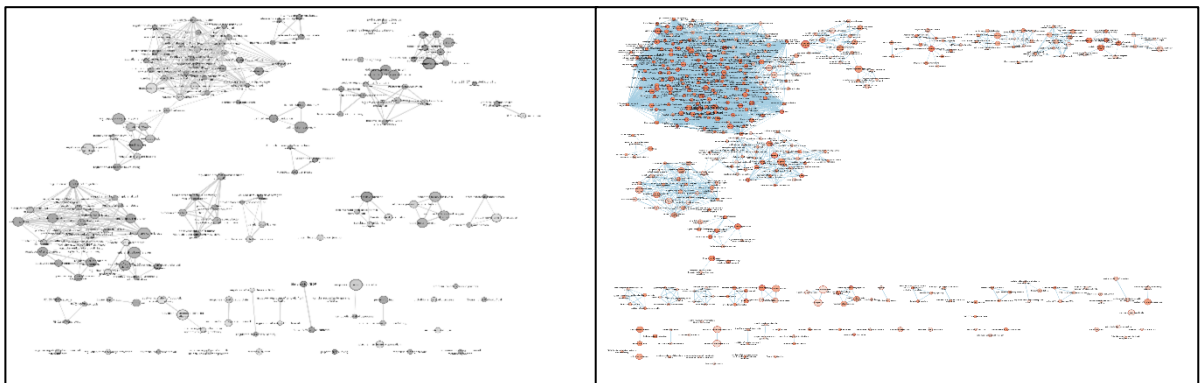


Figure S31: Enrichment of down (black) and upregulated (red) proteins after OPMA treatment. All BPs and pathways enriched in inflammation induced primary keratinocytes due to down and upregulated proteins were arranged according to function similarities. Each node (circle) represents a distinct biological process (GO:BP) or pathway (REAC) involving between 5 and 350 genes. Color gradient describes statistic linked to the identification of the biological process and pathways. Edges (lines) represent the number of genes overlapping between to biological processes or pathways, determined using the similarity coefficient.

THP1 cells
Viability testing for the determination of use level

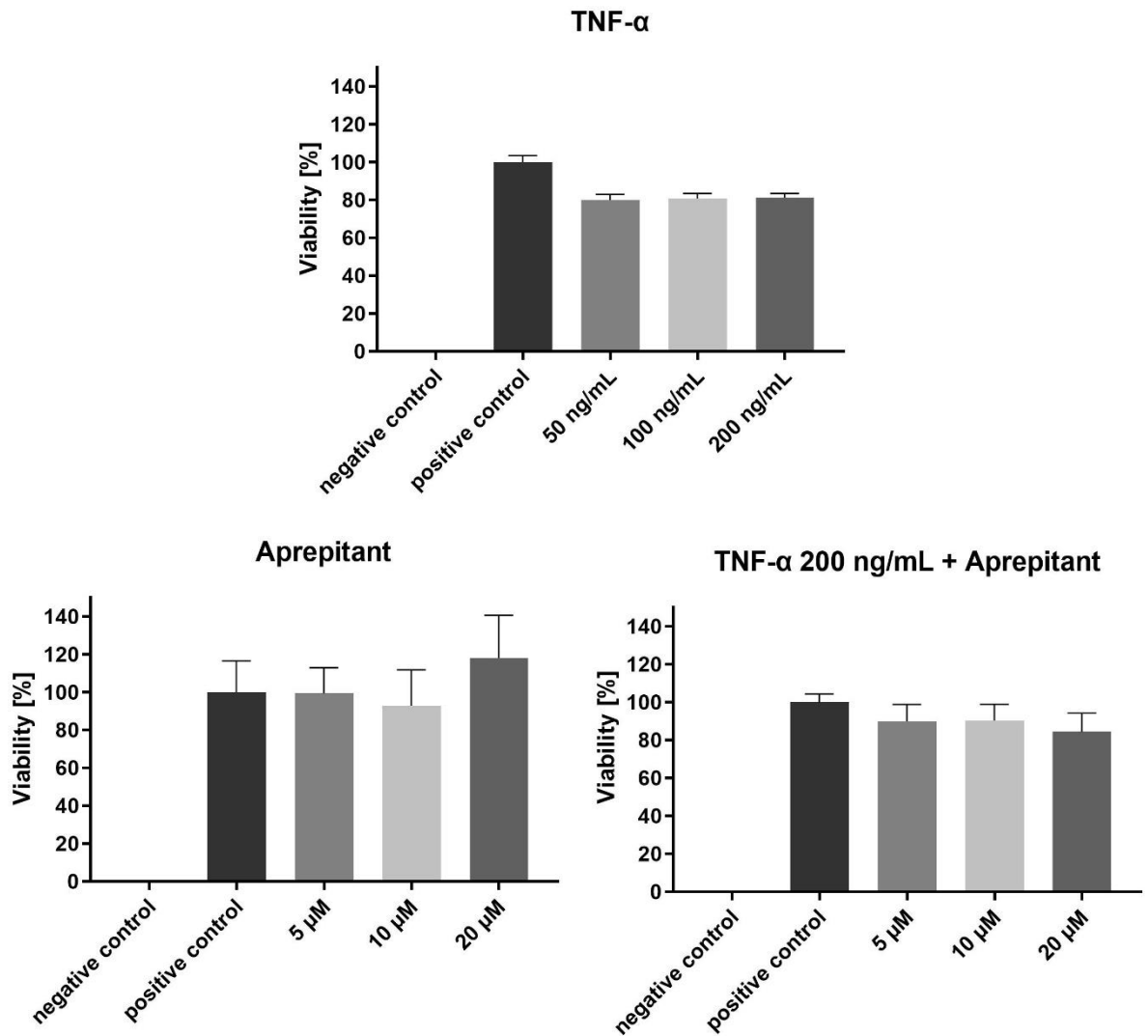


Figure S32: Viability testing of Inhibitor and inducer and in combination of both to determine use level on THP-1 cells. A viability of 80% was set as a limit for this assay. The resulting concentration was selected as working concentration for further experiments. neg. ctrl served as solvent control of 0,2% DMSO.

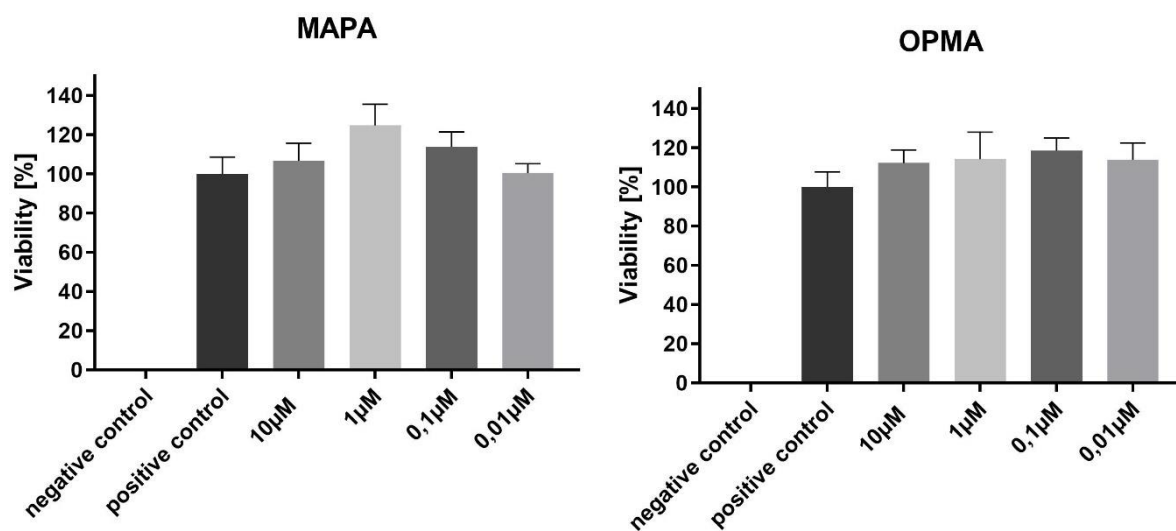


Figure S33: Viability testing of tested NCEs to determine use level on THP-1 cells. A viability of 80% was set as a limit for this assay. The resulting concentration was selected as working concentration for further experiments. neg. ctrl served as solvent control of 0,2% DMSO.

Proteomic Data on THP-1 cells after MAPA treatment

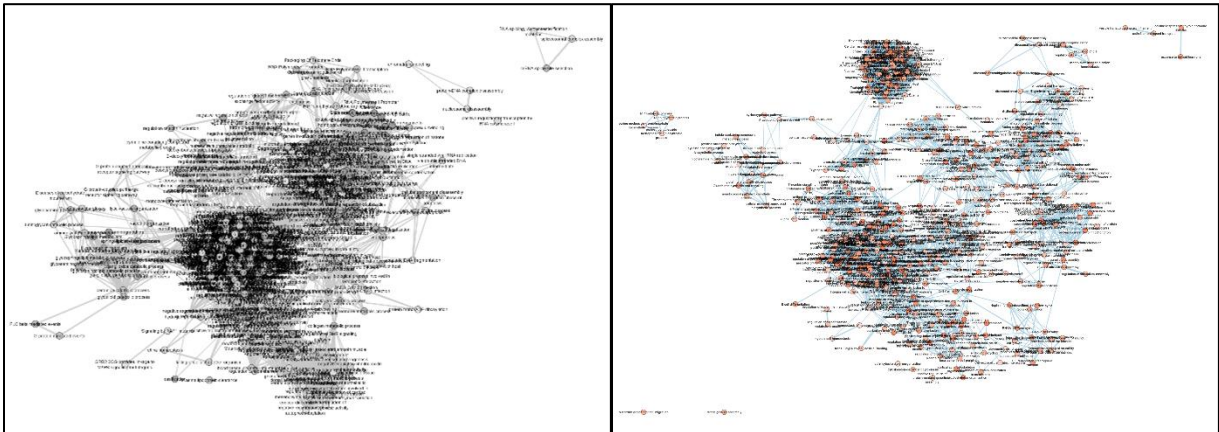


Figure S34: Enrichment of down (black) and upregulated (red) proteins in pro inflammatory induced THP-1 macrophages after treatment with secretom from HaCat cells treated with compound MAPA.

All BPs and pathways enriched in inflammation induced THP-1 cells were clustered according to their function similarities using Cytoscape. Each node (circle) represents a distinct biological process (GO:BP) or pathway (REAC) involving between 5 and 350 genes. Color gradient describes statistic linked to the identification of the biological process and pathways. Edges (lines) represent the number of genes overlapping between to biological processes or pathways, determined using the similarity coefficient.

Proteomic Data on THP-1 cells after OPMA treatment

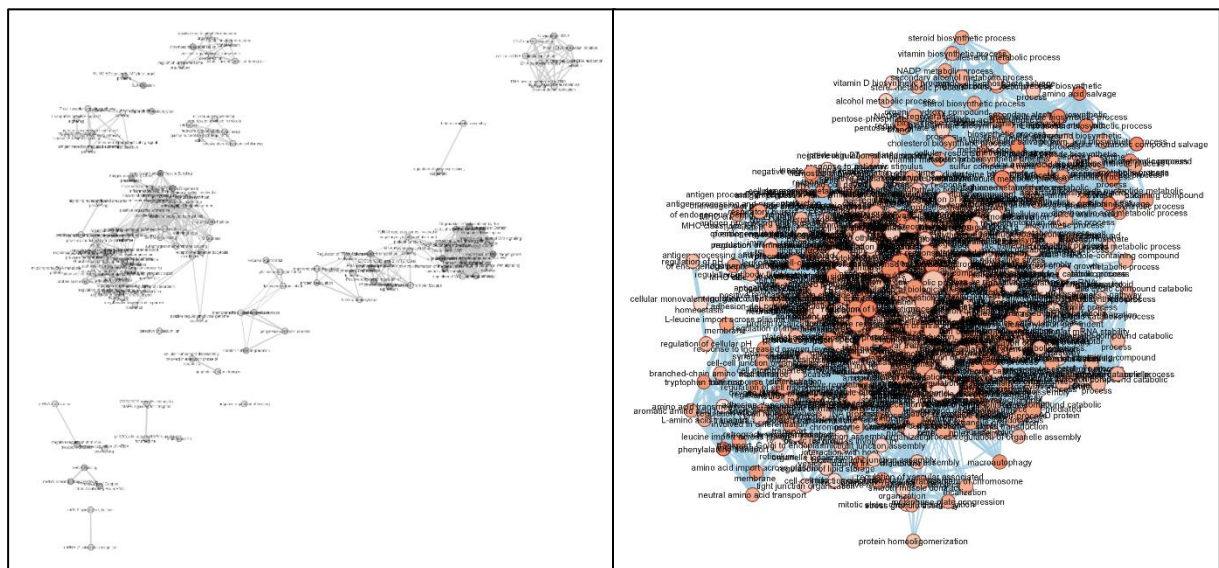


Figure S35: Enrichment of down (black) and upregulated (red) proteins in pro inflammatory induced THP-1 macrophages after treatment with secretom from HaCat cells treated with compound OPMA.

All BPs and pathways enriched in inflammation induced THP-1 cells were clustered according to their function similarities using Cytoscape. Each node (circle) represents a distinct biological process (GO:BP) or pathway (REAC) involving between 5 and 350 genes. Color gradient describes statistic linked to the identification of the biological process and pathways. Edges (lines) represent the number of genes overlapping between to biological processes or pathways, determined using the similarity coefficient.

Phosphorylated protein level of different signaling proteins after compound treatment in HaCat cells
NFkB

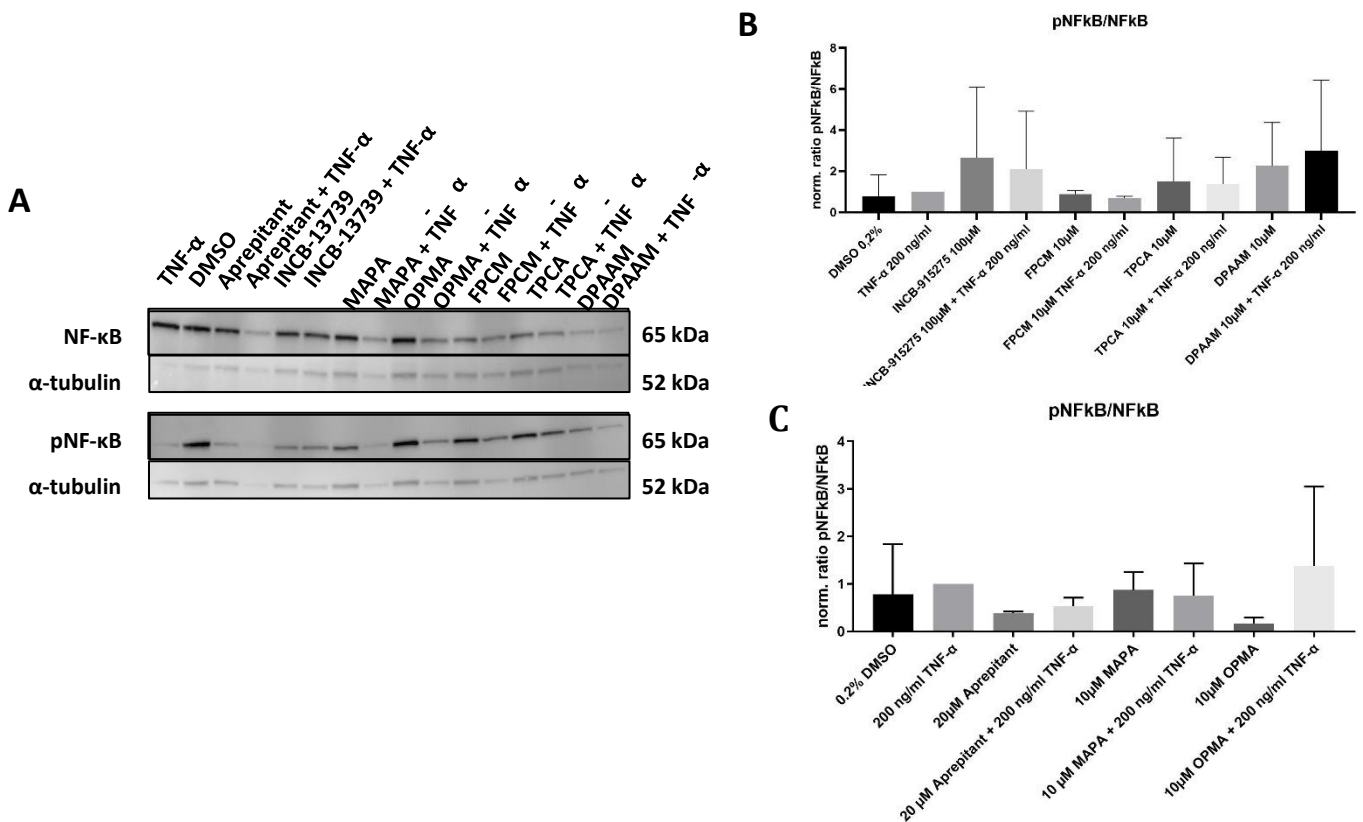


Figure S36: Quantification of NFkB and phosphorylated NFkB (A) after treatment with B: FPCM, TPCA and DPAAM and C: MAPA and OPMA
HaCat cells were seeded in 6-well plate and treated for 48h with substances in humidified atmosphere at 37°C and 5% CO₂ afterwards harvested and lysed in Lysis Buffer. Cell lysates were further used for Western Blot analysis. 0.2% DMSO served as negative control. 20µg protein lysate were used to assess the expression of NFkB. (n=3, One-way ANOVA followed by $\alpha = 0.05$. Significances (****): $p < 0.0001$, (***): $p < 0.001$, (**): $p < 0.01$, (*): $p < 0.05$, (ns): $p \geq 0.05$). Means \pm SD are shown.

ERK

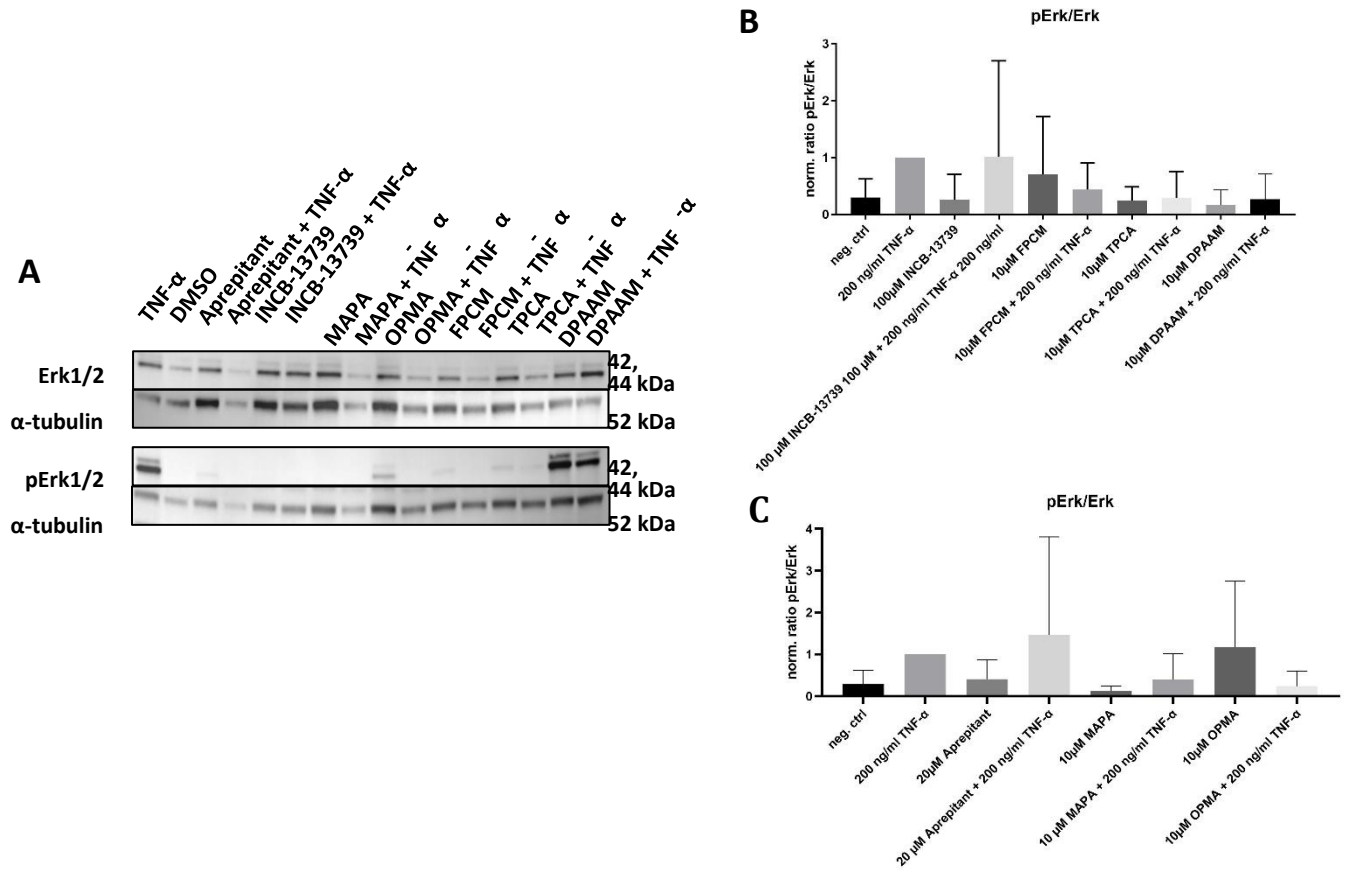


Figure S37: Quantification of ERK and phosphorylated ERK (A) after treatment with B: FPCM, TPCA and DPAAM and C: MAPA and OPMA

HaCat cells were seeded in 6-well plate and treated for 48h with substances in humidified atmosphere at 37°C and 5% CO₂ afterwards harvested and lysed in Lysis Buffer. Cell lysates were further used for Western Blot analysis. 0.2% DMSO served as negative control. 20 μ g protein lysate were used to assess the expression of ERK. (n=3, One-way ANOVA followed by $\alpha = 0.05$. Significances (****): $p < 0.0001$, (***) : $p < 0.001$, (**) : $p < 0.01$, (*) : $p < 0.05$, (ns): $p \geq 0.05$). Means \pm SD are shown.

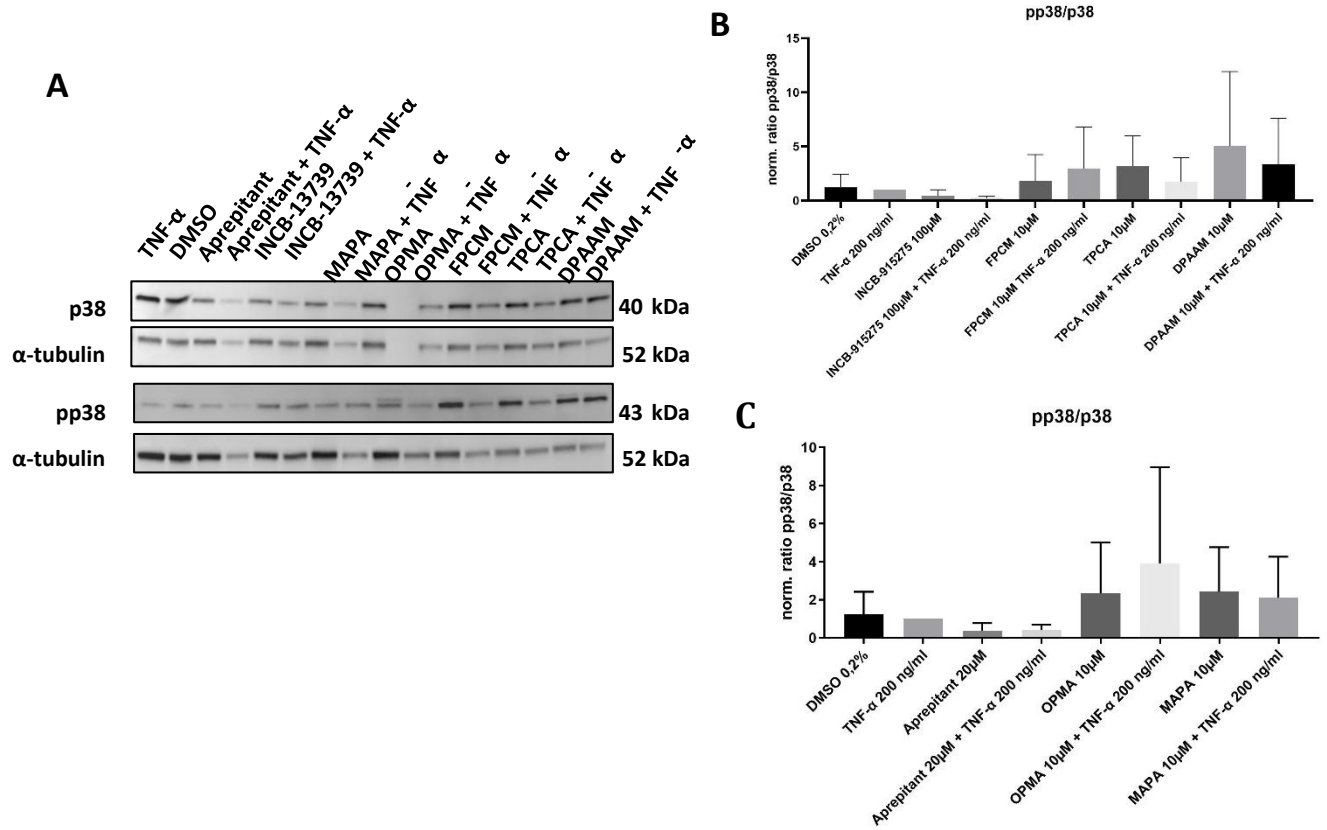


Figure S38: Quantification of p38 and phosphorylated p38 (A) after treatment with B: FPCM, TPCA and DPAAM and C: MAPA and OPMA

HaCat cells were seeded in 6-well plate and treated for 48h with substances in humidified atmosphere at 37°C and 5% CO₂ afterwards harvested and lysed in Lysis Buffer. Cell lysates were further used for Western Blot analysis. 0,2% DMSO served as negative control. 20 μ g protein lysate were used to assess the expression of p38. (n=3, One-way ANOVA followed by $\alpha = 0.05$. Significances (****): p < 0.0001, (**): p < 0.01, (*): p < 0.05, (ns): p \geq 0.05). Means \pm SD are shown.

Akt

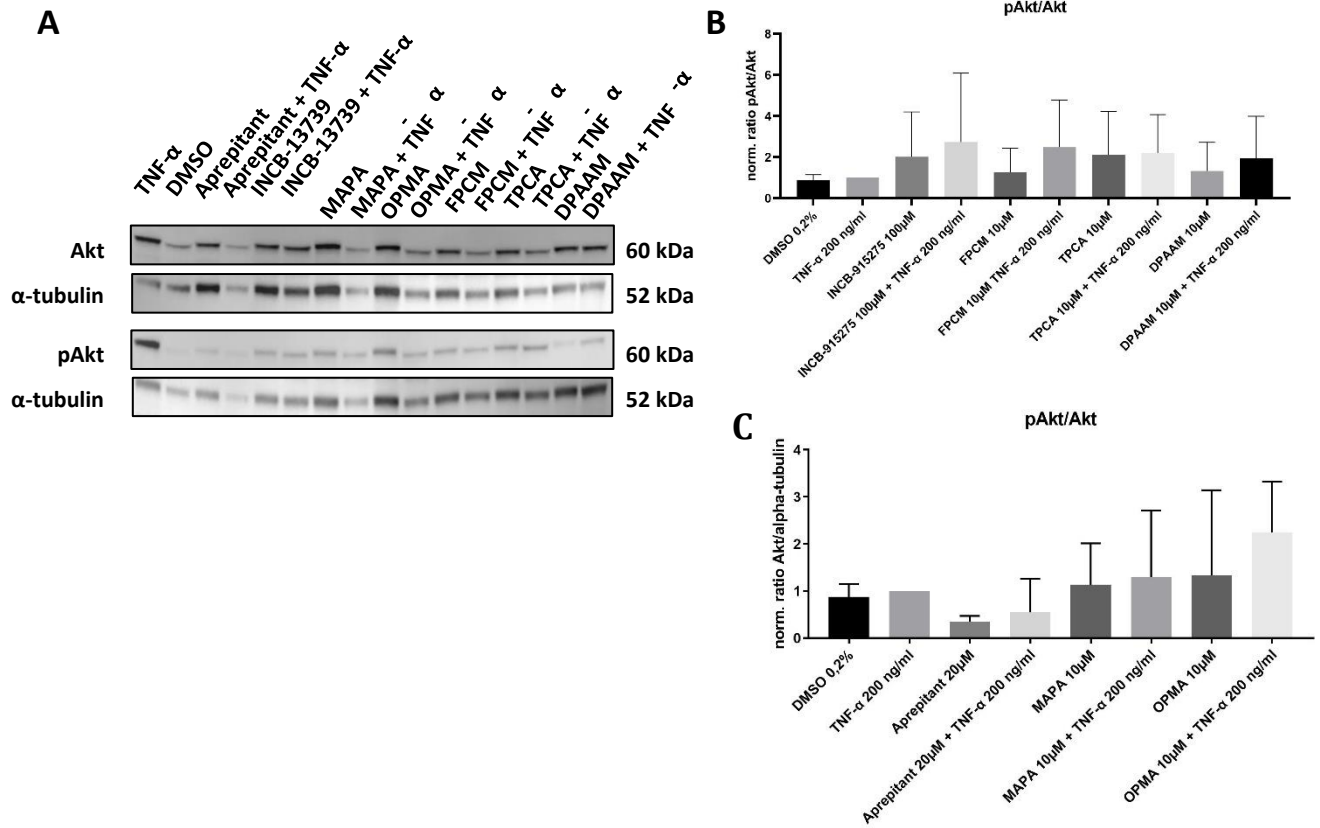


Figure S39: Quantification of Akt and phosphorylated Akt (A) after treatment with B: FPCM, TPCA and DPAAM and C: MAPA and OPMA

HaCat cells were seeded in 6-well plate and treated for 48h with substances in humidified atmosphere at 37°C and 5% CO₂ afterwards harvested and lysed in Lysis Buffer. Cell lysates were further used for Western Blot analysis. 0.2% DMSO served as negative control. 20 μ g protein lysate were used to assess the expression of Akt. (n=3, One-way ANOVA followed by $\alpha = 0.05$. Significances (****): $p < 0.0001$, (***) : $p < 0.001$, (**) : $p < 0.01$, (*) : $p < 0.05$, (ns): $p \geq 0.05$). Means \pm SD are shown.

Stat3

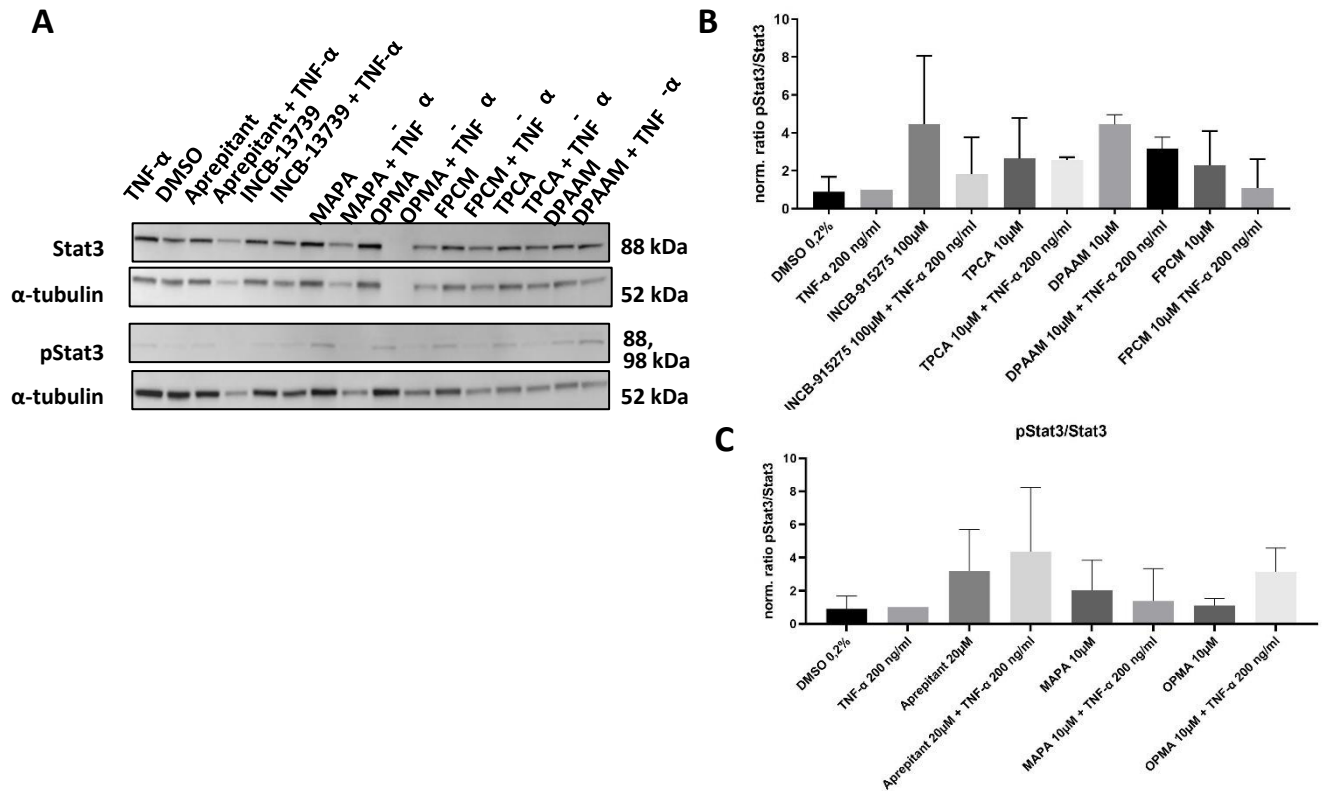


Figure S40: Quantification of Stat3 and phosphorylated Stat3 (A) after treatment with B: FPCM, TPCA and DPAAM and C: MAPA and OPMA

HaCat cells were seeded in 6-well plate and treated for 48h with substances in humidified atmosphere at 37°C and 5% CO₂ afterwards harvested and lysed in Lysis Buffer. Cell lysates were further used for Western Blot analysis. 0.2% DMSO served as negative control. 20 μ g protein lysate were used to assess the expression of Stat3. (n=3, One-way ANOVA followed by $\alpha = 0.05$. Significances (****): $p < 0.0001$, (***): $p < 0.001$, (**): $p < 0.01$, (*): $p < 0.05$, (ns): $p \geq 0.05$). Means \pm SD are shown.

Phosphorylated protein level of different signaling proteins after compound treatment in HaCat cells and transferred to THP-1 cells
P38

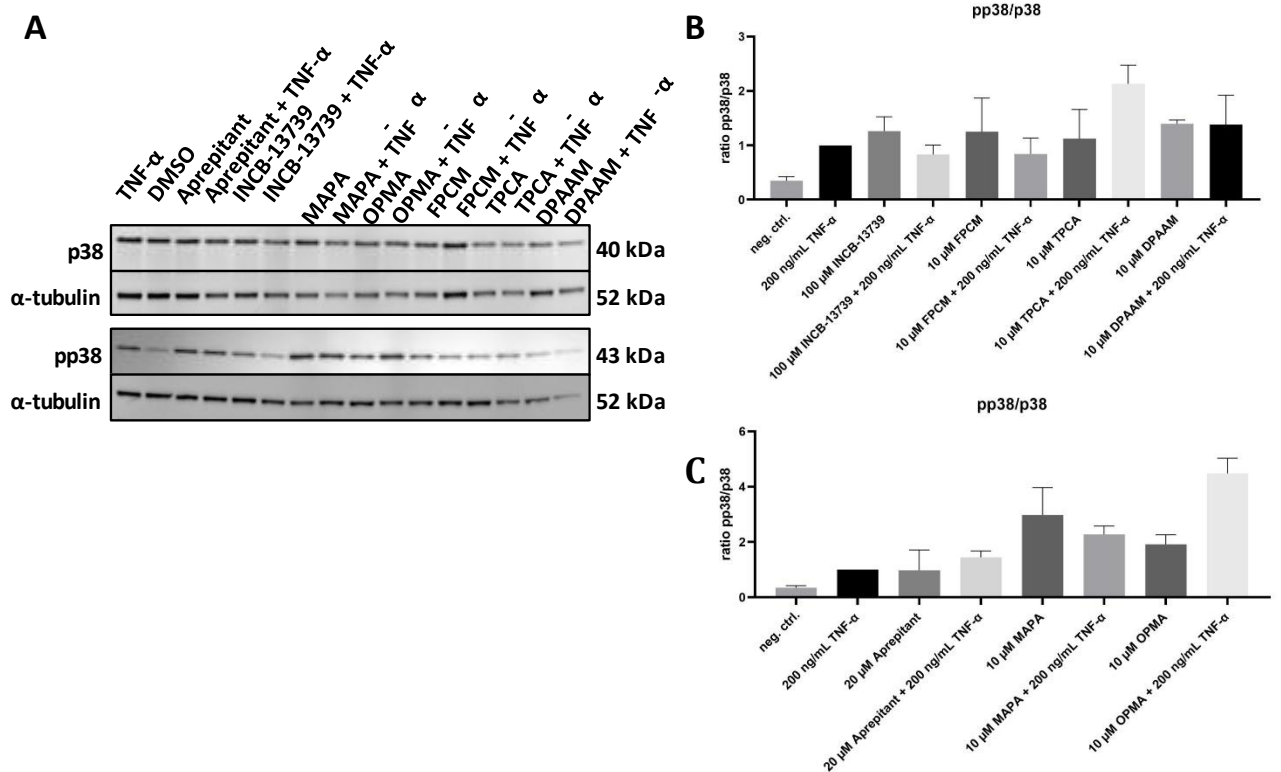


Figure S41: Quantification of A: p38 and phosphorylated p38 after treatment with B: FPCM, TPCA and DPAAM and C: MAPA and OPMA

THP-1 were seeded in 6well plates and treated for 24h with supernatant from 48h treated HaCat cells in humidified atmosphere at 37°C and 5% CO₂. Afterwards harvested and lysed in Lysis Buffer. Cell lysis were further used for protein concentration and Western Blot analysis. neg. ctrl served as solvent control of 0,2% DMSO. 20 μ g protein concentration were used to assess the expression of p38. (n=3, One-way ANOVA followed by $\alpha = 0.05$. Significances (****): $p < 0.0001$, (**): $p < 0.001$, (*): $p < 0.01$, (·): $p < 0.05$, (ns): $p \geq 0.05$). Means \pm SD are shown.

NFkB

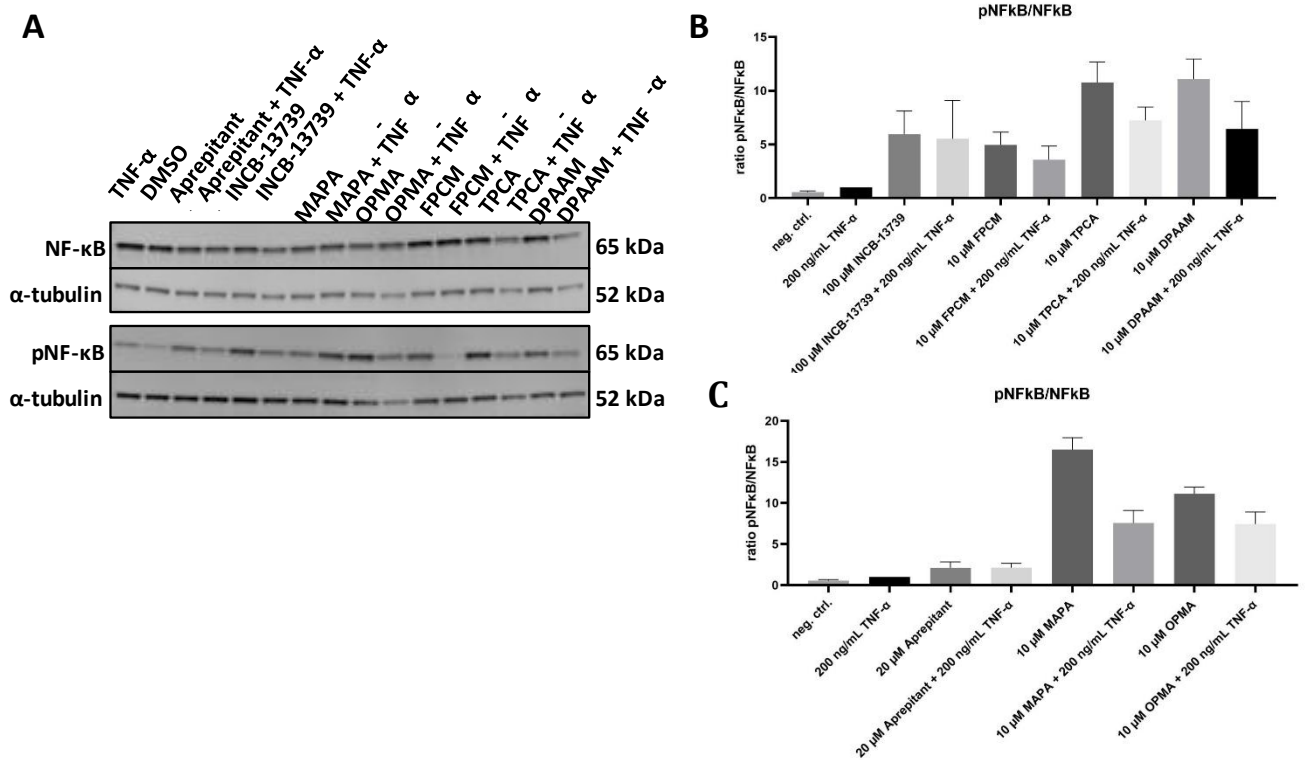


Figure S42: Quantification of A: NFkB and phosphorylated NFkB after treatment with B: FPCM, TPCA and DPAAM and C: MAPA and OPMA

THP-1 were seeded in 6well plates and treated for 24h with supernatant from 48h treated HaCat cells in humidified atmosphere at 37°C and 5% CO₂. Afterwards harvested and lysed in Lysis Buffer. Cell lysis were further used for protein concentration and Western Blot analysis. neg. ctrl served as solvent control of 0,2% DMSO. 20μg protein concentration were used to assess the expression NFkB. (n=3, One-way ANOVA followed by $\alpha = 0.05$. Significances (****): $p < 0.0001$, (**): $p < 0.001$, (*): $p < 0.01$, (*): $p < 0.05$, (ns): $p \geq 0.05$). Means \pm SD are shown.

Akt

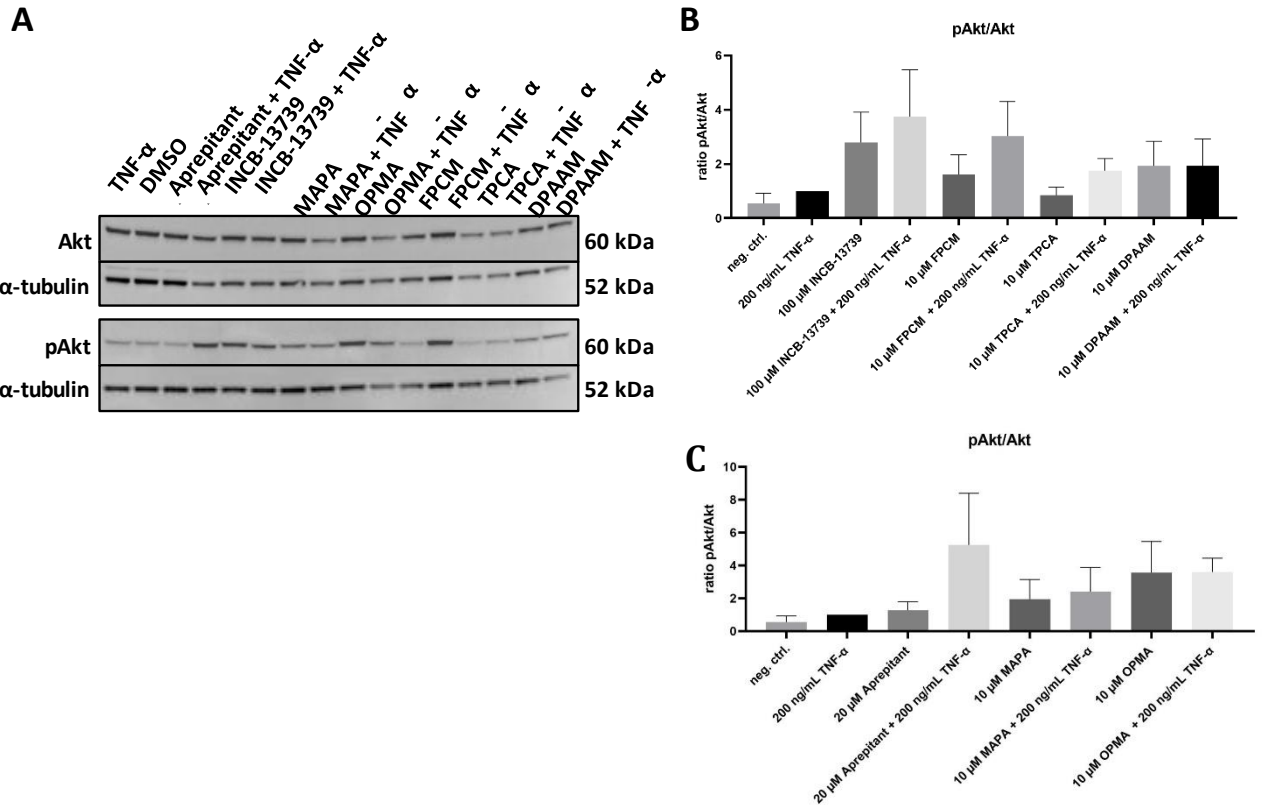


Figure S43: Quantification of A: Akt and phosphorylated Akt after treatment with B: FPCM, TPCA and DPAAM and C: MAPA and OPMA

THP-1 were seeded in 6well plates and treated for 24h with supernatant from 48h treated HaCat cells in humidified atmosphere at 37°C and 5% CO₂. Afterwards harvested and lysed in Lysis Buffer. Cell lysis were further used for protein concentration and Western Blot analysis. neg. ctrl served as solvent control of 0,2% DMSO. 20 μ g protein concentration were used to assess the expression Akt. (n=3, One-way ANOVA followed by $\alpha = 0.05$. Significances (****): $p < 0.0001$, (**): $p < 0.001$, (*): $p < 0.01$, (*) : $p < 0.05$, (ns): $p \geq 0.05$). Means \pm SD are shown.

Stat3

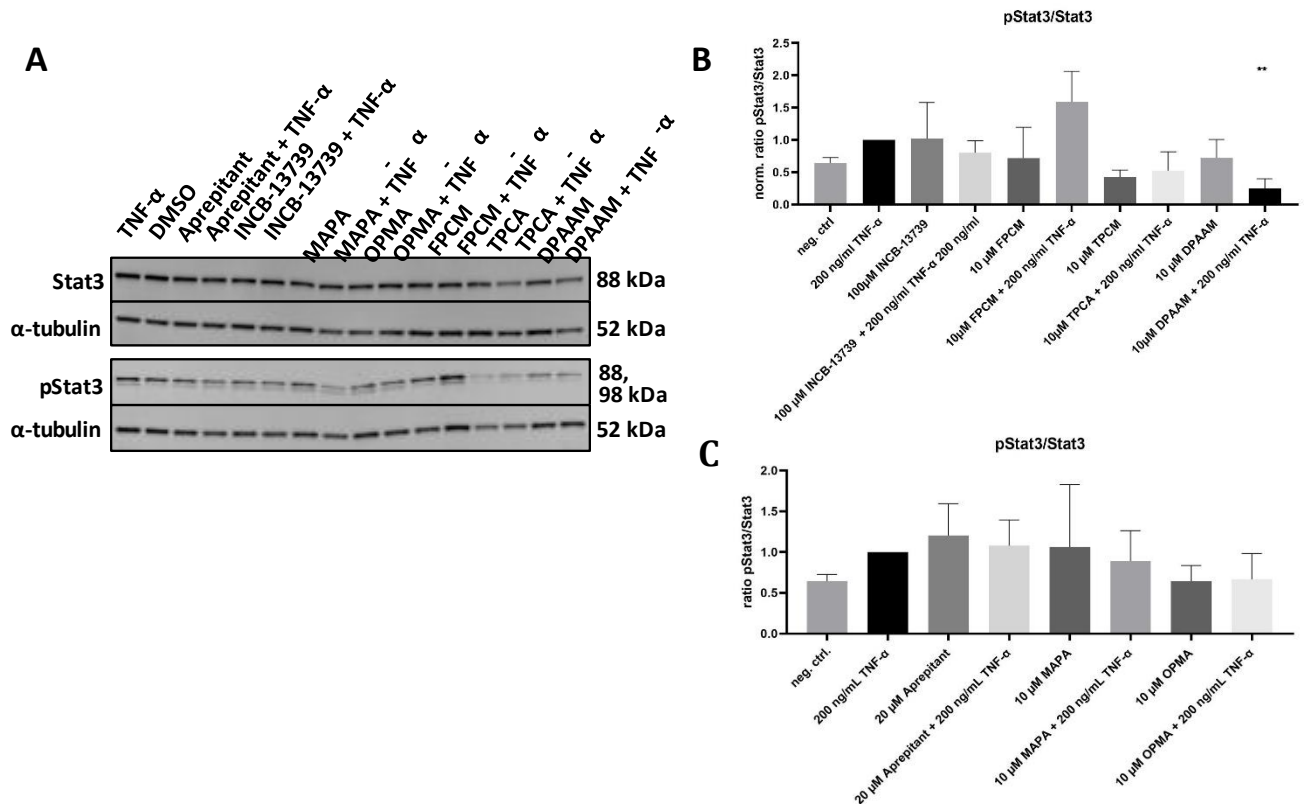


Figure S44: Quantification of A: Stat3 and phosphorylated Stat3 after treatment with B: FPCM, TPCA and DPAAM and C: MAPA and OPMA

THP1 were seeded in 6well plates and treated for 24h with supernatant from 48h treated HaCat cells in humidified atmosphere at 37°C and 5% CO₂. Afterwards harvested and lysed in Lysis Buffer. Cell lysis were further used for protein concentration and Western Blot analysis. neg. ctrl served as solvent control of 0,2% DMSO. 20μg protein concentration were used to assess the expression Stat3. (n=3, One-way ANOVA followed by $\alpha = 0.05$. Significances (****): $p < 0.0001$, (***): $p < 0.001$, (**): $p < 0.01$, (*): $p < 0.05$, (ns): $p \geq 0.05$). Means \pm SD are shown.

ERK

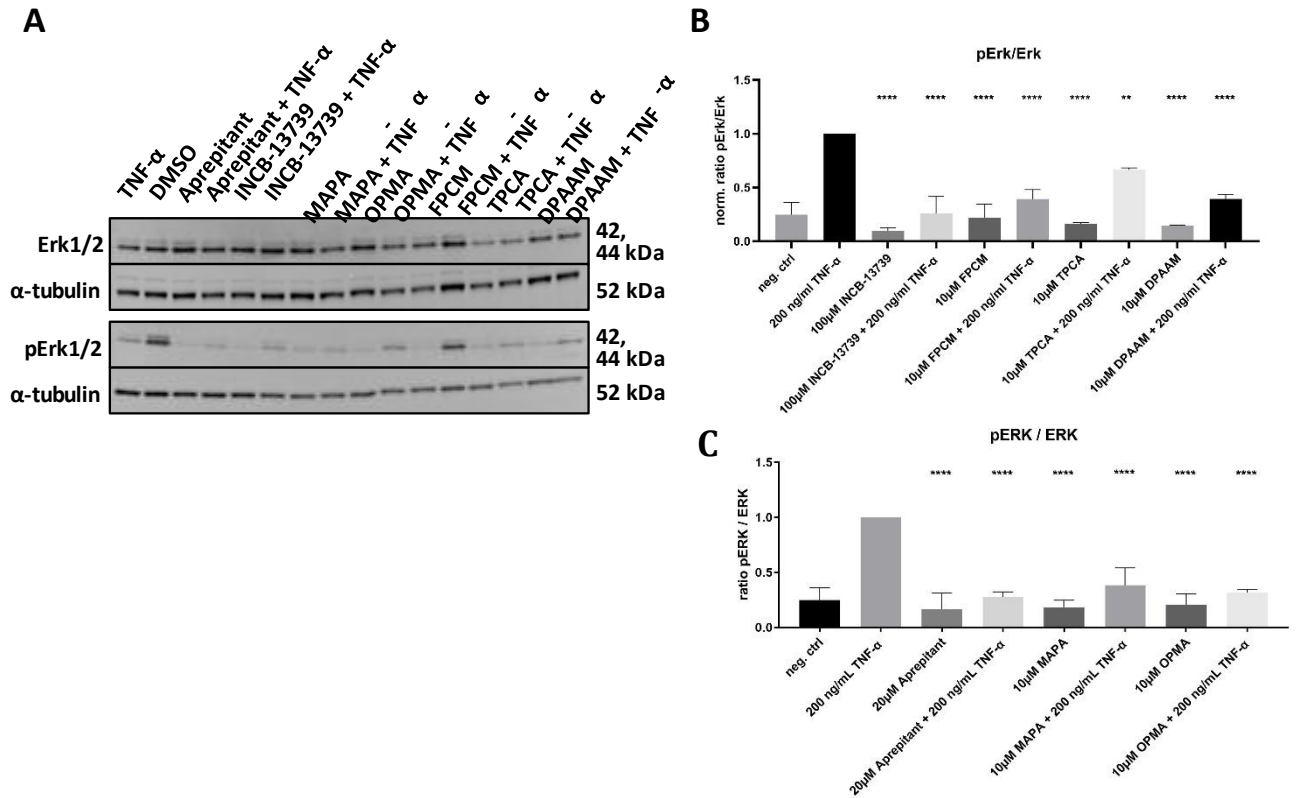


Figure S45: Quantification of A: ERK and phosphorylated ERK after treatment with B: FPCM, TPCA and DPAAM and C: MAPA and OPMA

THP1 were seeded in 6well plates and treated for 24h with supernatant from 48h treated HaCat cells in humidified atmosphere at 37°C and 5% CO₂. Afterwards harvested and lysed in Lysis Buffer. Cell lysis were further used for protein concentration and Western Blot analysis. neg. ctrl served as solvent control of 0,2% DMSO. 20µg protein concentration were used to assess the expression ERK. (n=3, One-way ANOVA followed by $\alpha = 0.05$. Significances (****): $p < 0.0001$, (***): $p < 0.001$, (**): $p < 0.01$, (*): $p < 0.05$, (ns): $p \geq 0.05$). Means \pm SD are shown.

10.5 Danksagung

An dieser Stelle möchte ich mich bei allen bedanken die mich bei der Anfertigung und dem Gelingen dieser Arbeit begleitet und unterstützt haben.

In erster Linie geht mein aufrichtiger Dank an meinen Doktorvater Prof. Dr. Harald Kolmar, für die Betreuung meiner Doktorarbeit an der TU Darmstadt. Ich bin sehr dankbar für den wissenschaftlichen Austausch, die Unterstützung und die Anregungen für den Verlauf meiner Arbeit.

Ein besonderer Dank geht an Prof. Dr. Dipl.-Ing. Jörg von Hagen, der mir die Möglichkeit gegeben hat, in diesem Forschungslabor meine Doktorarbeit anzufertigen. Danke, für deine Betreuung, für dein stets offenes Ohr, für deine Kompetenz und deine Zeit die du trotz allem immer für mich hattest. Vielen Dank für deine überwältigende fachliche Kompetenz, deine konstruktive Kritik und für deinen Rückhalt auch in schwierigen Situationen.

Ebenfalls vielen Dank an Dr. Andrew Salazar für deine Betreuung, dein Feedback und die Zeit die du dir bei meinen zahlreichen Fragen genommen hast. Vielen Dank für das Vertrauen, die Unterstützung und die Motivation dieses Thema zu bearbeiten.

Ein großer Dank geht auch an Prof. Dr. Katja Schmitz und Prof. Dr. Heribert Warzecha für die Übernahme des Amtes der Fachprüfer für meine Disputation. Vielen Dank Prof. Dr. Markus Biesalski für die Übernahme des Vorsitzenden bei meiner Verteidigung. Ich schätze Ihren wissenschaftlichen und fachlichen Input für meine Arbeit sehr.

Liebe AK Kolmar Doktoranden Tanja Lehmann und Melanie Nguyen bei Merck vielen Dank für die netten Mittagessen und die Gespräche, die wir über die Promotion und dessen Ablauf führen konnten und uns gegenseitig gut zugesprochen haben.

Danke liebe Kollegen, die ich während meiner Doktorarbeit kennen lernen durfte. Besonderer Dank geht an Paul Schiller, Lisa Eckelhöfer und Julia Volk die mir bei Fragen im Labor immer zur Seite gestanden haben. Danke, dass ich mich immer auf euch verlassen kann, für die wunderbare Arbeitsatmosphäre und den Spaß, den wir miteinander hatten. Mein Dank geht auch an Julian Osthoff, Marcus Brunner, Michael Termer, Joachim März, Christophe Carola, Stefan Bender und Ralf Petry für die Zeit und Hilfe von euch.

Vielen Dank auch an die Arbeitsgruppenübergreifende Unterstützung von Marc Krenkel und Christin Rakers mit Curia Team, die mir bei meinen Projekten unterstützend zur Seite standen. Ein Dank geht auch an Kollegen, die mich im Arbeitsalltag sehr motiviert und unterstützt haben: Jutta zur Lage, Gabi Witte, Sarah Kögler, Sabrina Lehrian, Annette Fritz, Alexandra Axt-Heidemann, Heike Schuchmann, Ines Keusch, Jörn Beck und Annika Reibold.

Vielen Dank an Prof. Johann Bauer, Hannelore Breitenbach, Andreas Friedrich, Adriana Rathner, Alesia Brodskaja und Dorothee Hölzl und Team der Universität Salzburg und Linz für die großartige Zusammenarbeit an und mit diversen Themengebieten. Vielen Dank für den Input und die Forschung mit meinen Molekülen in *in vivo* Studien. Die Zeit war sehr inspirierend und ich bin sehr dankbar für die Hilfe und Unterstützung.

Einen riesigen Dank geht an Antonia Pönicke, Elena Nickels und Kira Kopietz. Vielen Dank für die wunderbare Zusammenarbeit während eurer Bachelor- und Masterarbeiten. Ich habe sehr viel mit euch und von euch gelernt und bin dankbar für die fachspezifischen Diskussionen und die

Gespräche auch abseits des Labors. Durch euren Input habt ihr einen großen Teil zu einer produktiven Arbeit beigetragen.

Besonders möchte ich mich bei meiner Familie bedanken die mir stets den Rücken gestärkt und mir bei allem unterstützend und treu zur Seite gestanden hat. Danke Mama und Papa, dass ihr mich immer unterstützt, gefördert und aufgebaut habt. Ohne euch wäre ich nicht da, wo ich jetzt bin. Danke auch an meine Geschwister Sarah, Nathalie und David, dass ihr immer da wart und seid. Danke für euren Rückhalt und eure Unterstützung, das Zuhören und noch so unendlich viel mehr.

Danke!

10.6 Curriculum Vitae

Anita Jäger

Date of birth: 04/04/1995
Place of birth: Darmstadt
Marital status: single
Nationality: German

ACADEMIC CAREER

01/2020 – present day **Ph. D. at Merck KGaA (Darmstadt)**
Identification of novel antagonists against skin relevant molecular targets in mediation of itch and inflammation; under the supervision of Prof. Dr. Kolmar

04/2018 – 12/2019 **M. Sc. Applied Life Sciences**
University of Applied Sciences, Zweibrücken, Germany
Master Thesis: Elucidation of aging in human fibroblasts and establishing aged skin models for cosmetic research (Active Ingredients Innovation, Merck KGaA, Prof. Dipl. Ing. Jörg von Hagen)

09/2014 – 02/2018 **B. Sc. / B. Ing. Applied Life Sciences**
University of Applied Sciences, Zweibrücken, Germany
Bachelor Thesis: Role of the microglial Histone-Deacetylase 3 on Alzheimer pathogenesis in APP/PS1 transgenic mice (Alzheimer Forschung, Universität Saarbrücken, Dr. Alexander Liu)

08/2010 – 03/2014 **Abitur**
Leininger Gymnasium
Grünstadt, Rhineland-Palatine, Germany

Darmstadt, 15.12.2022

Anita Jäger

10.7 Affirmations

Erklärungen

§8 Abs. 1 lit. c der Promotionsordnung der TU Darmstadt

Ich versichere hiermit, dass die elektronische Version meiner Dissertation mit der schriftlichen Version übereinstimmt und für die Durchführung des Promotionsverfahrens vorliegt.

§8 Abs. 1 lit. d der Promotionsordnung der TU Darmstadt

Ich versichere hiermit, dass zu einem vorherigen Zeitpunkt noch keine Promotion versucht wurde und zu keinem früheren Zeitpunkt an einer in- oder ausländischen Hochschule eingereicht wurde. In diesem Fall sind nähere Angaben über Zeitpunkt, Hochschule, Dissertationsthema und Ergebnis dieses Versuchs mitzuteilen.

§9 Abs. 1 der Promotionsordnung der TU Darmstadt

Ich versichere hiermit, dass die vorliegende Dissertation selbstständig und nur unter Verwendung der angegebenen Quellen verfasst wurde.

§9 Abs. 2 der Promotionsordnung der TU Darmstadt

Die Arbeit hat bisher noch nicht zu Prüfungszwecken gedient.

Darmstadt, den

(Name und Unterschrift)